IN THE UNITED STATES PATENT AND TRADEMARK OFFICE

Applicants: Paul G. Ahlquist, et al.
Serial No.: 10/618,896
Filed: July 14, 2003
Title: *Yeast Genes That Affect Viral Replication*
Art Unit: 1632
Examiner: Shin-Lin Chen
Docket No.: 960296.00096
Confirm. No.: 7353

DECLARATION OF PAUL AHLQUIST, PH.D.

Mail Stop Amendment
Commissioner for Patents
P.O. Box 1450
Alexandria, VA 22313-145

Dear Sir:

I, Paul Ahlquist, Ph.D., declare that:

1. I am a Professor of Oncology and Molecular Virology at the University of Wisconsin-Madison School of Medicine and Public Health, Madison, Wisconsin. I am also a named inventor on the above-identified application. The focus of my laboratory is studying the novel, RNA-based pathways and virus-host interactions underlying replication, gene expression and evolution by positive-strand RNA viruses, the largest class of viruses. I have been asked by Attorney Jean Baker to comment on the December 19, 2008, Office Action in the above-identified application.

2. The Office Action has questioned the conserved nature of delta9 fatty acid desaturases (hereafter D9FADs, also called SCDs). Unsaturated fatty acids (UFAs) are key determinants of membrane fluidity and other important membrane properties. As established in the earlier part of the interview, all studied eukaryotes from yeast to humans use D9FADs/SCDs to carry out the first step in synthesizng UFAs. D9FAD/SCD activity is thus crucial to maintaining basic membrane properties essential for all membrane-linked processes.

3. Membranes are crucial to the replication of all well-studied positive-strand RNA viruses. In particular, all such viruses assemble the machinery for their genomic RNA replication (arguably the central event in their lifecycle) on one or more intracellular lipid bilayer

membranes. This is well documented, e.g., in a number of recent reviews that collectively refer to a great many distinct positive-strand RNA viruses, comprising many different genuses (genera) of positive-strand RNA viruses that infect humans, animals and plants. Such reviews include, e.g., Mackenzie 2005, Salonen 2005, and Ahlquist 2006.

4. Different positive-strand RNA viruses use different intracellular membranes, but my laboratory has shown in one case that one can engineer the retargeting of viral RNA replication complexes from one membrane (mitochondrial)) to another (endoplasmic reticulum [ER]), and that RNA replication proceeded at the new site at high levels (Miller 2003). Positive-strand RNA viruses commonly induce some type of membrane rearrangements at the membranes that they use for RNA replication, and for different viruses these membrane rearrangements can appear quite different. However, my lab has also shown that for a single virus (BMV), simple changes in the levels and interaction of the viral RNA replication factors dramatically alter the morphology of membrane arrangements (from vesicles to stacked membrane sheets), while preserving highly active RNA replication (Schwartz 2004 - this is also illustrated in Fig. 3c-d of Ahlquist 2006). As is discussed further in these references, this implies that, despite the differences in appearance, the various membrane-associated replication structures share common features (such as features of protein-membrane and protein-protein interaction) that are the crucial features for supporting RNA replication.

5. Examiner Chen has asked me to clarify the nature of brome mosaic virus (BMV) as a model system, particularly a model system for positive strand RNA virus replication. BMV has been a leading system in revealing the nature of positive strand RNA replication complex association with membranes. My lab has used BMV for many inquiries and to the nature of positive strand RNA replication, e.g., to show that the positive-strand RNA replication complexes use rearranged membranes to form new, infection-specific compartments in which to sequester viral RNA templates with their replication factors while protecting them from competing processes of RNA translation and decay. Key references in regard to these and other advances through BMV include, e.g., Schwartz 2002, the Ahlquist 2006 review and many references cited therein, and the Lee 2001 and 2003 papers that document the importance of the OLE1 D9FAD.

6. Examples of the importance of these BMV results as precedents for other positive-strand RNA viruses includes the frequent citation of these and other BMV papers from our group in many papers on positive-strand RNA viruses. Specific highly relevant examples include the adoption of our results on BMV as the major current model for RNA replication complex

formation by hepatitis C virus (HCV), one of the most clinically important human positive-strand RNA viruses. See, e.g., the repeated reference to our results on BMV-membrane interactions and membrane rearrangements in the Discussion of the HCV RNA replication paper by Miyanari 2003, and further compare the model proposed for HCV replication complexes in Fig. 6 of Quinkert 2005 to Fig 7 in our paper Schwartz 2002.

7. I have listed below the entire citation of references cited in this Declaration. Copies of these references are attached as Exhibit A.

Ahlquist P (2006) Parallels among positive-strand RNA viruses, reverse-transcribing viruses and double-stranded RNA viruses. Nat Rev Microbiol 4: 371–382.

Lee, W-M., M. Ishikawa and P. Ahlquist (2001). Mutation of host Δ9 fatty acid desaturase inhibits brome mosaic virus RNA replication between template recognition and RNA synthesis. J. Virol. 75:2097-2106.

Lee, W-M. and P. Ahlquist (2003). Membrane synthesis, specific lipid requirements, and localized lipid composition changes associated with a positive-strand RNA virus RNA replication protein. J. Virol. 77: 12819-12828.

Mackenzie J (2005) Wrapping things up about virus RNA replication. Traffic 6: 967–977.

Miller, D. J., M. D. Schwartz, B. T. Dye and P. Ahlquist (2003). Engineered retargeting of viral RNA replication complexes to an alternative intracellular membrane. J. Virol. 77:12193-12202.

Miyanari Y, Hijikata M, Yamaji M, Hosaka M, Takahashi H, Shimotohno K (2003) Hepatitis C virus non-structural proteins in the probable membranous compartment function in viral genome replication.
J Biol Chem 278:50301-8.

Quinkert D, Bartenschlager R, Lohmann V (2005) Quantitative analysis of the hepatitis C virus replication complex. J Virol. 79:13594-605.

Salonen A, Ahola T, Kääriäinen L (2005) Viral RNA replication in association with cellular membranes. Curr Top Microbiol Immunol. 285:139-73.

Schwartz, M., J. Chen, M. Janda, M. Sullivan, J. den Boon and P. Ahlquist (2002). A positive-strand RNA virus replication complex parallels form and function of retrovirus capsids. Molecular Cell 9:505-514.

Schwartz, M., J. Chen, W-M Lee, M. Janda and P. Ahlquist (2004). Alternate, virus-induced membrane rearrangements support positive-strand RNA virus genome replication. Proc. Natl. Acad. Sci. USA 101:11263-11268.

7. I declare that all statements made herein of my own knowledge are true and that all statements made on information and belief are believed to be true; and further that these statements were made with the knowledge that willful false statements and the like made are punishable by fine or imprisonment, or both, under Section 1001 of Title 18 of the United States Code and that such willful false statements may jeopardize the validity of the above-identified application or any patent issuing thereon.

Respectfully submitted,

Date: 4-20-09

Paul Ahlquist, Ph.D.

Parallels among positive-strand RNA viruses, reverse-transcribing viruses and double-stranded RNA viruses

Paul Ahlquist

Abstract | Viruses are divided into seven classes on the basis of differing strategies for storing and replicating their genomes through RNA and/or DNA intermediates. Despite major differences among these classes, recent results reveal that the non-virion, intracellular RNA-replication complexes of some positive-strand RNA viruses share parallels with the structure, assembly and function of the replicative cores of extracellular virions of reverse-transcribing viruses and double-stranded RNA viruses. Therefore, at least four of seven principal virus classes share several underlying features in genome replication and might have emerged from common ancestors. This has implications for virus function, evolution and control.

Positive-strand RNA virus
A virus, the infectious virions of which contain the genome in a single-stranded, messenger-sense RNA form.

Despite continuing advances, established and emerging viruses remain major causes of human disease, with dramatic costs in mortality, morbidity and economic terms. In addition to acute diseases, viruses cause at least 15–20% of human cancers[1,2] and are implicated in neurological and other chronic disorders. One of many challenges in controlling viruses and virus-mediated diseases is that viruses show an amazing diversity in basic characteristics and life cycles, including differences in virion structure, replication strategies, genetic organization, gene expression and many other fundamental processes. Therefore, even the very processes against which antivirals are targeted often differ radically among virus classes. Inherent in this remarkable variety are intriguing issues about the multiplicity of virus origins and the functional and evolutionary relations of existing viruses. Such issues have practical as well as academic importance, as underlying similarities among virus classes might serve as a foundation for broader-spectrum antiviral strategies.

One of the most elemental differences among viruses is their diversity in genome replication and encapsidation strategies, which define seven major classes (FIG. 1). Some viruses replicate their genomes solely through DNA intermediates, packaging these genomes in infectious virions either as double-stranded (ds)DNA or single-stranded (ss)DNA. By contrast, most viruses replicate their genomes solely through RNA intermediates. Such RNA viruses are divided into three classes based on whether their virions package the genome as mRNA-sense (positive-strand) ssRNA, antisense (negative-strand) ssRNA or dsRNA. Other viruses replicate by interconverting their genomes between RNA and DNA. The virions of such reverse-transcribing viruses always initially package the RNA forms of their genomes, and either might (for example, hepadnaviruses and foamy retroviruses) or might not (for example, orthoretroviruses) reverse-transcribe the RNA into DNA before the virion exits the initially infected producer cell.

Viruses in each of these seven classes tend to share additional features, such as gene-expression strategies and so on, that further cluster and differentiate their members from the other classes, showing that these classes represent meaningful, functionally distinct groupings and probable evolutionary lineages. Some of these variations arise because the type of nucleic acid delivered by the virion to a target cell dictates early infection and gene-expression steps. For example, to initiate viral gene expression, dsRNA virus virions and negative-strand RNA ((–)RNA) virus virions contain viral polymerases that transcribe the genome into translatable mRNA, and reverse-transcribing-virus virions contain polymerases that copy the genome into cell-transcribable DNA (BOX 1). Positive-strand RNA ((+)RNA) viruses, the virions of which deliver immediately translatable messenger-sense RNAs, encapsidate their RNA without a polymerase and form strictly intracellular RNA-replication and mRNAtranscription complexes (BOX 1).

Despite these and other differences, recent results have revealed fundamental parallels in the genome-replication processes of certain (+)RNA viruses, dsRNA viruses and reverse-transcribing viruses. In particular, the

Institute for Molecular Virology and Howard Hughes Medical Institute, University of Wisconsin–Madison, Madison, Wisconsin 53706, USA.
e-mail: ahlquist@wisc.edu
doi:10.1038/nrmicro1389
Published online 3 April 2006

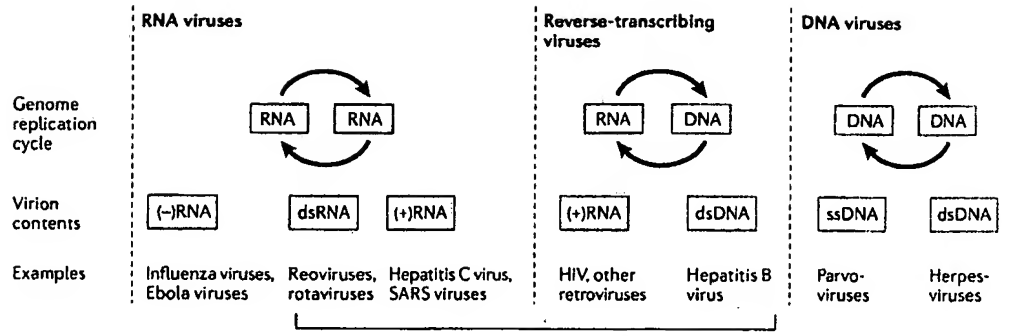

Figure 1 | **Seven classes of virus distinguished by genome replication and encapsidation strategies.** The bracket highlights the four virus classes emphasized in this review. (+)RNA, positive-strand RNA, which is single-stranded RNA of the same polarity as viral mRNA; (-)RNA, negative-strand RNA, which is single-stranded RNA of anti-mRNA polarity; dsRNA, double-stranded RNA; SARS, severe acute respiratory syndrome.

intracellular RNA-replication complexes of some, if not many, (+)RNA viruses share several similarities with the replicative cores of virions from both dsRNA viruses and reverse-transcribing viruses. This review outlines these similarities and their potential implications for virus function and evolution. As primary examples, we review similarities among (+)RNA viruses in the alphavirus-like superfamily, the dsRNA reoviruses and the retroviruses. Other shared characteristics with similar evolutionary implications have been recognized recently among certain other (+)RNA viruses, the dsRNA birnaviruses and the reverse-transcribing hepadnaviruses, including parallels in viral RNA-polymerase structure, capsid proteins and protein priming of genome replication[3–7].

Negative-strand RNA ((–)RNA) viruses (FIG. 1) also share similarities with some of the basic features reviewed here, suggesting that the functional and evolutionary parallels discussed below might be extended further. These possibilities are not discussed here in detail for reasons of space. In addition, whereas (+)RNA viruses, dsRNA viruses and reverse-transcribing viruses each use identical (+)RNA molecules as genome-replication intermediates and mRNAs, (–)RNA viruses are distinguished by using different forms of (+)RNA for these functions.

(+)RNA virus and retrovirus parallels

tRNAs and genome replication. One of the first similarities recognized between the replication of retroviruses and (+)RNA viruses was the role of tRNAs in initiating retroviral reverse transcription and of tRNA-like elements in initiating RNA replication by a subset of (+)RNA viruses such as the bromoviruses[8,9] (FIG. 2). Bromoviruses, discussed further below, have three genomic RNAs with highly conserved, structured, tRNA-like 3′ ends (FIG. 2b). These 3′ ends terminate in 3′-CCA_{OH} sequences that are completed by tRNA-nucleotidyl transferase, they are specifically aminoacylated *in vitro* and *in vivo* with tyrosine, and they contain the promoter for (–)RNA synthesis[10–13].

tRNA-related sequences initiate negative-strand synthesis for genomic RNA replication in both retroviruses and (+)RNA viruses, but the mechanisms are distinct. For retroviruses, a cellular tRNA covalently primes negative-strand cDNA synthesis, whereas for the relevant (+)RNA viruses, a viral tRNA-like element serves as a recognition site and template for (–)RNA synthesis that is initiated *de novo*, without a primer. A natural intermediate and potential evolutionary link between these processes was identified by Lambowitz and colleagues, who showed that a *Neurospora crassa* mitochondrial retroplasmid initiates reverse transcription without a primer at the tRNA-like 3′ end of its genomic RNA, paralleling negative-strand initiation by (+)RNA viruses[14].

Membrane-associated RNA-replication complexes. As noted above, (+)RNA viruses differ from retroviruses and other RNA viruses in that they do not encapsidate their polymerases in extracellular virions. Nevertheless, emerging results show that similarities between (+)RNA-virus RNA replication and retrovirus reverse transcription are not limited to aspects of negative-strand initiation and the general similarities of RNA and DNA polymerases. Instead, as detailed below, (+)RNA-virus RNA replication occurs in virus-induced compartments which have many similarities to the replicative cores or capsids of retrovirus virions.

(+)RNA-virus replication is invariably localized to intracellular membranes. Different (+)RNA viruses target distinct but usually specific membranes, such as those of the endoplasmic reticulum (ER)[15–19], endosomes[20,21], mitochondria[22] or chloroplasts[23]. RNA replication is usually associated with rearrangements of these target membranes, often giving rise to membrane invaginations, single- or double-membrane vesicles, membrane-bound vesicle packets and other structures.

For many (+)RNA viruses, RNA synthesis localizes to membranes bearing 50–70-nm vesicular compartments that are invaginated away from the cytoplasm into the lumen of the affected secretory compartment or organelle. Such invaginations, termed spherules, were first visualized in early electron microscopy (EM) studies of alphavirus-infected cells[20,21]. There are many other examples of such invaginations in and beyond the alphavirus-like superfamily, such as those associated with bromoviruses[24,25], nodaviruses[22] and tymoviruses[23].

Negative-strand RNA virus
A virus, the infectious virions of which contain the genome in a single-stranded, anti-messenger-sense RNA form.

Retroplasmid
A DNA plasmid that replicates by transcription and reverse transcription of an RNA intermediate.

Box 1 | Distinct life cycles of dsRNA viruses, (+)RNA viruses and retroviruses

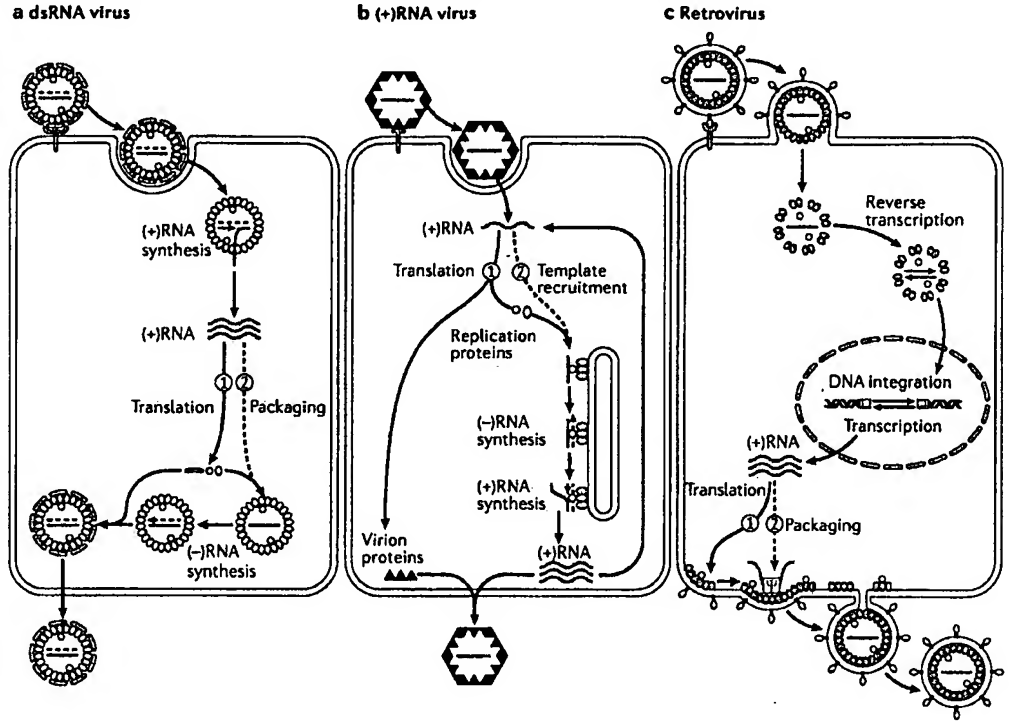

All three classes of virus replicate through positive-strand RNA ((+)RNA) intermediates (red strands in the figure) that are templates for both translation and genome replication. For each class, the figure shows a simplified, representative life cycle.

Double-stranded (ds)RNA viruses

As shown in part a of the figure, virus attachment and endocytosis deliver a virion core that contains viral genomic dsRNA and viral RNA polymerase (yellow) into the cytoplasm. The core transcribes and extrudes (+)mRNAs that are first translated (1) and then packaged (2) by the resulting viral proteins into new virion cores. Cores mature by synthesizing negative-strand (–)RNA (dotted strand) and adding exterior proteins. They exit by cell lysis or secretion.

(+)RNA viruses

As shown in part b of the figure, endocytosed virions release messenger-sense genomic RNA into the cytoplasm for translation. Newly translated viral RNA-replication proteins recruit this genomic RNA into a membrane-associated, intracellular RNA-replication complex. Small amounts of (–)RNA are produced and used as templates to greatly amplify viral (+)RNA, which is encapsidated into new progeny virions.

Retroviruses

As shown in part c of the figure, virion attachment and envelope fusion release a subviral complex that contains viral genomic (+)RNA and reverse transcriptase (yellow). After cDNA synthesis by reverse transcription, proviral cDNA is integrated into the host chromosome and transcribed to produce (+)RNA that is translated (1) and then packaged (2) into new virions that are released by budding.

As illustrated in FIG. 3a–c, for nodaviruses and bromoviruses, such spherules frequently occur in contiguous clusters and are often light-bulb-shaped structures, the interiors of which are connected to the cytoplasm through membranous necks.

Parallels with retrovirus capsids. Retroviruses package their reverse transcriptase (also designated Pol) and their genomic RNA templates into membrane-enveloped capsid shells assembled by the major capsid protein, Gag[26–28] (FIG. 4a). For most retroviruses, these capsids bud from the cell together with viral envelope proteins and are delivered to new cells by infection, giving rise to intracellular complexes in which reverse transcription occurs[29–31]. For foamy retroviruses and retrovirus-like LTR (long terminal repeat) retrotransposons, reverse transcription occurs in such capsids without leaving the producer cell[32–34]. Such capsids contain hundreds[35] to thousands[36] of Gag proteins and approximately 10–20-fold fewer Gag–Pol fusion proteins[28,37]. Retrovirus genomic RNAs are selectively packaged in these capsids by Gag interaction with specific *cis*-acting signals, often designated as Ψ[38,39].

Recently, links between the intracellular spherules of (+)RNA viruses and retrovirus capsids emerged from studies of brome mosaic virus (BMV) RNA replication.

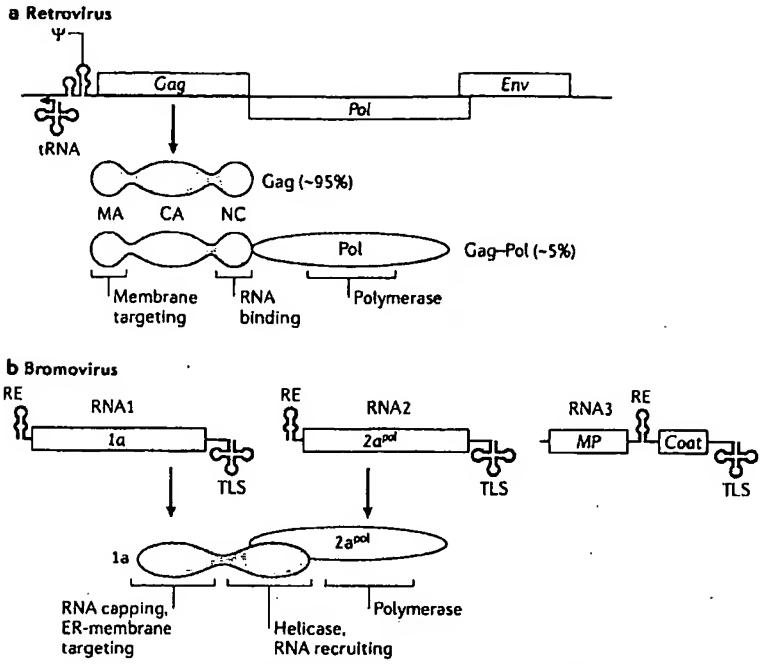

Figure 2 | **Schematic overview of retrovirus and bromovirus genomes. a** | Schematic of the genomic RNA of a simple retrovirus and encoded virion proteins Gag and Gag–Pol. **b** | Schematic of bromovirus genomic RNAs 1, 2 and 3 and encoded RNA-replication factors 1a and $2a^{pol}$. CA, capsid; Env, envelope-protein gene; ER, endoplasmic reticulum; MA, matrix; NC, nucleocapsid; RE, RNA template recruiting element for genomic RNA replication; TLS, 3′ tRNA-like sequence, which contains the promoter for negative-strand RNA synthesis; tRNA, host tRNA primer for negative-strand cDNA synthesis; Ψ, RNA-packaging signal.

BMV is the type member of the bromoviruses and a representative member of the alphavirus-like superfamily of (+)RNA viruses. This superfamily includes many viruses that infect animals or plants, all of which share three conserved protein domains that are involved in RNA replication[40,41]. In BMV, these domains are distributed across two replication proteins, 1a and $2a^{pol}$ (FIG. 2b), that co-localize on ER membranes at the sites of viral RNA synthesis[15,16]. 1a contains an RNA-helicase-like domain and an RNA-capping domain with m^7G methyltransferase and covalent m^7G binding activities required for capping of viral RNAs *in vivo*[42–44]. $2a^{pol}$ contains a central polymerase domain.

Protein 1a is a multifunctional protein with central roles in the genesis and operation of BMV RNA-replication complexes (FIG. 4b). In the absence of other viral factors, 1a localizes to ER membranes[16] and induces invagination of the spherular replication compartments[45]. 1a also recruits nascent or full-length $2a^{pol}$ to ER membranes by an interaction between the 1a helicase-like domain and the N-terminal extension that precedes the $2a^{pol}$ polymerase domain[46–48].

Protein 1a also transfers BMV genomic RNA-replication templates to a new state, which was first recognized because the stability and accumulation of BMV genomic RNAs was dramatically increased by 1a co-expression in yeast[49–51]. Subsequent work showed that 1a induces the transfer of BMV genomic RNAs to a novel, membrane-associated, nuclease-resistant state[45]. The location of the nuclease-resistant RNA and the site of RNA synthesis seem to be the spherule interior, as (+)RNA and (–)RNA templates and nascent BMV RNAs show identical membrane association and nuclease resistance, and immunogold EM localizes 5-bromo-UTP (BrUTP)-labelled nascent RNAs to the spherule interior[45].

Recruitment of BMV genomic RNAs to the RNA-replication complex by 1a is controlled in *cis* by internal (RNA3) or 5′ proximal (RNA1 and RNA2) recruitment elements (REs) on each genomic RNA (FIG. 2b), which are necessary and sufficient for 1a responsiveness[51,52]. Mutational studies show that the RE activity of BMV RNA derivatives in 1a-induced recruitment is closely linked to their relative template activity in (–)RNA synthesis and full RNA replication[51,52]. Therefore, 1a-responsive RNA-template recruitment seems to be a crucial step that precedes replication.

As shown in FIG. 4a,b, the roles of 1a, $2a^{pol}$ and the *cis*-acting REs parallel the roles of Gag, Pol and Ψ in retrovirus replication. Similar to Gag, 1a localizes to the cytoplasmic face of membranes as a peripheral membrane protein[53], self-interacts[54], and is the sole viral factor required to induce membrane invagination[45]. Immunogold EM labelling and biochemical analyses show that each spherule contains hundreds of 1a proteins[45]. The resulting spherules (FIG. 3c) are remarkably similar to the necked vesicles that result when retrovirus budding is arrested by mutations in the Gag late domain that recruits host factors required for membrane breakage and fusion[55]. Moreover, the high multiplicity of 1a in spherules, its strong membrane association and self-interaction, and the dependence of endocytic and secretory vesicle formation and enveloped-virion budding on protein coats or shells[56,57] indicate that 1a might induce membrane invagination by forming a capsid-like shell similar to that of Gag. Similarly, the 1a–RE interaction in RNA-template recruitment parallels the Gag–Ψ interaction in retrovirus RNA packaging. Like retrovirus Pol, BMV $2a^{pol}$ is not required for spherule formation or RNA recruitment. However, when expressed, $2a^{pol}$ is incorporated into the replication complex in a $1a/2a^{pol}$ ratio of ~25, similar to the Gag/Pol ratio of 10/20 (REFS 37,45).

Similarities with other (+)RNA viruses

The universal association of (+)RNA-virus RNA replication with modified intracellular membranes, often in association with membrane invaginations, and other shared features imply that the RNA-replication complexes of a wide variety of (+)RNA viruses might use principles that are similar to those illustrated in FIG. 4b. Such parallels include the following: both alphavirus- and cucumovirus-induced membrane spherules contain dsRNA[25,58]; BrUTP labelling implies that the interiors of alphavirus spherules are the sites of viral RNA synthesis[59]; hepatitis C virus and coronavirus (–)RNA-replication templates are in a membrane-associated, nuclease-resistant state[60–62]; hepatitis C virus replication proteins are present in active replication complexes at >100-fold excess over viral RNA and are sequestered in a protease-resistant

BrUTP labelling
Labelling RNA by replacing the substrate UTP with 5-bromo-UTP (BrUTP). The labelled RNA can be localized using electron microscopy following immunogold labelling with an antibody directed against BrU.

state[61,62]; poliovirus polymerase and possibly other replication factors self-oligomerize in extended lattices[63]; and tombusvirus genomic RNA possesses an internal *cis* signal for initial template recruitment and separate 3′ terminal sequences for negative-strand initiation[64].

Furthermore, just as for retrovirus Gag and BMV 1a, the membrane structures associated with genome replication by many (+)RNA viruses can be induced by a subset of viral RNA-replication proteins that do not include the polymerase. Examples include the RNA-replication-associated membrane structures induced by alphavirus nsP123 (REF. 65), arterivirus nsp2 and nsp3 (REF. 66), hepatitis C virus nsP4B (REFS 19,67) and picornavirus 2BC (REFS 18,68,69).

As explained further below, the parallels among (+)RNA-virus RNA-replication complexes, retrovirus capsids and dsRNA-virus capsids (FIG. 4) imply possible mechanistic explanations for several common features of (+)RNA-virus RNA replication, such as the ability of the replication complex to retain (−)RNA templates for positive-strand synthesis, differential regulation of (−)RNA and (+)RNA synthesis, and frequent down-regulation of polymerase expression.

Pol regulation in retroviruses and (+)RNA viruses. In retrovirus genomes, the Pol open reading frame (ORF) follows that of Gag and is expressed by a rare translational frameshift or translational readthrough event, generating an ~20-fold ratio of Gag/Gag–Pol (FIG. 2a) that is incorporated into the final virion (FIG. 4a). This highly asymmetric ratio regulates the free volume and other parameters of the capsid, and is functionally important, as increasing the level of Gag–Pol relative to Gag inhibits retrovirus virion assembly, release and infectivity[37,70,71].

Similarly, many (+)RNA viruses downregulate expression of their polymerase relative to RNA-replication proteins related in sequence and/or functions to 1a. The finding that BMV 1a parallels Gag in acting at high multiplicity to induce the RNA-replication compartment (FIG. 4a,b) implies that such polymerase downregulation might satisfy functional requirements similar to those governing the Gag/Gag–Pol ratio in retrovirus capsids. Like retroviruses, many (+)RNA viruses use translational readthrough or frameshift to downregulate polymerase expression. Well-studied examples include the animal alphaviruses and arteriviruses and plant tobamoviruses and tombusviruses. In each case, the ORF upstream to that of polymerase encodes a protein(s) with parallels to 1a. Specifically, alphavirus nsP123 and tobamovirus p130 are homologous to 1a (REF. 40), and nsP123 is sufficient to induce membrane spherules[65]; arterivirus ORF1a proteins induce membrane rearrangements associated with RNA replication[66]; and tombusvirus p33 self-interacts and directs membrane association of itself, viral RNA and polymerase[72]. As with Gag and Pol, increasing expression of the polymerase-containing fusion proteins at the expense of the upstream membrane-interacting proteins inhibits tobamovirus and alphavirus replication[73,74].

Unlike the above examples, bromoviruses express 1a and $2a^{pol}$ from separate genomic RNAs (FIG. 2b). In this regard, they parallel the foamy virus genus of retroviruses, which express Gag and Pol as independent proteins from separate mRNAs[34]. Although expressed separately, direct *in vivo* interaction between the C-terminal 1a helicase domain and N-terminal sequences of nascent $2a^{pol}$ results in a 1a–$2a^{pol}$ complex with a polarity that is reminiscent

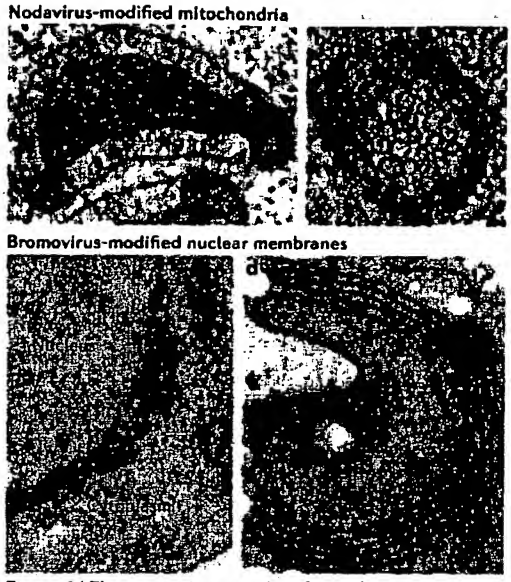

Figure 3 | **Electron micrographs of membrane rearrangements associated with nodavirus and bromovirus RNA replication. a** | Mitochondria in a flock-house-nodavirus-infected *Drosophila* cell, showing the typical 50–70-nm, light-bulb-shaped spherular invaginations of the outer mitochondrial membrane into the expanded lumen between the inner and outer membranes. Reproduced with permission from REF. 22 © (2001) American Society for Microbiology. **b** | Mitochondrion in a flock-house-nodavirus-infected *Drosophila* cell that has been sectioned perpendicular to the axis of the spherule necks, rather than parallel to these axes as in panel **a**. This view reveals a 'vesicle packet' appearance (B. Kopek and P.A., unpublished results). Note that invagination into the lumen of any closed membrane compartment such as the endoplasmic reticulum (ER) or mitochondrial envelope creates a spherule interior that remains connected to the cytoplasm, but that in the section shown in **b**, the spherule appears separated from the cytoplasm by two or more bounding membranes. **c** | Similar 50–70-nm spherular vesicles invaginated from the outer perinuclear ER membrane into the ER lumen, in a yeast cell expressing brome mosaic virus (BMV) replication factor 1a in the absence of other viral components. Indistinguishable spherules occur in cells expressing 1a and BMV $2a^{pol}$ in a 20/1 ratio and replicating BMV RNA3. Reproduced with permission from REF. 45 © (2002) Elsevier. **d** | Karmellae-like layering of the outer perinuclear ER membrane in cells expressing BMV 1a plus elevated levels of BMV $2a^{pol}$, and replicating BMV RNA3. Note at top and bottom left that the ~60-nm intermembrane space is contiguous with the cytoplasm. Reproduced with permission from REF. 84 © (2004) National Academy of Sciences, USA.

Translational frameshift
A site-specific, programmed shift of some translating ribosomes from one reading frame to another, allowing a fraction of translation products to be extended in the new frame.

Translational readthrough
Programmed translation of some ribosomes through a termination codon, allowing a fraction of translation products to be extended beyond the normal stop site.

of orthoretrovirus Gag–Pol[46–48] (FIG. 2). Moreover, whereas translation from separate mRNAs precludes regulation by frameshift or readthrough, BMV downregulates $2a^{pol}$ at translation initiation[75] and by degradation of $2a^{pol}$ that is not complexed with 1a (REF. 76). 1a–$2a^{pol}$ interaction itself is downregulated by competing 1a–1a interaction[54] and $2a^{pol}$ phosphorylation[77]. Therefore, like alphaviruses[78], bromoviruses have evolved several mechanisms to reduce polymerase accumulation and incorporation to achieve the retrovirus-like 1a to $2a^{pol}$ ratio of 25/1 in RNA-replication complexes[45].

Some other (+)RNA viruses, such as hepatitis C virus and picornaviruses, use polyprotein expression strategies that translate all viral ORFs, including polymerase, at equimolar levels. In at least some of these cases, only a fraction of polymerase sequences might be active owing to production of processing intermediates that lack polymerase sequences or activity, polymerase-active and -inactive conformers, polymerase sequestration in the nucleus and/or inclusion bodies, and other effects[62,79]. Some retrotransposons that produce equimolar levels of Gag and Pol appear to use related strategies to regulate polymerase incorporation or activity[80,81].

Alternative membrane rearrangements. Whereas RNA replication by many (+)RNA viruses induces spherular membrane invaginations similar to those shown in FIG. 3a–c, some (+)RNA viruses induce alternative membrane rearrangements. In many cases, the topologies of these rearranged membranes remain under investigation and, as discussed below, some superficially distinct membrane structures might share underlying parallels in topology, assembly and function. Similarly, depending on the conditions, retrovirus Gag not only assembles normal capsids but also sheets, tubes and other structures[82].

Flavivirus RNA replication localizes to packets in which an outer bounding membrane surrounds 50–100-nm vesicles that label with antibodies to viral RNA-replication proteins and dsRNA[83]. These vesicle packets are similar to EM views of BMV spherules invaginated into the ER lumen[84] or nodavirus spherules invaginated into the lumen between the inner and outer mitochondrial membranes[22], when sectioned perpendicular to the direction of invagination (FIG. 3b). BrUTP-labelled RNA synthesis by the related hepatitis C virus localizes to potentially similar clusters of ~85-nm vesicles surrounded by undulating membranes, termed

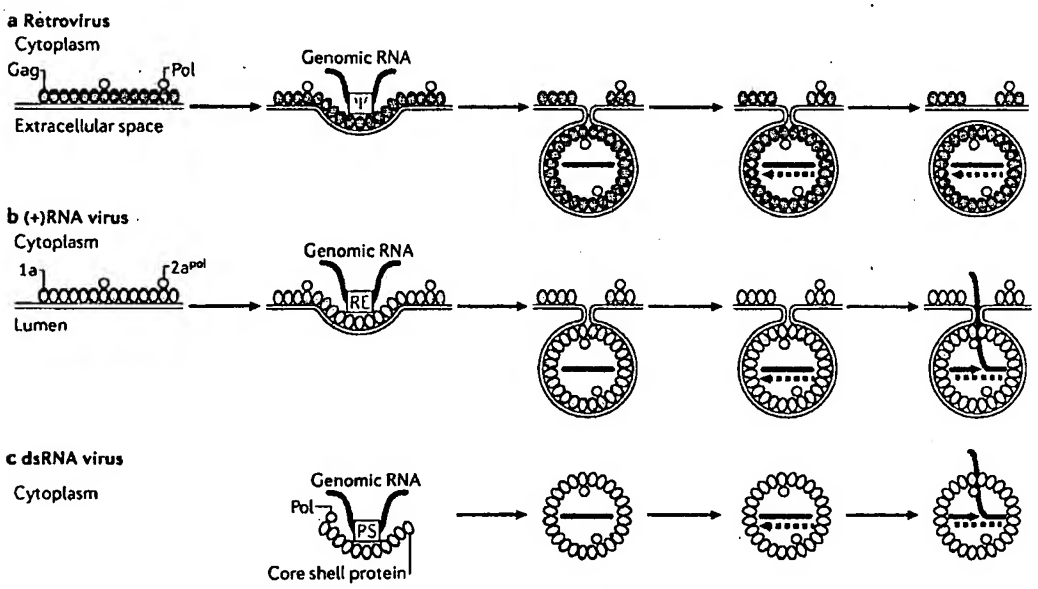

Figure 4 | **Parallels between structure, assembly and function of retrovirus capsids, dsRNA-virus capsids and (+)RNA-virus RNA-replication complexes.** Highly simplified schematics are shown in each case. **a** | Assembly of a retrovirus capsid includes the interaction of membrane-associated Gag and Gag–Pol. Gag-dependent genomic RNA encapsidation takes place through packaging signal Ψ, and this is followed by budding. To emphasize similarities with panels **b** and **c**, synthesis of negative-strand cDNA (dashed lines) is shown prior to budding, as occurs for foamy retroviruses. **b** | Assembly and function of a bromovirus RNA-replication complex at the outer endoplasmic-reticulum membrane includes interaction of membrane-associated 1a and $2a^{pol}$. 1a-dependent genomic RNA encapsidation takes place through the recruitment element (RE) template recruitment signal. This is followed by synthesis and retention of negative-strand RNA (dashed black lines), and asymmetric synthesis and export of positive-strand progeny RNA (red lines), which for at least some positive-strand RNA ((+)RNA) viruses proceeds by a semi-conservative mechanism as shown[143]. **c** | Assembly and function of the capsid core of a generalized double-stranded (ds)RNA virus includes encapsidation of genomic RNAs by a packaging signal (PS), synthesis and retention of negative-strand RNA (dashed black lines) and subsequent asymmetric synthesis and export of positive-strand progeny RNA (red lines). (+)RNA synthesis by dsRNA viruses can be either semi-conservative[144], as shown, or conservative[90,145].

the membranous web[19,67]. Recently, models with strong parallels to bromovirus replication complexes have been proposed for RNA-replication complexes of hepatitis C virus[62,85].

RNA replication by picornaviruses, arteriviruses and coronaviruses occurs in conjunction with double-membrane vesicles, that is, vesicles bearing two closely appressed bounding membranes[17,18,86]. Similar to spherules, arterivirus double-membrane vesicles are thought to form by invagination of appressed ER membranes[17]. Some EM sections of poliovirus double-membrane vesicles display a narrow neck that connects the inner and outer membranes to each other, and that also connects the vesicle interior to the cytoplasm[87], indicating possible genesis by invagination, continuing connection with the cytoplasm, or both.

Interconversion of membrane rearrangements. Further evidence linking seemingly distinct membrane rearrangements in RNA replication is that altering the relative levels and interactions of BMV replication factors 1a and $2a^{pol}$ shifts the associated membrane rearrangements between two dramatically distinct forms[84]. Expressing 1a plus low levels of $2a^{pol}$ (1a/$2a^{pol}$≈20) induces spherular replication complexes matching those of natural bromovirus[24,25] and alphavirus[21] infections (FIG. 3c). By contrast, expressing 1a plus higher levels of $2a^{pol}$ induces stacks of appressed double membranes that support RNA replication to levels as high as spherules[84] (FIG. 3d). The spaces between these double membrane layers parallel spherule interiors in being 50–60 nm wide, containing 1a and $2a^{pol}$, and being directly connected to the cytoplasm. Therefore, BMV-induced spherules and double membrane layers seem to be functionally and topologically equivalent forms that are built from the same protein–protein and protein–membrane interactions, but in altered proportions.

Similar stacked, double-membrane ER layers and other ordered ER membrane arrays are induced by overexpression of membrane-associated picornavirus replication factors 2B and 2BC (REFS 68,88). Moreover, the double-membrane vesicles associated with picornavirus RNA replication, the spherule-bearing mitochondrial membranes associated with nodavirus RNA replication and the spherule-bearing chloroplast membranes associated with tymovirus RNA replication all cluster by interaction of surface membranes bearing viral replication factors[22,23,63,89]. Therefore, a continuum of vesicle-forming and planar membrane interactions seems to be a normal part of RNA replication by many (+)RNA viruses.

(+)RNA virus and dsRNA virus parallels

Many of the above parallels between (+)RNA viruses and retroviruses extend to dsRNA viruses, which also sequester genomic RNA templates, viral polymerase and, often, RNA-capping functions in a protein shell for genome replication[90,91] (FIG. 4c). Possible connections between certain (+)RNA and dsRNA viruses were recognized previously, based on conservation of polymerase[5,92] and, in one case, on additional replication-factor sequences[93].

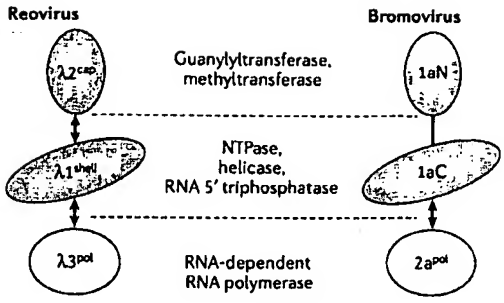

Figure 5 | **Structure–function parallels between reovirus and bromovirus RNA-replication factors.** The schematics illustrate similarities between interaction and function of reovirus core shell-forming protein λ1, RNA-capping protein λ2 and RNA-dependent polymerase λ3, and the interactions and functions of the brome mosaic virus (BMV) 1a C-proximal NTPase/helicase domain (1aC), 1a N-proximal RNA-capping domain (1aN) and $2a^{pol}$ RNA-dependent RNA polymerase. The reovirus λ1–λ2–λ3 interactions shown in the schematic occur at each of the twelve 5-fold axes of the reovirus core.

Similarities with* Reoviridae *cores. BMV RNA-replication factors and replication complexes share several similarities with the icosahedrally symmetric replicative cores of the dsRNA-virus family *Reoviridae* (FIG. 4). *Reoviridae* virions consist of one or more outer-protein shells that are shed during cell entry, surrounding an RNA-containing core that synthesizes RNA *in vivo* and *in vitro*[90]. For the Orthoreovirus genus of the *Reoviridae*, the transcriptionally active, dsRNA-containing core is bound by an ~60-nm icosahedral shell made from 60 dimers of protein λ1 (REF. 94). At each of the twelve 5-fold axes of the core, one copy of the λ3 polymerase resides inside the shell[95], whereas on the shell exterior, a pentamer turret of the λ2 capping proteins surrounds the 5-fold axis[94]. The λ3 polymerase copies the genomic dsRNA templates into new (+)RNA progeny, exporting the nascent RNAs to the cytoplasm through the λ2 pentamer turret, which adds m^7G caps to the 5′ ends.

BMV 1a shows many parallels in function and protein–protein interactions with reovirus core proteins λ1 and λ2, implying potentially similar roles in RNA synthesis (FIG. 5). 1a parallels λ1 as the self-interacting, high-copy-number inducer of the viral RNA-replication compartment, yielding the spherular BMV replication complexes. The 50–70-nm intra-membrane diameter of these spherules is similar to the reovirus λ1 core-protein shell. The C-terminal 1a NTPase/helicase domain and its alphavirus homologues have NTPase, RNA 5′-triphosphatase and helicase activities[96–99], matching λ1 (REFS 100,101). The 1a NTPase/helicase domain also anchors BMV RNA polymerase $2a^{pol}$ to the replication complex by direct interaction[102], whereas λ1 performs the same role for reovirus RNA polymerase λ3 (REF. 95). The resulting twelve λ3 polymerases per core are similar to the estimated 10–15 $2a^{pol}$ per BMV RNA-replication complex[45]. Continuing these parallels, λ1 and the 1a NTPase/helicase domain each anchor RNA-capping

functions to the RNA-synthesis complex in the form of reovirus λ2 protein and the BMV 1a N-terminal domain, respectively. λ2 (REFS 103,104) and the 1a N-terminal domain[42–44,105] both possess guanylyltransferase and methyltransferase activities that add m⁷G caps to the 5′ ends of the (+)RNA products of their respective RNA-synthesis complexes.

RNA packaging, synthesis and export. Recent results indicate possible parallels between the recruitment of (+)RNA templates to BMV RNA-replication complexes and the packaging of (+)RNAs in dsRNA viruses. For dsRNA bacteriophage φ6, viral (+)RNAs are translocated into a pre-formed, empty core by a hexameric viral NTPase/helicase, P4 (REFS 106,107). Similarly, recruitment of BMV genomic RNAs from a membrane-bound, nuclease-sensitive state into the nuclease-resistant spherule replication complex, but not formation of the membrane-invaginated spherules themselves, is blocked by single amino-acid substitutions that inhibit the NTPase activity of the 1a NTPase/helicase domain[99]. Also, like φ6 P4, the 1a-homologous NTPase/helicase domain of protein p126 of tobacco mosaic virus forms hexamers[108]. For the *Reoviridae*, packaging viral (+)RNAs for replication also involves a viral protein with NTPase, RNA-binding and helix-destabilizing activities — the octameric NSP2 for the Rotavirus genus[109,110] and, potentially, μ2 for the Orthoreovirus genus[90,110,111]. Like φ6 P4 (REF. 106) and BMV 1a (REF. 112), μ2 also seems to be a co-factor for (+)RNA synthesis[111].

For dsRNA viruses, packaging of (+)RNAs is associated with, or followed by, (−)RNA synthesis, yielding dsRNAs that are protected in cores or core-like precursors[90,91]. Similarly, BMV (−)RNA synthesis depends on 1a-mediated (+)RNA recruitment[51,52], and the resulting (−)RNA products are exclusively retained in the nuclease-resistant, membrane-associated RNA-replication compartment[45]. This retention in a virus-induced RNA-replication compartment explains the efficient, repetitive *in vivo* use of (−)RNAs as templates for (+)RNA synthesis, and the lack of (−)RNA exchange between RNA-replication complexes in the same cell[113]. Compartmentalization of RNA templates also seems to be important in protecting dsRNA-virus genomes and the potentially dsRNA-replication intermediates of (+)RNA viruses[25,58] from dsRNA-induced host defences, including interferon responses and RNA interference[90,91,114–116].

A reovirus-like pathway for (+)RNA replication (FIG. 4b,c) would also explain the common early shutoff of (−)RNA synthesis in BMV and other (+)RNA viruses, while (+)RNA synthesis continues unabated[112,117,118], and the dependence of (−)RNA synthesis on continuing protein synthesis[118]. In such a model, (−)RNAs might be synthesized primarily during or immediately after replication-complex assembly from newly synthesized proteins, forming dsRNAs that would preferentially or exclusively be templates for (+)RNA synthesis in the resulting stable replication complexes. Replication-complex assembly and negative-strand synthesis seem to cease on exhaustion of a limiting host factor, possibly the target membrane for replication-complex formation[15,118]. Pre-formed replication complexes, however, remain active in (+)RNA synthesis[112,118].

For both the *Reoviridae*[90] and the alphavirus-like superfamily[119,120], (−)RNAs are not capped. By contrast, (+)RNA products are modified with 5′ m⁷G caps and exported to the cytoplasm from both dsRNA virus cores[94,95,121] and BMV spherules[43–45]. This and the parallels noted above between the capping functions and polymerase interactions of the responsible reovirus proteins and 1a suggest that the transcription/capping/export complexes at the 5-fold axes of dsRNA-virus cores might provide models for at least some aspects of the corresponding processes at the spherule necks of BMV and other (+)RNA-virus replication complexes.

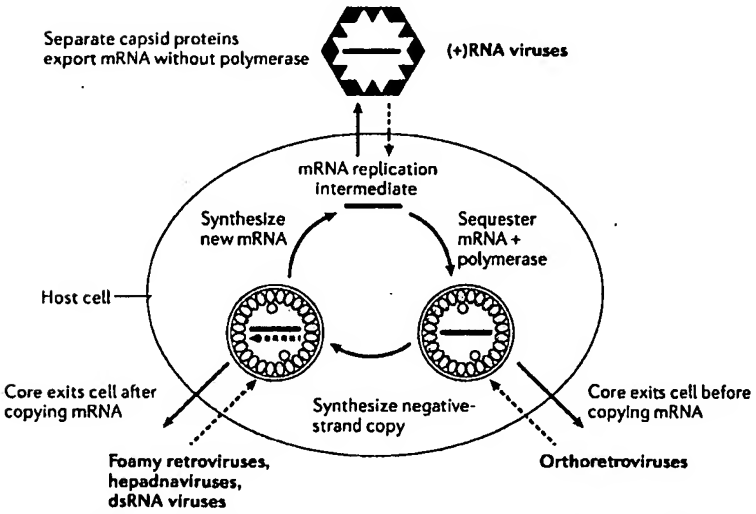

Figure 6 | **Parallels and distinctions among the life cycles of reverse-transcribing viruses, (+)RNA viruses and dsRNA viruses.** All three classes of virus share a similar replication cycle for their genomic RNA (central cyclical steps) but derive their infectious virions from different intermediates in that cycle (radial arrows). See text for further details. (+)RNA, positive-strand RNA; dsRNA, double-stranded RNA.

Possible evolutionary relationships

The above results show that reverse-transcribing viruses, dsRNA viruses and many, if not all, (+)RNA viruses share central features of genome replication (FIG. 6). Most fundamentally, all replicate their genome through an RNA intermediate that also functions as an mRNA. In all three cases, viral proteins that are translated from these mRNAs capture the mRNA template with its polymerase in a multi-subunit core, sequestering viral RNA from competing processes such as translation and degradation, and sequestering polymerase from competing templates. The polymerase then copies the mRNA into a complementary template from which more mRNA is produced.

The variations on this theme that distinguish the three virus classes primarily relate to possessing an RNA-dependent RNA or DNA polymerase, and to deriving infectious virions from different intermediates in the common replication cycle. Orthoretroviruses, such as HIV, export the replicative core prior to copying

the mRNA intermediate (FIG. 6, bottom right). By contrast, foamy viruses, hepadnaviruses and dsRNA viruses export the replicative core after copying the mRNA intermediate (FIG. 6, bottom left). For (+)RNA viruses, the virion is separate from the replication complex, and capsid proteins that are not involved in RNA replication package and export the mRNA intermediate before it is sequestered with polymerase (FIG. 6, top). These distinct virion-assembly choices have important consequences, as noted in the introduction, but from some perspectives could be considered temporary extracellular excursions because, as soon as the next cell is infected, each virus re-enters the central, shared replication pathway.

Although no set of shared features can distinguish divergent from convergent evolution, the many parallels summarized here suggest that (+)RNA viruses, dsRNA viruses and reverse-transcribing viruses might have arisen from common ancestors. The transitions required for such evolution can be readily envisioned, and in some cases have precedents. RNA-dependent RNA and DNA polymerases, for example, have related structures[122,123], and a shift between the two has generally been postulated as the basis for the emergence of DNA-based biology from the RNA world[9]. In keeping with the potential for such transitions, BMV RNA-dependent RNA polymerase can copy DNA templates[124], and reverse transcriptase can, with single point mutations, incorporate ribonucleotide triphosphates (rNTPs) to produce RNA[125].

Established and emerging results further indicate that the intracellular RNA-replication complexes of (+)RNA viruses might evolve into infectious extracellular virions, similar to those of dsRNA or reverse-transcribing viruses, by relatively simple modifications. The spherule RNA-replication complexes of alphaviruses, for example, occur on endosomal membranes and, in lesser numbers, at the plasma membrane, where their appearance closely mimics budding virions[59]. Such spherules are released into the medium at low frequency[59], which might explain the novel infectious particles released from cells replicating alphavirus derivatives with all natural virion proteins deleted and replaced by envelope protein G of vesicular stomatitis virus[126]. As G protein is readily incorporated into many particles that bud from the plasma membrane and confers the ability to attach to, and fuse membranes with, many cells, incorporation of G protein into spherule membranes might confer infectivity by allowing released replication complexes or their RNAs to enter new cells.

Once acquired, infectivity might be enhanced and optimized through subsequently selected events. For retroviruses and other enveloped viruses, efficient virion budding requires recruiting functions from the host-cell multivesicular-body pathway[57]. This host machinery can be recruited by incorporating into viral proteins any of a range of short protein-interaction motifs or L domains, which function in a largely position-independent manner[55]. RNA-recombination events that are suitable to acquire such L domains, favourable envelope-protein genes or other relevant functions from cellular or other viral RNAs are rampant in (+)RNA viruses and retroviruses, representing a major force in virus evolution[127–129].

Additional pathways for evolutionary transitions between the intracellular RNA-replication complexes of (+)RNA viruses and dsRNA virions have recently been suggested[6,130]. As the replication complexes of (+)RNA viruses are invariably membrane-associated, it is notable that virions of the Rotavirus genus of the dsRNA *Reoviridae* bud through membranes during assembly and exit from cells[131]. Moreover, rotavirus transmembrane protein nsP4, which mediates virion-core association with ER membranes, is required for correct assembly of the viroplasms in which core assembly and replicative RNA synthesis occur, indicating linkage of these processes with membranes[132,133]. dsRNA bacteriophage ϕ6 virions also become membrane-enveloped during exit[134].

Whereas most views of virus relationships have tended to emphasize the features and classes depicted in FIG. 1, it is intriguing that several alternative, orthogonal virus groupings are defined and mutually distinguished by features that are more strongly conserved across two or more of the classes in FIG. 1. Selected examples include the conservation of an unusual polymerase-sequence rearrangement between (+)RNA tetraviruses and dsRNA birnaviruses[5], or the use of protein-primed genome replication by the (+)RNA picornaviruses, dsRNA birnaviruses and reverse-transcribing hepadnaviruses[3,4,7], in contrast to the use of tRNA-like elements by bromoviruses and retroviruses. Such relationships suggest that transitions between the virus classes depicted in FIG. 1 might have evolved on more than one occasion, and that links between viruses within a class might not always be as strong as links between classes.

Implications for virus control

The emergence of common underlying principles in the central replication processes of (+)RNA viruses, reverse-transcribing viruses and dsRNA viruses suggests that some of these shared features might provide useful targets for broader-spectrum or generalizable approaches for virus control. One approach might be to modulate membrane lipid composition, as recent results show that assembly and function of membrane-associated (+)RNA-virus replication complexes and retrovirus caspids are highly sensitive to the lipid composition of their target membranes, which in at least some cases can be manipulated by small-molecule therapeutics[135–138]. Another general approach might be to interfere with oligomerization or function of oligomerizing replication factors such as retrovirus Gag and BMV 1a by dominant negative mutants[43,99], inhibition of required chaperones[139,140], targeted incorporation of destructive ligands or other approaches. Further interventions might be based on interfering with viral RNA interactions that are essential for genome packaging, replication and other steps, using nucleic-acid aptamers or other inhibitors[141]. Other approaches might interfere with the trafficking of viral replication factors and RNAs to their required intracellular sites of assembly[142]. Opportunities for such interference will continue to increase as further aspects of these processes are understood in greater detail.

Concluding remarks

An exciting aspect of current virology is that advancing results have not only continued to enrich our understanding of individual viruses, but also to reveal unifying principles that link many aspects of virus infection, replication and host interactions across a surprisingly wide breadth of virus–host systems. The resulting insights display a fundamental order within the vast and sometimes apparently chaotic diversity of known viruses, with important ramifications for virus function and evolution. As the full extent of this tapestry of relations is still emerging, ongoing studies will continue to extend and refine the underlying mechanistic connections. In association with their mechanistic importance, the results should have a growing impact on our abilities to limit the continuing toll and emerging threat of viral diseases, and to develop the beneficial uses of viruses.

1. Butel, J. S. Viral carcinogenesis: revelation of molecular mechanisms and etiology of human disease. *Carcinogenesis* **21**, 405–426 (2000).
2. Talbot, S. J. & Crawford, D. H. Viruses and tumours — an update. *Eur. J. Cancer* **40**, 1998–2005 (2004).
3. Paul, A. V., Rieder, E., Kim, D. W., van Boom, J. H. & Wimmer, E. Identification of an RNA hairpin in poliovirus RNA that serves as the primary template in the *in vitro* uridylylation of VPg. *J. Virol.* **74**, 10359–10370 (2000).
4. Murray, K. E. & Barton, D. J. Poliovirus CRE-dependent VPg uridylylation is required for positive-strand RNA synthesis but not for negative-strand RNA synthesis. *J. Virol.* **77**, 4739–4750 (2003).
References 3 and 4 reveal and refine parallels in protein-primed genome replication by RNA picornaviruses and reverse-transcribing hepatitis B virus.
5. Gorbalenya, A. E. *et al.* The palm subdomain-based active site is internally permuted in viral RNA-dependent RNA polymerases of an ancient lineage. *J. Mol. Biol.* **324**, 47–62 (2002).
Reveals that an unusual re-ordering of polymerase domains is shared by certain (+)RNA viruses and dsRNA viruses.
6. Coulibaly, F. *et al.* The birnavirus crystal structure reveals structural relationships among icosahedral viruses. *Cell* **120**, 761–772 (2005).
7. Ahlquist, P. Virus evolution: fitting lifestyles to a T. *Curr. Biol.* **15**, R465–R467 (2005).
8. Weiner, A. M. & Maizels, N. tRNA-like structures tag the 3′ ends of genomic RNA molecules for replication: implications for the origin of protein synthesis. *Proc. Natl Acad. Sci. USA* **84**, 7383–7387 (1987).
Proposes evolutionary relationships among tRNA-like 3′ ends of certain (+)RNA-virus genomic RNAs, retroviral tRNA priming and chromosomal telomeres.
9. Maizels, N. & Weiner, A. M. in *The RNA World* (eds Gesteland, R. F., Cech, T. R. & Atkins, J. F.) 79–111 (Cold Spring Harbor Laboratory Press, Cold Spring Harbor, 1999).
10. Miller, W. A., Bujarski, J. J., Dreher, T. W. & Hall, T. C. Minus-strand initiation by brome mosaic virus replicase within the 3′ tRNA-like structure of native and modified RNA templates. *J. Mol. Biol.* **187**, 537–546 (1986).
11. Dreher, T. W. & Hall, T. C. Mutational analysis of the tRNA mimicry of brome mosaic virus RNA. Sequence and structural requirements for aminoacylation and 3′-adenylation. *J. Mol. Biol.* **201**, 41–55 (1988).
12. Dreher, T. W. & Hall, T. C. Mutational analysis of the sequence and structural requirements in brome mosaic virus RNA for minus strand promoter activity. *J. Mol. Biol.* **201**, 31–40 (1988).
13. Choi, S. K., Hema, M., Gopinath, K., Santos, J. & Kao, C. Replicase-binding sites on plus- and minus-strand brome mosaic virus RNAs and their roles in RNA replication in plant cells. *J. Virol.* **78**, 13420–13429 (2004).
14. Wang, H. & Lambowitz, A. M. The Mauriceville plasmid reverse transcriptase can initiate cDNA synthesis *de novo* and may be related to reverse transcriptase and DNA polymerase progenitor. *Cell* **75**, 1071–1081 (1993).
Identifies a natural intermediate between tRNA-primed retrovirus reverse transcription and *de novo* RNA synthesis on tRNA-like 3′ ends of some RNA viruses.
15. Restrepo-Hartwig, M. & Ahlquist, P. Brome mosaic virus helicase- and polymerase-like proteins colocalize on the endoplasmic reticulum at sites of viral RNA synthesis. *J. Virol.* **70**, 8908–8916 (1996).
16. Restrepo-Hartwig, M. & Ahlquist, P. Brome mosaic virus RNA replication proteins 1a and 2a colocalize and 1a independently localizes on the yeast endoplasmic reticulum. *J. Virol.* **73**, 10303–10309 (1999).
17. Pedersen, K. W., van der Meer, Y., Roos, N. & Snijder, E. J. Open reading frame 1-a-encoded subunits of the arterivirus replicase induce endoplasmic reticulum-derived double-membrane vesicles which carry the viral replication complex. *J. Virol.* **73**, 2016–2026 (1999).
18. Suhy, D. A., Giddings, T. H., Jr & Kirkegaard, K. Remodeling the endoplasmic reticulum by poliovirus infection and by individual viral proteins: an autophagy-like origin for virus-induced vesicles. *J. Virol.* **74**, 8953–8965 (2000).
19. Gosert, R. *et al.* Identification of the hepatitis C virus RNA replication complex in Huh-7 cells harboring subgenomic replicons. *J. Virol.* **77**, 5487–5492 (2003).
20. Grimley, P. M., Berezesky, I. & Friedman, R. M. Cytoplasmic structures associated with an arbovirus infection: loci of viral ribonucleic acid synthesis. *J. Virol.* **2**, 1326–1338 (1968).
21. Froshauer, S., Kartenbeck, J. & Helenius, A. Alphavirus RNA replicase is located on the cytoplasmic surface of endosomes and lysosomes. *J. Cell Biol.* **107**, 2075–2086 (1988).
References 20 and 21 are classic papers showing association of alphavirus RNA synthesis with modified intracellular membranes.
22. Miller, D. J., Schwartz, M. D. & Ahlquist, P. Flock house virus RNA replicates on outer mitochondrial membranes in *Drosophila* cells. *J. Virol.* **75**, 11664–11676 (2001).
23. Prod'homme, D., Le Panse, S., Drugeon, G. & Jupin, I. Detection and subcellular localization of the turnip yellow mosaic virus 66K replication protein in infected cells. *Virology* **281**, 88–101 (2001).
24. Kim, K. S. An ultrastructural study of inclusions and disease in plant cells infected by cowpea chlorotic mottle virus. *J. Gen. Virol.* **35**, 535–543 (1977).
25. Hatta, T. & Francki, R. I. B. Cytopathic structures associated with tonoplasts of plant cells infected with cucumber mosaic and tomato aspermy viruses. *J. Gen. Virol.* **53**, 343–346 (1981).
26. Morikawa, Y. HIV capsid assembly. *Curr. HIV Res.* **1**, 1–14 (2003).
27. Scarlata, S. & Carter, C. Role of HIV-1 Gag domains in viral assembly. *Biochim. Biophys. Acta* **1614**, 62–72 (2003).
28. Swanstrom, R. & Wills, J. W. in *Retroviruses* (eds Coffin, J. M., Hughes, S. H. & Varmus, H. E.) 263–334 (Cold Spring Harbor Laboratory Press, Cold Spring Harbor, 1997).
29. Ansari-Lari, M. A. & Gibbs, R. A. Expression of human immunodeficiency virus type 1 reverse transcriptase in *trans* during virion release and after infection. *J. Virol.* **70**, 3870–3805 (1996).
30. Yuan, B., Fassati, A., Yueh, A. & Goff, S. P. Characterization of Moloney murine leukemia virus p12 mutants blocked during early events of infection. *J. Virol.* **76**, 10801–10810 (2002).
31. Nermut, M. V. & Fassati, A. Structural analyses of purified human immunodeficiency virus type 1 intracellular reverse transcription complexes. *J. Virol.* **77**, 8196–8206 (2003).
32. Garfinkel, D. J., Boeke, J. D. & Fink, G. R. Ty element transposition: reverse transcriptase and virus-like particles. *Cell* **42**, 507–517 (1985).
33. Eichinger, D. J. & Boeke, J. D. The DNA intermediate in yeast Ty1 element transposition copurifies with virus-like particles: cell-free Ty1 transposition. *Cell* **54**, 955–966 (1988).
34. Linial, M. L. Foamy viruses are unconventional retroviruses. *J. Virol.* **73**, 1747–1755 (1999).
35. Palmer, K. J. *et al.* Cryo-electron microscopy structure of yeast Ty retrotransposon virus-like particles. *J. Virol.* **71**, 6863–6868 (1997).
36. Briggs, J. A. *et al.* The stoichiometry of Gag protein in HIV-1. *Nature Struct. Mol. Biol.* **11**, 672–675 (2004).
37. Shehu-Xhilaga, M., Crowe, S. M. & Mak, J. Maintenance of the Gag/Gag–Pol ratio is important for human immunodeficiency virus type 1 RNA dimerization and viral infectivity. *J. Virol.* **75**, 1834–1841 (2001).
38. Berkowitz, R., Fisher, J. & Goff, S. P. RNA packaging. *Curr. Top. Microbiol. Immunol.* **214**, 177–218 (1996).
39. D'Souza, V. & Summers, M. F. Structural basis for packaging the dimeric genome of Moloney murine leukaemia virus. *Nature* **431**, 586–590 (2004).
40. Ahlquist, P. *et al.* Sindbis virus proteins nsP1 and nsP2 contain homology to nonstructural proteins from several RNA plant viruses. *J. Virol.* **53**, 536–542 (1985).
41. van Regenmortel, M. H. V. (ed.) *Virus Taxonomy* (Academic Press, San Diego, 2000).
42. Ahola, T. & Ahlquist, P. Putative RNA capping activities encoded by brome mosaic virus: methylation and covalent binding of guanylate by replicase protein 1a. *J. Virol.* **73**, 10061–10069 (1999).
43. Ahola, T., den Boon, J. A. & Ahlquist, P. Helicase and capping enzyme active site mutations in brome mosaic virus protein 1a cause defects in template recruitment, negative-strand RNA synthesis, and viral RNA capping. *J. Virol.* **74**, 8803–8811 (2000).
44. Kong, F., Sivakumaran, K. & Kao, C. The N-terminal half of the brome mosaic virus 1a protein has RNA capping-associated activities: specificity for GTP and *S*-adenosylmethionine. *Virology* **259**, 200–210 (1999).
45. Schwartz, M. *et al.* A positive-strand RNA virus replication complex parallels form and function of retrovirus capsids. *Mol. Cell* **9**, 505–514 (2002).
Reveals parallels between the structure, assembly and function of bromovirus RNA-replication complexes and retrovirus virions.
46. Kao, C. C. & Ahlquist, P. Identification of the domains required for direct interaction of the helicase-like and polymerase-like RNA replication proteins of brome mosaic virus. *J. Virol.* **66**, 7293–7302 (1992).
47. Chen, J. & Ahlquist, P. Brome mosaic virus polymerase-like protein 2a is directed to the endoplasmic reticulum by helicase-like viral protein 1a. *J. Virol.* **74**, 4310–4318 (2000).
48. Chen, J., Noueiry, A. & Ahlquist, P. An alternate pathway for recruiting template RNA to the brome mosaic virus RNA replication complex. *J. Virol.* **77**, 2568–2577 (2003).
49. Janda, M. & Ahlquist, P. Brome mosaic virus RNA replication protein 1a dramatically increases *in vivo* stability but not translation of viral genomic RNA3. *Proc. Natl Acad. Sci. USA* **95**, 2227–2232 (1998).
50. Sullivan, M. & Ahlquist, P. *Cis*-acting signals in bromovirus RNA replication and gene expression: networking with viral proteins and host factors. *Semin. Virol.* **8**, 221–230 (1997).
51. Chen, J., Noueiry, A. & Ahlquist, P. Brome mosaic virus protein 1a recruits viral RNA2 to RNA replication through a 5′ proximal RNA2 signal. *J. Virol.* **75**, 3207–3219 (2001).
52. Sullivan, M. & Ahlquist, P. A brome mosaic virus intergenic RNA3 replication signal functions with viral replication protein 1a to dramatically stabilize RNA *in vivo*. *J. Virol.* **73**, 2622–2632 (1999).
53. den Boon, J., Chen, J. & Ahlquist, P. Identification of sequences in brome mosaic virus replicase protein 1a that mediate association with endoplasmic reticulum membranes. *J. Virol.* **75**, 12370–12381 (2001).

54. O'Reilly, E. K., Wang, Z., French, R. & Kao, C. C. Interactions between the structural domains of the RNA replication proteins of plant-infecting RNA viruses. *J. Virol.* **72**, 7160–7169 (1998).
55. Freed, E. O. Viral late domains. *J. Virol.* **76**, 4679–4687 (2002).
56. McMahon, H. T. & Mills, I. G. COP and clathrin-coated vesicle budding: different pathways, common approaches. *Curr. Opin. Cell Biol.* **16**, 379–391 (2004).
57. Morita, E. & Sundquist, W. I. Retrovirus budding. *Annu. Rev. Cell Dev. Biol.* **20**, 395–425 (2004).
58. Lee, J.-Y., Marshall, J. A. & Bowden, D. S. Characterization of rubella virus replication complexes using antibodies to double-stranded RNA. *Virology* **200**, 307–312 (1994).
59. Kujala, P. *et al.* Biogenesis of the Semliki Forest virus RNA replication complex. *J. Virol.* **75**, 3873–3884 (2001).
60. Sethna, P. B. & Brian, D. A. Coronavirus genomic and subgenomic minus-strand RNAs copartition in membrane-protected replication complexes. *J. Virol.* **71**, 7744–7749 (1997).
61. Miyanari, Y. *et al.* Hepatitis C virus non-structural proteins in the probable membranous compartment function in viral genome replication. *J. Biol. Chem.* **278**, 50301–50308 (2003).
62. Quinkert, D., Bartenschlager, R. & Lohmann, V. Quantitative analysis of the hepatitis C virus replication complex. *J. Virol.* **79**, 13594–13605 (2005).
63. Lyle, J. M., Bullitt, E., Bienz, K. & Kirkegaard, K. Visualization and functional analysis of RNA-dependent RNA polymerase lattices. *Science* **296**, 2218–2222 (2002).
Shows that poliovirus RNA polymerase can self-interact in extended networks consistent with RNA replication on membrane surfaces.
64. Panaviene, Z., Panavas, T. & Nagy, P. D. Role of an internal and two 3′-terminal RNA elements in assembly of tombusvirus replicase. *J. Virol.* **79**, 10608–10618 (2005).
65. Salonen, A. *et al.* Properly folded nonstructural polyprotein directs the Semliki Forest virus replication complex to the endosomal compartment. *J. Virol.* **77**, 1691–1702 (2003).
66. Snijder, E. J., van Tol, H., Roos, N. & Pedersen, K. W. Non-structural proteins 2 and 3 interact to modify host cell membranes during the formation of the arterivirus replication complex. *J. Gen. Virol.* **82**, 985–994 (2001).
67. Egger, D. *et al.* Expression of hepatitis C virus proteins induces distinct membrane alterations including a candidate viral replication complex. *J. Virol.* **76**, 5974–5984 (2002).
68. Cho, M. W., Teterina, N., Egger, D., Bienz, K. & Ehrenfeld, E. Membrane rearrangement and vesicle induction by recombinant poliovirus 2C and 2BC in human cells. *Virology* **202**, 129–145 (1994).
69. Teterina, N. L. *et al.* Requirements for assembly of poliovirus replication complexes and negative-strand RNA synthesis. *J. Virol.* **75**, 3841–3850 (2001).
70. Felsenstein, K. M. & Goff, S. P. Expression of the Gag–Pol fusion protein of Moloney murine leukemia virus without Gag protein does not induce virion formation or proteolytic processing. *J. Virol.* **62**, 2179–2182 (1988).
71. Karacostas, V., Wolffe, E. J., Nagashima, K., Gonda, M. A. & Moss, B. Overexpression of the HIV-1 Gag–Pol polyprotein results in intracellular activation of HIV-1 protease and inhibition of assembly and budding of virus-like particles. *Virology* **193**, 661–671 (1993).
72. Panavas, T., Hawkins, C. M., Panaviene, Z. & Nagy, P. D. The role of the p33:p33/p92 interaction domain in RNA replication and intracellular localization of p33 and p92 proteins of Cucumber necrosis tombusvirus. *Virology* **338**, 81–95 (2005).
73. Ishikawa, M., Meshi, T., Motoyoshi, F., Takamatsu, N. & Okada, Y. *In vitro* mutagenesis of the putative replicase genes of tobacco mosaic virus. *Nucleic Acids Res.* **14**, 8291–8305 (1986).
74. Li, G. & Rice, C. M. Mutagenesis of the in-frame opal termination codon preceding nsP4 of Sindbis virus: studies of translational readthrough and its effect on virus replication. *J. Virol.* **63**, 1326–1337 (1989).
75. Noueiry, A. O., Chen, J. & Ahlquist, P. A mutant allele of essential, general translation initiation factor DED1 selectively inhibits translation of a viral mRNA. *Proc. Natl Acad. Sci. USA* **97**, 12985–12990 (2000).
76. Ishikawa, M., Diez, J., Restrepo-Hartwig, M. & Ahlquist, P. Yeast mutations in multiple complementation groups inhibit brome mosaic virus RNA replication and transcription and perturb regulated expression of the viral polymerase-like gene. *Proc. Natl Acad. Sci. USA* **94**, 13810–13815 (1997).
77. Kim, S. H., Palukaitis, P. & Park, Y. I. Phosphorylation of cucumber mosaic virus RNA polymerase 2a protein inhibits formation of replicase complex. *EMBO J.* **21**, 2292–2300 (2002).
78. deGroot, R. J., Rümenapf, T., Kuhn, R. J., Strauss, E. G. & Strauss, J. H. Sindbis virus RNA polymerase is degraded by the N-end rule pathway. *Biochemistry* **88**, 8967–8971 (1991).
79. Hajimorad, M. R. *et al.* Nia and Nib of peanut stripe potyvirus are present in the nucleus of infected cells, but do not form inclusions. *Virology* **224**, 368–379 (1996).
80. Levin, H. L., Weaver, D. C. & Boeke, J. D. Novel gene expression mechanism in a fission yeast retroelement: Tf1 proteins are derived from a single primary translation product. *EMBO J.* **12**, 4885–4895 (1993).
81. Teysset, L., Dang, V. D., Kim, M. K. & Levin, H. L. A long terminal repeat-containing retrotransposon of *Schizosaccharomyces pombe* expresses a Gag-like protein that assembles into virus-like particles which mediate reverse transcription. *J. Virol.* **77**, 5451–5463 (2003).
82. Ganser, B. K., Cheng, A., Sundquist, W. I. & Yeager, M. Three-dimensional structure of the M-MuLV CA protein on a lipid monolayer: a general model for retroviral capsid assembly. *EMBO J.* **22**, 2886–2892 (2003).
83. Westaway, E., Mackenzie, J., Kenney, M., Jones, M. & Khromykh, A. Ultrastructure of Kunjin virus-infected cells: colocalization of NS1 and NS3 with double-stranded RNA, and of NS2B with NS3, in virus-induced membrane structures. *J. Virol.* **71**, 6650–6661 (1997).
84. Schwartz, M., Chen, J., Lee, W. M., Janda, M. & Ahlquist, P. Alternate, virus-induced membrane rearrangements support positive-strand RNA virus genome replication. *Proc. Natl Acad. Sci. USA* **101**, 11263–11268 (2004).
Shows that outwardly distinct membrane rearrangements, similar to those associated with RNA replication by different viruses, can be induced by the same viral replication proteins.
85. Aizaki, H., Lee, K. J., Sung, V. M., Ishiko, H. & Lai, M. M. Characterization of the hepatitis C virus RNA replication complex associated with lipid rafts. *Virology* **324**, 450–461 (2004).
86. Gosert, R., Kanjanahaluethai, A., Egger, D., Bienz, K. & Baker, S. C. RNA replication of mouse hepatitis virus takes place at double-membrane vesicles. *J. Virol.* **76**, 3697–3708 (2002).
87. Schlegel, A., Giddings, J., T., Ladinsky, M. & Kirkegaard, K. Cellular origin and ultrastructure of membranes induced during poliviruis infection. *J. Virol.* **70**, 6576–6588 (1996).
88. Teterina, N. L., Bienz, K., Egger, D., Gorbalenya, A. E. & Ehrenfeld, E. Induction of intracellular membrane rearrangements by HAV proteins 2C and 2BC. *Virology* **237**, 66–77 (1997).
89. Egger, D., Pasamontes, L., Bolten, R., Boyko, V. & Bienz, K. Reversible dissociation of the poliovirus replication complex: functions and interactions of its components in viral RNA synthesis. *J. Virol.* **70**, 8675–8683 (1996).
90. Nibert, M. L. & Schiff, L. A. In *Fields Virology* (eds Knipe, D. M. & Howley, P. M.) 1679–1728 (Lippincott, Williams & Wilkins, Philadelphia, 2001).
91. Patton, J. T. & Spencer, E. Genome replication and packaging of segmented double-stranded RNA viruses. *Virology* **277**, 217–225 (2000).
92. Koonin, E. V., Gorbalenya, A. E. & Chumakov, K. M. Tentative identification of RNA-dependent RNA polymerases of dsRNA viruses and their relationship to positive strand RNA viral polymerases. *FEBS Lett.* **252**, 42–46 (1989).
93. Koonin, E. V., Choi, G. H., Nuss, D. L., Shapira, R. & Carrington, J. C. Evidence for common ancestry of a chestnut blight hypovirulence-associated double-stranded RNA and a group of positive-strand RNA plant viruses. *Proc. Natl Acad. Sci. USA* **88**, 10647–10651 (1991).
94. Reinisch, K. M., Nibert, M. L. & Harrison, S. C. Structure of the reovirus core at 3.6 Å resolution. *Nature* **404**, 960–967 (2000).
95. Zhang, X., Walker, S. B., Chipman, P. R., Nibert, M. L. & Baker, T. S. Reovirus polymerase λ3 localized by cryo-electron microscopy of virions at a resolution of 7.6 Å. *Nature Struct. Biol.* **10**, 1011–1018 (2003).
References 94 and 95 define the structure of transcriptionally active cores of dsRNA reovirus.
96. Gomez de Cedron, M., Ehsani, N., Mikkola, M. L., Garcia, J. A. & Kaariainen, L. RNA helicase activity of Semliki Forest virus replicase protein NSP2. *FEBS Lett.* **448**, 19–22 (1999).
97. Vasiljeva, L., Merits, A., Auvinen, P. & Kaariainen, L. Identification of a novel function of the alphavirus capping apparatus. RNA 5′-triphosphatase activity of Nsp2. *J. Biol. Chem.* **275**, 17281–17287 (2000).
98. Li, Y. I. *et al.* The helicase-like domain of plant potexvirus replicase participates in formation of RNA 5′ cap structure by exhibiting RNA 5′-triphosphatase activity. *J. Virol.* **75**, 12114–12120 (2001).
99. Wang, X. *et al.* Brome mosaic virus 1a nucleoside triphosphatase/helicase domain plays crucial roles in recruiting RNA replication templates. *J. Virol.* **79**, 13747–13758 (2005).
100. Bisaillon, M., Bergeron, J. & Lemay, G. Characterization of the nucleoside triphosphate phosphohydrolase and helicase activities of the reovirus λ1 protein. *J. Biol. Chem.* **272**, 18298–18303 (1997).
101. Bisaillon, M. & Lemay, G. Characterization of the reovirus λ1 protein RNA 5′-triphosphatase activity. *J. Biol. Chem.* **272**, 29954–29957 (1997).
102. Kao, C. C., Quadt, R., Hershberger, R. P. & Ahlquist, P. Brome mosaic virus RNA replication proteins 1a and 2a form a complex *in vitro*. *J. Virol.* **66**, 6322–6329 (1992).
103. Luongo, C. L., Contreras, C. M., Farsetta, D. L. & Nibert, M. L. Binding site for *S*-adenosyl-L-methionine in a central region of mammalian reovirus λ2 protein. Evidence for activities in mRNA cap methylation. *J. Biol. Chem.* **273**, 23773–23780 (1998).
104. Luongo, C. L., Reinisch, K. M., Harrison, S. C. & Nibert, M. L. Identification of the guanylyltransferase region and active site in reovirus mRNA capping protein λ2. *J. Biol. Chem.* **275**, 2804–2810 (2000).
105. Li, Y. I., Chen, Y. J., Hsu, Y. H. & Meng, M. Characterization of the AdoMet-dependent guanylyltransferase activity that is associated with the N terminus of bamboo mosaic virus replicase. *J. Virol.* **75**, 782–788 (2001).
106. Pirttimaa, M. J., Paatero, A. O., Frilander, M. J. & Bamford, D. H. Nonspecific nucleoside triphosphatase P4 of double-stranded RNA bacteriophage φ6 is required for single-stranded RNA packaging and transcription. *J. Virol.* **76**, 10122–10127 (2002).
107. Kainov, D. E. *et al.* RNA packaging device of double-stranded RNA bacteriophages, possibly as simple as hexamer of P4 protein. *J. Biol. Chem.* **278**, 48084–48091 (2003).
108. Goregaoker, S. P. & Culver, J. N. Oligomerization and activity of the helicase domain of the tobacco mosaic virus 126- and 183-kilodalton replicase proteins. *J. Virol.* **77**, 3549–3556 (2003).
109. Jayaram, H., Taraporewala, Z., Patton, J. T. & Prasad, B. V. Rotavirus protein involved in genome replication and packaging exhibits a HIT-like fold. *Nature* **417**, 311–315 (2002).
110. Taraporewala, Z. F. & Patton, J. T. Nonstructural proteins involved in genome packaging and replication of rotaviruses and other members of the *Reoviridae*. *Virus Res.* **101**, 57–66 (2004).
111. Kim, J., Parker, J. S., Murray, K. E. & Nibert, M. L. Nucleoside and RNA triphosphatase activities of orthoreovirus transcriptase cofactor μ2. *J. Biol. Chem.* **279**, 4394–4403 (2004).
112. Kroner, P. A., Young, B. M. & Ahlquist, P. Analysis of the role of brome mosaic virus 1a protein domains in RNA replication, using linker insertion mutagenesis. *J. Virol.* **64**, 6110–6120 (1990).
113. Ishikawa, M., Kroner, P., Ahlquist, P. & Meshi, T. Biological activities of hybrid RNAs generated by 3′-end exchanges between tobacco mosaic and brome mosaic viruses. *J. Virol.* **65**, 3451–3459 (1991).
114. Ahlquist, P. RNA-dependent RNA polymerases, viruses, and RNA silencing. *Science* **296**, 1270–1273 (2002).
115. Silvestri, L. S., Taraporewala, Z. F. & Patton, J. T. Rotavirus replication: plus-sense templates for double-stranded RNA synthesis are made in viroplasms. *J. Virol.* **78**, 7763–7774 (2004).
116. Gitlin, L., Stone, J. K. & Andino, R. Poliovirus escape from RNA interference: short interfering RNA-target recognition and implications for therapeutic approaches. *J. Virol.* **79**, 1027–1035 (2005).

117. Ishikawa, M., Meshi, T., Ohno, T. & Okada, Y. Specific cessation of minus-strand RNA accumulation at an early stage of tobacco mosaic virus infection. *J. Virol.* **65**, 861–868 (1991).
118. Strauss, J. H. & Strauss, E. G. The alphaviruses: gene expression, replication, and evolution. *Microbiol. Rev.* **58**, 491–562 (1994).
119. Wengler, G., Wengler, G. & Gross, H. J. Terminal sequences of Sindbis virus-specific nucleic acids: identity in molecules synthesized in vertebrate and insect cells and characteristic properties of the replicative form RNA. *Virology* **123**, 273–283 (1982).
120. Collmer, C. W. & Kaper, J. M. Double-stranded RNAs of cucumber mosaic virus and its satellite contain an unpaired terminal guanosine: implications for replication. *Virology* **145**, 249–259 (1985).
121. Diprose, J. M. *et al.* Translocation portals for the substrates and products of a viral transcription complex: the bluetongue virus core. *EMBO J.* **20**, 7229–7239 (2001).
122. Hansen, J., Long, A. & Schultz, S. Structure of the RNA-dependent RNA polymerase of poliovirus. *Structure* **5**, 1109–1122 (1997).
123. Lesburg, C. A. *et al.* Crystal structure of the RNA-dependent RNA polymerase from hepatitis C virus reveals a fully encircled active site. *Nature Struct. Biol.* **6**, 937–943 (1999).
124. Siegel, R. W., Bellon, L., Beigelman, L. & Kao, C. C. Use of DNA, RNA, and chimeric templates by a viral RNA-dependent RNA polymerase: evolutionary implications for the transition from the RNA to the DNA world. *J. Virol.* **73**, 6424–6429 (1999). **Shows that a (+)RNA-virus RNA-dependent RNA polymerase has substantial activity on DNA templates.**
125. Gao, G., Orlova, M., Georgiadis, M. M., Hendrickson, W. A. & Goff, S. P. Conferring RNA polymerase activity to a DNA polymerase: a single residue in reverse transcriptase controls substrate selection. *Proc. Natl Acad. Sci. USA* **94**, 407–411 (1997).
126. Rolls, M. M., Webster, P., Balba, N. H. & Rose, J. K. Novel infectious particles generated by expression of the vesicular stomatitis virus glycoprotein from a self-replicating RNA. *Cell* **79**, 497–506 (1994).
127. Lai, M. M. RNA recombination in animal and plant viruses. *Microbiol. Rev.* **56**, 61–79 (1992).
128. Nagy, P. D. & Simon, A. E. New insights into the mechanisms of RNA recombination. *Virology* **235**, 1–9 (1997).
129. Worobey, M. & Holmes, E. C. Evolutionary aspects of recombination in RNA viruses. *J. Gen. Virol.* **80**, 2535–2543 (1999).
130. Ahlquist, P. *et al.* Viral and host determinants of RNA virus vector replication and expression. *Vaccine* **23**, 1784–1787 (2005).
131. Estes, M. K. in *Fields Virology* (eds Knipe, D. M. & Howley, P. M.) 1747–1785 (Lippincott, Williams & Wilkins, Philadelphia, 2001).
132. Lopez, T. *et al.* Silencing the morphogenesis of rotavirus. *J. Virol.* **79**, 184–192 (2005).
133. Silvestri, L. S., Tortorici, M. A., Vasquez-Del Carpio, R. & Patton, J. T. Rotavirus glycoprotein NSP4 is a modulator of viral transcription in the infected cell. *J. Virol.* **79**, 15165–15174 (2005). **References 132 and 133 reveal links between rotavirus transmembrane protein nsP4 and formation of viroplasms in which dsRNA virion-core assembly occurs.**
134. Laurinavicius, S., Kakela, R., Bamford, D. H. & Somerharju, P. The origin of phospholipids of the enveloped bacteriophage ϕ6. *Virology* **326**, 182–190 (2004).
135. Lee, W. M., Ishikawa, M. & Ahlquist, P. Mutation of host Δ9 fatty acid desaturase inhibits brome mosaic virus RNA replication between template recognition and RNA synthesis. *J. Virol.* **75**, 2097–2106 (2001).
136. Lee, W. M. & Ahlquist, P. Membrane synthesis, specific lipid requirements, and localized lipid composition changes associated with a positive-strand RNA virus RNA replication protein. *J. Virol.* **77**, 12819–12828 (2003).
137. Ono, A. & Freed, E. O. Plasma membrane rafts play a critical role in HIV-1 assembly and release. *Proc. Natl Acad. Sci. USA* **98**, 13925–13930 (2001).
138. Kushner, D. B. *et al.* Systematic, genome-wide identification of host genes affecting replication of a positive-strand RNA virus. *Proc. Natl Acad. Sci. USA* **100**, 15764–15769 (2003).
139. Hu, J., Toft, D. O. & Seeger, C. Hepadnavirus assembly and reverse transcription require a multi-component chaperone complex which is incorporated into nucleocapsids. *EMBO J.* **16**, 59–68 (1997).
140. Tomita, Y. *et al.* Mutation of host *dnaJ* homolog inhibits brome mosaic virus negative-strand RNA synthesis. *J. Virol.* **77**, 2990–2997 (2003).
141. Held, D. M., Kissel, J. D., Patterson, J. T., Nickens, D. G. & Burke, D. H. HIV-1 inactivation by nucleic acid aptamers. *Front. Biosci.* **11**, 89–112 (2006).
142. Resh, M. D. Intracellular trafficking of HIV-1 Gag: how Gag interacts with cell membranes and makes viral particles. *AIDS Rev.* **7**, 84–91 (2005).
143. Khromykh, A. A., Kondratieva, N., Sgro, J. Y., Palmenberg, A. & Westaway, E. G. Significance in replication of the terminal nucleotides of the flavivirus genome. *J. Virol.* **77**, 10623–10629 (2003).
144. Yang, H., Makeyev, E. V., Butcher, S. J., Gaidelyte, A. & Bamford, D. H. Two distinct mechanisms ensure transcriptional polarity in double-stranded RNA bacteriophages. *J. Virol.* **77**, 1195–1203 (2003).
145. Wickner, R. B. Double-stranded RNA viruses of *Saccharomyces cerevisiae*. *Microbiol. Rev.* **60**, 250–265 (1996).

Acknowledgements
We thank all members of our laboratory for helpful discussions. This work was supported by the National Institutes of Health.

Competing interests statement
The author declares no competing financial interests.

DATABASES
The following terms in this article are linked online to:
Entrez Genome: http://www.ncbi.nlm.nih.gov/entrez/query.fcgi?db=genome
hepatitis C virus | HIV | poliovirus | RNA1 | RNA2 | RNA3 | tobacco mosaic virus | vesicular stomatitis virus
UniProtKB: http://ca.expasy.org/sprot
1a | 2a^{pol} | λ1 | λ2 | λ3 | P4

FURTHER INFORMATION
Paul Ahlquist's homepage: http://mcardle.oncology.wisc.edu/faculty/bio/ahlquist_p.html
Access to this links box is available online.

JOURNAL OF VIROLOGY, Mar. 2001, p. 2097–2106 Vol. 75, No. 5
0022-538X/01/$04.00+0 DOI: 10.1128/JVI.75.5.2097–2106.2001

Mutation of Host Δ9 Fatty Acid Desaturase Inhibits Brome Mosaic Virus RNA Replication between Template Recognition and RNA Synthesis

WAI-MING LEE,[1,2] MASAYUKI ISHIKAWA,[2] AND PAUL AHLQUIST[1,2]*

Howard Hughes Medical Institute[1] and Institute for Molecular Virology,[2] University of Wisconsin—Madison, Madison, Wisconsin 53706

Received 18 July 2000/Accepted 30 November 2000

All positive-strand RNA viruses assemble their RNA replication complexes on intracellular membranes. Brome mosaic virus (BMV) replicates its RNA in endoplasmic reticulum (ER)-associated complexes in plant cells and the yeast *Saccharomyces cerevisiae*. BMV encodes RNA replication factors 1a, with domains implicated in RNA capping and helicase functions, and 2a, with a central polymerase-like domain. Factor 1a interacts independently with the ER membrane, viral RNA templates, and factor 2a to form RNA replication complexes on the perinuclear ER. We show that BMV RNA replication is severely inhibited by a mutation in *OLE1*, an essential yeast chromosomal gene encoding Δ9 fatty acid desaturase, an integral ER membrane protein and the first enzyme in unsaturated fatty acid synthesis. *OLE1* deletion and medium supplementation show that BMV RNA replication requires unsaturated fatty acids, not the Ole1 protein, and that viral RNA replication is much more sensitive than yeast growth to reduced unsaturated fatty acid levels. In *ole1* mutant yeast, 1a still becomes membrane associated, recruits 2a to the membrane, and recognizes and stabilizes viral RNA templates normally. However, RNA replication is blocked prior to initiation of negative-strand RNA synthesis. The results show that viral RNA synthesis is highly sensitive to lipid composition and suggest that proper membrane fluidity or plasticity is essential for an early step in RNA replication. The strong unsaturated fatty acid dependence also demonstrates that modulating fatty acid balance can be an effective antiviral strategy.

All positive-strand RNA viruses of eukaryotes studied to date have RNA replication complexes localized to intracellular membranes, often in association with infection-specific membrane proliferation and or vesiculation (28, 29, 38, 39, 41). Multiple results indicate that membrane association is important for viral RNA synthesis. In vitro synthesis of positive-strand RNAs of picornaviruses and nodaviruses depends on membranes (31, 48). Activation of the alphavirus Semliki Forest virus (SFV) RNA-capping enzyme requires lipids with anionic head groups (3). Cerulenin, an inhibitor of lipid synthesis, inhibits RNA replication by poliovirus and SFV (16, 34). Brefeldin A, an inhibitor of secretory vesicle formation, severely inhibits RNA replication by poliovirus and rhinovirus, though not by some other picornaviruses (11, 20, 30). Despite these results, the nature and function of membrane association in positive-strand RNA virus replication remain poorly understood.

Brome mosaic virus (BMV) is a representative member of the alphavirus-like superfamily of human, animal, and plant positive-strand RNA viruses. The BMV genome is composed of three RNAs. RNA1 and RNA2 respectively encode 1a and 2a, the only BMV proteins required for RNA replication. 1a and 2a interact (25) and contain three domains conserved with those of other superfamily members. 1a contains an N-terminal domain with m^7G methyltransferase and m^7GMP covalent binding activities required for capping viral RNA in vivo (1, 26) and a C-terminal DEAD box RNA helicase domain. 2a contains a central polymerase-like domain. 1a directs itself and 2a to the endoplasmic reticulum (ER) membrane to form replication complexes that colocalize with viral RNA synthesis (7, 37, 38). RNA3 encodes a cell-to-cell movement protein (3a) and the coat protein, which are dispensable for RNA replication. The 3′-end-proximal coat protein gene is not translatable from RNA3 but only from a subgenomic mRNA, RNA4, synthesized from negative-strand RNA3 (Fig. 1).

As well as in BMV's natural plant hosts, 1a and 2a direct RNA3 replication and subgenomic mRNA synthesis in the yeast *Saccharomyces cerevisiae* (24). This yeast system reproduces all known features of BMV RNA replication in plant cells, including localization of replication complexes to the perinuclear ER (7, 37). When RNA3 or its derivatives are introduced by transfection or in vivo DNA-dependent transcription into yeast expressing 1a and 2a, negative-strand RNA3 is synthesized and used as a template for RNA-directed synthesis of more positive-strand RNA3 and subgenomic mRNA to express the coat protein gene or its replacements (Fig. 1A). Replacing the coat gene with suitable reporter genes thus provides colony-selectable or -screenable phenotypes linked to BMV RNA replication (22, 24).

To identify cellular factors and functions required for BMV RNA replication, we screened for yeast mutants with defects in their support of BMV-directed gene expression. Here we describe the isolation and characterization of one such yeast mutant, herein designated *ole1w* yeast, which inhibited BMV RNA replication by more than 95%. The affected *OLE1* gene encodes an integral ER membrane protein, Δ9 fatty acid desaturase, essential for conversion of saturated fatty acids

* Corresponding author. Mailing address: Institute for Molecular Virology, University of Wisconsin—Madison, 1525 Linden Dr., Madison, WI 53706-1596. Phone: (608) 263-5916. Fax: (608) 265-9214. E-mail: ahlquist@facstaff.wisc.edu.

EXHIBIT A

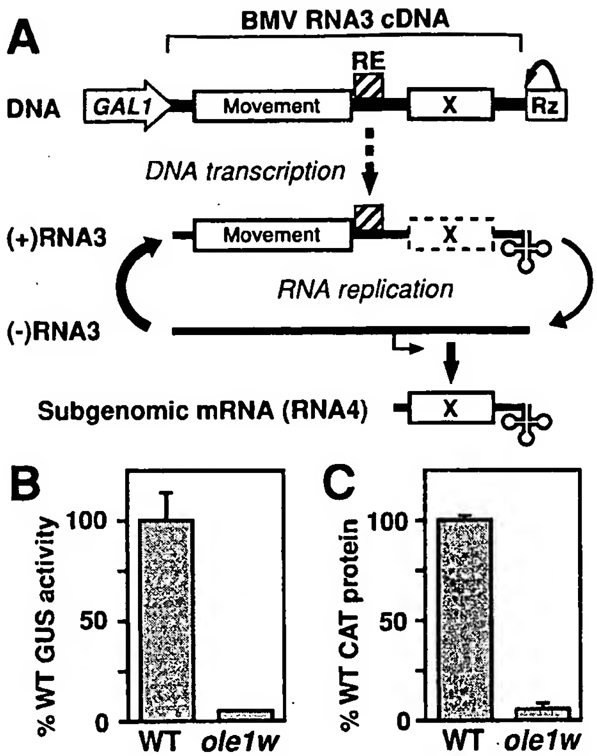

FIG. 1. (A) Pathway for initiating BMV-directed, RNA-dependent RNA replication and subgenomic mRNA synthesis from DNA. (Top) cDNA-based RNA3 launching cassette including BMV noncoding regions (single lines), movement protein gene, intergenic replication enhancer (RE), 5′-end-flanking *GAL1* promoter, and 3′-end-flanking hepatitis delta virus ribozyme (Rz). ORF X represents the BMV coat gene or its replacements, *URA3*, GUS, or CAT. On galactose induction, cellular RNA polymerase II synthesizes positive-strand RNA3 transcripts that serve as the templates for 1a- and 2a-directed RNA3 replication and subgenomic mRNA (RNA4) synthesis required to express the coat protein gene or its replacements. The bent arrow below negative-strand RNA3 represents the RNA4 start site. (B) BMV-directed GUS expression in wt YMI04 and mutant *ole1w* yeast. Yeast cells were grown in Gal-containing liquid medium for 48 h, and GUS activity per milligram of total protein was measured. Averages and standard deviations from three independent cultures of each yeast are shown. (C) BMV-directed CAT expression in wt YMI04 and mutant *ole1w* yeast transfected with B3CAT in vitro transcripts. Transfected spheroplasts were incubated 12 h in Gal medium, and CAT expression per milligram of total protein was measured. Data are presented as in panel B.

(SFAs) to unsaturated fatty acids (UFAs) (44, 45). These UFAs are incorporated into membrane lipids and are major determinants of membrane fluidity and plasticity (10, 36, 40, 42, 47). We found that the *OLE1* protein was not required for BMV RNA replication but that one or more steps between template recognition and initiation of viral RNA synthesis required UFAs at levels far above those required for yeast growth. Thus, the *ole1* mutation reveals linkage between lipid composition and specific early steps in viral RNA replication. Through its ability to block RNA replication at a particular step, the *ole1* mutation should be valuable for further study of RNA synthesis initiation and the membrane association of RNA replication. These results also suggest new directions for antiviral strategies.

MATERIALS AND METHODS

Plasmids. Yeast 2μm plasmids, pB1CT19 (*HIS3* marker gene) and pB2CT15 (*LEU2* marker) (24), and centromeric plasmids, pB1YT3H (*HIS3* marker) and pB2YT5 (*LEU2* marker) (7), were used to express 1a and 2a from the *ADH1* and *GAL1* promoters, respectively. pB1YT3H was made by substituting the *HIS3* gene for the *URA3* gene in pB1YT3 (Y. Tomita and M. Ishikawa, unpublished results), a yeast centromeric plasmid with the 1a open reading frame (ORF) linked to the *GAL1* promoter. All plasmids expressing RNA3 or its derivatives were derived from pB3RQ39, a centromeric plasmid with the *TRP1* marker gene, as described previously (22). A yeast genomic DNA library, ATCC 77164, containing yeast strain YPH1 genomic DNA fragments (average size, 8.8 kb) in the centromeric vector pRS200 (*TRP1* marker) (18) was used to identify the complementing gene. The *ole1w* mutation was isolated by using the gap repair method (12) to clone an *Hpa*I-*Pac*I DNA fragment containing the first 90% of the *OLE1* ORF and 220 bp of 5′ noncoding sequence (Fig. 2B) from the mutant yeast into the vector pRS200. DNA sequencing was performed at the Automated DNA Sequencing Facility, University of Wisconsin Biotechnology Center.

Yeast strains, cell growth, and transformation. Yeast strain YPH500 (*MAT*α *ura3-52 lys2-801 ade2-101 tyr1-63 his3-200 leu2-1*) and its derivatives (21) were used throughout, except that YM106, a derivative of YPH499 (*MAT*a *ura3-52 lys2-801 ade2-101 trp1-63 his3-200 leu2-1*), (21) was used for mating. YM104, the parental strain for mutant isolation, was a YPH500 derivative containing chromosomally integrated B3URA3 and B3GUS expression cassettes and plasmids pB1CT19 and pB2CT15. *ole1*Δ::*URA3* yeast was constructed by integrative transformation (12) of YM104 with the *Nhe*I-*Bsr*GI fragment of Fig. 2B with the *Eco*NI-*Pac*I fragment, containing 400 bp of the 5′ noncoding sequence and 90% of the *OLE1* ORF, replaced by the transcriptionally active *URA3* gene. The isogenic strains $ole1w_i$ and $ole1w_i'$ were constructed by integrative transformation of the *Nhe*I-*Bsr*GI fragment (Fig. 2B) containing the *ole1w* mutation into, respectively, *ole1*Δ::*URA3* and an equivalent *ole1*Δ::*URA3* derivative of YPH500. Correct integration was verified by Southern blot analysis.

Yeast cultures were grown at 30°C until mid-logarithmic phase (optical density at 600 nm = 0.5 to 0.7) in defined synthetic medium with relevant amino acids omitted to maintain selection for plasmids as described previously (22). Yeast cell pellets, harvested by low-speed centrifugation, were stored at −70°C until RNA or protein extraction. Tergitol Nonidet P-40 (1%) was added to the medium to solubilize fatty acids (44). Plasmid transformation was performed with a FROZEN-EZ yeast transformation kit (Zymo Research).

RNA transfection. Capped in vitro RNA transcripts of B3CAT were synthesized from pB3CA101, spheroplasts were prepared from yeast grown for 24 h in Gal medium, and RNA transfections were performed as described previously (24).

GUS and CAT assays. β-Glucuronidase (GUS) filter lifts and quantitative assays were performed as described previously (22). For chloramphenicol acetyltransferase (CAT) assays, yeast lysate was prepared as for the quantitative GUS assay but a different extraction buffer (50 mM Tris [pH 7.5], 5 mM EDTA, 0.1% *N*-lauroylsarcosine, 0.1% Triton X-100, and 1× protease inhibitors [0.5 mM phenylmethylsulfonyl fluoride, 2.5 mM benzamidine, 1 μg of pepstatin A per ml, and 2.5 μg each of aprotinin and leupeptin per ml]) was used. CAT protein levels were measured with a CAT enzyme-linked immunosorbent assay kit (Boehringer Mannheim), and total protein was determined with a Bradford protein assay kit (Bio-Rad) using bovine serum albumin as a concentration standard.

Western blotting. Protein was prepared as for the CAT assays except that the extraction buffer was augmented with 20 mM 2-mercaptoethanol and a 2X solution of the protease inhibitors and the clarified cell lysate was supplemented with 1% sodium dodecyl sulfate and boiled for 5 min to inactivate the proteases. Total protein of each cell lysate was determined by a sodium dodecyl sulfate-tolerant Bio-Rad DC Protein Assay (Lowry assay). Equal amounts of total protein were electrophoresed and transferred to nylon membrane. 1a and 2a proteins were probed with corresponding antibodies and detected by chemiluminescence (38).

Northern blotting. Total yeast RNA isolation, RNA concentration determination by absorbance at 260 nm, agarose-formaldehyde gel electrophoresis, and transfer to nylon membrane were performed as described previously (4, 24). Positive-strand RNA3 and RNA4 were detected with a ^{32}P-labeled RNA probe complementary to their 3′ 200 bases. Negative-strand RNA3 was detected with a ^{32}P-labeled RNA probe corresponding to the CAT gene (for B3CAT) or coat gene (for B3 and B3CP^{fs}) coding sequence (24). Radioactive signals were measured with a Molecular Dynamics PhosphorImager.

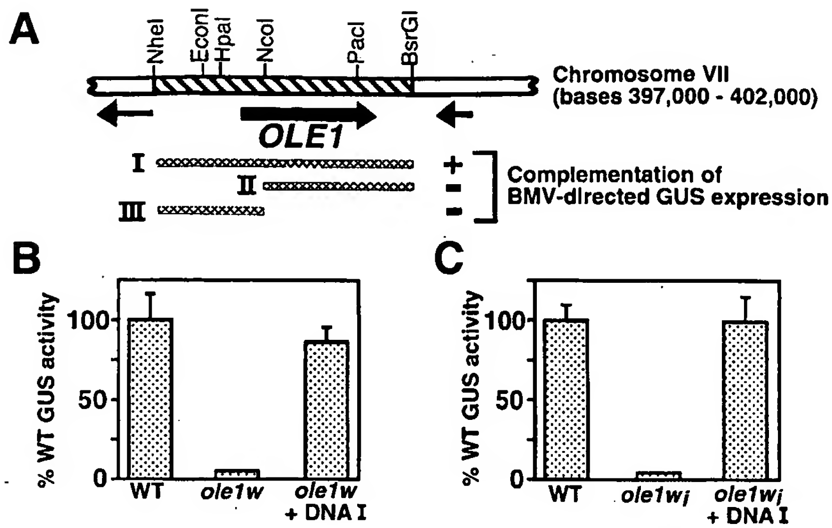

FIG. 2. (A) Schematic of a 5-kb region of yeast chromosome VII containing the *OLE1* ORF (thick arrow), showing 2.9-kb fragment I, which complements BMV-directed GUS expression in *ole1w* yeast, and noncomplementing fragments II and III. Arrows show flanking ORFs. (B) Complementation of BMV-directed GUS expression in *ole1w* yeast by fragment I of panel A. wt and *ole1w* yeast cells were transformed with the yeast centromeric plasmid pRS200 carrying fragment I or with the empty plasmid vector. Transformants were grown, and GUS activity was measured as described in the legend to Fig. 1B. (C) The isogenic strain *ole1w*$_i$, constructed by replacing the *OLE1* gene in wt YM104 with the *ole1w* gene from mutant yeast, reproduced the phenotype of the original *ole1w* mutant.

RESULTS

Isolation of a yeast mutant strongly inhibiting BMV-directed gene expression. To isolate mutants with a reduced ability to support BMV-directed gene expression, we used yeast strain YM104 (21). YM104 contains plasmids expressing BMV 1a and 2a from the constitutive *ADH1* promoter and chromosomally integrated cassettes expressing B3URA3 and B3GUS from the galactose (Gal)-inducible *GAL1* promoter. B3URA3 and B3GUS are BMV RNA3 derivatives with the coat gene replaced by the *URA3* and GUS genes, respectively. *URA3* or GUS expression requires both Gal to induce B3URA3 and B3GUS transcription and BMV 1a- and 2a-directed RNA replication and subgenomic mRNA synthesis (Fig. 1A).

To isolate mutants, UV-mutagenized YM104 yeast cells were plated on Gal medium containing 0.1% 5-fluoroorotic acid to select against cells with BMV-directed *URA3* expression. After 5 to 7 days, about 0.1% of the plated cells developed into colonies. Six thousand such colonies were examined for BMV-expressed GUS activity by filter lift assays. Three hundred isolates with blue color development lacking or delayed relative to that of wild-type (wt) YM104 were selected and mated with YM106, which contained no BMV sequences and had the mating type (*MAT*a) opposite to that of YM104 (*MAT*α). Of the resulting 300 diploids, 100 showed restored GUS activity, implying that inhibition of BMV-directed GUS expression in the corresponding YM104-derived parental haploids was due to recessive yeast chromosomal mutations complemented by the YM106 genome. One such Gus$^-$ haploid isolate, in which BMV-directed GUS expression was reduced 20-fold, was chosen for further analysis. Complementation experiments showed that this mutation was independent of the previously described BMV-inhibiting yeast mutations *mab1*, *-2*, and *-3* (21).

This original mutant strain is herein designated *ole1w* yeast because, as shown below, the causal mutation that inhibits BMV RNA replication maps to the yeast *OLE1* gene. *w* is an allele designation to distinguish this mutation from other *ole1* mutations. *ole1w* yeast grew normally. Its doubling time in defined Gal medium, about 5 h, paralleled that of wt YM104 yeast. Nevertheless, BMV-directed gene expression was strongly inhibited: GUS activity per milligram of total protein in extracts of *ole1w* yeast averaged 5% of that of wt YM104 yeast (Fig. 1B). To determine if this inhibition was due to defective DNA-directed transcription or nucleocytoplasmic transport of B3GUS RNA3, these nuclear steps were bypassed by transfecting *ole1w* yeast with in vitro transcripts of B3CAT, an RNA3 derivative with the coat gene replaced by the CAT gene. Since the ratio of CAT expression in *ole1w* yeast to that in wt yeast was equal to that for GUS (Fig. 1B to C), cytoplasmic steps of BMV RNA synthesis must be inhibited in *ole1w* yeast.

The yeast *OLE1* gene complements the mutant defect in BMV-directed gene expression. To identify genes able to complement this recessive defect in supporting BMV-directed gene expression, *ole1w* yeast cells were transformed with a yeast genomic DNA library carried by the shuttle vector pRS200, which bears the yeast *TRP1* gene (18). Of 20,000 transformants screened by filter lift assays for BMV-directed GUS activity, 5 reproducibly showed wt blue color development. From each of these transformants, a pRS200-based plasmid was isolated by its ability to permit *E. coli* auxotrophic strain KC8 to grow on medium lacking tryptophan (4). Each of these plasmids complemented the *ole1w* mutation when it was retransformed into

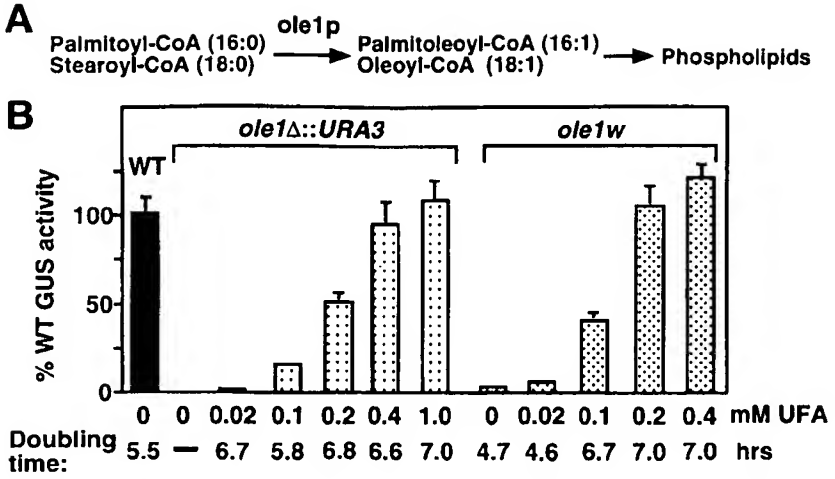

FIG. 3. (A) Pathway of unsaturated fatty acid synthesis and incorporation into membrane phospholipids. Ole1p, Δ9 fatty acid desaturase, synthesizes palmitoleoyl coenzyme A (CoA) and oleoyl-CoA by introducing a double bond between C-9 and C-10 of palmitoyl-CoA and stearoyl-CoA, respectively. (B) UFAs restore BMV-directed GUS expression in yeast lacking *OLE1* (*ole1*Δ::*URA3*) and *ole1w* yeast. wt YMI04, *ole1*Δ::*URA3*, and *ole1w* yeast cells were grown in defined Gal media containing the indicated amounts of UFA (an equimolar mixture of palmitoleic and oleic acids; see Results) until mid-log phase. GUS activity was measured as described in the legend to Fig. 1B. Cell doubling time was calculated from the increase in A_{600} during log-phase growth.

ole1w yeast. Sequencing both ends of the yeast genomic DNA in these plasmids revealed two overlapping fragments of yeast chromosome VII: bases 397187 to 406757 and bases 398499 to 407045. The 8.25-kb region common to both fragments contained five ORFs of 100 or more codons and two tRNA genes.

By deletion mapping and filter lift assays for BMV-directed GUS activity, complementing activity was assigned to a 2.9-kb *Nhe*I-*Bsr*GI fragment containing only the *OLE1* ORF (Fig. 2A). When transformed into *ole1w* yeast, this fragment restored BMV-directed GUS expression to wt levels (Fig. 2B). Moreover, the complete *OLE1* gene was required for full complementation (Fig. 2A).

To determine whether *OLE1* was the originally mutated gene or an extragenic suppressor, the *ole1w* gene was cloned from the mutant yeast by gap repair and used to replace the *OLE1* gene in wt YMI04 yeast by integrative transformation. The resulting *ole1w*$_i$ isogenic strain reproduced the original *ole1w* mutant phenotype, inhibiting BMV-directed GUS expression to 5% of that of the wt, and this phenotype was suppressed by a plasmid bearing the wt *OLE1* gene (Fig. 2C).

To identify the causal mutation in the *ole1w* allele, restriction fragments were exchanged between the mutant and wt *OLE1* genes and the recombinant plasmids were tested for the ability to complement *ole1w* yeast. The mutant phenotype was mapped to a 280-bp DNA fragment encoding Arg_{167}-Leu_{262} of the *OLE1*-encoded protein, Ole1p. DNA sequencing of this region in the wt and mutant genes revealed a single A-to-G substitution, causing a Tyr_{212} (TAT)-to-Cys (TGT) substitution in Ole1p.

UFAs restore BMV-directed gene expression in *ole1w* and *ole1*Δ yeast. Ole1p is the Δ9 fatty acid desaturase, a 510-amino-acid (57-kDa) integral ER membrane protein that converts saturated palmitic (16:0) and stearic (18:0) acids into unsaturated palmitoleic (16:1) and oleic (18:1) acids (Fig. 3A). These UFAs exist in yeast cells primarily (>95% of the time) as acyl chains of membrane phospholipids and are important determinants of membrane fluidity and other physical properties. Transcriptional and posttranscriptional regulation of *OLE1* by UFAs, SFAs, and other conditions are largely responsible for regulating the UFA/SFA ratio and thus membrane fluidity (9, 17). As the only enzyme converting SFAs to UFAs, *OLE1* is essential for yeast growth in media lacking UFAs (44). Δ9 fatty acid desaturase is also the rate-limiting, initial enzyme for UFA synthesis in animals (32).

Because BMV RNA synthesis is also associated with yeast ER membranes (37), the function and localization of Ole1p suggested two possible explanations for the inhibition of BMV-directed gene expression in mutant yeast. First, the *ole1w* mutation might alter the level of UFAs in yeast membranes, which might inhibit BMV RNA replication, subgenomic mRNA synthesis, or both through effects on membrane fluidity or other physical properties. In keeping with this hypothesis, the *ole1w* mutation (Tyr_{212} to Cys) is located in the predicted catalytic domain of Ole1p (45). Alternatively, Ole1p itself, as an integral membrane protein, may be required as an anchor for the BMV RNA replication complex on the ER.

To determine whether BMV-directed gene expression required Ole1p itself or only UFAs, we used integrative transformation to delete the *OLE1* ORF of wt YMI04 yeast and replace it with the *URA3* gene, creating *ole1*Δ::*URA3* yeast. As expected, *ole1*Δ::*URA3* yeast was unable to grow in medium lacking UFAs (Fig. 3B). The growth of *ole1*Δ::*URA3* yeast and its ability to support BMV-directed gene expression were then tested in medium supplemented with increasing amounts of UFA. UFA was provided as an equimolar mixture of the Ole1p products palmitoleic and oleic acids, which results in a cellular fatty acid composition similar to that in unsupplemented wt yeast (6). UFA (0.02 to 0.1 mM) was sufficient to restore *ole1*Δ::*URA3* yeast to growth with a wt doubling time, but BMV-directed GUS expression remained inhibited to 5 to

EXHIBIT A

15% of wt levels (Fig. 3B). Higher UFA levels progressively improved BMV-directed GUS expression, with nearly wt levels being restored by 0.4 mM UFA. Thus, UFAs but not Ole1p were important for BMV-directed GUS expression. The ability of *ole1* mutant yeast to grow with substantially reduced UFA levels is consistent with the finding that UFA levels in wt yeast membranes are five- to ninefold higher than required for growth under optimal conditions (19, 44). The excess UFA is thought to provide extra membrane fluidity required to adapt to environmental changes such as a fall in temperature. Consistent with this, *ole1w* and $ole1w_i$ yeast lost viability within a few days in storage at 4°C while wt yeast was stable for several weeks.

Supplementing the original *ole1w* yeast with UFAs also restored BMV-directed GUS expression (Fig. 3B), implying that the original mutant phenotype was caused by reduced desaturase activity. *ole1w* yeast required less UFA supplementation than its $ole1\Delta$::*URA3* counterpart to restore a similar level of BMV-directed GUS expression. This finding is consistent with the fact that *ole1w* yeast cells were isolated and grow normally on defined medium lacking UFAs (see above) and so must retain sufficient desaturase activity for cell growth. When either *ole1* mutant was grown in high levels of UFA, some increase in doubling time was noted. However, a similar result was seen with wt yeast and mild inhibitory effects of UFAs on yeast growth have been reported previously (49).

1a and 2a protein accumulation and membrane association in mutant yeast. To facilitate the viral RNA accumulation experiments described below, we made an additional isogenic yeast strain, $ole1w_i'$, bearing the *ole1w* allele but lacking the chromosomally integrated B3URA3 and B3GUS expression cassettes of YMI04 and $ole1w_i$. This $ole1w_i'$ strain allowed study of wt RNA3 and RNA3 derivatives introduced on plasmids, while avoiding interference from B3URA3 and B3GUS RNAs in Northern blot analysis of BMV RNA replication products. The initial BMV RNA template used was B3CAT, which combines an easily assayed reporter gene with higher accumulations of BMV RNA replication products than are found with B3GUS.

wt and $ole1w_i'$ yeast were transformed with plasmids expressing B3CAT, 1a, and 2a. With *ADH1*-expressed 1a and 2a, $ole1w_i'$ yeast showed wt 1a protein accumulation and slightly reduced 2a protein accumulation (Fig. 4A, lanes 1 to 3). Since 2a levels can be reduced substantially without inhibiting BMV RNA replication (13), it was unclear if this reduction contributed to the *ole1w* RNA replication phenotype. To resolve this, we tested plasmids expressing 1a and 2a from the *GAL1* promoter which yield higher levels of and more stable 1a and 2a expression in yeast (12). As intended, *GAL1*-promoted expression increased 1a and 2a accumulation in wt yeast, and these higher 1a and 2a levels were reproduced in $ole1w_i'$ yeast with or without UFA supplementation (Fig. 4A, lanes 4 to 6).

BMV-directed CAT expression in $ole1w_i'$ yeast with *ADH1*-expressed 1a and 2a was 5% of that of the wt (Fig. 4B, left side), duplicating the original *ole1w* phenotype (Fig. 1C). Adding 0.2 mM UFA to the medium restored 2a accumulation and CAT expression to wt levels. The *GAL1*-promoted increase in 1a and 2a accumulation coincided with a fivefold increase in BMV-directed CAT expression in wt yeast and UFA-supplemented $ole1w_i'$ yeast (Fig. 4B). However, despite wt 1a and 2a

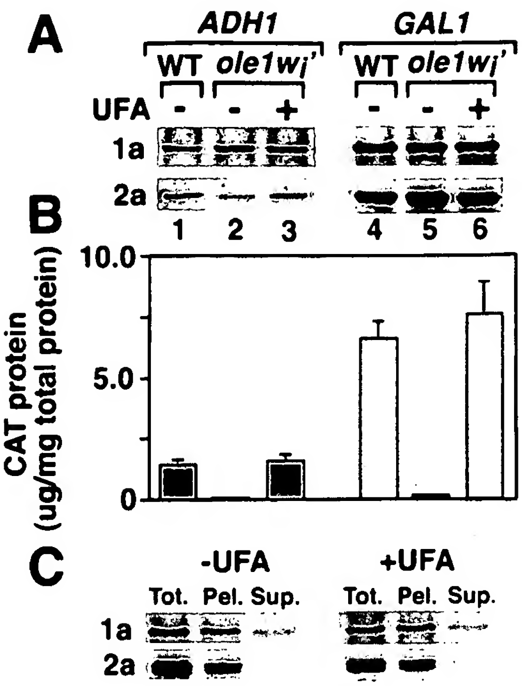

FIG. 4. (A) Western blot analysis of 1a and 2a protein accumulation in wt and $ole1w_i'$ yeast containing a plasmid expressing B3CAT and either *ADH1*-promoted 1a and 2a expression plasmids (lanes 1 to 3) or *GAL1*-promoted 1a and 2a expression plasmids (lanes 4 to 6). Yeast was grown to mid-log phase in Gal medium containing no UFA (−) or 0.2 mM UFA (+). Cell lysates were prepared, and equal amounts of total protein were electrophoresed and Western blotted as described in Materials and Methods. (B) BMV-directed CAT expression in the yeast cells described in the legend to panel A. (C) Distribution of 1a and 2a between membrane and soluble cytoplasmic fractions in $ole1w_i'$ yeast with or without the UFA supplementation. $ole1w_i'$ yeast cells expressing *GAL1*-promoted 1a, 2a, and RNA3 were harvested at mid-log phase, and total protein (Tot.) was extracted. A portion of the lysate was centrifuged at 10,000 × *g* to yield pellet (Pel.) and supernatant (Sup.) fractions. The same percentage of each fraction was analyzed by electrophoresis and Western blotting.

levels, CAT expression in unsupplemented $ole1w_i'$ yeast with *GAL1*-promoted 1a and 2a was only 2% of that in the wt (Fig. 4B). Thus, the *ole1w* mutation inhibited BMV-directed gene expression at one or more steps after 1a and 2a protein production. To provide equal levels of 2a accumulation in wt and *ole1* mutant yeast, all subsequent experiments were performed with *GAL1*-expressed 1a and 2a.

Confocal microscopy and cell fractionation show that 1a and 2a are associated with ER membrane in wt yeast that replicates BMV RNA (7, 37). To determine if the *ole1w* mutation inhibited membrane association of 1a and 2a, $ole1w_i'$ spheroplasts with *GAL1*-expressed 1a, 2a, and RNA3 were osmotically lysed, membranes were pelleted at 10,000 × *g*, and Western blotting was used to examine the distribution of 1a and 2a between the membrane and soluble cytoplasmic fractions (7). As shown in Fig. 4C, patterns of distribution were identical in $ole1w_i'$ yeast with or without the UFA supplementation and identical to that in wt yeast (7). Thus, the *ole1w* mutation did not impede membrane association of 1a or its ability to direct 2a to membrane.

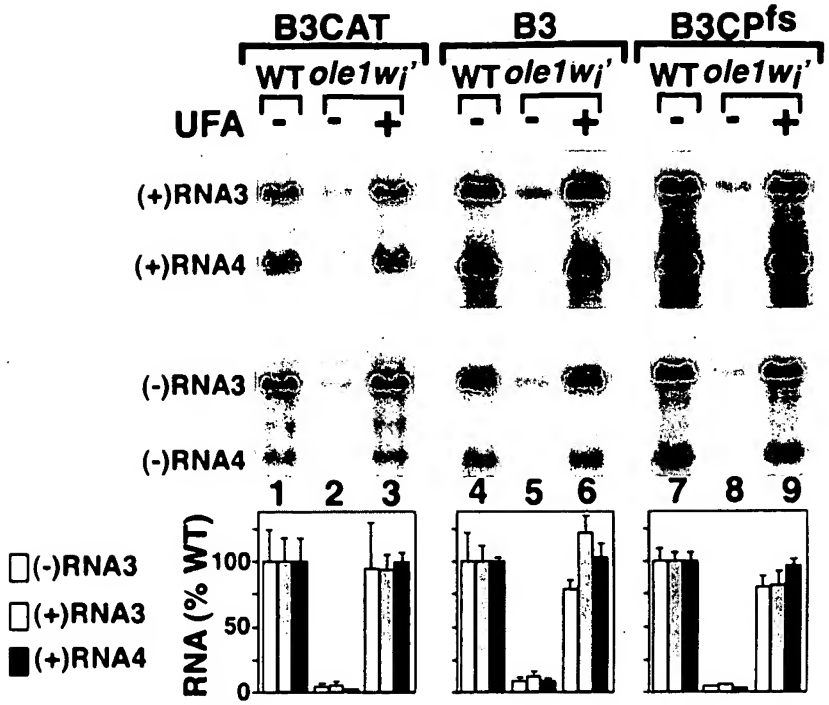

FIG. 5. Northern blot analysis of RNA3 and RNA4 accumulation in wt and *ole1w$_i$'* yeast containing plasmids directing *GAL1*-promoted expression of 1a, 2a, and the indicated RNA3 derivatives. Yeast cells were grown as described for Fig. 4. Total RNA was prepared, and equal amounts of total RNA were electrophoresed and Northern blotted as described in Materials and Methods. Because negative-strand RNA3 accumulates to 30- to 100-fold-lower levels than those of positive-strand RNA3 in wt yeast, negative-strand blots were printed at a higher intensity to facilitate visualization. Negative-strand RNA3 (open bars), positive-strand RNA3 (shaded bars), and positive-strand RNA4 (filled bars) accumulations were measured with a PhosphorImager (Molecular Dynamics) and normalized to that of wt yeast. The histogram shows averages and standard deviations from three experiments.

Inhibited accumulation of BMV RNA replication products in *ole1w$_i$'* yeast. To determine whether inhibition of BMV-directed gene expression by *ole1w* mutation was due to a defect in subgenomic mRNA (RNA4) synthesis or translation, we measured B3CAT RNA4 accumulation in wt and *ole1w$_i$'* yeast. Positive-strand RNA4 accumulation in *ole1w$_i$'* yeast was only 2% of that of the wt (Fig. 5, lanes 1 to 3), fully accounting for the reduction of BMV-directed CAT protein expression (Fig. 4B). Similar inhibition of positive- and negative-strand B3CAT genomic RNA (RNA3) accumulation was seen in *ole1w$_i$'* yeast (7 and 5% of wt levels). All of these viral RNA accumulation defects were suppressed by medium supplementation with 0.2 mM UFA (Fig. 5, lanes 2 to 3).

Since B3CAT is not a natural BMV RNA replication template, we also tested wt RNA3 replication in *ole1w$_i$'* yeast. As shown in Fig. 5, lanes 4 to 6, negative- and positive-strand RNA3 and positive-strand RNA4 accumulations in unsupplemented *ole1w$_i$'* yeast were 9, 13, and 9% of wt levels. The slightly larger accumulations of wt RNA3 and RNA4 in *ole1w$_i$'* yeast (13 and 9% of wt levels) relative to levels of B3CAT RNA3 and RNA4 (7 and 2% of wt levels) could be due to expression of small amounts of coat protein, which selectively encapsidates and stabilizes BMV RNAs (27). To explore this, we tested B3CP^{fs}, in which coat protein expression was eliminated by a 4-base frameshifting insertion immediately after the initiating AUG codon and simultaneous mutation of the second in-frame AUG codon to AUC (46). As shown in Fig. 5, lanes 7 to 9, B3CP^{fs} RNA3 and RNA4 accumulated in *ole1w$_i$'* yeast to 7 and 3% of wt levels, implying that coat protein was largely responsible for increased wt RNA3 and -4 accumulations relative to those in B3CAT. To eliminate any effects of coat protein on RNA3 stability and accumulation (see above), B3CP^{fs} and its derivatives were used in all subsequent experiments.

Normal 1a-induced RNA3 stabilization in *ole1w$_i$'* yeast. In wt yeast lacking 2a, 1a acts through the *cis*-acting intergenic replication enhancer (RE) of positive-strand RNA3 (Fig. 1A) to dramatically increase the stability and accumulation of RNA3 transcripts while inhibiting their translation (23). Multiple results, including parallel inhibitory and stimulatory effects of RE mutations on 1a-induced RNA3 stabilization and RNA3 replication, indicate that these 1a-induced effects reflect the initial recruitment of RNA3 templates from translation to RNA replication (12, 46). To better determine the stage at which RNA3 replication was inhibited in *ole1w$_i$'* yeast, we tested for 1a-induced stimulation of RNA3 transcript accumulation in *ole1w$_i$'* yeast.

In the absence of 1a and 2a, plasmid-derived, positive-strand RNA3 transcripts accumulated to equal levels in *ole1w$_i$'* yeast with or without the UFA supplementation that suppresses the *ole1w* phenotype (Fig. 6, lanes 1 to 2). Thus, the *ole1w* mutation did not affect DNA-dependent synthesis or accumulation of RNA3 transcripts. In the presence of 1a, RNA3 accumulation increased 16-fold in *ole1w$_i$'* yeast, again independently of

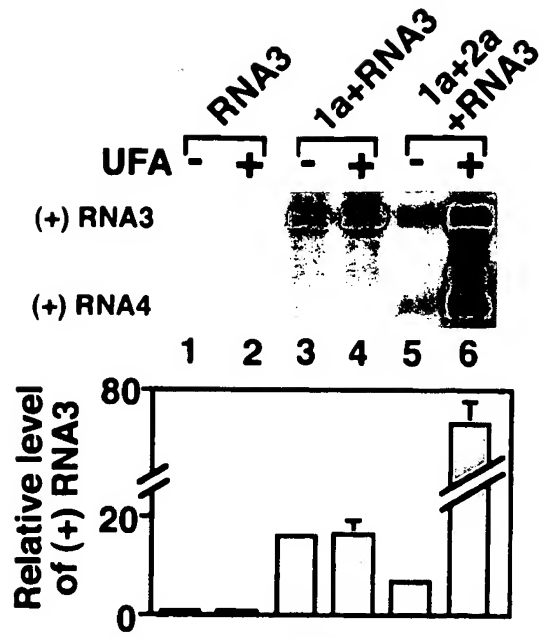

FIG. 6. Northern blot analysis of BMV positive-strand RNA3 accumulation in *ole1w$_i$'* yeast expressing the indicated BMV components. The B3CP^{fs} derivative of RNA3 was used to avoid the effects of coat protein on RNA accumulation (see Results). Yeast cells were grown, and positive-strand RNA3 accumulation was analyzed as described for Fig. 5. The histogram shows averages and standard deviations for positive-strand RNA3 accumulation, normalized to the level in UFA-supplemented *ole1w$_i$'* yeast (lane 2), from three experiments. Thus, the histogram scale represents the fold increase in RNA3 accumulation in the presence of 1a (lanes 3 to 4) or 1a plus 2a (lanes 5 to 6), relative to the level of DNA-directed transcription in the absence of 1a and 2a (lanes 1 and 2).

UFA supplementation (lanes 3 to 4). Thus, 1a-induced stimulation of RNA3 accumulation was also not inhibited by the *ole1w* mutation. Nevertheless, RNA3 replication and subgenomic mRNA synthesis in *ole1w$_i$'* yeast remained strongly dependent on UFAs (lanes 5 to 6).

Unexpectedly, the *ole1w*-dependent inhibition of RNA3 replication in lane 5 revealed that less positive-strand RNA3 accumulated in the presence of 1a and 2a than with 1a alone (lanes 3 to 4). Further results below (Fig. 7) show that, when RNA3 replication is inhibited by a *cis*-acting mutation, this 2a-induced decrease in RNA3 accumulation occurs even when the *ole1w* mutant phenotype is suppressed by UFA supplementation. Thus, 2a interference with 1a stabilization of RNA3 appears to be a normal feature of 1a and 2a interaction. Since 2a protein interacts directly with 1a (25) and since 2a mRNA is derived from BMV RNA2, another RNA replication template, either 2a or its mRNA, might competitively inhibit RNA3 interaction with 1a.

Inhibition of negative-strand RNA3 synthesis in *ole1w$_i$'* yeast. The negative-strand RNA3 synthesis pathway in yeast is not saturated by DNA-transcribed positive-strand RNA3 templates, so that negative-strand RNA3 accumulation is stimulated by RNA-dependent amplification of positive-strand RNA3 templates (22). Consequently, due to the cyclical nature of wt RNA3 replication (Fig. 1A), the reduced negative-strand

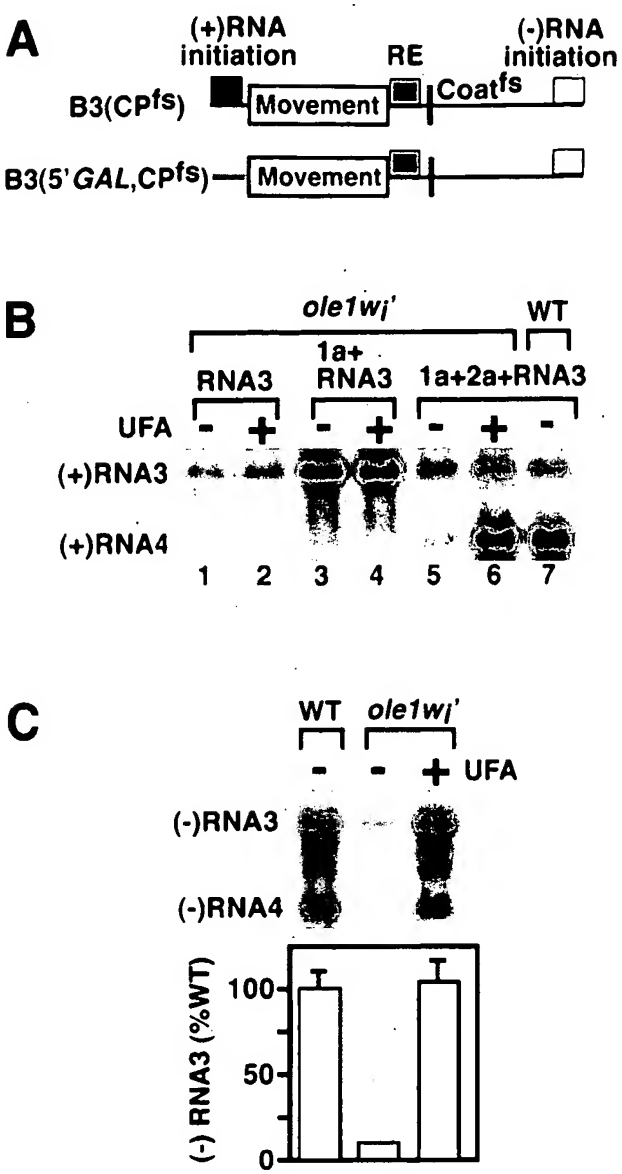

FIG. 7. Inhibition of negative-strand RNA3 synthesis in *ole1w$_i$'* yeast. (A) Schematic of B3(5'*GAL*, CP^{fs}) and its parent B3CP^{fs}, indicating *cis*-acting elements required for template recruitment (RE), negative-strand initiation, and positive-strand initiation. B3(5'GAL, CP^{fs}) was constructed by replacing the complete viral 5' NCR of B3CP^{fs} with the 5' NCR of yeast *GAL1* mRNA. (B) Northern blot analysis of positive-strand RNA3 accumulation in wt and *ole1w$_i$'* yeast expressing the indicated BMV components. Yeast cells were grown, and the amount of positive-strand RNA3 in each sample was analyzed as described for Fig. 5. (C) Northern blot analysis of negative-strand RNA3 accumulation in wt and *ole1w$_i$'* yeast expressing 1a, 2a, and B3(5'*GAL*, CP^{fs}). The histogram shows averages and standard deviations for negative-strand RNA3 accumulation, normalized to that in wt yeast, from three experiments.

accumulation in *ole1w$_i$'* yeast (Fig. 5) is consistent either with direct inhibition of negative-strand synthesis or with a primary defect in positive-strand synthesis, reducing the templates available for negative-strand synthesis.

To block RNA-dependent positive-strand RNA synthesis

and test negative-strand RNA synthesis directly, the wt BMV 5′ noncoding region (NCR) of B3CP^{fs} was replaced with the 5′ NCR of the yeast *GAL1* mRNA in an expression plasmid designated B3(5′*GAL*, CP^{fs}) (Fig. 7A). The resulting B3(5′*GAL*, CP^{fs}) transcript retained the RE region and, like wt RNA3, showed a strong 1a-dependent increase in accumulation (Fig. 7B, lanes 1 to 4). Moreover, as expected, B3(5′*GAL*, CP^{fs}) directed UFA-dependent subgenomic mRNA synthesis (Fig. 7B, lane 6). However, even in UFA-supplemented yeast, co-expression of 1a and 2a did not produce the dramatic further increase in positive-strand RNA3 accumulation seen for B3CP^{fs} and wt RNA3 (Fig. 7B, lanes 5 to 6). Rather, with or without UFA supplementation, positive-strand RNA3 accumulation in the presence of 1a and 2a was less than with 1a alone (Fig. 7B, lanes 3 to 6). Thus, B3(5′*GAL*, CP^{fs}) RNA3 supported little or no BMV-directed positive-strand RNA3 synthesis, confirming prior results that the wt RNA3 5′ NCR contains signals required for positive-strand synthesis (22).

Thus, for B3(5′*GAL*, CP^{fs}), the only templates for negative-strand RNA3 synthesis were provided by *GAL1*-promoted DNA transcription, which was unaffected by the $ole1w_i'$ mutation (Fig. 7B, lanes 1 to 2). Accordingly, in wt yeast (2) and in UFA-supplemented $ole1w_i'$ yeast (Fig. 7C and data not shown), the 5′ *GAL* substitution reduced negative-strand RNA3 accumulation to 15% of that of replicating wt RNA3. More importantly, in unsupplemented $ole1w_i'$ yeast, negative-strand RNA accumulation for B3(5′ *GAL*, CP^{fs}) was reduced a further 10-fold relative to that from the same template in wt yeast or UFA-supplemented $ole1w_i'$ yeast (Fig. 7C). Thus, in unsupplemented $ole1w_i'$ yeast, BMV RNA replication was inhibited at or before negative-strand RNA3 synthesis.

DISCUSSION

The studies presented here show that BMV RNA replication in yeast is severely inhibited by mutation of *OLE1*, an essential yeast gene encoding the Δ9 fatty acid desaturase required for unsaturated fatty acids synthesis. UFA supplementation of an engineered *ole1* deletion strain showed that BMV RNA replication did not require the Ole1 protein but rather required UFA levels well above those required for yeast cell growth. These results demonstrate in vivo the functional importance of lipids for BMV RNA replication and, as discussed below, imply an intimate and potentially dynamic relationship between RNA replication factors and the lipid bilayer.

The RNA replication defect in *ole1w* mutant yeast was traced to a narrow interval in early replication. In *ole1w* yeast, RNA replication factor 1a carried out several normal functions. 1a still became membrane associated and directed the membrane association of 2a (Fig. 4C). The 2a-independent ability of 1a to stabilize RNA3 transcripts, a function strongly linked to selection of RNA3 templates for replication (12, 46), was also unimpaired in $ole1w_i'$ yeast (Fig. 6). Nevertheless, negative-strand RNA3 synthesis was reduced to 10% or less of that of the wt (Fig. 7C). Thus, BMV RNA synthesis was inhibited after initial recognition of the positive-strand RNA3 template but at or before the first phase of RNA synthesis, i.e., negative-strand RNA synthesis. While this defect in negative-strand synthesis is sufficient to explain the overall reduction in BMV RNA replication, the results do not rule out additional defects in later steps of positive-strand RNA3 and subgenomic mRNA synthesis. For flock house virus, e.g., complete in vitro replication of viral RNA and positive-strand synthesis in particular depends on glycerophospholipids (48). Also, the capping functions of the alphavirus SFV nsP1 are activated by lipids, with a requirement for anionic head groups (3). While BMV may be subject to similar influences from polar head groups of membrane lipids, the results presented here show that BMV RNA replication is also highly sensitive to the fatty acid composition of the lipid bilayer.

Recently, BMV RNA replication was also found to be inhibited by mutation of the yeast gene *LSM1* (12). *LSM1* and *OLE1* show many disparate characteristics and appear to be involved in distinct aspects of BMV RNA replication. Unlike *OLE1*, *LSM1* is dispensable for yeast growth in minimal medium at 30°C, though it is required at 37°C. The *LSM1*-encoded protein, Lsm1p, is not membrane associated but distributed throughout the cytoplasm. Lsm1p is not a biosynthetic enzyme but rather is related to RNA splicing factors and implicated in the metabolism of viral and cellular mRNAs, including the transition of mRNAs from translation to other fates such as degradation and replication (5, 12). Accordingly, *LSM1* mutation inhibits 1a-induced stabilization of RNA3, which is unimpaired in $ole1w_i'$ mutants (Fig. 6). These results, isolation of additional BMV-inhibiting yeast mutations, and other findings suggest that many if not most steps in viral RNA replication depend on distinct host factors (12, 21).

UFA dependence of RNA replication. Cerulenin, an inhibitor of lipid synthesis, inhibits RNA replication by poliovirus and the alphavirus SFV (16, 34). While alternate interpretations cannot be ruled out due to cerulenin's ability to inhibit processes other than lipid synthesis (33), this inhibition of RNA replication suggests a possible requirement for continued lipid and/or membrane synthesis. The inhibition of BMV RNA replication in *ole1w* yeast, however, is not due to a general block of lipid or membrane synthesis. Ole1p is the desaturase that converts newly synthesized SFAs to UFAs. When UFA levels in yeast are limited by *ole1* mutations, membrane synthesis proceeds at normal rates but the UFA/SFA ratio in membrane phospholipids drops (44). Moreover, our experiments showed that *ole1w* yeast cells had a normal growth rate and size, and this did not change when the cells expressed 1a, 2a, and RNA3.

The UFA/SFA ratio affects many membrane-associated functions because of its strong effect on membrane fluidity and other physical properties (14, 42). wt BMV RNA replication required approximately five times more UFA supplementation than did normal growth of mutant yeast (Fig. 3), suggesting that optimal assembly or function of the RNA replication complex requires a highly fluid membrane. After membrane association, rapid diffusion might be required for 1a, 2a, or another replication factor to locate a required interaction partner before being trapped in a competing nonproductive interaction. During replication, rotation or translation of membrane-associated RNA replication factors might be required for RNA unwinding, translocation along RNA templates, or necessary cyclical alterations in protein-protein interactions.

In addition to kinetic effects, reduced UFA levels may also impede BMV RNA synthesis by perturbing the form or stability of replication factor interactions. Under conditions of reduced UFA levels, increased lipid packing density and mem-

brane microviscosity tend to displace membrane-associated proteins farther into the aqueous phase, altering their potential for interacting with other factors and the position of such interactions relative to the membrane (8, 42). Since introducing a *cis* double bond shifts lipids from a cylindrical to a more cone-shaped profile, UFAs also influence membrane curvature and flexibility (40). Modulating any of these parameters may impede the functional interaction of 1a, 2a, viral RNA, or host components with each other. Since the *ole1w* mutation did not inhibit 1a association with membrane or 1a-directed membrane association of 2a (Fig. 4C), the required interaction of the N-terminal 120 amino acids of 2a with the 1a C-terminal helicase-like domain (7) was not affected in *ole1w* yeast. However, other 1a-2a interactions required for later RNA replication steps may be perturbed. For example, BMV RNA replication also depends on an independent interaction between 1a and the central 2a polymerase domain (43).

While negative-strand RNA synthesis was strongly dependent on UFAs in vivo, a preformed, template-dependent negative-strand RNA synthesis activity can be solubilized from membranes of BMV-infected plant cells or yeast expressing 1a, 2a, and RNA3 (35). Thus, the UFA requirement may lie in assembly of a functional RNA synthesis complex. Alternatively, in vivo UFA dependence and membrane association of negative-strand RNA synthesis may relate to functions missing from the solubilized, in vitro negative-strand synthesis activity. Anomalous characteristics of the in vitro system include low efficiency of template usage (<0.1% of added template) and a lack of response to the intercistronic replication enhancer, which in vivo directs 1a-dependent RNA3 stabilization and stimulates negative-strand RNA3 synthesis and RNA3 replication approximately 100-fold (35, 46).

While unsaturated oleic and/or palmitoleic acids were required for BMV RNA replication, oleic acid disrupts poliovirus RNA replication in HeLa cells (15) or HeLa cell extracts (31). These results may be related to more complex effects of oleic acid on HeLa cells. Supplementing *ole1* mutant yeast with oleic acid, palmitoleic acid, or other UFAs yields a direct increase in membrane glycerophospholipids containing these UFAs (44). However, treating of HeLa cells with oleic acid resulted in major changes in the synthesis of many lipids, including dramatic increases in the synthesis of cholesterol and other neutral lipids, a reduced phosphatidylserine/phosphatidylcholine ratio, and other changes (15). Similarly, in HeLa cell extracts, oleic acid inhibited in vitro translation as well as poliovirus RNA replication (31).

In conclusion, we find that BMV RNA replication is strongly dependent on UFA levels in vivo. When UFAs were limited, ER-associated RNA replication was blocked after 1a and 2a membrane association and RNA3 template recognition and stabilization but before negative-strand RNA synthesis. The ability to use the *ole1w* mutation to block RNA replication at this stage should help to elucidate the early events in initiation of RNA synthesis. Dependence of BMV RNA replication on UFA levels in particular implies a requirement for host membrane fluidity, suggesting that the membrane is not just a static anchoring site for RNA replication complexes. Accordingly, further study of *ole1w* yeast should help to illuminate the nature and function of membrane association in RNA replication in positive-strand RNA viruses.

Since membrane-associated RNA replication appears to be a universal feature of positive-strand RNA viruses of eukaryotes, the replication of other viruses in this class may also be dependent on the fatty acid compositions of membrane lipids. Thus, while different host cells and viruses may function optimally over different lipid composition ranges, the finding that BMV RNA replication is much more sensitive than normal yeast cell growth to reduced levels of UFAs suggests that genetic or pharmacological approaches to modulate the lipid composition of host membranes may provide useful antiviral strategies.

ACKNOWLEDGMENTS

We thank Yukio Tomita for pB1YT3, Michael Sullivan for pB3(5′ *GAL*, CP^{6x}), Amine Noueiry and Juana Diez for valuable experimental advice, and Cindy Dorner for excellent technical assistance.

This work was supported by the National Institutes of Health through grant GM35072. P.A. is an investigator of the Howard Hughes Medical Institute.

REFERENCES

1. **Ahola, T., and P. Ahlquist.** 1999. Putative RNA capping activities encoded by brome mosaic virus: methylation and covalent binding of guanylate by replicase protein 1a. J. Virol. 73:10061–10069.
2. **Ahola, T., J. den Boon, and P. Ahlquist.** 2000. Helicase and capping enzyme active site mutations in brome mosaic virus protein 1a cause defects in template recruitment, negative-strand RNA synthesis, and viral RNA capping. J. Virol. 74:8803–8811.
3. **Ahola, T., A. Lampio, P. Auvinen, and L. Kaariainen.** 1999. Semliki Forest virus mRNA capping enzyme requires association with anionic membrane phospholipids for activity. EMBO J. 18:3164–3172.
4. **Ausubel, F. M., R. Brent, R. E. Kingston, D. D. Moore, J. G. Seidman, J. A. Smith, and K. Struhl (ed.).** 1987. Current protocols in molecular biology. John Wiley & Sons, New York, N.Y.
5. **Boeck, R., B. Lapeyr, C. E. Brown, and A. B. Sachs.** 1998. Capped mRNA degradation intermediates accumulate in the yeast *spb8–2* mutant. Mol. Cell. Biol. 18:5062–5072.
6. **Bossie, M. A., and C. E. Martin.** 1989. Nutritional regulation of yeast Δ-9 fatty acid desaturase activity. J. Bacteriol. 171:6409–6413.
7. **Chen, J., and P. G. Ahlquist.** 2000. Brome mosaic virus polymerase-like protein 2a is directed to the endoplasmic reticulum by helicase-like viral protein 1a. J. Virol. 74:4310–4318.
8. **Cherry, R. J., U. Muller, C. Holenstein, and M. P. Heyn.** 1980. Lateral segregation of proteins induced by cholesterol in bacteriorhodopsin-phospholipid vesicles. Biochim. Biophys. Acta 596:145–151.
9. **Choi, J. Y., J. Stukey, S. Y. Hwang, and C. E. Martin.** 1996. Regulatory elements that control transcription activation and unsaturated fatty acid-mediated repression of the *Saccharomyces cerevisiae OLE1* gene. J. Biol. Chem. 271:3581–3589.
10. **Cronan, J. E. J., and E. P. Gelmann.** 1975. Physical properties of membrane lipids: biological relevance and regulation. Bacteriol. Rev. 39:232–256.
11. **Cuconati, A., A. Molla, and E. Wimmer.** 1998. Brefeldin A inhibits cell-free, de novo synthesis of poliovirus. J. Virol. 72:6456–6464.
12. **Diez, J., M. Ishikawa, M. Kaido, and P. Ahlquist.** 2000. Identification and characterization of a host protein required for efficient template selection in viral RNA replication. Proc. Natl. Acad. Sci. USA 97:3913–3918.
13. **Dinant, S., M. Janda, P. A. Kroner, and P. Ahlquist.** 1993. Bromovirus RNA replication and transcription require compatibility between the polymerase- and helicase-like viral RNA synthesis proteins. J. Virol. 67:7181–7189.
14. **Emmerson, P. J., M. J. Clark, F. Medzihradsky, and A. E. Remmers.** 1999. Membrane microviscosity modulates mu-opioid receptor conformational transitions and agonist efficacy. J. Neurochem. 73:289–300.
15. **Guinea, R., and L. Carrasco.** 1991. Effects of fatty acids on lipid synthesis and viral RNA replication in poliovirus-infected cells. Virology 185:473–476.
16. **Guinea, R., and L. Carrasco.** 1990. Phospholipid biosynthesis and poliovirus genome replication, two coupled phenomena. EMBO J. 9:2011–2016.
17. **Gyorfy, Z., I. Horvath, G. Balogh, A. Domonkos, E. Duda, B. Maresca, and L. Vigh.** 1997. Modulation of lipid unsaturation and membrane fluid state in mammalian cells by stable transformation with the Δ9-desaturase gene of *Saccharomyces cerevisiae*. Biochem. Biophys. Res. Commun. 237:362–366.
18. **Halbrook, J., and M. F. Hoekstra.** 1994. Mutations in the *Saccharomyces cerevisiae CDC1* gene affect double-strand-break-induced intrachromosomal recombination. Mol. Cell. Biol. 14:8037–8050.
19. **Henry, S. A.** 1982. Membrane lipids of yeast: biochemical and genetic studies, p. 101–149. *In* J. Strathern, E. W. Jones, and J. R. Broach (ed.), The

molecular biology of the yeast *Saccharomyces*: metabolism and gene expression. Cold Spring Harbor Laboratory, Cold Spring Harbor, N.Y.
20. **Irurzun, A., L. Perez, and L. Carrasco.** 1992. Involvement of membrane traffic in the replication of poliovirus genomes: effects of brefeldin A. Virology **191**:166–175.
21. **Ishikawa, M., J. Diez, M. Restrepo-Hartwig, and P. Ahlquist.** 1997. Yeast mutations in multiple complementation groups inhibit brome mosaic virus RNA replication and transcription and perturb regulated expression of the viral polymerase-like gene. Proc. Natl. Acad. Sci. USA **94**:13810–13815.
22. **Ishikawa, M., M. Janda, M. A. Krol, and P. Ahlquist.** 1997. In vivo DNA expression of functional brome mosaic virus RNA replicons in *Saccharomyces cerevisiae*. J. Virol. **71**:7781–7790.
23. **Janda, M., and P. Ahlquist.** 1998. Brome mosaic virus RNA replication protein 1a dramatically increases in vivo stability but not translation of viral genomic RNA3. Proc. Natl. Acad. Sci. USA **95**:2227–2232.
24. **Janda, M., and P. Ahlquist.** 1993. RNA-dependent replication, transcription, and persistence of brome mosaic virus RNA replicons in *S. cerevisiae*. Cell **72**:961–970.
25. **Kao, C. C., and P. Ahlquist.** 1992. Identification of the domains required for direct interaction of the helicase-like and polymerase-like RNA replication proteins of brome mosaic virus. J. Virol. **66**:7293–7302.
26. **Kong, F., K. Sivakumaran, and C. C. Kao.** 1999. The N-terminal half of the brome mosaic virus 1a protein has RNA capping-associated activities: specificity for GTP and S-adenosylmethionine. Virology **259**:200–210.
27. **Krol, M. A., N. H. Olson, J. Tate, J. E. Johnson, T. S. Baker, and P. Ahlquist.** 1999. RNA-controlled polymorphism in the in vivo assembly of 180-subunit and 120-subunit virions from a single capsid protein. Proc. Natl. Acad. Sci. USA **96**:13650–13655.
28. **Mackenzie, J. M., M. K. Jones, and E. G. Westaway.** 1999. Markers for trans-Golgi membranes and the intermediate compartment localize to induced membranes with distinct replication functions in flavivirus-infected cells. J. Virol. **73**:9555–9567.
29. **Magliano, D., J. A. Marshall, D. S. Bowden, N. Vardaxis, J. Meanger, and J. Y. Lee.** 1998. Rubella virus replication complexes are virus-modified lysosomes. Virology **240**:57–63.
30. **Maynell, L. A., K. Kirkegaard, and M. W. Klymkowsky.** 1992. Inhibition of poliovirus RNA synthesis by brefeldin A. J. Virol. **66**:1985–1994.
31. **Molla, A., A. V. Paul, and E. Wimmer.** 1993. Effects of temperature and lipophilic agents on poliovirus formation and RNA synthesis in a cell-free system. J. Virol. **67**:5932–5938.
32. **Ntambi, J. M.** 1999. Regulation of stearoyl-CoA desaturase by polyunsaturated fatty acids and cholesterol. J. Lipid Res. **40**:1549–1558.
33. **Oda, T., and H. C. Wu.** 1993. Cerulenin inhibits the cytotoxicity of ricin, modeccin, Pseudomonas toxin, and diphtheria toxin in brefeldin A-resistant cell lines. J. Biol. Chem. **268**:12596–12602.
34. **Perez, L., R. Guinea, and L. Carrasco.** 1991. Synthesis of Semliki Forest virus RNA requires continuous lipid synthesis. Virology **183**:74–82.
35. **Quadt, R., M. Ishikawa, M. Janda, and P. Ahlquist.** 1995. Formation of brome mosaic virus RNA-dependent RNA polymerase in yeast requires coexpression of viral proteins and viral RNA. Proc. Natl. Acad. Sci. USA **92**:4892–4896.
36. **Rattray, J. B., A. Schibeci, and D. K. Kidby.** 1975. Lipids of yeasts. Bacteriol. Rev. **39**:197–231.
37. **Restrepo-Hartwig, M., and P. Ahlquist.** 1999. Brome mosaic virus RNA replication proteins 1a and 2a colocalize and 1a independently localizes on the yeast endoplasmic reticulum. J. Virol. **73**:10303–10309.
38. **Restrepo-Hartwig, M. A., and P. Ahlquist.** 1996. Brome mosaic virus helicase- and polymerase-like proteins colocalize on the endoplasmic reticulum at sites of viral RNA synthesis. J. Virol. **70**:8908–8916.
39. **Schaad, M. C., P. E. Jensen, and J. C. Carrington.** 1997. Formation of plant RNA virus replication complexes on membranes: role of an endoplasmic reticulum-targeted viral protein. EMBO J. **16**:4049–4059.
40. **Schneiter, R., and S. D. Kohlwein.** 1997. Organelle structure, function, and inheritance in yeast: a role for fatty acid synthesis? Cell **88**:431–434.
41. **Sethna, P. B., and D. A. Brian.** 1997. Coronavirus genomic and subgenomic minus-strand RNAs copartition in membrane-protected replication complexes. J. Virol. **71**:7744–7749.
42. **Shinitzky, M.** 1984. Membrane fluidity and cellular functions, p. 1–51. *In* M. Shinitzky (ed.), Physiology of membrane fluidity, vol. 1. CRC Press, Boca Raton, Fla.
43. **Smirnyagina, E., N. S. Lin, and P. Ahlquist.** 1996. The polymerase-like core of brome mosaic virus 2a protein, lacking a region interacting with viral 1a protein in vitro, maintains activity and 1a selectivity in RNA replication. J. Virol. **70**:4729–4736.
44. **Stukey, J., V. M. McDonough, and C. E. Martin.** 1989. Isolation and characterization of *OLE1*, a gene affecting fatty acid desaturation from *Saccharomyces cerevisiae*. J. Biol. Chem. **264**:16537–16544.
45. **Stukey, J., V. M. McDonough, and C. E. Martin.** 1990. The *OLE1* gene of *Saccharomyces cerevisiae* encodes the Δ9 fatty acid desaturase and can be functionally replaced by the rat stearoyl-CoA desaturase gene. J. Biol. Chem. **265**:20144–20149.
46. **Sullivan, M. L., and P. Ahlquist.** 1999. A brome mosaic virus intergenic RNA3 replication signal functions with viral replication protein 1a to dramatically stabilize RNA in vivo. J. Virol. **73**:2622–2632.
47. **van der Rest, M. E., A. H. Kamminga, A. Nakano, Y. Anraku, B. Poolman, and W. N. Konings.** 1995. The plasma membrane of *Saccharomyces cerevisiae*: structure, function, and biogenesis. Microbiol. Rev. **59**:304–322.
48. **Wu, S. X., P. Ahlquist, and P. Kaesberg.** 1992. Active complete in vitro replication of nodavirus RNA requires glycerophospholipid. Proc. Natl. Acad. Sci. USA **89**:11136–11140.
49. **Zhang, S., Y. Skalsky, and D. J. Garfinkel.** 1999. *MGA2* or *SPT23* is required for transcription of the Δ9 fatty acid desaturase gene, *OLE1*, and nuclear membrane integrity in *Saccharomyces cerevisiae*. Genetics **151**:473–483.

JOURNAL OF VIROLOGY, Dec. 2003, p. 12819–12828 Vol. 77, No. 23
0022-538X/03/$08.00+0 DOI: 10.1128/JVI.77.23.12819–12828.2003

Membrane Synthesis, Specific Lipid Requirements, and Localized Lipid Composition Changes Associated with a Positive-Strand RNA Virus RNA Replication Protein

Wai-Ming Lee* and Paul Ahlquist*

Howard Hughes Medical Institute and Institute for Molecular Virology, University of Wisconsin—Madison, Madison, Wisconsin 53706

Received 13 June 2003/Accepted 15 August 2003

Multifunctional RNA replication protein 1a of brome mosaic virus (BMV), a positive-strand RNA virus, localizes to the cytoplasmic face of endoplasmic reticulum (ER) membranes and induces ER lumenal spherules in which viral RNA synthesis occurs. We previously showed that BMV RNA replication in yeast is severely inhibited prior to negative-strand RNA synthesis by a single-amino-acid substitution in the *ole1w* allele of yeast Δ9 fatty acid (FA) desaturase, which converts saturated FAs (SFAs) to unsaturated FAs (UFAs). Here we further define the relationships between 1a, membrane lipid composition, and RNA synthesis. We show that 1a expression increases total membrane lipids in wild-type (wt) yeast by 25 to 33%, consistent with recent results indicating that the numerous 1a-induced spherules are enveloped by invaginations of the outer ER membrane. 1a did not alter total membrane lipid composition in wt or *ole1w* yeast, but the *ole1w* mutation selectively depleted 18-carbon, monounsaturated (18:1) FA chains and increased 16:0 SFA chains, reducing the UFA-to-SFA ratio from ~2.5 to ~1.5. Thus, *ole1w* inhibition of RNA replication was correlated with decreased levels of UFA, membrane fluidity, and plasticity. The *ole1w* mutation did not alter 1a-induced membrane synthesis, 1a localization to the perinuclear ER, or colocalization of BMV 2a polymerase, nor did it block spherule formation. Moreover, BMV RNA replication templates were still recovered from cell lysates in a 1a-induced, 1a- and membrane-associated, and nuclease-resistant but detergent-susceptible state consistent with spherules. However, unlike nearby ER membranes, the membranes surrounding spherules in *ole1w* cells were not distinctively stained with osmium tetroxide, which interacts specifically with UFA double bonds. Thus, in *ole1w* cells, spherule-associated membranes were locally depleted in UFAs. This localized UFA depletion helps to explain why BMV RNA replication is more sensitive than cell growth to reduced UFA levels. The results imply that 1a preferentially interacts with one or more types of membrane lipids.

The RNA replication complexes of all well-studied, eukaryotic positive-strand RNA viruses are found on intracellular membranes. In association with RNA replication, infection by such viruses often induces proliferation, vesiculation, and sometimes redistribution of specific intracellular membranes (6, 10, 11, 20, 22, 23, 25, 32, 35, 36, 39, 40, 42). RNA replication by poliovirus, Semliki Forest virus, and cowpea mosaic virus is sensitive to cerulenin, a lipid synthesis inhibitor, implying a requirement for lipid and/or membrane synthesis (5, 12, 30). Brefeldin A, an inhibitor of secretory vesicle formation, blocks RNA replication by poliovirus and rhinovirus (24). Furthermore, in vitro studies show that some steps of positive-strand RNA virus RNA replication are sensitive to membrane-disrupting, nonionic detergents or are activated by added membrane lipids (3, 44, 47). Nevertheless, present knowledge of the contributions of membranes to the assembly and function of viral RNA replication complexes is very limited.

One positive-strand RNA virus for which membrane association of RNA replication has been studied is brome mosaic virus (BMV), a representative member of the alphavirus-like superfamily of human, animal, and plant viruses (1). BMV has three genomic RNAs. RNA1 and RNA2 encode proteins 1a and 2a, respectively, which are the only viral proteins required for RNA replication. 1a contains an N-terminal domain with m^7G methyltransferase and putative guanylyltransferase activities required for capping viral RNA and a C-terminal RNA helicase-like domain (2). 2a contains a central polymerase domain and an N-terminal domain that interacts with the 1a helicase domain (17). RNA3 encodes a cell-to-cell movement protein (3a) and the coat protein. The 3′-proximal coat protein gene is not translatable from RNA3 but only from a subgenomic mRNA, RNA4, synthesized from negative-strand RNA3 (26).

BMV replicates its genomic RNAs and synthesizes subgenomic mRNA in the budding yeast *Saccharomyces cerevisiae* (16), duplicating the known features of BMV RNA replication in its natural host plant cells. 1a localizes to the outer nuclear envelope or perinuclear endoplasmic reticulum (ER) membrane and induces this membrane to invaginate into the ER lumen, forming 50- to 70-nm diameter spherular vesicles or spherules (9, 33, 39). 1a also directs 2a polymerase and viral RNA templates to these spherules, which become the sites of viral RNA synthesis (7, 33, 39, 43). The interior of these spherules remains connected to the cytoplasm via a membranous neck contiguous with the ER membrane. Similar membrane spherules are associated with RNA replication by other members of the alphavirus superfamily, nodaviruses, and other pos-

* Corresponding author. Mailing address: Institute for Molecular Virology, University of Wisconsin—Madison, 1525 Linden Dr., Madison, WI 53706-1596. Phone: (608) 263-5916. Fax: (608) 265-9214. E-mail for W.-M. Lee: wlee5@facstaff.wisc.edu. E-mail for P. Ahlquist: ahlquist@wisc.edu.

itive-strand viruses (references 25 and 39 and references therein). The structure, assembly, and function of BMV spherules have multiple similarities to the replicative cores of retrovirus and double-stranded RNA virus virions (39).

We previously reported the isolation of a yeast mutant that inhibits BMV RNA replication approximately 50-fold due to a mutation in the essential yeast gene *OLE1* (21). *OLE1* encodes Δ9 fatty acid (FA) desaturase (Ole1p), an integral ER membrane protein and the only enzyme for unsaturated FA (UFA) synthesis in yeast (29). Ole1p converts saturated palmitic acid (having C_{16} FA chains with no double bonds; hereafter 16:0) and stearic acid (18:0) into unsaturated palmitoleic (16:1) and oleic (18:1) acids. The BMV-inhibiting allele *ole1w* has a single amino acid substitution (Y_{212} to C) in the predicted catalytic domain of Ole1p. This mutation blocks BMV RNA replication prior to negative-strand RNA synthesis but does not inhibit cell growth in the absence or presence of BMV components. *OLE1* deletion and medium supplementation experiments showed that all effects of the *ole1w* mutation on BMV replication are due to reduced UFA levels; i.e., BMV RNA replication depends on UFAs but not directly on Ole1p. The results show that BMV RNA replication is highly sensitive to membrane lipid composition and that manipulation of lipid composition by pharmacological as well as genetic approaches may be a useful antiviral strategy.

To better understand the effects of the *ole1w* mutation and to obtain further insights into the roles of membranes in RNA replication, we combined biochemical, confocal fluorescence, and electron microscopy (EM) analyses to study membrane lipid composition and 1a-membrane, 1a-2a, and 1a-RNA interactions involved in forming the functional RNA replication complex. Here we show that BMV replication protein 1a stimulates membrane lipid accumulation in the absence of other viral components, that the *ole1w* mutation blocked RNA replication despite allowing all known 1a functions in replication complex formation, and that *ole1w* not only globally reduced the cellular UFA-to-SFA ratio but preferentially depleted osmium-reactive UFA levels in 1a-associated perinuclear ER membranes.

MATERIALS AND METHODS

Yeast and plasmids. Yeast strain YPH500 (*MAT ura3-52 lys2-801 ade2-101 tyr1-63 his3-200 leu2-1*) and its isogenic *ole1w* derivative (21), bearing a single Y_{212}-to-C mutation in *OLE1*, were used throughout. Centromeric plasmids pB1YT3H, pB2YT5, and pB2YT5-G2 were used to express BMV 1a, 2a, and 2a-green fluorescent protein (GFP), respectively (7, 21). RNA3 was expressed from pB3CPfs, a centromeric plasmid with the *TRP1* marker (21). sec63p-GFP was expressed from pJK59, kindly provided by J. A. Kahanab and P. Silver (Department of Biological Chemistry and Molecular Pharmacology, Harvard Medical School). Plasmid transformation and yeast cultivation were performed as described earlier (21).

FA analysis. Total FA from 10 optical densities at 600 nm (OD_{600}) of yeast were extracted and were converted to methyl esters as described earlier (27). FA species were separated according to chain length and degree of saturation by gas-liquid chromatography and were identified by retention time. The molar amount of each species was measured by using a flame ionization detector (27).

Cell fractionation and RNase sensitivity assays. Yeast cells were treated with lyticase to remove the cell wall as described earlier (39). The resulting spheroplasts were lysed in YLB buffer (50 mM Tris-Cl [pH 8.0], 2.5 mM EDTA, 1 mM phenylmethylsulfonyl fluoride, 5 μg of pepstatin/ml, 10 μg of leupeptin/ml, 10 μg of aprotinin/ml, and 10 mM benzamidine) and were centrifuged 5 min at 20,000 × *g* to yield membrane-enriched pellet and membrane-depleted supernatant fractions. To assay the RNase sensitivity of RNA3 in the pellet fractions, membrane pellets were resuspended in YLB and were divided into three portions. Portions A and B received no initial treatment, while portion C was treated with 0.5% NP-40 for 15 min at 4°C. Portions B and C then were treated with 0.01 U of micrococcal nuclease/μl for 15 min at 30°C (39). RNA was extracted from each fraction and were analyzed by Northern blotting as described earlier (21).

Confocal microscopy. A Bio-Rad 1024 double-channel confocal microscope (at the W. M. Keck Laboratory for Biological Imaging of the University of Wisconsin—Madison) was used to visualize and compare the intracellular sites of accumulation of 1a protein, 2a protein, and sec63p. To detect 1a protein, yeast cells were fixed with formaldehyde, permeabilized with Triton X-100, and immunostained with rabbit anti-1a serum followed by donkey anti-rabbit antibodies conjugated to Texas red as described previously (33). GFP-2a and sec63p-GFP were visualized by their intrinsic fluorescence. GFP was fused to the N terminus of 2a (7) and C terminus of sec63p (J. Kahanab and P. Silver, unpublished results). GFP fusion did not interfere with the normal localization and function of 2a or sec63p-GFP in yeast. Images of the intracellular distribution of 1a (red) and 2a (green) or sec63p (green) within the same optical section (0.5 μm) were acquired sequentially and were digitally superimposed to compare the two distributions. To ensure the reproducibility of the results, each experiment was performed several times, and in each experiment hundreds of cells were examined. Representative results are shown in the figures. The effective resolution of the images is about 100 to 200 nm.

EM. For the experiment whose results are shown in Fig. 5, yeast cells were fixed in 4% paraformaldehyde and 2% glutaraldehyde, postfixed with 1% osmium tetroxide and 1% potassium ferricyanide, stained with 1% uranyl acetate, dehydrated in a graded series of ethanol solutions, and embedded in Spurr's resin (Electron Microscopy Sciences, Ft. Washington, Pa.) as described earlier (39). Seventy-nanometer sections were cut and placed on copper grids, poststained with 8% uranyl acetate in 50% methanol and Reynold's lead citrate, and analyzed with a Philips CM120 transmission electron microscope at the Medical School Electron Microscope Facility of the University of Wisconsin. For immunogold EM experiments (see Fig. 6), yeast cells were similarly fixed except that the preembedding osmium tetroxide and uranyl acetate steps were omitted, samples were embedded in LR White resin (Polysciences, Inc., Warrington, Pa.) and sections were placed on nickel grids. Grids were blocked with 0.5% gelatin, immunostained with anti-1a rabbit serum and 12-nm gold-labeled secondary antibodies, poststained, and analyzed by transmission EM as described above.

RESULTS

***ole1w* mutation but not 1a expression alters yeast FA composition.** Our prior results suggested that the *ole1w* mutation inhibited BMV RNA replication by reducing UFA levels (21). To verify this directly, to define the specific lipid species affected, and to determine the magnitude of the effects, we determined the FA composition of wt and isogenic *ole1w* yeast. In addition, because our earlier results suggested interrelationships between 1a, *OLE1* desaturase activity, and BMV RNA replication (21), we analyzed wt and *ole1w* yeast lacking or expressing 1a to determine if 1a expression influenced the FA composition of membrane lipids. To determine FA levels and composition, total cellular FAs were extracted from yeast, converted to methyl esters, and fractionated by chain length and degree of saturation by using gas-liquid chromatography. Each species was identified by its retention time during chromatography and its molar amount was measured by using a flame ionization detector.

In *S. cerevisiae*, palmitic acid (16:0), stearic acid (18:0), palmitoleic acid (16:1), and oleic acid (18:1) comprise well over 90% of total FA (14). As shown in Fig. 1A, comparing these major FA species revealed that the *ole1w* mutation had little effect on 16:1 or 18:0 levels but caused an approximately 25% drop in 18:1 and an ~50% rise in 16:0. The selective decrease in 18:1 but not 16:1 FA levels suggests that the *ole1w* mutation preferentially inhibits action of the encoded desaturase on 18:0 substrates. Similar differential effects of mutations on desatu-

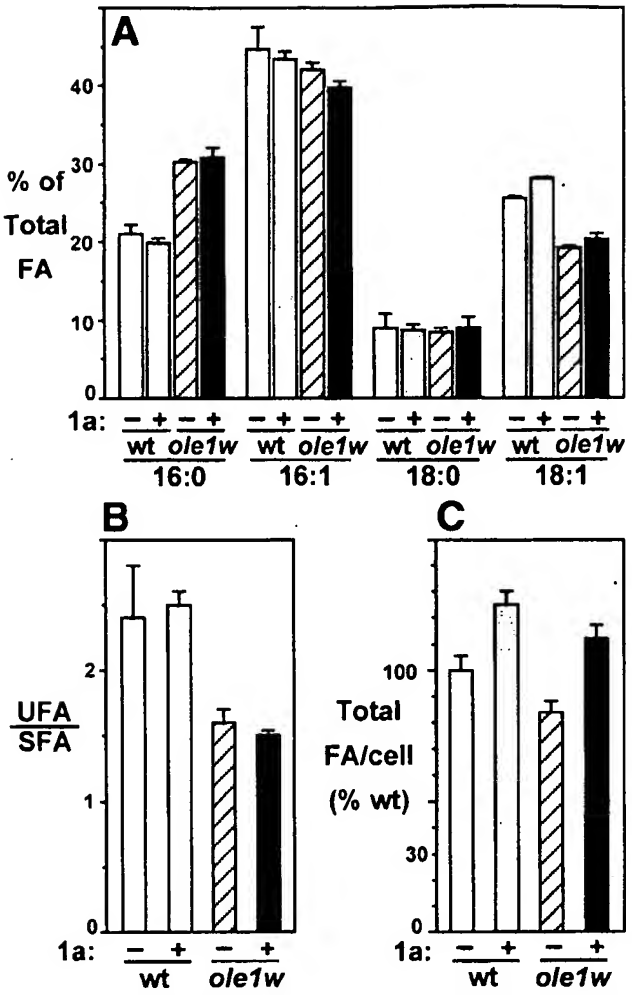

FIG. 1. Effect of BMV 1a expression and the yeast *ole1w* mutation on total accumulation and composition of yeast FAs. wt yeast and mutant yeast were grown in defined, galactose-containing medium to mid-log phase. Total FA was extracted, converted to methyl esters, and separated by chain length and degree of saturation by using gas-liquid chromatography. The molar amount of 16:0, 16:1, 18:0, and 18:1 FA was measured by using a flame ionization detector and was normalized to the OD_{600} of each yeast culture. (A) Relative levels of 16:0, 16:1, 18:0, and 18:1 FA in each sample, as a molar percentage of total FA. Yeast genotype (wt or *ole1w*) and the presence or absence of 1a (− or +) are indicated at the bottom for each sample. Total FA is the sum of 16:0, 16:1, 18:0, and 18:1 in each sample. (B) Ratio of total UFA (16:1 + 18:1) to SFA (16:0 + 18:0). (C) Total FA per cell, shown as a percentage of the total FA per cell of wt yeast lacking 1a. Each histogram shows the averages and standard deviations of four experiments.

rase specificity for 16:0 and 18:0 substrates have been reported before (46). The associated increase of 16:0 levels may be a secondary consequence of inhibiting 18:1 synthesis, since 16:0 is a substrate for synthesizing 18:0 and thus 18:1.

On first inspection of these results, it appeared surprising that the *ole1w* mutation induces such a severe, UFA-suppressible inhibition of BMV RNA replication, since the level of the major UFA species, 16:1, was nearly wild type (wt) and since the less abundant UFA 18:1 was reduced by only ~25%. However, due to the simultaneous increase in 16:0, the ratio of total UFA to SFA, which strongly influences membrane fluidity and plasticity, was reduced from approximately 2.5 in wt yeast to 1.5 in *ole1w* yeast (Fig. 1B). Moreover, further results below imply that variations in local as well as total FA composition may be important in the effects of the *ole1w* mutation on BMV RNA replication complexes.

TABLE 1. 1a expression and *ole1w* mutation had no effect on the sizes of yeast cells

Yeast	Avg size (μm^2)[a]
wt	18.4 ± 4.8
wt + 1a	17.5 ± 4.5
ole1w	18.3 ± 4.3
ole1w + 1a	19.0 ± 5.0

[a] Yeast was visualized with a light microscope; well-focused images were recorded digitally. The size of each cell in each image was measured as a one-dimensional area with the IPLab Spectrum program. For each sample, average and standard deviation of 150 to 300 cells are shown.

In contrast to the effects of the *ole1w* mutation, expression of 1a had little or no effect on FA composition in either wt or *ole1w* yeast (Fig. 1A and B). Thus, 1a did not directly or indirectly regulate the activity of the *OLE1*-encoded Δ9 FA desaturase.

1a expression increases yeast FA levels. To compare total FA levels per cell, the molar amounts of various FA for each culture were summed, normalized to the OD_{600} of the culture, and expressed as a percentage of the total FA value for wt yeast lacking 1a (Fig. 1C). To determine whether any differences in total FA content might relate to *ole1w*- or 1a-induced changes in cell size and whether OD_{600} accurately reflected cell density, we examined samples of each culture by light microscopy. In addition to visual examination, the cross-sectional areas of 150 to 300 cells from each culture were measured digitally (IPLab Spectrum program; Scanalytics, Inc. Fairfax, Va.). As shown in Table 1, there were no significant differences in cell size for wt or *ole1w* yeast with or without 1a.

Figure 1C shows that 1a expression increased total FA levels per cell by 25% in wt yeast. Since over 95% of all FA in yeast exist as fatty acyl chains of membrane lipids, total FA levels reflect yeast membrane content (31) and the 1a-induced increase in FA must represent an increase in membrane content. Furthermore, since 1a did not increase cell size (Table 1) and hence did not increase plasma membrane area, this change must reflect an increase in intracellular membranes. This is consistent with and confirms recent EM results showing that the numerous, ER lumenal, spherular replication complexes induced by 1a are formed in and enveloped by invaginations of the outer ER membrane, considerably increasing the surface area of the outer ER membrane (39).

In the absence of 1a, the *ole1w* mutation reduced total FA per cell by 16% relative to wt yeast (Fig. 1C). The basis for this reduction is not yet clear. It appeared tempting to speculate that total membrane synthesis in *ole1w* mutant yeast might be limited by the mutant's reduced capacity for UFA synthesis and the need to maintain the UFA-to-SFA ratio within viable limits of membrane fluidity. However, in *ole1w* yeast, 1a expression increased total FA accumulation by 33% (Fig. 1C). The size of this 1a-induced increase in total FA levels, which

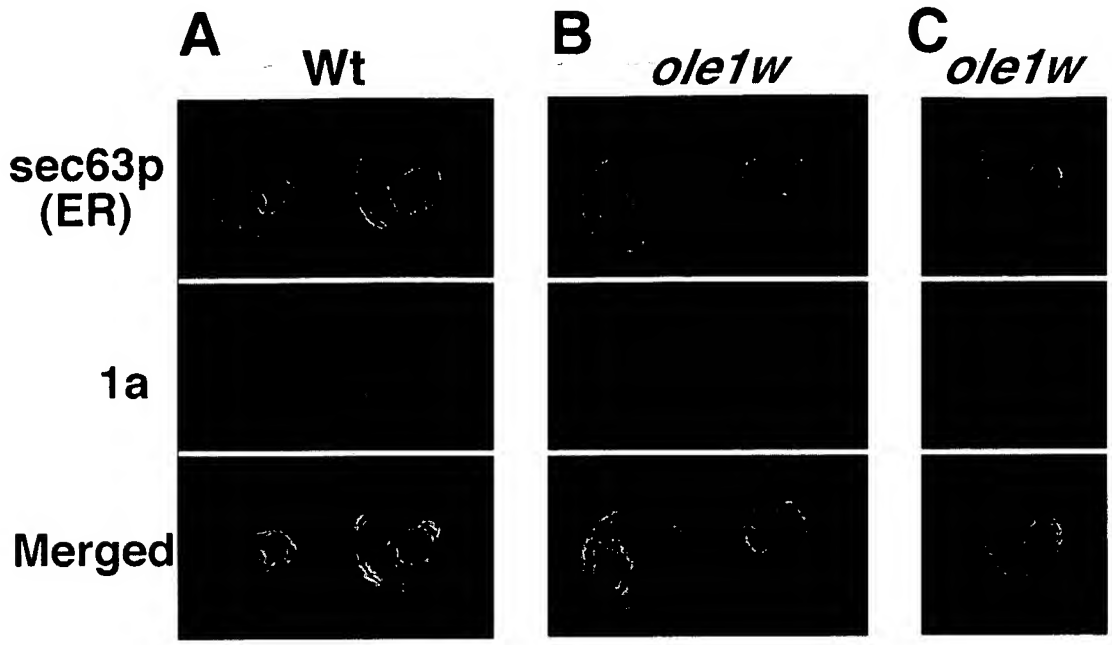

FIG. 2. *ole1w* yeast supports normal localization of BMV 1a protein to ER membranes. wt yeast and *ole1w* mutant yeast expressing 1a and a fusion protein linking GFP to sec63p, an integral ER membrane protein, were fixed with formaldehyde, spheroplasted, permeabilized with Triton X-100, and immunostained with rabbit anti-1a antiserum followed by secondary antibodies conjugated to Texas red. sec63p-GFP was visualized by its intrinsic fluorescence. The intracellular distributions of sec63p-GFP (top row, green) and 1a (middle row, red) were sequentially imaged in the same 0.5-μm optical section by confocal microscopy and were digitally superimposed for further comparison (bottom row). Representative images are shown. (A) wt yeast. (B) *ole1w* yeast. Shown are 1a and sec63p-GFP distributions representative of >95% of the cells. (C) *ole1w* yeast. Shown are 1a and sec63p-GFP distributions seen in a small percentage of the cells.

was even greater than that for wt yeast in both relative and absolute terms, implied that the *ole1w* mutation did not inhibit BMV RNA replication by preventing 1a-induced synthesis of additional membrane to support formation of the membrane-enveloped spherular replication complexes.

Reduced UFA levels do not alter ER localization of 1a. In wt yeast and in BMV's natural plant host cells, 1a localizes to ER membranes (33, 34). In lysates of *ole1w* yeast, we previously found that 1a cofractionates with total cellular membranes (21). Thus, the *ole1w* mutation does not prevent membrane association of 1a. To determine whether 1a localized to its normal ER membrane sites in *ole1w* yeast, we used confocal microscopy to compare the intracellular distributions of 1a and a yeast ER marker, sec63p, in wt and *ole1w* yeast. In over 95% of *ole1w* cells (Fig. 2B), 1a colocalized with sec63p in a pattern indistinguishable from that of 1a in wt yeast (Fig. 2A). In both cases, 1a colocalized with sec63p on perinuclear ER membranes and, to a lesser degree, on peripheral ER membrane strands, which in yeast are frequently appressed to the outer edge of the cell.

Interestingly, a small fraction of *ole1w* yeast cells, comprising only a small percentage of the total, showed a different pattern of 1a localization (Fig. 2C). In these cells, 1a was not found in a normal ER pattern but rather localized to relatively large, amorphous bodies, usually directly adjacent to the nucleus. In the same cells, sec63p was found in its normal perinuclear and peripheral ER patterns, but, in addition, a fraction of sec63p colocalized with 1a in the amorphous bodies. Since 1a self interacts (28), such structures may represent aggregations of ER membrane-associated 1a, possibly triggered by high levels of 1a expression since 1a signals in such cells were often unusually bright. Similar 1a-associated amorphous bodies were not found in wt yeast expressing 1a.

Reduced UFA levels do not alter 1a-induced ER colocalization of 2a. In *ole1w* yeast, the 1a functions tested in Fig. 2 and in prior work (21) appeared normal, but viral positive-strand, negative-strand, and subgenomic RNA synthesis was blocked (21). Since viral RNA synthesis requires not only 1a but also BMV 2a polymerase, the possible effects of the *ole1w* mutation on 2a, its interactions with 1a, or its interactions with cellular components were of particular interest.

When expressed without 1a in wt yeast, BMV 2a polymerase has been found distributed throughout cells (7). However, in the presence of 1a, an N-terminal segment of 2a interacts with the helicase-like region of 1a and colocalizes on ER membranes (7). We showed previously that, in *ole1w* yeast expressing 1a and 2a, 2a cofractionates with total cell membranes (21). To determine whether 2a colocalized normally with 1a to ER membranes in *ole1w* yeast, or if 2a might alter the distribution of 1a in such cells, we used confocal microscopy to compare the intracellular distributions of 1a and 2a. Because 2a normally accumulates to low levels relative to 1a and gives fainter signals by immunofluorescence, these experiments used a previously studied, functional GFP-2a fusion that supports BMV RNA replication (7). In the absence of 1a, this GFP-2a was distributed throughout the cell in wt and *ole1w* yeast (reference 7 and results not shown). When 1a and GFP-2a were coexpressed in *ole1w* yeast, they were found colocalized in ER-associated pat-

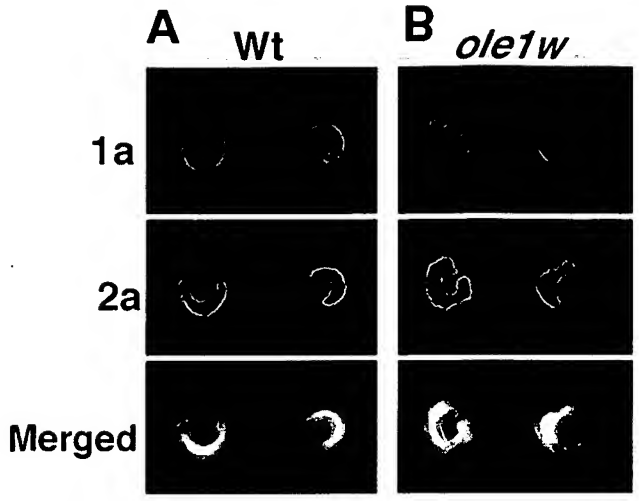

FIG. 3. *ole1w* yeast supports normal, 1a-induced localization of BMV 2a protein to ER membranes. wt yeast (A) and *ole1w* yeast (B) expressing BMV 1a and a 2a-GFP fusion protein were processed as described in the Fig. 2 legend. 1a (top row, red) was visualized by indirect immunofluorescence, 2a-GFP (middle row, green) was visualized by intrinsic fluorescence, and the images were digitally superimposed for futher comparison (bottom row). Representative images are shown.

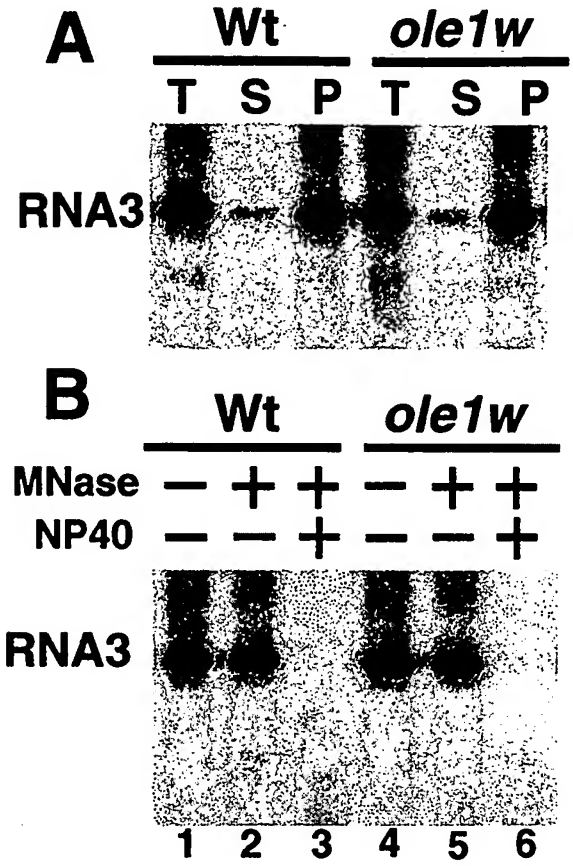

FIG. 4. *ole1w* yeast supports normal, 1a-induced transfer of BMV RNA3 to a membrane-associated, nuclease-resistant state. (A) Membrane association of RNA3. wt yeast and *ole1w* yeast expressing 1a and RNA3 were spheroplasted and lysed osmotically, and the total lysate (T) was fractionated by centrifugation (5 min at 20,000 × *g*) into a membrane-depleted supernatant (S) and a membrane-enriched pellet (P). RNA3 levels in each fraction were analyzed by Northern blotting. (B) Nuclease resistance of RNA3. Northern blot analysis of RNA3 in the pellet fraction (P) from panel A after no additional treatment (lanes 1 and 4), incubation with 0.01 U of micrococcal nuclease (MNase)/μl for 15 min at 30°C (lanes 2 and 5), or incubation with 0.5% NP-40 for 15 min at 0°C followed by micrococcal nuclease (lanes 3 and 6).

terns indistinguishable from those in wt yeast (Fig. 3). In both wt and *ole1w* yeast, as observed previously, 1a and 2a signals were particularly strong on perinuclear ER but also extended to peripheral ER strands. Therefore, reduced UFA levels did not detectably perturb 1a-directed 2a localization to the ER, nor did they cause 2a to alter the intracellular distribution of 1a. As in Fig. 2C, a small percentage of *ole1w* yeast cells showed 1a and 2a colocalization in relatively large, amorphous bodies (results not shown).

Reduced UFA levels do not inhibit recovery of BMV RNAs in a 1a-induced, membrane-associated, nuclease-resistant state. In wt yeast in the absence of 2a polymerase, 1a acts through specific *cis*-acting RNA signals to dramatically increase the stability and thus the accumulation of BMV genomic RNAs (15, 43). In *ole1w* yeast, this 1a-induced stimulation of BMV RNA accumulation proceeds to wt levels (21). Recent findings show that, in wt yeast, this increased stability results from 1a-mediated recruitment of BMV RNA replication templates into a novel, membrane-associated, protected compartment (39). Multiple results imply that this compartment corresponds to the interior of the 1a-induced, membrane-enveloped spherules. In lysates of wt yeast, 1a-stabilized BMV RNA copurifies with spherule-bearing, perinuclear ER membranes in a 1a-dependent, nuclease-resistant, nonionic detergent-disruptible state (39). Moreover, nascent BMV RNA replication products cofractionate in an indistinguishable membrane-associated, nuclease-resistant state and are localized to the interior of spherules by in vivo BrUTP labeling and immunogold EM (39).

To determine if the *ole1w* mutation and associated changes in membrane lipid composition affected the formation, stability, or membrane association of this protected RNA pool, we tested lysates of wt and *ole1w* yeast expressing 1a and BMV RNA3. 1a-dependent membrane association of RNA3 can be assayed by fractionating such lysates into a membrane-enriched pellet and a membrane-depleted supernatant (39). As shown in Fig. 4A, the degree of 1a-induced membrane association of RNA3 in *ole1w* yeast was as high as that in wt yeast. Moreover, as shown in Fig. 4B, the membrane-associated RNA3 from *ole1w* and wt yeast was equally protected from micrococcal nuclease but was equally susceptible to nonionic detergent NP-40 plus micrococcal nuclease. Thus, the *ole1w* mutation did not detectably alter 1a-dependent membrane association, nuclease protection, or nonionic detergent susceptibility of RNA3.

***ole1w* mutation preferentially alters spherule membranes.** As noted above, expressing 1a alone in wt yeast induces invaginations of the outer, perinuclear ER (nuclear envelope) membrane to form spherular compartments associated with

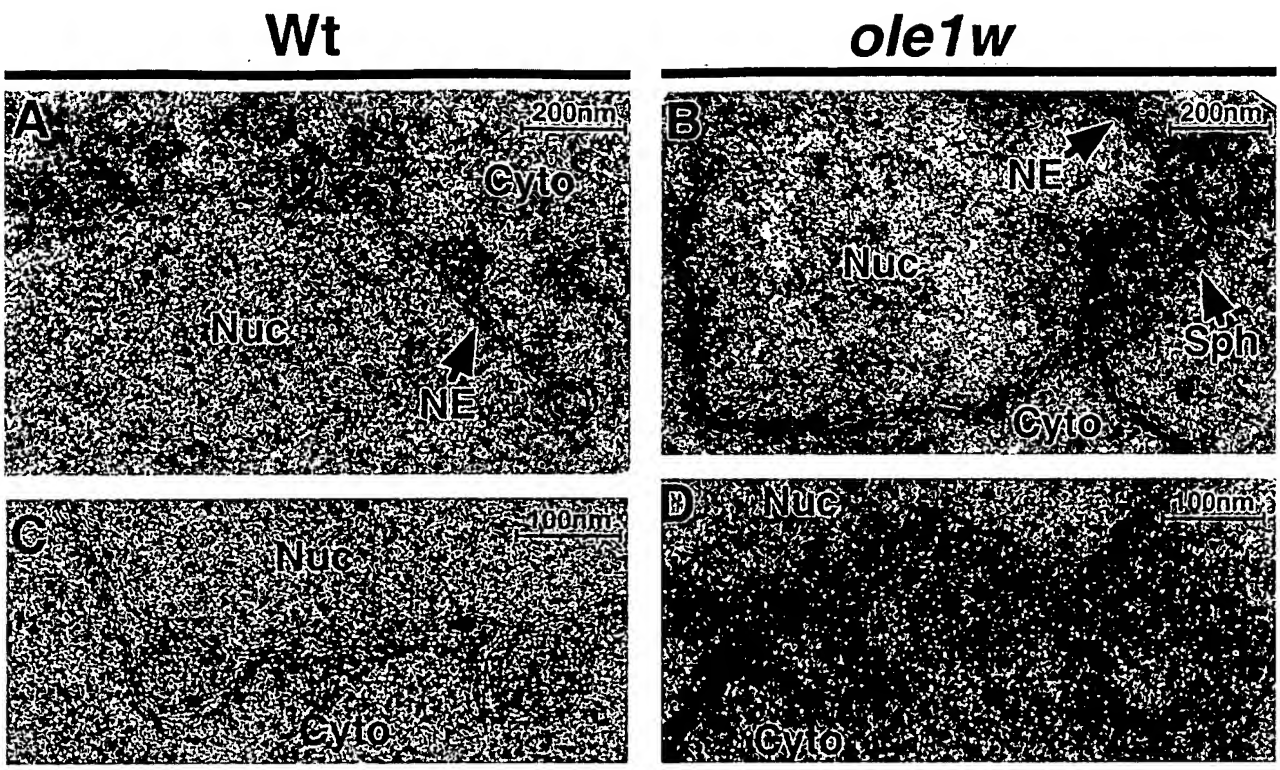

FIG. 5. Yeast *ole1w* mutation preferentially alters the membranes bounding 1a-induced spherules. Representative electron micrographs of wt yeast (panels A and C) and *ole1w* mutant yeast (panels B and D) expressing 1a are shown. Panels C and D show enlarged portions of panels A and B, respectively, to reveal further details of the spherule membranes. Labels represent nucleoplasm (Nuc), nuclear envelope (NE), cytoplasm (Cyto), and 1a-induced spherules (Sph). Please see Results for further comments.

BMV RNA protection and replication (39). To determine whether the formation or structure of such spherules was affected in *ole1w* yeast by the decreased UFA-to-SFA ratio and its associated changes in membrane fluidity and plasticity, we compared the ultrastructure of wt and *ole1w* yeast by EM. Following standard practices, yeast cells were fixed for EM with glutaraldehyde and paraformaldehyde followed by osmium tetroxide (OsO_4). The aldehydes stabilize membranes and other protein complexes by cross-linking proteins. OsO_4 fixes and stains membranes by reacting with the double bonds of unsaturated lipids at the rate of one per double bond (13). The products of this reaction include stable diester linkages between unsaturated acyl chains of adjacent membrane lipids and OsO_2, which is deposited at the hydrophilic sides of the lipid bilayer, marking the membrane with two parallel, electron-dense lines in high-resolution electron micrographs.

Figure 5 shows representative electron micrographs of wt and *ole1w* yeast expressing 1a. In wt yeast, the lipid bilayers of the inner and outer perinuclear ER membranes and the invaginated spherule membranes were marked by the typical paired lines of osmium staining (Fig. 5A and 5C). In *ole1w* yeast (Fig. 5B and D), most sections of the general, perinuclear ER membranes also were marked by osmium staining. However, in these yeast mutants, the lipid bilayer-associated lines of OsO_2 deposition often were not as distinctive and clear as those in wt yeast and occasionally were disrupted by short gaps. These results appear consistent with the dependence of osmium staining on adjacent UFA chains and the reduced membrane UFA levels in these cells. This partial, general decline in membrane definition was seen in the peripheral ER and other membranes in *ole1w* yeast with or without 1a but was slightly more pronounced in the presence of 1a.

In addition, even more notable effects of the *ole1w* mutation were found in 1a-expressing yeast in specific subdomains of the perinuclear ER membrane (Fig. 5B and D). In *ole1w* cells expressing 1a, portions of the nuclear border were marked by 50- to 60-nm spherular cores similar to those found in the ER lumen of wt yeast expressing 1a (Fig. 5A and C). However, in the *ole1w* yeast these regions lacked well-defined osmium staining of either the inner and outer nuclear envelope membrane or of the spherule-bounding membranes surrounding such cores in wt yeast. Immediately flanking regions of the nuclear envelope, however, showed visible osmium staining (Fig. 5B and D). Thus, reactivity of the nuclear envelope membrane with the UFA-dependent reagent OsO_4 was significantly reduced in the immediate vicinity of these cores.

To determine whether the 1a-induced, perinuclear, spherule core-like structures in *ole1w* yeast were counterparts of spherule cores in wt yeast, we used immunogold EM with anti-1a antisera to determine if these structures contained 1a. As is required to preserve 1a antigenicity, for this analysis yeast was fixed only with aldehydes (39). Without OsO_4 fixation, membrane lipids are depleted during later alcohol dehydration steps of sample processing for thin sectioning. However, an

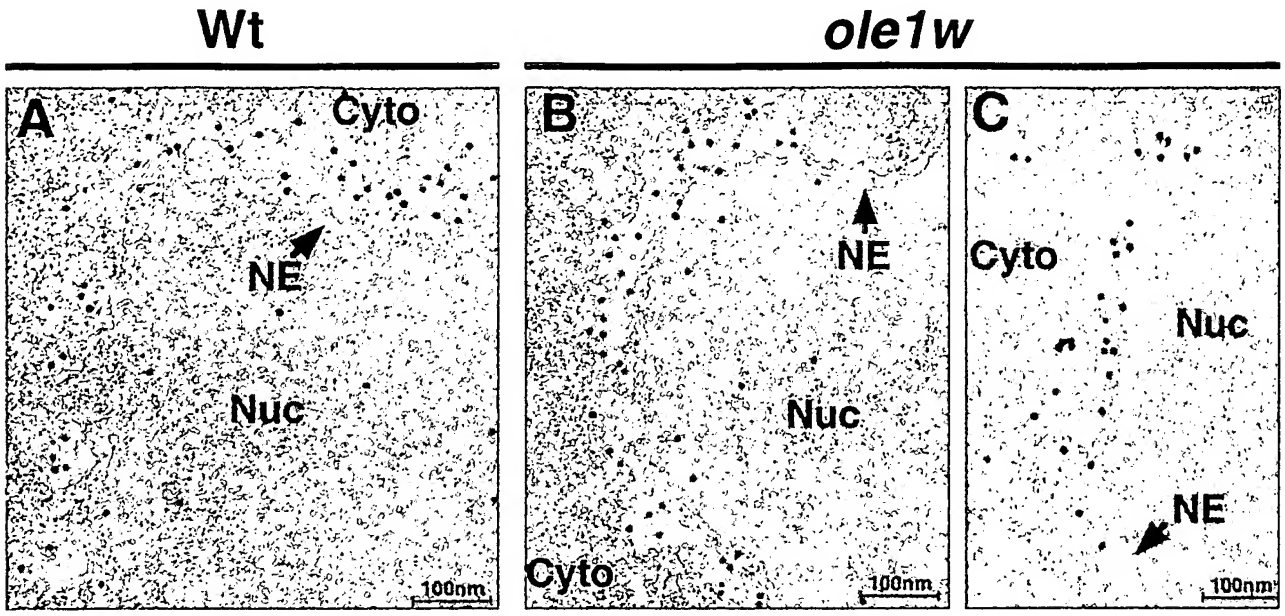

FIG. 6. BMV 1a protein is localized to perinuclear spherule cores in both wt and *ole1w* yeast. Representative electron micrographs of immunogold localization of 1a in wt yeast (A) and *ole1w* mutant yeast (B and C) expressing 1a are shown. Labels indicate nucleoplasm (Nuc), nuclear envelope (NE), and cytoplasm (Cyto). To preserve 1a antigenicity for immunogold staining, yeast expressing 1a was fixed by using aldehydes without OsO_4, causing membranes to appear as white, electron-lucent strips, rather than as osmium-stained black lines in Fig. 5A and C. 1a was visualized by immunostaining thin sections with rabbit anti-1a antiserum and secondary antibodies conjugated to 12-nm gold particles.

outline of the membrane normally is preserved due to aldehyde cross-linking of membrane proteins, which comprise about 50% of the total mass of yeast membranes. Consequently, in the resulting electron micrographs, the aldehyde-cross-linked, lipid-depleted membranes generally appear as white, electron-lucent strips, rather than as osmium-stained black lines.

In wt yeast, as seen previously (39), 1a localized primarily to the 50- to 70-nm spherical cores that were found between the inner and outer perinuclear ER membranes (Fig. 6A). Within this ER lumen in wt yeast, these cores usually were separated by additional electron-lucent layers that appeared to correspond to the spherule-bounding membranes seen in Fig. 5A and B. In *ole1w* yeast (Fig. 6B and C), 1a similarly localized primarily to the dilated, 50- to 70-nm space between the inner and outer nuclear envelopes. However, while close inspection of the micrographs revealed that this dilated ER lumen contained individual spherule cores as in Fig. 5B and D, the separation between these cores was less defined than in wt yeast. Thus, in contrast to Fig. 5, this osmium-independent processing allowed visualization of the expected inner and outer nuclear membranes bordering the 1a-induced spherule cores in *ole1w* yeast but further illustrated that the membranes flanking spherules in *ole1w* yeast differed in structure, composition, or both from those in wt yeast.

DISCUSSION

In this study, we further explored the relationships among BMV replication protein 1a, membrane lipid synthesis and composition, and viral RNA replication. We found that 1a expression markedly increased membrane lipid accumulation per cell, in parallel with 1a induction of numerous, 1a-containing, intralumenal ER membrane invaginations (Fig. 5 and 6) that constitute the viral RNA replication complex (39). Though fully rescuable by UFA feeding and therefore due to reduced UFA levels, the strong RNA replication block of the *ole1w* mutant allele of Δ9 FA desaturase was caused by much smaller shifts in lipid balance than in previously isolated *OLE1* mutants affecting cellular processes (Fig. 1). Thus, viral RNA synthesis was highly sensitive to membrane lipid composition. Moreover, although blocked in even the earliest forms of viral RNA synthesis, *ole1w* yeast supported all known steps in 1a interaction with ER membranes, BMV 2a polymerase, and viral RNA templates for replication complex assembly, including forming 1a-containing perinuclear spherule cores (Fig. 2 to 6). However, in *ole1w* yeast, 1a-associated perinuclear membranes were locally deficient in reactivity with the UFA-specific stain OsO_4, implying that 1a caused local variations in membrane lipid composition and that the already reduced UFA levels in the mutant yeast were preferentially further depleted in the vicinity of 1a. The relation of these results to other viral and cellular processes is discussed further below.

1a stimulates membrane lipid accumulation. As noted in the introduction, RNA replication by positive-strand RNA viruses occurs on intracellular membranes, often in association with membrane proliferation and vesiculation that, for some viruses, has been shown to be functionally important for RNA replication (5, 12, 24, 30). Here we showed that expressing BMV RNA replication factor 1a alone in yeast increased total membrane lipid accumulation per cell by 25 to 33% (Fig. 1C). The absence of any corresponding increase in cell size or plasma membrane area (Table 1) shows that this must reflect

an increase in intracellular membranes, consistent with recent observations that 1a induces vesicle-like invaginations that greatly increase the area of the affected ER membrane and form the compartment in which RNA replication occurs (39). Besides the production of these perinuclear ER spherules, 1a expression did not induce any discernible proliferation of intracellular membranes. 1a may stimulate lipid synthesis indirectly, since 1a accumulation on the ER membrane and possible 1a exclusion of some cell membrane proteins may trigger pathways that normally induce lipid synthesis for maintaining proper lipid-to-protein ratios in cellular membranes. Alternatively, we cannot rule out that 1a directly stimulates lipid synthesis by interacting with one or more of the ER membrane-associated enzymes involved in FA and lipid synthesis.

Globally and locally altered membrane lipid balance in *ole1w* yeast. In *ole1w* yeast, BMV RNA replication was blocked by relatively modest shifts in membrane lipid composition (Fig. 1), underscoring that viral RNA replication was much more dependent on lipid composition than was cell growth. Temperature-sensitive (*ts*) mutations that more severely inhibit *OLE1* expression or activity block cell growth and disrupt the morphology of multiple cellular membranes. When shifted to the nonpermissive temperature of 37°C, a yeast strain with *ts* mutations in *MGA2* and *SPT23*, encoding transcription factors required for *OLE1* expression, decreased *OLE1* mRNA by 15-fold, total UFA levels by 35%, and the UFA-to-SFA ratio by 2.5-fold; blocked yeast growth; and caused separation of the inner and outer nuclear membranes (48). Shifting *mdm2*, a *ts* allele of *OLE1*, to 37°C decreased UFA levels by threefold and the UFA-to-SFA ratio by over 10-fold, abolished transfer of mitochondria from mother cells to budding daughter cells, and caused the remaining mitochondria to fragment (41). Both strains were rescued by UFA feeding at nonpermissive temperature, confirming that their defects were caused by depleting UFAs.

In contrast, the *ole1w* mutation blocked BMV RNA replication without detectable defects in yeast growth or morphology. *ole1w* yeast had normal doubling times, normal cell sizes (Table 1), and no observable abnormality in the morphology of subcellular structures in the presence or absence of BMV components. This lack of cell growth or morphology defects is consistent with the finding that wt yeast maintains UFA levels well above the minimum required for growth under optimal conditions, providing extra membrane fluidity to cope with changes in temperature or other environmental conditions (4). Moreover, the *ole1w* mutation caused little or no change in the levels of total FA or of the more abundant 16:1 UFA and only a 25 to 30% decrease in the less abundant 18:1 UFA (Fig. 1A and C). Overall, total UFA levels decreased by only 12%, and the UFA-to-SFA ratio fell by only 40%.

Nevertheless, the 12% decrease in UFA levels in *ole1w* yeast inhibits BMV RNA replication by 95% or more (21). The *ole1w* mutation did not inhibit 1a-induced membrane synthesis (Fig. 1C), 1a-induced transfer of viral RNA to a membrane-associated, nonionic detergent-susceptible, nuclease-protected compartment (Fig. 4), or formation of 1a-containing, perinuclear membrane-associated spherule cores (Fig. 5 and 6). In *ole1w* yeast, the normal 1a stimulation of membrane synthesis (Fig. 1C) and lumenal location of 1a-containing cores (Fig. 5B and 6B) suggest that formation of the 1a-containing spherule cores involved ER membrane invagination, as in wt yeast. However, as shown in Fig. 5B, osmium staining of the membranes around the spherule cores was specifically reduced relative to flanking sections of the perinuclear ER membranes. Since such staining depends on osmium reaction with the double bonds of UFA chains in membrane lipids, this implies that the regions of the perinuclear ER membranes containing 1a and 1a-induced spherules were preferentially depleted in UFA-containing lipids.

Since osmium staining involves diester formation between the double bonds of adjacent lipids with UFA chains, the localized reduction in staining may not represent complete UFA exclusion but only depletion below a threshold at which adjacent UFAs become rare. Consistent with this, 1a-containing membranes might have a lower-than-average affinity for UFA-containing lipids even in wt yeast, but the reduction in their UFA concentration might reach an osmium-discernible threshold only when the UFA-to-SFA ratio drops sufficiently below wt, as in *ole1w* yeast.

The ability of 1a to locally modulate membrane lipid composition is understandable, as 1a is present on the membrane at high local concentration. 1a is one of the most abundant proteins in total nuclear membrane preparations (39), interacts with itself (28), accumulates in localized patches on ER membranes (33, 34), and is present in hundreds of copies per spherule (39).

Any of several mechanisms might contribute to localized depletion of osmium-stainable UFA chains from 1a-containing, spherule-associated membranes. For example, self-interaction (28) and multimerization (39) of membrane-associated 1a proteins might create a membrane zone with reduced protein and lipid mobility. Since the rigid bends of the *cis* double bonds in UFAs favor a less densely packed, more fluid state, UFA-containing lipids might tend to be excluded from this relatively static membrane zone into the more fluid surrounding membrane, leaving behind a higher concentration of more tightly packing, less fluid, SFA-containing lipids. Alternatively, 1a might selectively interact with and retain SFA-containing lipids, so that the high local 1a concentration would tend to exclude UFAs. Finally, 1a might preferentially interact with UFA-containing lipids but in a way that disrupted their ability to stain with osmium. 1a is a peripheral membrane protein on the cytoplasmic face of the ER but possesses a membrane affinity that is unusually high for a peripheral membrane protein (9). Some peripheral membrane proteins, including cytochrome *c*, appear to achieve high-affinity membrane interaction by using a hydrophobic protein cavity to bind UFAs on membrane lipids (18, 45). Such binding requires the UFA to extend out of the membrane via rotation around the C_2—C_3 carbon bond of the phospholipid glycerol backbone. Similar interaction of 1a with UFA-containing lipids might sequester UFAs out of the lipid bilayer and prevent their effective interaction with OsO_4 and other lipids, thus further lowering the already reduced membrane UFA levels in *ole1w* yeast and leading to the locally poor membrane fixation and staining.

Blocked RNA replication in *ole1w* yeast. The *ole1w* mutation did not inhibit 1a and 2a colocalization on ER membranes (Fig. 2 and 3), formation of ER-lumenal, 1a-containing spherule cores (Fig. 5 and 6), or 1a transfer of BMV RNA to a membrane-associated, nuclease-protected compartment (Fig.

4). Nevertheless, the *ole1w*-induced shift in lipid balance, which is particularly pronounced in 1a-associated membranes, induces a severe, UFA-suppressible block to viral RNA replication at or before synthesis of negative-strand RNA (21). This strong sensitivity implies that the membrane is an essential, functional component of the RNA replication complex. While the results presented here define a narrow interval between unaffected and affected steps in replication complex assembly and function, the precise nature of the replication block remains to be determined. Fluid membranes and specific lipids are required to activate some protein functions and to facilitate formation or modulation of protein-protein interactions (18, 19). For example, UFA-containing lipids activate the membrane-associated *Escherichia coli* DNA replication initiator protein DnaA (8). Similarly, membrane fluidity, UFA-containing lipids, or both may be needed for 1a or 2a polymerase to function properly or to interact properly with each other or host factors.

In addition, local variations in lipid composition have central roles in regulating the formation and properties of curved membranes. Specific lipids are crucial for stabilizing the highly curved membrane junction between nuclear pores and the surrounding nuclear envelope (38). Formation and budding of synaptic vesicles require specific lipid modifications that convert inverted cone-shaped lipids to cone-shaped lipids, thereby favoring a specific polarity of membrane curvature (37). Similarly, local variations in lipid composition likely are crucial for the formation and properties of the vesicular, spherular membrane invaginations that envelope the replication complexes of BMV, nodaviruses, and many other positive-strand RNA viruses (references 25 and 39 and references therein). Since the bend introduced by a *cis* double bond gives UFA-containing lipids a cone shape promoting negative membrane curvature, the *OLE1*-dependent UFA-to-SFA ratio is an important contributor to the properties of such curved membranes. Just as for budding synaptic vesicles, lipid composition might be particularly vital for the properties of the highly curved membrane necks joining the light bulb-shaped spherules to the outer perinuclear membranes. These necks appear crucial for RNA synthesis as the likely channels for ribonucleotide import and product RNA export (39).

ACKNOWLEDGMENTS

We thank Makoto Miyazaki and James Ntambi of the the Department of Biochemistry, University of Wisconsin—Madison, for valuable assistance with lipid analysis, Benjamin August and Randall Massey of the Medical School Electron Microscope Facility for assistance with EM, Mark Tengowski and Lance Rodenkirch of the W. M. Keck Laboratory for Biological Imaging for assistance with confocal microscopy, and Jason Kahanab and Pamela Silver of Harvard Medical School for generously providing the sec63p-GFP expression plasmid. We also thank Michael Schwartz and other members of our laboratory for helpful discussions throughout these experiments.

This work was supported by the National Institutes of Health through grant GM35072. P.A. is an Investigator of the Howard Hughes Medical Institute.

REFERENCES

1. **Ahlquist, P.** 1992. Bromovirus RNA replication and transcription. Curr. Opin. Genet. Dev. **2**:71–76.
2. **Ahola, T., J. den Boon, and P. Ahlquist.** 2000. Helicase and capping enzyme active site mutations in brome mosaic virus protein 1a cause defects in template recruitment, negative-strand RNA synthesis, and viral RNA capping. J. Virol. **74**:8803–8811.
3. **Ahola, T., A. Lampio, P. Auvinen, and L. Kaariainen.** 1999. Semliki Forest virus mRNA capping enzyme requires association with anionic membrane phospholipids for activity. EMBO J. **18**:3164–3172.
4. **Barber, E. D., and W. E. Lands.** 1973. Quantitative measurement of the effectiveness of unsaturated fatty acids required for the growth of *Saccharomyces cerevisiae*. J. Bacteriol. **115**:543–551.
5. **Carette, J. E., M. Stuiver, J. van Lent, J. Wellink, and A. van Kammen.** 2000. Cowpea mosaic virus infection induces a massive proliferation of endoplasmic reticulum but not Golgi membranes and is dependent on de novo membrane synthesis. J. Virol. **74**:6556–6563.
6. **Carette, J. E., J. van Lent, S. A. MacFarlane, J. Wellink, and A. van Kammen.** 2002. Cowpea mosaic virus 32- and 60-kilodalton replication proteins target and change the morphology of endoplasmic reticulum membranes. J. Virol. **76**:6293–6301.
7. **Chen, J., and P. Ahlquist.** 2000. Brome mosaic virus polymerase-like protein 2a is directed to the endoplasmic reticulum by helicase-like viral protein 1a. J. Virol. **74**:4310–4318.
8. **Crooke, E.** 2001. Escherichia coli DnaA protein-phospholipid interactions: in vitro and in vivo. Biochimie **83**:19–23.
9. **den Boon, J. A., J. Chen, and P. Ahlquist.** 2001. Identification of sequences in Brome mosaic virus replicase protein 1a that mediate association with endoplasmic reticulum membranes. J. Virol. **75**:12370–12381.
10. **Egger, D., B. Wolk, R. Gosert, L. Bianchi, H. E. Blum, D. Moradpour, and K. Bienz.** 2002. Expression of hepatitis C virus proteins induces distinct membrane alterations including a candidate viral replication complex. J. Virol. **76**:5974–5984.
11. **Gosert, R., A. Kanjanahaluethai, D. Egger, K. Bienz, and S. C. Baker.** 2002. RNA replication of mouse hepatitis virus takes place at double-membrane vesicles. J. Virol. **76**:3697–3708.
12. **Guinea, R., and L. Carrasco.** 1990. Phospholipid biosynthesis and poliovirus genome replication, two coupled phenomena. EMBO J. **9**:2011–2016.
13. **Hayat, M. A.** 2000. Principles and techniques of electron microscopy: biological applications, 4th ed. Cambridge University Press, Cambridge, United Kingdom.
14. **Hunter, K., and A. H. Rose.** 1972. Lipid composition of Saccharomyces cerevisiae as influenced by growth temperature. Biochim. Biophys. Acta **260**:639–653.
15. **Janda, M., and P. Ahlquist.** 1998. Brome mosaic virus RNA replication protein 1a dramatically increases in vivo stability but not translation of viral genomic RNA3. Proc. Natl. Acad. Sci. USA **95**:2227–2232.
16. **Janda, M., and P. Ahlquist.** 1993. RNA-dependent replication, transcription, and persistence of brome mosaic virus RNA replicons in S. cerevisiae. Cell **72**:961–970.
17. **Kao, C. C., and P. Ahlquist.** 1992. Identification of the domains required for direct interaction of the helicase-like and polymerase-like RNA replication proteins of brome mosaic virus. J. Virol. **66**:7293–7302.
18. **Kinnunen, P. K.** 1996. On the molecular-level mechanisms of peripheral protein: membrane interactions induced by lipids forming inverted nonlamellar phases. Chem. Phys. Lipids **81**:151–166.
19. **Kinnunen, P. K., A. Koiv, J. Y. Lehtonen, M. Rytomaa, and P. Mustonen.** 1994. Lipid dynamics and peripheral interactions of proteins with membrane surfaces. Chem. Phys. Lipids **73**:181–207.
20. **Kujala, P., A. Ikaheimonen, N. Ehsani, H. Vihinen, P. Auvinen, and L. Kaariainen.** 2001. Biogenesis of the Semliki Forest virus RNA replication complex. J. Virol. **75**:3873–3884.
21. **Lee, W. M., M. Ishikawa, and P. Ahlquist.** 2001. Mutation of host Δ9 fatty acid desaturase inhibits brome mosaic virus RNA replication between template recognition and RNA synthesis. J. Virol. **75**:2097–2106.
22. **Mackenzie, J. M., M. K. Jones, and E. G. Westaway.** 1999. Markers for *trans*-Golgi membranes and the intermediate compartment localize to induced membranes with distinct replication functions in flavivirus-infected cells. J. Virol. **73**:9555–9567.
23. **Magliano, D., J. A. Marshall, D. S. Bowden, N. Vardaxis, J. Meanger, and J. Y. Lee.** 1998. Rubella virus replication complexes are virus-modified lysosomes. Virology **240**:57–63.
24. **Maynell, L. A., K. Kirkegaard, and M. W. Klymkowsky.** 1992. Inhibition of poliovirus RNA synthesis by brefeldin A. J. Virol. **66**:1985–1994.
25. **Miller, D. J., M. D. Schwartz, and P. Ahlquist.** 2001. Flock house virus RNA replicates on outer mitochondrial membranes in *Drosophila* cells. J. Virol. **75**:11664–11676.
26. **Miller, W. A., T. W. Dreher, and T. C. Hall.** 1985. Synthesis of brome mosaic virus subgenomic RNA in vitro by internal initiation on (-)-sense genomic RNA. Nature (London) **313**:68–70.
27. **Miyazaki, M., H. J. Kim, W. C. Man, and J. M. Ntambi.** 2001. Oleoyl-CoA is the major de novo product of stearoyl-CoA desaturase 1 gene isoform and substrate for the biosynthesis of the Harderian gland 1-alkyl-2, 3-diacylglycerol. J. Biol. Chem. **276**:39455–39461.
28. **O'Reilly, E. K., Z. Wang, R. French, and C. C. Kao.** 1998. Interactions between the structural domains of the RNA replication proteins of plant-infecting RNA viruses. J. Virol. **72**:7160–7169.
29. **Paltauf, F., S. A. Henry, and S. D. Kohlwein.** 1993. Regulation and compartmentalization of lipid synthesis in yeast. p. 415–500. *In* E. W. Jones, J. R.

Pringle, and J. R. Broach (ed.), The molecular and cellular biology of the yeast Saccharomyces: gene expression, vol. 2. Cold Spring Harbor Laboratory, Cold Spring Harbor, N.Y.

30. **Perez, L., R. Guinea, and L. Carrasco.** 1991. Synthesis of Semliki Forest virus RNA requires continuous lipid synthesis. Virology **183:**74–82.
31. **Rattray, J. B., A. Schibeci, and D. K. Kidby.** 1975. Lipids of yeasts. Bacteriol. Rev. **39:**197–231.
32. **Reichel, C., and R. N. Beachy.** 1998. Tobacco mosaic virus infection induces severe morphological changes of the endoplasmic reticulum. Proc. Natl. Acad. Sci. USA **95:**11169–11174.
33. **Restrepo-Hartwig, M., and P. Ahlquist.** 1999. Brome mosaic virus RNA replication proteins 1a and 2a colocalize and 1a independently localizes on the yeast endoplasmic reticulum. J. Virol. **73:**10303–10309.
34. **Restrepo-Hartwig, M. A., and P. Ahlquist.** 1996. Brome mosaic virus helicase- and polymerase-like proteins colocalize on the endoplasmic reticulum at sites of viral RNA synthesis. J. Virol. **70:**8908–8916.
35. **Ritzenthaler, C., C. Laporte, F. Gaire, P. Dunoyer, C. Schmitt, S. Duval, A. Piequet, A. M. Loudes, O. Rohfritsch, C. Stussi-Garaud, and P. Pfeiffer.** 2002. Grapevine fanleaf virus replication occurs on endoplasmic reticulum-derived membranes. J. Virol. **76:**8808–8819.
36. **Rubino, L., A. Di Franco, and M. Russo.** 2000. Expression of a plant virus non-structural protein in Saccharomyces cerevisiae causes membrane proliferation and altered mitochondrial morphology. J. Gen. Virol. **81:**279–286.
37. **Scales, S. J., and R. H. Scheller.** 1999. Lipid membranes shape up. Nature **401:**123–124.
38. **Schneiter, R., and S. D. Kohlwein.** 1997. Organelle structure, function, and inheritance in yeast: a role for fatty acid synthesis? Cell **88:**431–434.
39. **Schwartz, M., J. Chen, M. Janda, M. Sullivan, J. den Boon, and P. Ahlquist.** 2002. A positive-strand RNA virus replication complex parallels form and function of retrovirus capsids. Mol. Cell **9:**505–514.
40. **Snijder, E. J., H. van Tol, N. Roos, and K. W. Pedersen.** 2001. Non-structural proteins 2 and 3 interact to modify host cell membranes during the formation of the arterivirus replication complex. J. Gen. Virol. **82:**985–994.
41. **Stewart, L. C., and M. P. Yaffe.** 1991. A role for unsaturated fatty acids in mitochondrial movement and inheritance. J. Cell Biol. **115:**1249–1257.
42. **Suhy, D. A., T. H. Giddings, and K. Kirkegaard.** 2000. Remodeling the endoplasmic reticulum by poliovirus infection and by individual viral proteins: an autophagy-like origin for virus-induced vesicles. J. Virol. **74:**8953–8965.
43. **Sullivan, M. L., and P. Ahlquist.** 1999. A brome mosaic virus intergenic RNA3 replication signal functions with viral replication protein 1a to dramatically stabilize RNA in vivo. J. Virol. **73:**2622–2632.
44. **Takegami, T., R. J. Kuhn, C. W. Anderson, and E. Wimmer.** 1983. Membrane-dependent uridylylation of the genome-linked protein VPg of poliovirus. Proc. Natl. Acad. Sci. USA **80:**7447–7451.
45. **Tuominen, E. K., C. J. Wallace, and P. K. Kinnunen.** 2002. Phospholipid-cytochrome c interaction: evidence for the extended lipid anchorage. J. Biol. Chem. **277:**8822–8826.
46. **Whittle, E., and J. Shanklin.** 2001. Engineering delta 9-16:0-acyl carrier protein (ACP) desaturase specificity based on combinatorial saturation mutagenesis and logical redesign of the castor delta 9-18:0-ACP desaturase. J. Biol. Chem. **276:**21500–21505.
47. **Wu, S. X., and P. Kaesberg.** 1991. Synthesis of template-sense, single-strand Flockhouse virus RNA in a cell-free replication system. Virology **183:**392–396.
48. **Zhang, S., Y. Skalsky, and D. J. Garfinkel.** 1999. MGA2 or SPT23 is required for transcription of the delta9 fatty acid desaturase gene, OLE1, and nuclear membrane integrity in Saccharomyces cerevisiae. Genetics **151:**473–483.

Traffic 2005; 6: 967–977
Blackwell Munksgaard

doi: 10.1111/j.1600-0854.2005.00339.x

EXPERT Review

Wrapping Things up about Virus RNA Replication

Jason Mackenzie*

School of Molecular and Microbial Sciences, University of Queensland, St. Lucia, Queensland 4072, Australia
**Corresponding author: Jason Mackenzie, j.mackenzie@uq.edu.au*

All single-stranded 'positive-sense' RNA viruses that infect mammalian, insect or plant cells rearrange internal cellular membranes to provide an environment facilitating virus replication. A striking feature of these unique membrane structures is the induction of 70–100 nm vesicles (either free within the cytoplasm, associated with other induced vesicles or bound within a surrounding membrane) harbouring the viral replication complex (RC). Although similar in appearance, the cellular composition of these vesicles appears to vary for different viruses, implying different organelle origins for the intracellular sites of viral RNA replication. Genetic analysis has revealed that induction of these membrane structures can be attributed to a particular viral gene product, usually a non-structural protein. This review will highlight our current knowledge of the formation and composition of virus RCs and describe some of the similarities and differences in RNA-membrane interactions observed between the virus families *Flaviviridae* and *Picornaviridae*.

Key words: cellular ultrastructure, membrane rearrangements, virus-host interactions, virus RNA replication

Received 1 June 2005, revised and accepted for publication 4 August 2005, published on-line 5 September 2005

Membrane wrapping is an important principle that many viruses use during their life cycles. As a virologist, I have learnt to appreciate that many years of evolution have 'educated' viruses in the ways of the cell. We have learnt many new aspects of cell biology from existing virus models, and I am sure that many more insights are yet to come. In this context, various laboratories have toiled long and hard to understand the cellular principles associated with virus replication. All RNA viruses, whether they infect mammalian, insect or plant cells, induce membrane structures. Replication of positive-sense RNA viruses is intimately linked to unique membrane structures that ultimately wrap around the active replication complexes (RCs), providing a membrane-bounded microenvironment in which RNA synthesis can occur. In many cases, these consist of small vesicles, approximately 70–100 nm in diameter, that accumulate in the perinuclear region of infected cells (1–7). These vesicles or spherules appear to be common to a number of virus families including alphaviruses (e.g. Semliki Forest virus), rubiviruses (e.g. Rubella virus), alphavirus-like superfamily (e.g. Brome mosaic virus), flaviviruses (e.g. Kunjin virus), tombusviruses (e.g. Carnation Italian ringspot virus) and alphanodaviruses (e.g. Flock House virus) (4–6,8–16). In each case, the spherules/vesicles themselves present as invaginations of a cellular membrane, of differing origins. Thus, the lumen is enclosed or bounded by a membrane but still has access to cytoplasmic constituents via an open neck. The presence of readily visible threads within these spherules/vesicles has lead to the belief that they contain the viral RNA. This idea has been strengthened by immunolabelling the spherules/vesicles with antibodies to double-stranded RNA (5,6,10,17) or exogenously added bromouridine (4,14,18), *in situ* hybridization (19,20) or treatment of infected cells with RNAse leading to the digestion and thus absence of the threads after embedding and microscopy (21). Hepatitis C virus (HCV), a member of the *Hepacivirus* genera within the *Flaviviridae* family of viruses, appears to induce more heterogenously sized vesicles within the perinuclear region (1,22). These vesicles were also shown to contain the viral RNA by *in situ* hybridization and *in vivo* labelling with bromouridine triphosphate (22). In contrast to the above morphology, coronaviruses and arteriviruses induce double-membrane vesicles (DMV) of approximately 80–100 nm in diameter (7,23,24). *In situ* experiments with BrUTP and conjugated riboprobes have established that these DMVs house the replicating RNA (7,23,24). Picornaviruses on the other hand still induce dramatic cytoplasmic vesiculation of cellular membranes to wrap the active replicating viral RNA. However, these membranes are much more heterogenous in size and shape (3,25–27). It is quite clear though that in each virus family the RC becomes surrounded by cellular membranes. More than likely, this wrapping of the RC ensures protection from host-response proteins recognizing the viral RNA, i.e. protein kinase R, but in addition also provides a stable and confined surface area for the polymerase and RC to assemble and function. As most of these structures appear morphologically similar, common modes of biogenesis must exist that are 'shared' by the virus families. It appears that almost each genera has its own way of exploiting host-cell machinery. This is especially true for the *picornaviruses*.

As there have been two recent reviews on RCs of other virus families (28,29), I will concentrate on two similar virus families – the *Flaviviridae* and the *Picornaviridae*

that differ in their mechanisms of RNA replication. Both families contain members of great health concerns for humans and domesticated animals.

The flavivirus replication complex and associated membranes

The *Flaviviridae* family consists of three genera: *Flavivirus*, *Pestivirus* and *Hepacivirus* (30). As the majority of the studies investigating the RC have been analysed using the flavivirus Kunjin virus (KUNV) as a model, this review will only discuss the *Flavivirus* genus. The *Flavivirus* genus comprises over 60 species, by far the largest member of the *Flaviviridae* family. These include a range of pathogens, such as dengue virus (DENV), West Nile virus (WNV), Yellow fever virus (YFV) and Tick-borne encephalitis virus (TBEV) that are important to both man and animals (30) (World Health Organization, Fact Sheet no. 117, 2002). Superficially, the flaviviruses appear to be relatively simple in structure and replication. They have a membrane and a genome consisting of an 11-kb single positive-sense RNA molecule that encodes one long open reading frame with no overlapping gene sequences or subgenomic RNA species. The translated proteins are post- and co-translationally cleaved by both host and viral proteases to yield the mature proteins (Figure 1) (30). The genes encoding the three structural proteins core (C), premembrane (prM) and envelope (E) are the first to be translated and are the only proteins found in secreted virions. The remaining seven non-structural (NS) proteins appear to play roles primarily in replication of the viral RNA (31); however, recent evidence suggests that some also contribute to virion assembly and/or maturation (32,33).

Flavivirus infection of cultured cells is associated with a reasonably long latent period of infection, approximately 12 h (34). Subsequently, replication increases exponentially which is associated with the induction and proliferation of unique and characteristic cytoplasmic membrane structures (35). These membranes have been described as convoluted membranes (CM), paracrystalline arrays (PC) and small vesicular structures (SMS; after chemical fixation) or vesicle packets [VPs; after cryofixation (36); Figure 2]. Our studies with WNV strain KUNV have provided a comprehensive and detailed analysis of the composition and function of the individual membranes during KUNV replication (31,37).

The first indication that these induced membranes were associated with RNA replication came from the seminal experiments by Chu and Westaway (38). Membrane fractions were isolated from cytoplasmic extracts separated by sucrose density centrifugation and analysed for protein composition and viral RNA species [either after direct separation or for RNA-dependent RNA polymerase (RdRp) activity in the isolated fractions]. Electron microscopy (EM) of the RdRp-active fractions revealed a striking correlation of KUNV NS proteins implicated in viral RNA synthesis with the KUNV-induced membranes in infected cells. Immunolabelling of thawed cryosections prepared from DENV-infected cells revealed a significant accumulation of NS1 within distinct morphological membrane structures, that we termed VP (6,36). Double-labelling with antibodies to dsRNA revealed co-localization of both antibodies only within the VP, strongly suggesting the VPs were the intracellular sites of DENV RNA replication (6). *In situ* hybridization of resin-embedded sections from DENV-infected cells supported the proposal that the VPs are the same structure as the SMS (19). We could show that the NS proteins NS1, NS2A, NS3, NS4A, NS5 and dsRNA were all localized to VP (17,39), whereas NS2B, NS3

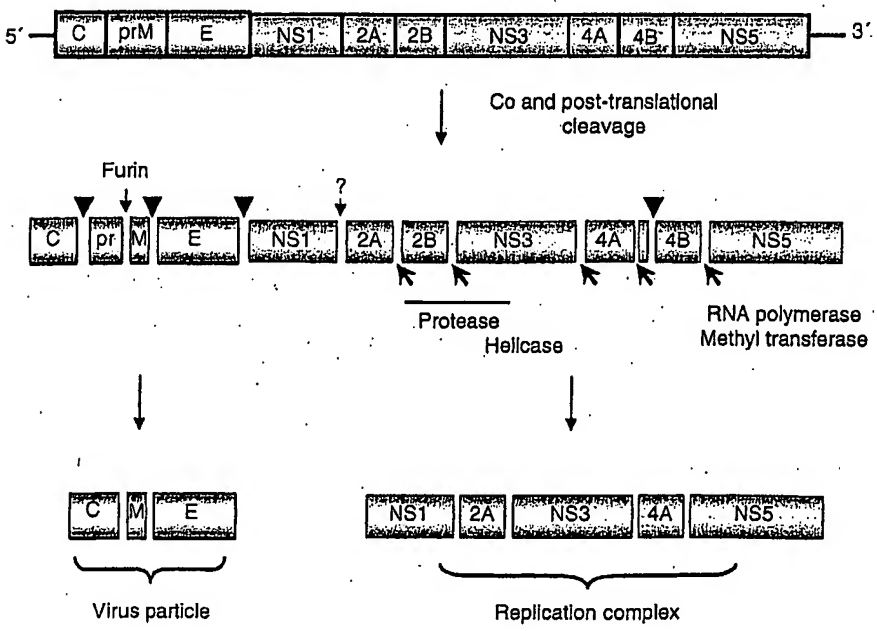

Figure 1: Schematic representation of the *Flavivirus* genome organization and polyprotein-processing events associated with replication. Cleavage sites depicted with a ▼ represent cleavage by host-signal peptidase within the lumen of the endoplasmic reticulum. Sites represented with a ↖ depict cleavage by the viral-encoded protease NS3 with cofactor NS2B. The cleavage between NS1 and NS2A is currently not well understood but is performed by a host-cell protease in the lumen of the endoplasmic recticulum.

NS4A and
localized to
the nucleus
NS3 that v
proposed t
and proteol
protease N
and KUNV
indicated th
synthesis.
additionally
with bromc

The immun
biochemica
ing model
(31). Our a
NS5 binds
NS3 then a
ing RC is th
brane thro
NS4A and I
in the pres
dicted that
the VP (ste
invaginatior
continues,
This is ana
and *alphav*
the cytopla
within the i
It is presur
required f
through th
translocate
NS4A pres
ER membr
that this in
the cytopl
interaction
mide treatr
the RC is u
recruitmen
within the
RNA is exp
tic processi
tion and re
nascent R
Following t
to the rEI
immature v

An importa
membrane
For flaviviri
plex. As d
brane struc
the rER, Cl

EXHIBIT A

NS5 localized to CM/PC (17,39), and NS4B localized to proliferated endoplasmic recticulum (ER) and the nucleus (40). Based on the known protease activity of NS3 that works in concert with its cofactor NS2B, we proposed the CM/PC to be sites of protein translation and proteolytic cleavage of the polyprotein by the KUNV protease NS2B-NS3 (17). Whereas localization of dsRNA and KUNV proteins associated with RNA replication (17) indicated that the VPs constitute the sites of viral RNA synthesis. The role of VP in viral RNA synthesis was additionally confirmed by *in situ* labelling of nascent RNA with bromouridine (18).

The immunolocalization data, together with molecular and biochemical results (41–44), led us to propose the following model of the events during flavivirus RNA replication (31). Our assumption is that on completion of translation, NS5 binds the 3′ end of the (+) RNA molecule. NS2A and NS3 then also bind to the RNA and/or NS5. This preforming RC is then directed to the cytoplasmic face of a membrane through interaction with two additional proteins, NS4A and NS2A. Importantly, this interaction only occurs in the presence of viral RNA (39). At this point, we predicted that the RC-bound viral RNA becomes wrapped in the VP (step 1 in Figure 2B) and is contained within this invagination where efficient replication of the viral RNA continues, hidden from the host-surveillance proteins. This is analogous to models proposed for *alphaviruses* and *alphavirus*-like superfamily (8,14), whereby access of the cytoplasmic viral RNA to the active viral RC housed within the indented vesicular pits is through an open neck. It is presumed that other cellular factors and nucleotides required for efficient RNA replication can also pass through the vesicle neck. Interestingly, although NS1 translocates into the ER lumen, it is able to interact with NS4A presumably via regions of NS4A that transverse the ER membrane. However, genetic studies have suggested that this interaction is mediated by residues in NS4A on the cytoplasmic face of the membrane (45). How this interaction occurs is not fully understood. As cycloheximide treatment does not affect replication, it is likely that the RC is used for multiple rounds of replication/membrane recruitment of the RC facilitated by its confined location within the VP (18). Following replication within the VP, the RNA is exported to the CM/PC for translation and proteolytic processing (step 2 in Figure 2B). It is known that translation and replication are coupled and that replication of a nascent RNA molecule is required for packaging (46). Following translation, the RNA molecule is then transported to the rER where assembly of the nucleocapsid and immature virion occurs (47) (Step 3 in figure 2B).

An important focus for virologists is the cellular origins of membranes and proteins involved in viral RNA replication. For flaviviruses, this process appears bewilderingly complex. As described above, there are three distinct membrane structures associated with the flavivirus life cycle – the rER, CM/PC and VP – all of which are to some extent related to membranes derived from the early secretory pathway (Figure 2). Interestingly, each of these membrane structures contains a distinct set of viral proteins with apparently different functions (see above). Furthermore, each of the membrane structures appears to contain a different subset of host proteins (48). Significantly, the *trans*-Golgi marker β-1,4-galactosyltransferase (GalT) localized to the VPs in KUNV-infected Vero cells (48); GalT was especially concentrated in membranes of the vesicles within the packet and not the bounding membrane itself. Other *trans*-Golgi network (TGN) markers such as p230 and TGN46 also localize within the VP, whereas p200 and γ-adaptin were not observed (Jason Mackenzie, unpublished observations). Notably, although much of the GalT, TGN46 and p230 redistributed to the VP, a subset of these proteins remained associated with the Golgi apparatus, which appeared morphologically unperturbed and had the normal distribution of the Golgi *cis*- and *medial*-cisternae protein Giantin (48). An intact Golgi apparatus is a strict requirement for flavivirus replication, because the fully assembled virions exit the cell through the Golgi apparatus (47), and furin cleavage of prM (which occurs at the *trans* side of the Golgi) to M is essential for virus infectivity (49). In contrast to TGN proteins, ERGIC-53, a recognized marker for the intermediate compartment (IC) (50), did not localize to the VP but accumulated within the CM/PC. Protein disulphide isomerase (PDI; an rER resident protein) was observed to label rER continuous with the CM/PC but was not significantly found within the CM/PC (48). Thus, it would appear that a subset of TGN/Golgi protein associates intimately with the ER/IC-derived CM/PC and that the CM/PC are physically continuous with the rER.

Our data offer insights into the long-standing controversy about the organization of the IC. In one, still popular view, the IC is considered as a compartment distinct from the ER and the Golgi (51–53). Others propose that the IC is continuous with the ER and the *cis* Golgi (52,53). Our data, in flavivirus-infected cells, show clearly that the rER and IC appear as continuous structures: the rER (identified with anti-PDI antibodies) and the CM/PC (defined as the IC by its labelling with anti-ERGIC-53 antibodies). Our observations strongly support a transport model, whereby proteins are transported from the rER to the IC via a continuous membrane rather than via vesicular steps.

Brefeldin A (BFA) is a fungal metabolite and a potent inhibitor of anterograde membrane transport due to its effects on the activity of ADP ribosylation factor (ARF). Among other activities, the action of BFA prevents coatomer proteins binding to membranes (54), culminating in the disassembly of the Golgi apparatus and redistribution of Golgi proteins to the ER. Our studies with BFA-treated, KUNV-infected cells have clearly indicated that anterograde membrane and/or protein transport are required for biogenesis of the KUNV membrane structures, but only at an early step in the replication cycle (48). Membrane

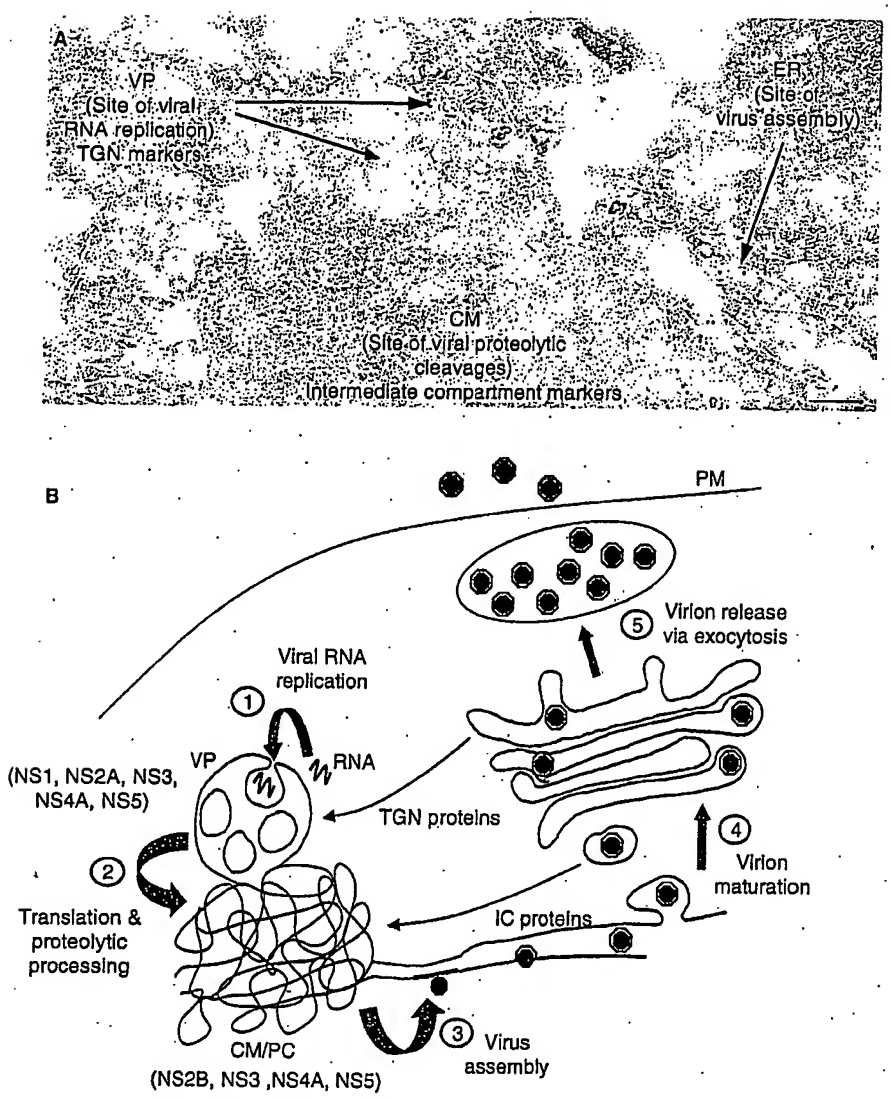

Figure 2: Ultrastructural observations of Kunjin virus-infected Vero cells at 24 h post-infection. Panel A reveals immunogold labelling of a thawed cryosection prepared from Kunjin virus-infected cells with antibodies raised against protein disulphide isomerase (PDI) and 10 nm protein-A gold. Note the labelling of the lumen of the rER continuous with the convoluted membranes (CM) but no labelling within this structure. Adjacent vesicle packets (VPs) are also devoid of the PDI antibodies. Magnification bar represents 200 nm. Schematic representation of the flavivirus life cycle is depicted in Panel B. Step 1 proposes the incorporation of cytoplasmic viral RNA into the VP for replication by the replication complex. (2) The transcribed viral RNA is then transported to the CM/PC for translation and proteolytic cleavage via both host- and viral-encoded proteases. (3) Subsequently, the RNA is encapsidated by the core protein, and virion assembly proceeds via budding into the ER lumen. (4) Virion maturation occurs via transit through the Golgi apparatus before release through the plasma membrane (PM) via exocytosis (5). Redistribution of *trans*-Golgi network (TGN) and intermediate compartment (IC) host proteins to the VP and CM/paracrystalline arrays (PC), respectively, are highlighted.

induction was not inhibited once the membranes themselves were formed, after the latent period (48). Additionally, GalT localized within the VP was also resistant to dispersion; this is in contrast to the redistribution of GalT observed in uninfected cells treated under similar conditions (48).

It is not clear at present which of the flaviviral proteins are responsible for membrane induction. However, after examination of cell lines bearing KUNV replicons of variable replication efficiencies, the 'induced' membranes were only found in cell lines that harboured efficiently replicating replicons (55). This suggested that one or more of the NS proteins is required for membrane induction and indicated a direct correlation between the extents of viral protein synthesis/accumulation and membrane proliferation/alteration. Analysis of the cellular origins of these membranes in replicon-transduced cells was in

total agreement with that observed during virus infection, except for the notable difference in the distribution of dsRNA and GalT (55). The subcellular distribution of the replicon dsRNA appeared as small foci scattered throughout the cytoplasm by immunofluorescence (IF) that presented as isolated foci on the cytoplasmic face of the ER when observed by cryo-immunoelectron microscopy with anti-dsRNA antibodies (55). This labelling pattern is strikingly similar to the pattern obtained in cell lines harbouring HCV replicons, using *in situ* hybridization or *in vivo* labelling of nascent viral RNA with BrUTP (22). Recent evidence has indicated that the HCV NS4B proteins has the capacity to induce membrane rearrangements resembling those observed in cell lines replicating a HCV replicon (1,56). However, our recent results argue that at least the KUNV polyprotein NS2B-NS3-NS4A by itself contains the required attributes to induce cytoplasmic membrane structures analogous to those observed during flavivirus infection (Jason Mackenzie, unpublished observations).

Replication complex of the picornaviridae

Investigation of the RCs of picornaviruses has been pioneered by the elegant and comprehensive studies of Kurt Bienz and Denise Egger (Basel, Switzerland). Their systematic approach has been an inspiration for other investigators (including myself) who have studied the RCs of their own viruses.

Like the *Flaviviridae*, the *Picornaviridae* genomic RNA is translated as a polyprotein, albeit initiated by an internal ribosomal entry site and post- and co-translationally cleaved by host- and viral-encoded proteases (Figure 3). The mature proteins assemble on the 3′ end of the (+)-strand RNA to initiate (–)-strand synthesis. It is proposed that this occurs on the cytoplasmic face of membranes facilitated by the interaction of the hydrophobic viral proteins with host membranes. Poliovirus (PV) proteins 2B, 2C and 3A are all tightly associated with ER membranes, and 2C binds specifically to the 3′ end of the minus-strand RNA, and 3Dpol specifically associates with the input positive-sense RNA to generate minus-strand RNA. Specific protein–protein interactions within the RC are difficult to dissect, as all the PV proteins, both structural and NS, reside within the RC (Figure 4). Furthermore, the presence of different polyprotein species makes it difficult to specifically identify individual proteins by immunolabelling. An antibody raised against one protein could also recognize the polyprotein it is derived from. The early stages of replication likely occur on rER membranes until sufficient viral protein accumulates and cellular membranes are rearranged.

The initial connection between 'induced' vesicles and RNA replication was revealed by high-resolution autoradiography (2) and subsequently extended using detailed *in situ* hybridization and immunogold labelling of prepared embedded sections from PV-infected cells (57,58); similar techniques were used on membranes isolated from sucrose density gradient fractions containing active RNA polymerase activity (58–60). These experiments showed not only that the viral RNA and proteins involved in replication were associated with the proliferating membranes, but also that these membranes supported active replication (61). More intriguing was the appearance of the isolated membranes which were observed as vesicle rosettes (60). An interesting property of these rosettes was that they readily dissociate at low temperature or under low ionic conditions into tubulo vesicular structures and can reassemble into a functional complex on increased incubation at 30 °C (61).

Infection of mammalian cells with members of the *Picornaviridae* family results in a dramatic vesiculation and disintegration of internal membrane structures (3,25,62–64). The vesicles within these clusters range in size from 70 to 500 nm in diameter and appear to accumulate within the perinuclear area (Figure 4). Evidence for a requirement for continuous lipid synthesis to facilitate

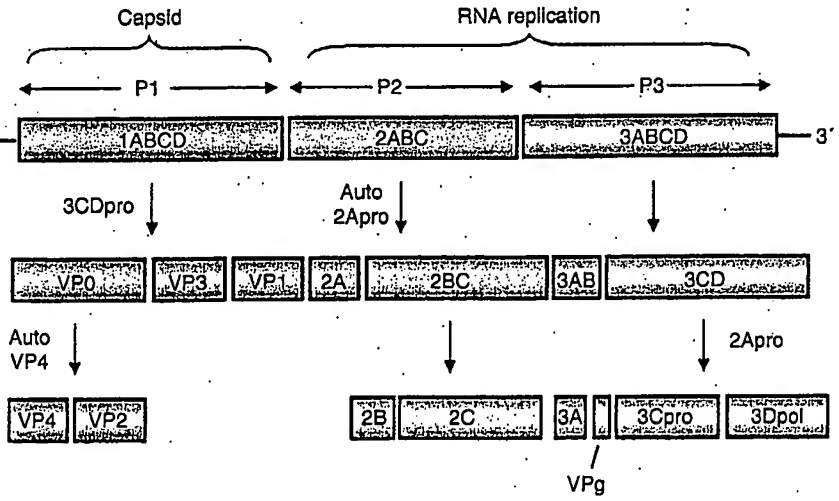

Figure 3: Schematic representation of the genomic organization of the *Picornavirus* genome and polyprotein species generated via virus-specific proteolysis. Many of these polyprotein species have specific roles during replication of *picornaviruses*.

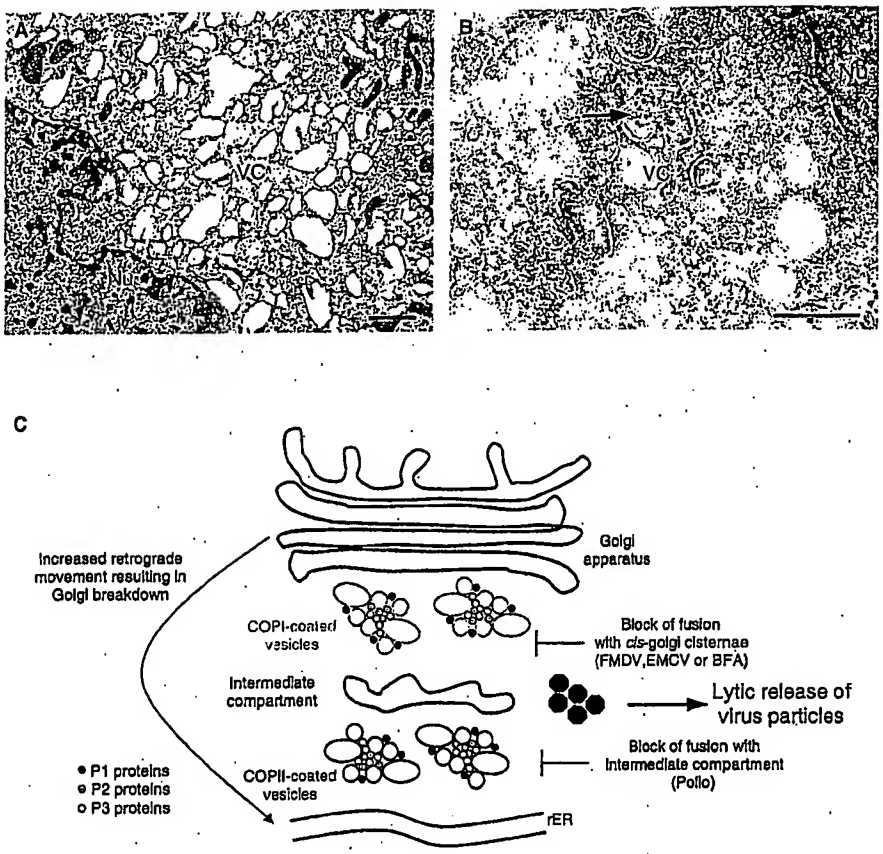

Figure 4: Ultrastructural analysis of *Parechovirus*-infected BSC-1 cells at 6 h post-infection. In (A), the resin-embedded section reveals vesicle clusters (VCs) accumulating in the perinuclear region. The vesicles range in size from approximately 100–800 nm. B) immunogold labelling of cryosections from parechovirus-infected cells reveals the vesicle clusters heavily decorated with antibodies to dsRNA and 10 nm protein-A gold. C) Schematic representation of membrane rearrangements observed during picornavirus infection. Anterograde transport carriers are restricted at different stages of the secretory pathway depending on the different viruses investigated. This restriction in transport of protein and membrane to the Golgi apparatus leads to the eventual disintegration of the Golgi due to the redistribution of Golgi proteins and membrane to the ER via retrograde movement. Nu, nucleus. Magnification bars represent 1 μm and 200 nm in Panels A and B, respectively.

viral RNA replication has emerged from two independent observations. Firstly, experiments using the phospholipid synthesis inhibitor cerulenin showed that replication and infectivity of members of the *Picornaviridae* was greatly reduced in the presence of the drug (65–67). Subsequent studies indicated that many other RNA viruses are equally sensitive to the action of cerulenin suggesting a broad spectrum activity against viruses requiring lipid moieties (68,69). Secondly, PV-induced vesicles, and thus the RC formed from defective viruses, cannot support the replication of superinfecting wild-type PV (26,70). This suggests that each membranous RC must be formed in *cis* from nascent translated viral proteins recruiting cellular membranes. This inability to 'recycle' RCs may explain some of the difficulties in *trans*-complementing defective PV genomes (71).

One model in the PV field speculates that the virally induced membranes in the peri-nuclear area of the cell reflect the inhibition of the host secretory pathway leading to an accumulation of anterograde transport carriers. Such a process is potentially blocked by BFA, as this drug stops anterograde transport by inhibiting the ARF-exchange factor resulting in dissociation of the COP1 coat. However, experiments using BFA have revealed that different viruses within the *Picornaviridae* family have different susceptibilities to BFA (3,72,73) and may use different host membrane components. Poliovirus and Echovirus 11 are extremely sensitive to BFA treatment (3,73), whereas foot-and-mouth disease virus (FMDV) and encephalomyocarditis virus (EMCV) are resistant to BFA effects (3,27), and Parechovirus displays some partial sensitivity (3). For the susceptible viruses, the effects of BFA can be rationalized by results indicating a role for host coat proteins in the formation of picornavirus RCs. Poliovirus appears to use COPII proteins early in the formation of the RC to induce the viral vesicles (74). However, late in infection most cellular proteins are also associated with the PV

vesicles (75).
posed that th
nents occurr
transport ves
grade transp
observed to
p63) (74,76,7
dent formatio
replication is
of COPII pro
by this drug (
experiments
replication pr
the PV protei
membranes
interesting to
(81,82), and
observed to
the PV 2C pr
vesicles with
11 infections
viral replicati
sitive to BFA
can be ass
Interestingly,
throughout 1
BFA itself, w
Additionally,
to the RC (J
observations
these vesicl
require neith
effects of BI
very little re
the IC during
ing that th

Figure 5: Im
localization o
observed wit
tion is recogr

EXHIBIT A

vesicles (75). Based on these observations, it was proposed that the PV vesicle induction using COPII components occurred in a manner similar to the formation of transport vesicles in uninfected cells (74). Like anterograde transport vesicles, the PV vesicles were also observed to exclude ER-resident marker proteins (e.g. p63) (74,76,77). Nevertheless, the apparent COPII-dependent formation of the PV vesicles does not explain why PV replication is sensitive to BFA. The dynamics and activity of COPII proteins is generally assumed to be unaffected by this drug (78). Rather, BFA sensitivity and some *in vitro* experiments strongly implicate ARF directly in the virus replication process (79,80). Recent data has implied that the PV proteins 3A or 3CD can induce ARF translocation to membranes facilitating active PV replication (79). It is interesting to note that the PV 2C protein is a GTPase (81,82), and a single point mutation within 2C was observed to render PV resistant to BFA (83). Perhaps, the PV 2C protein may stabilize coatomer proteins on the vesicles within the clusters. In contrast to PV, Echovirus 11 infections lead to an active redistribution of COPI to the viral replication sites, and infection is also extremely sensitive to BFA (3). Therefore, a direct role of COPI proteins can be assumed in the replication of Echovirus 11. Interestingly, Parechovirus infection dispersed COPI throughout the cytoplasm (3), similar to the action of BFA itself, with some COPI also observed within the RC. Additionally, we and others have observed GalT to localize to the RC (Jason Mackenzie and E. Gazina, unpublished observations) (62) suggesting a possible Golgi origin of these vesicles. In contrast, EMCV and FMDV appear to require neither COPI or COPII and are both resistant to the effects of BFA (3,27). In this context, it is surprising that very little research has sought to investigate the role of the IC during picornavirus replication, especially considering that the IC represents a crossroads within the secretory pathway, where a switching of COPII to COPI proteins on transport carriers is thought to occur (84). Experiments with FMDV showed a slight dispersion of ERGIC-53 from the perinuclear region to scattered foci within the cytoplasm (27). However, our preliminary data suggest some excellent co-localization of Echovirus 11 and EMCV RC with anti-ERGIC-53 antibodies by IF (Figure 5). The distribution of ERGIC-53 appears relatively unaffected during these infections with coincident labelling observed both in the perinuclear region and in isolated cytoplasmic foci (Figure 5).

The results summarized above strongly implicate a dynamic association of ARF, COPI and COPII components with *picornavirus* replication, possibly regulated and/or stabilized by the viral proteins 2C, 3A and 3CD. The effect of BFA may relate to the activity of protein 2C, to release COPII and/or bind and stabilize COPI to the vesicle membranes. This stabilizing of COPI and ARF to cellular membranes may explain why large vesicles are observed during picornavirus infection, as the COPI-bound vesicles would retain the capacity to fuse to other membranes bearing the appropriate tether. Whether or not the COP proteins are directly required for RNA replication and/or virus assembly is not currently known, but siRNA knockdown experiments may provide a better understanding in the future. It has been speculated that perhaps this dismantling of the secretory pathway is an active measure to prevent cell-surface expression of immunoregulatory molecules such as MHC I (85–87). It is important to note that *picornaviruses* do not require an intact secretory pathway for virion maturation, as the virions have no membranes and consist of assembled capsid subunits that are released via a lytic process (rather than through exocytosis; Figure 4C). Additionally, the capsid proteins required for virus assembly are also intimately associated

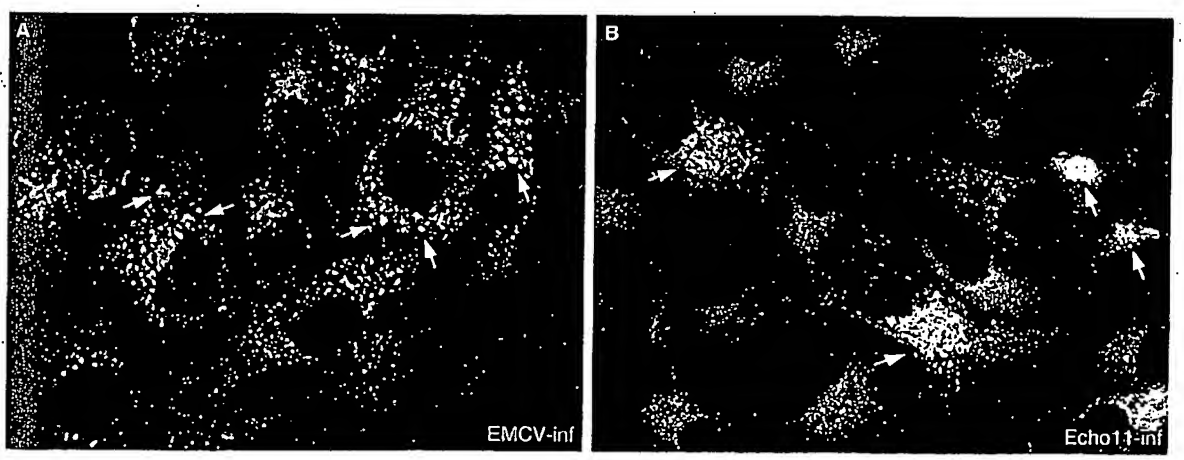

Figure 5: Immunofluorescene analysis of EMCV-infected (A) and Echovirus 11-infected (B) BSC-1 cells at 6 h post-infection. Co-localization of anti-dsRNA (labelled with Alexa Fluor 488; green) and anti-ERGIC53 (labelled with Alexa Fluor 568; red) antibodies is observed within discrete cytoplasmic foci representing the picornavirus replication complex (highlighted with arrowheads). Dual localization is recognized as a yellow hue in both panels.

with the vesicle clusters (61,88) (Figure 4C), exemplifying the organized membranous microenvironment facilitating virus replication.

Another model proposed by the Kirkegaard laboratory (Stanford, USA) suggests a role for autophagy in the generation of the PV vesicle clusters (75,77). Autophagy is a membrane-dependent engulfment of cytoplasmic constituent destined for degradation typified by the presence of DMV structures (89). Using high-pressure freezing and EM, the PV vesicles were presented as DMVs resembling autophagic vesicles (75). Earlier studies investigating Mouse Hepatitis virus (MHV) and Equine Arterivirus RNA replication revealed the presence of DMVs harbouring the viral RC (23,24,90). The studies by van der Meer *et al.* (24) identified the presence of the endosomal markers lamp-1 and endocytosed BSA-gold in the MHV RC; however, the role of autophagy was not investigated. Recent studies on MHV have suggested that the process of autophagy may contribute to the formation and stability of MHV RCs, as MHV replication was impaired in an autophagy knock-out cell line (91). Immunogold labelling indicated the presence of the autophagosomal protein LC3 (92–94) as well as cellular markers from different organelles within the PV RC (75). Additionally, when MHV- and PV-infected cells were incubated in the presence of a chemical inhibitor of autophagy, 3-methyladenine, there was decreased viral replication (91,94). Consistent with this biogenesis model is the fact that although dramatic breakdown of the Golgi apparatus occurs during PV infection, an intact Golgi apparatus or *trans*-Golgi network is not essential for the formation of autophagic vacuoles (95). Yet in contrast, BFA does not seem to prevent the formation of autophagic vacuoles but rather tends to increase the volume fraction of autophagic vacuoles (95). These contradictory results could suggest that more than one mechanism underlies PV vesicle formation, perhaps implying a combined use of anterograde membrane transport and autophagy. It can be envisaged that on prevention and accumulation of anterogade transport vesicles, the Golgi apparatus breaks down due to the retrograde movement of Golgi enzymes and proteins to the ER (as observed during treatment of uninfected cells with BFA). This accumulation of proteins within the ER may trigger host-cell responses to signal proteolysis of the accumulated proteins within the ER, possibly initiating autophagy. With such a rapid life cycle, the window of opportunity for researchers to dissect the steps of picornavirus replication is limited.

To gain additional insights into the process of membrane induction in the absence of viral replication, viral proteins have been expressed individually. Such studies have been successful in identifying viral factors involved in membrane proliferation for a number of *picornaviruses*. In each case, expression of proteins from the P2 and P3 region of the genome leads to membrane alterations analogous to those observed during wild-type infection. Further experiments indicate a role for the polyprotein precursor 2BC and 2C itself in inducing vesicle clusters (96–98). Expression of each of the individual proteins alone has highlighted the membrane association and destabilizing effects of proteins 2B, 2C and 3A (99,100). Both 2B and 3A are efficient immobilizers of membrane and protein trafficking through the secretory pathway, with 2B displaying some specificity for the Golgi apparatus (101). By contrast, 3A appears to restrict protein export from the ER (102) perhaps inducing the dispersion of coat proteins from newly forming transport vesicles. However, recent observations have indicated that only the FMDV protein 2BC can inhibit protein trafficking to the cell plasma membrane, and FMDV proteins 2B, 2C and 3A do not convey these properties (100). On the other hand, protein 2C does not block protein transport, yet induces vesicle clusters analogous to those observed in the cytoplasm during wild-type infection (98,103). The PV protein 3D – the virus encoded RdRp – has been the focus of many structural analyses. The goal of these studies has been to identify peptide-binding pockets that might be targets for chemical inhibitors. Nevertheless, some interesting observations were made after EM analysis of the purified protein. The higher order structure of purified 3D was observed to be an ordered sheet or lattice (104). These arrays also had the capacity to form tubules. It was thus proposed that 3D is recruited to the membrane via interaction with 3AB and that this physical interaction between the 3D molecules induces assembly of the observed lattices forming a uniform surface area that can subsequently be utilized for RNA replication (104).

Concluding Remarks

In reviewing our current knowledge of the replication of two well-studied families of viruses, it is clear that we still have a long way to go. Like all viruses, the subversion of cellular machinery and pathways is crucial for virus propagation and survival. The specific interaction and recruitment of host factors and distinct membrane domains to virus replication sites imply different strategies for the manipulation of host components. Dissection of the steps taken during biogenesis of the viral RC has highlighted some basic cell biology principles, especially relating to membrane traffic from the ER to IC and Golgi apparatus and possible subdomains within the *trans*-Golgi. Questions still remain as to why different picornaviruses use distinct host components in producing morphologically similar vesicle structures. Also, what role does the apparent dynamic exchange of ARF and COP proteins play in the virus lifecycle? Is it merely a mechanism to prevent surface expression and secretion of immune regulatory molecules or is it directly involved in the assembly process? In contrast, flaviviruses redistribute *trans*-Golgi proteins to their sites of viral RNA replication. What roles do host glycosylation and sorting proteins play in viral RNA replication and why do positive-sense RNA viruses wrap their replicative machinery? Is it simply

to ensure gre
proteins and
environment
area for RC a
translation a
tions? Or are
(i.e. dsRNA)
stranded RN
case, viruses
and dissect r
doubt contin
'wrap up' th
these familie

Acknowle

I thank Gareth C
the manuscript
I thank Elena Ga
53 immunofluor
our research by
Australia.

Reference

1. Egger D, V
K. Express
alterations
2002;76:5
2. Bienz K, E
the P2 ge
induced r
immunocy
220–226.
3. Gazina EV
requireme
among thr
4. Kujala P, Ik
Biogenesis
2001;75:3
5. Magliano D
Rubella vi
Virology 1
6. Mackenzie
dengue vi
RNA replic
7. Pedersen
frame 1a-
plasmic re
viral replic
8. Froshauer
located o
J Cell Biol
9. Kujala P,
Intracellul
J Virol 19
10. Lee JY, M
replicatio
Virology 1

EXHIBIT A

to ensure greater efficiency of replication by concentrating proteins and molecules within a desired membranous environment? Is it to provide a greater membrane surface area for RC assembly and increased cellular machinery for translation and subsequent post-translational modifications? Or are the viruses hiding potential cell activators (i.e. dsRNA) from host surveillance molecules like double-stranded RNA-dependent protein kinase (PKR)? In any case, viruses have provided us with models to understand and dissect many cellular trafficking pathways and will no doubt continue to do so. I hope that eventually we can 'wrap up' the events associated with the replication of these families of pathogenic positive-sense RNA viruses.

Acknowledgments

I thank Gareth Griffiths and Jacomine Krijnse-Locker for critical review of the manuscript and making it a much better manuscript than the original. I thank Elena Gazina for the Parechovirus-infected cells and for the ERGIC-53 immunofluorescence pictures. I also want to acknowledge support of our research by the National Health and Medical Research Council of Australia.

References

1. Egger D, Wolk B, Gosert R, Bianchi L, Blum HE, Moradpour D, Bienz K. Expression of hepatitis C virus proteins induces distinct membrane alterations including a candidate viral replication complex. J Virol 2002;76:5974–5984.
2. Bienz K, Egger D, Pasamontes L. Association of polioviral proteins of the P2 genomic region with the viral replication complex and virus-induced membrane synthesis as visualized by electron microscopic immunocytochemistry and autoradiography. Virology 1987;160:220–226.
3. Gazina EV, Mackenzie JM, Gorrell RJ, Anderson DA. Differential requirements for COPI coats in formation of replication complexes among three genera of Picornaviridae. J Virol 2002;76:11113–11122.
4. Kujala P, Ikaheimonen A, Ehsani N, Vihinen H, Auvinen P, Kaariainen L. Biogenesis of the Semliki Forest virus RNA replication complex. J Virol 2001;75:3873–3884.
5. Magliano D, Marshall JA, Bowden DS, Vardaxis N, Meanger J, Lee JY. Rubella virus replication complexes are virus-modified lysosomes. Virology 1998;240:57–63.
6. Mackenzie JM, Jones MK, Young PR. Immunolocalization of the dengue virus nonstructural glycoprotein NS1 suggests a role in viral RNA replication. Virology 1996;220:232–240.
7. Pedersen KW, van der Meer Y, Roos N, Snijder EJ. Open reading frame 1a-encoded subunits of the arterivirus replicase induce endoplasmic reticulum-derived double-membrane vesicles which carry the viral replication complex. J Virol 1999;73:2016–2026.
8. Froshauer S, Kartenbeck J, Helenius A. Alphavirus RNA replicase is located on the cytoplasmic surface of endosomes and lysosomes. J Cell Biol 1988;107 (6 Pt 1):2075–2086.
9. Kujala P, Ahola T, Ehsani N, Auvinen P, Vihinen H, Kaariainen L. Intracellular distribution of rubella virus nonstructural protein P150. J Virol 1999;73:7805–7811.
10. Lee JY, Marshall JA, Bowden DS. Characterization of rubella virus replication complexes using antibodies to double-stranded RNA. Virology 1994;200:307–312.
11. Lee JY, Marshall JA, Bowden DS. Replication complexes associated with the morphogenesis of rubella virus. Arch Virol 1992;122:95–106.
12. Ng ML. Ultrastructural studies of Kunjin virus-infected Aedes albopictus cells. J Gen Virol 1987;68:577–582.
13. Hatta T, Bullivant S, Matthews RE. Fine structure of vesicles induced in chloroplasts of Chinese cabbage leaves by infection with turnip yellow mosaic virus. J Gen Virol 1973;20:37–50.
14. Schwartz M, Chen J, Janda M, Sullivan M, den Boon J, Ahlquist P. A positive-strand RNA virus replication complex parallels form and function of retrovirus capsids. Mol Cell 2002;9:505–514.
15. Russo M, Di Franco A, Martelli GP. Cytopathology in the identification and classification of tombusviruses. Intervirology 1987;28:134–143.
16. Miller DJ, Schwartz MD, Ahlquist P. Flock house virus RNA replicates on outer mitochondrial membranes in Drosophila cells. J Virol 2001;75:11664–11676.
17. Westaway EG, Mackenzie JM, Kenney MT, Jones MK, Khromykh AA. Ultrastructure of Kunjin virus-infected cells: colocalization of NS1 and NS3 with double-stranded RNA, and of NS2B with NS3, in virus-induced membrane structures. J Virol 1997;71:6650–6661.
18. Westaway EG, Khromykh AA, Mackenzie JM. Nascent flavivirus RNA colocalized in situ with double-stranded RNA in stable replication complexes. Virology 1999;258:108–117.
19. Grief C, Galler R, Cortes LM, Barth OM. Intracellular localisation of dengue-2 RNA in mosquito cell culture using electron microscopic in situ hybridisation. Arch Virol 1997;142:2347–2357.
20. Restrepo-Hartwig M, Ahlquist P. Brome mosaic virus RNA replication proteins 1a and 2a colocalize and 1a independently localizes on the yeast endoplasmic reticulum. J Virol 1999;73:10303–10309.
21. Di Franco A, Russo M, Martelli GP. Ultrastructural and origin of cytoplasmic multivesicular bodies induced by Carnation Italian Ringspot virus. J Gen Virol 1984;65:1233–1237.
22. Gosert R, Egger D, Lohmann V, Bartenschlager R, Blum HE, Bienz K, Moradpour D. Identification of the hepatitis C virus RNA replication complex in Huh-7 cells harboring subgenomic replicons. J Virol 2003;77:5487–5492.
23. Gosert R, Kanjanahaluethai A, Egger D, Bienz K, Baker SC. RNA replication of mouse hepatitis virus takes place at double-membrane vesicles. J Virol 2002;76:3697–3708.
24. van der Meer Y, Snijder EJ, Dobbe JC, Schleich S, Denison MR, Spaan WJ, Locker JK. Localization of mouse hepatitis virus nonstructural proteins and RNA synthesis indicates a role for late endosomes in viral replication. J Virol 1999;73:7641–7657.
25. Bienz K, Egger D, Rasser Y, Bossart W. Intracellular distribution of poliovirus proteins and the induction of virus-specific cytoplasmic structures. Virology 1983;131:39–48.
26. Egger D, Bienz K. Recombination of poliovirus RNA proceeds in mixed replication complexes originating from distinct replication start sites. J Virol 2002;76:10960–10971.
27. Knox C, Moffat K, Ali S, Ryan M, Wileman T. Foot-and-mouth disease virus replication sites form next to the nucleus and close to the Golgi apparatus, but exclude marker proteins associated with host membrane compartments. J Gen Virol 2005;86:687–696.
28. Salonen A, Ahola T, Kaarialnen L. Viral RNA replication in association with cellular membranes. Curr Top Microbiol Immunol 2005;285:139–173.
29. Novoa RR, Calderita G, Arranz R, Fontana J, Granzow H, Risco C. Virus factories: associations of cell organelles for viral replication and morphogenesis. Biol Cell 2005;97:147–172.
30. Lindenbach BD, Rice CM. Flaviviridae: the viruses and their replication, 4th edn. In: Fields BN, Knipe DN, Howley PM, editors. Fields Virology. New York: Lippincott-Raven; 2001, pp. 991–1041.
31. Westaway EG, Mackenzie JM, Khromykh AA. Replication and gene function in Kunjin virus. Curr Top Microbiol Immunol 2002;267:323–351.

32. Liu WJ, Sedlak PL, Kondratieva N, Khromykh AA. Complementation analysis of the flavivirus Kunjin NS3 and NS5 proteins defines the minimal regions essential for formation of a replication complex and shows a requirement of NS3 in cis for virus assembly. J Virol 2002;76:10766–10775.
33. Kummerer BM, Rice CM. Mutations in the yellow fever virus nonstructural protein NS2A selectively block production of infectious particles. J Virol 2002;76:4773–4784.
34. Westaway EG. Replication of flaviviruses. In: Schlesinger RW, editor. Togaviruses. New York: Academic Press; 1980, pp. 531–581.
35. Murphy FA. Morphology and morphogenesis. In: Monath TP, editor. St. Louis Encephalitis. Washington DC: American Public Health Association Inc, 1980, pp. 65–103.
36. Mackenzie JM, Jones MK, Young PR. Improved membrane preservation of flavivirus-infected cells with cryosectioning. J Virol Methods 1996;56:67–75.
37. Westaway EG, Mackenzie JM, Khromykh AA. Kunjin RNA replication and applications of Kunjin replicons. Adv Virus Res 2003;59:99–140.
38. Chu PW, Westaway EG. Molecular and ultrastructural analysis of heavy membrane fractions associated with the replication of Kunjin virus RNA. Arch Virol 1992;125:177–191.
39. Mackenzie JM, Khromykh AA, Jones MK, Westaway EG. Subcellular localization and some biochemical properties of the flavivirus Kunjin nonstructural proteins NS2A and NS4A. Virology 1998;245:203–215.
40. Westaway EG, Khromykh AA, Kenney MT, Mackenzie JM, Jones MK. Proteins C and NS4B of the flavivirus Kunjin translocate independently into the nucleus. Virology 1997;234:31–41.
41. Khromykh AA, Westaway EG. Completion of Kunjin virus RNA sequence and recovery of an infectious RNA transcribed from stably cloned full-length cDNA. J Virol 1994;68:4580–4588.
42. Khromykh AA, Westaway EG. Subgenomic replicons of the flavivirus Kunjin: construction and applications. J Virol 1997;71:1497–1505.
43. Rice CM, Grakoui A, Galler R, Chambers TJ. Transcription of infectious yellow fever RNA from full-length cDNA templates produced by in vitro ligation. New Biol 1989;1:285–296.
44. Lindenbach BD, Rice CM. trans-Complementation of yellow fever virus NS1 reveals a role in early RNA replication. J Virol 1997;71:9608–9617.
45. Lindenbach BD, Rice CM. Genetic interaction of flavivirus nonstructural proteins NS1 and NS4A as a determinant of replicase function. J Virol 1999;73:4611–4621.
46. Khromykh AA, Varnavski AN, Sedlak PL, Westaway EG. Coupling between replication and packaging of flavivirus RNA: evidence derived from the use of DNA-based full-length cDNA clones of Kunjin virus. J Virol 2001;75:4633–4640.
47. Mackenzie JM, Westaway EG. Assembly and maturation of the flavivirus Kunjin virus appear to occur in the rough endoplasmic reticulum and along the secretory pathway, respectively. J Virol 2001;75:10787–10799.
48. Mackenzie JM, Jones MK, Westaway EG. Markers for trans-Golgi membranes and the intermediate compartment localize to induced membranes with distinct replication functions in flavivirus-infected cells. J Virol 1999;73:9555–9567.
49. Stadler K, Allison SL, Schalich J, Heinz FX. Proteolytic activation of tick-borne encephalitis virus by furin. J Virol 1997;71:8475–8481.
50. Schweizer A, Fransen JA, Bachi T, Ginsel L, Hauri HP. Identification, by a monoclonal antibody, of a 53-kD protein associated with a tubulo-vesicular compartment at the cis-side of the Golgi apparatus. J Cell Biol 1988;107:1643–1653.
51. Pelham HR. Sorting and retrieval between the endoplasmic reticulum and Golgi apparatus. Curr Opin Cell Biol 1995;7:530–535.
52. Mironov AA, Mironov AA Jr, Beznoussenko GV, Trucco A, Lupetti P, Smith JD, Geerts WJ, Koster AJ, Burger KN, Martone ME, Deerinck TJ, Ellisman MH, Luini A. ER-to-Golgi carriers arise through direct en bloc protrusion and multistage maturation of specialized ER exit domains. Dev Cell 2003;5:583–594.
53. Krijnse-Locker J, Ericsson M, Rottier PJ, Griffiths G. Characterization of the budding compartment of mouse hepatitis virus: evidence that transport from the RER to the Golgi complex requires only one vesicular transport step. J Cell Biol 1994;124:55–70.
54. Donaldson JG, Klausner RD. ARF: a key regulatory switch in membrane traffic and organelle structure. Curr Opin Cell Biol 1994;6:527–532.
55. Mackenzie JM, Khromykh AA, Westaway EG. Stable expression of noncytopathic Kunjin replicons simulates both ultrastructural and biochemical characteristics observed during replication of Kunjin virus. Virology 2001;279:161–172.
56. Konan KV, Giddings TH Jr, Ikeda M, Li K, Lemon SM, Kirkegaard K. Nonstructural protein precursor NS4A/B from hepatitis C virus alters function and ultrastructure of host secretory apparatus. J Virol 2003;77:7843–7855.
57. Troxler M, Pasamontes L, Egger D, Bienz K. In situ hybridization for light and electron microscopy. a comparison of methods for the localization of viral RNA using biotinylated DNA and RNA probes. J Virol Methods 1990;30:1–14.
58. Bienz K, Egger D. Immunocytochemistry and in situ hybridization in the electron microscope: combined application in the study of virus-infected cells. Histochem Cell Biol 1995;103:325–338.
59. Bienz K, Egger D, Pfister T, Troxler M. Structural and functional characterization of the poliovirus replication complex. J Virol 1992;66:2740–2747.
60. Bienz K, Egger D, Troxler M, Pasamontes L. Structural organization of poliovirus RNA replication is mediated by viral proteins of the P2 genomic region. J Virol 1990;64:1156–1163.
61. Egger D, Pasamontes L, Bolten R, Boyko V, Bienz K. Reversible dissociation of the poliovirus replication complex: functions and interactions of its components in viral RNA synthesis. J Virol 1996;70:8675–8683.
62. Krogerus C, Egger D, Samuilova O, Hyypia T, Bienz K. Replication complex of human parechovirus 1. J Virol 2003;77:8512–8523.
63. Gosert R, Egger D, Bienz K. A cytopathic and a cell culture adapted hepatitis A virus strain differ in cell killing but not in intracellular membrane rearrangements. Virology 2000;266:157–169.
64. Monaghan P, Cook H, Jackson T, Ryan M, Wileman T. The ultrastructure of the developing replication site in foot-and-mouth disease virus-infected BHK-38 cells. J Gen Virol 2004;85 (Pt 4):933–946.
65. Molla A, Paul AV, Wimmer E. Effects of temperature and lipophilic agents on poliovirus formation and RNA synthesis in a cell-free system. J Virol 1993;67:5932–5938.
66. Guinea R, Carrasco L. Phospholipid biosynthesis and poliovirus genome replication, two coupled phenomena. Embo J 1990;9:2011–2016.
67. Carette JE, Stuiver M, Van Lent J, Wellink J, Van Kammen A. Cowpea mosaic virus infection induces a massive proliferation of endoplasmic reticulum but not Golgi membranes and is dependent on de novo membrane synthesis. J Virol 2000;74:6556–6563.
68. Perez L, Guinea R, Carrasco L. Synthesis of Semliki Forest virus RNA requires continuous lipid synthesis. Virology 1991;183:74–82.
69. Perez L, Carrasco L. Cerulenin, an inhibitor of lipid synthesis, blocks vesicular stomatitis virus RNA replication. FEBS Lett 1991;280:129–133.
70. Egger D, Teterina N, Ehrenfeld E, Bienz K. Formation of the poliovirus replication complex requires coupled viral translation, vesicle production, and viral RNA synthesis. J Virol 2000;74:6570–6580.
71. Teterina NL, Zhou WD, Cho MW, Ehrenfeld E. Inefficient complementation activity of poliovirus 2C and 3D proteins for rescue of lethal mutations. J Virol 1995;69:4245–4254.
72. O'Donnell VK, Pacheco JM, Henry TM, Mason PW. Subcellular distribution of the foot-and-mouth disease virus 3A protein in cells

infected with
forms of 3A. \
73. Maynell LA, K
RNA synthesi
74. Rust RC, Land
Bienz K. Cell
vesicles that
2001;75:9808
75. Schlegel A, G
and ultrastruc
J Virol 1996;7
76. Schweizer A
Reassessmer
1995;108:247
77. Suhy DA, Gic
reticulum by
autophagy-lik
8953–8965.
78. Ward TH, Pol
Maintenance
ER export. J
79. Belov GA, F
brane asso
2005;79:720
80. Cuconati A, I
synthesis of
81. Rodriguez F
GTPase acti
82. Rodriguez P
involved in F
83. Crotty S, S
replication r
targets a hc
84. Hauri HP, K
traffic in the
85. Deitz SB, I
dependent
Proc Natl A
86. Neznanov N
Agol VI, Gu
(TNF) -induc
surface. J V
87. Neznanov I
receptors c
Sci Monit 2
88. Pfister T,
Immunocy
lular fractic

infected with viruses encoding wild-type and bovine-attenuated forms of 3A. Virology 2001;287:151–162.
73. Maynell LA, Kirkegaard K, Klymkowsky MW. Inhibition of poliovirus RNA synthesis by brefeldin A. J Virol 1992;66:1985–1994.
74. Rust RC, Landmann L, Gosert R, Tang BL, Hong W, Hauri HP, Egger D, Bienz K. Cellular COPII proteins are involved in production of the vesicles that form the poliovirus replication complex. J Virol 2001;75:9808–9818.
75. Schlegel A, Giddings TH Jr, Ladinsky MS, Kirkegaard K. Cellular origin and ultrastructure of membranes induced during poliovirus infection. J Virol 1996;70:6576–6588.
76. Schweizer A, Rohrer J, Slot JW, Geuze HJ, Kornfeld S. Reassessment of the subcellular localization of p63. J Cell Sci 1995;108:2477–2485.
77. Suhy DA, Giddings TH Jr, Kirkegaard K. Remodeling the endoplasmic reticulum by poliovirus infection and by individual viral proteins: an autophagy-like origin for virus-induced vesicles. J Virol 2000;74:8953–8965.
78. Ward TH, Polishchuk RS, Caplan S, Hirschberg K, Lippincott-Schwartz J. Maintenance of Golgi structure and function depends on the integrity of ER export. J Cell Biol 2001;155:557–570.
79. Belov GA, Fogg MH, Ehrenfeld E. Poliovirus proteins induce membrane association of GTPase ADP-ribosylation factor. J Virol 2005;79:7207–7216.
80. Cuconati A, Molla A, Wimmer E. Brefeldin A inhibits cell-free, de novo synthesis of poliovirus. J Virol 1998;72:6456–6464.
81. Rodriguez PL, Carrasco L. Poliovirus protein 2C has ATPase and GTPase activities. J Biol Chem 1993;268:8105–8110.
82. Rodriguez PL, Carrasco L. Poliovirus protein 2C contains two regions involved in RNA binding activity. J Biol Chem 1995;270:10105–10112.
83. Crotty S, Saleh MC, Gitlin L, Beske O, Andino R. The poliovirus replication machinery can escape inhibition by an antiviral drug that targets a host cell protein. J Virol 2004;78:3378–3386.
84. Hauri HP, Kappeler F, Andersson H, Appenzeller C. ERGIC-53 and traffic in the secretory pathway. J Cell Sci 2000;113:587–596.
85. Deitz SB, Dodd DA, Cooper S, Parham P, Kirkegaard K. MHC I-dependent antigen presentation is inhibited by poliovirus protein 3A. Proc Natl Acad Sci USA 2000;97:13790–13795.
86. Neznanov N, Kondratova A, Chumakov KM, Angres B, Zhumabayeva B, Agol VI, Gudkov AV. Poliovirus protein 3A inhibits tumor necrosis factor (TNF) -induced apoptosis by eliminating the TNF receptor from the cell surface. J Virol 2001;75:10409–10420.
87. Neznanov N, Chumakov KP, Ullrich A, Agol VI, Gudkov AV. Unstable receptors disappear from cell surface during poliovirus infection. Med Sci Monit 2002;8:BR391–BR396.
88. Pfister T, Pasamontes L, Troxler M, Egger D, Bienz K. Immunocytochemical localization of capsid-related particles in subcellular fractions of poliovirus-infected cells. Virology 1992;188:676–684.
89. Levine B, Klionsky DJ. Development by self-digestion: molecular mechanisms biological functions autophagy. Dev Cell 2004;6:463–477.
90. van der Meer Y, van Tol H, Locker JK, Snijder EJ. ORF1a-encoded replicase subunits are involved in the membrane association of the arterivirus replication complex. J Virol 1998;72:6689–6698.
91. Prentice E, Jerome WG, Yoshimori T, Mizushima N, Denison MR. Coronavirus replication complex formation utilizes components of cellular autophagy. J Biol Chem 2004;279:10136–10141.
92. Kirkegaard K, Taylor MP, Jackson WT. Cellular autophagy: surrender, avoidance and subversion by microorganisms. Nat Rev Microbiol 2004;2:301–314.
93. Sodeik B, Schramm B, Suomalainen M, Locker JK. Meeting report: EMBO workshop 'Cell Biology of Virus Infection', September 25–29, 2004, EMBL, Heidelberg, Germany. Traffic 2005;6:351–356.
94. Jackson WT, Giddings THJ, Taylor MP, Mulinyawe S, Rabinovitch M, Kopito RR, Kirkegaard K. Subversion of cellular autophagosomal machinery by RNA viruses. PLoS Biol 2005;3:e156.
95. Purhonen P, Pursiainen K, Reunanen H. Effects of brefeldin A on autophagy in cultured rat fibroblasts. Eur J Cell Biol 1997;74:63–67.
96. Aldabe R, Carrasco L. Induction of membrane proliferation by poliovirus proteins 2C and 2BC. Biochem Biophys Res Commun 1995;206:64–76.
97. Cho MW, Teterina N, Egger D, Bienz K, Ehrenfeld E. Membrane rearrangement and vesicle induction by recombinant poliovirus 2C and 2BC in human cells. Virology 1994;202:129–145.
98. Teterina NL, Bienz K, Egger D, Gorbalenya AE, Ehrenfeld E. Induction of intracellular membrane rearrangements by HAV proteins 2C and 2BC. Virology 1997;237:66–77.
99. Aldabe R, Barco A, Carrasco L. Membrane permeabilization by poliovirus proteins 2B and 2BC. J Biol Chem 1996;271:23134–23137.
100. Moffat K, Howell G, Knox C, Belsham GJ, Monaghan P, Ryan MD, Wileman T. Effects of foot-and-mouth disease virus nonstructural proteins on the structure and function of the early secretory pathway: 2BC but not 3A blocks endoplasmic reticulum-to-golgi transport. J Virol 2005;79:4382–4395.
101. Sandoval I, Carrasco L. Poliovirus infection and expression of the poliovirus protein 2B provoke the disassembly of the Golgi complex, the organelle target for the antipoliovirus drug Ro-090179. J Virol 1997;71:4679–4693.
102. Doedens JR, Kirkegaard K. Inhibition of cellular protein secretion by poliovirus proteins 2B and 3A. Embo J 1995;14:894–907.
103. Teterina NL, Gorbalenya AE, Egger D, Bienz K, Ehrenfeld E. Poliovirus 2C protein determinants of membrane binding and rearrangements in mammalian cells. J Virol 1997;71:8962–8972.
104. Lyle JM, Bullitt E, Bienz K, Kirkegaard K. Visualization and functional analysis of RNA-dependent RNA polymerase lattices. Science 2002;296:2218–2222.

JOURNAL OF VIROLOGY, Nov. 2003, p. 12193–12202 Vol. 77, No. 22
0022-538X/03/$08.00+0 DOI: 10.1128/JVI.77.22.12193–12202.2003

Engineered Retargeting of Viral RNA Replication Complexes to an Alternative Intracellular Membrane

David J. Miller,[1,2]† Michael D. Schwartz,[2,3]‡ Billy T. Dye,[2,3] and Paul Ahlquist[2,3]*

Department of Medicine,[1] Institute for Molecular Virology,[2] and Howard Hughes Medical Institute,[3] University of Wisconsin—Madison, Madison, Wisconsin 53706

Received 11 June 2003/Accepted 15 August 2003

Positive-strand RNA virus replication complexes are universally associated with intracellular membranes, although different viruses use membranes derived from diverse and sometimes multiple organelles. We investigated whether unique intracellular membranes are required for viral RNA replication complex formation and function in yeast by retargeting protein A, the Flock House virus (FHV) RNA-dependent RNA polymerase. Protein A, the only viral protein required for FHV RNA replication, targets and anchors replication complexes to outer mitochondrial membranes in part via an N-proximal sequence that contains a transmembrane domain. We replaced the FHV protein A mitochondrial outer membrane-targeting sequence with the N-terminal endoplasmic reticulum (ER)-targeting sequence from the yeast NADP cytochrome P450 oxidoreductase or inverted C-terminal ER-targeting sequences from the hepatitis C virus NS5B polymerase or the yeast t-SNARE Ufe1p. Confocal immunofluorescence microscopy confirmed that protein A chimeras retargeted to the ER. FHV subgenomic and genomic RNA accumulation in yeast expressing ER-targeted protein A increased 2- to 13-fold over that in yeast expressing wild-type protein A, despite similar protein A levels. Density gradient flotation assays demonstrated that ER-targeted protein A remained membrane associated, and in vitro RNA-dependent RNA polymerase assays demonstrated an eightfold increase in the in vitro RNA synthesis activity of the ER-targeted FHV RNA replication complexes. Electron microscopy showed a change in the intracellular membrane alterations from a clustered mitochondrial distribution with wild-type protein A to the formation of perinuclear layers with ER-targeted protein A. We conclude that specific intracellular membranes are not required for FHV RNA replication complex formation and function.

A universal feature of positive-strand RNA viruses is the involvement of host intracellular membranes in RNA replication complex formation and function. This conclusion is based primarily on four observations. First, immunofluorescence and immunoelectron microscopy have localized viral replicase proteins and nascent viral RNA synthesis to intracellular membranes (16, 18, 24, 28, 29, 33, 42, 47, 51, 53, 56). Second, in vitro viral RNA-dependent RNA polymerase (RdRp) activity cofractionates with cellular membranes (6, 8, 12, 51, 58). Third, detergents suppress, and in some instances, phospholipids enhance the in vitro activities of viral replicase proteins (2, 8, 57, 58). Fourth, lipid synthesis inhibitors (20, 30, 36) and mutations in lipid synthesis genes (26) inhibit viral RNA replication. Recent results also show that at least some positive-strand RNA viruses use membrane rearrangements to create virus-specific, membrane-bounded compartments in which RNA replication occurs (51).

Despite these observations, many fundamental questions remain about the interaction of viral replication factors with host intracellular membranes and the specific roles of membranes in viral RNA replication complex formation and function. Moreover, while most viruses assemble their replication complexes on a specific membrane or membranes, different viruses use different membranes. For various positive-strand RNA viruses, membranes derived from the endoplasmic reticulum (ER) (26, 29, 35, 42, 46–48, 51), Golgi apparatus (47), lysosomes (18, 24, 28, 47), endosomes (18, 24), vacuoles (52), mitochondria (10, 15, 32, 33), perixosomes (9, 10), and chloroplasts (14) have all been implicated in viral RNA replication complex formation and function. The significance of this diversity of intracellular membranes used by different viruses is unknown.

The wide variety of intracellular membrane compartments used by different positive-strand RNA viruses, and their specific targeting, suggests that individual viruses may have unique host factor requirements supplied by specific intracellular membranes. Alternatively, many or all host intracellular membranes could provide the functions necessary for viral RNA replication complex formation and function, and the specific intracellular localization of individual viruses may be related to other steps in the viral life cycle, such as viral protein translation or encapsidation. Results that help distinguish between these competing hypotheses potentially have significant therapeutic implications, as antiviral drugs designed to block viral RNA replication complex formation or function on a specific intracellular membrane compartment will be ineffective if alternative membranes can be used efficiently.

To study intracellular viral RNA replication complex targeting, we use Flock House virus (FHV), an alphanodavirus that has been used as a model to investigate viral capsid formation and RNA packaging (49, 50, 59), viral RNA replication and

* Corresponding author. Mailing address: Institute for Molecular Virology, University of Wisconsin—Madison, 1525 Linden Dr., Madison, WI 53706-1596. Phone: (608) 263-5916. Fax: (608) 265-9214. E-mail: ahlquist@facstaff.wisc.edu.

† Present address: Departments of Medicine and Microbiology and Immunology, University of Michigan Medical School, Ann Arbor, MI 48109-0620.

‡ Present address: Department of Biological Sciences, Vanderbilt University, Nashville, TN 37235-1634.

subgenomic synthesis (3, 5, 22, 27), and RNA replication complex assembly and function (32, 33, 57, 58). FHV replicates in a wide variety of cells (4), including the yeast *Saccharomyces cerevisiae* (37–39). FHV contains a 4.5-kb bipartite genome, in which the larger RNA segment (RNA1) encodes protein A, the FHV RdRp (4, 13). Protein A is the only viral protein needed for FHV RNA replication (3, 21, 38), and it contains the sequences necessary for the intracellular targeting of FHV RNA replication complexes to outer mitochondrial membranes (32, 33). The protein A mitochondrial outer membrane-targeting sequence is located in the N-terminal 46 amino acids and contains a 19-amino-acid transmembrane domain (TMD) (32). The presence of a single essential viral protein, a defined N-terminal targeting sequence, and the intracellular localization of viral RNA replication complexes to a single organelle all make FHV an attractive model to investigate whether viral RNA replication complexes can be retargeted to an alternative intracellular membrane.

In this report, we show that FHV RNA replication complexes can be retargeted from the mitochondria to the ER via the introduction of chimeric sequences into the protein A N-terminal region. In addition, FHV RNA replication complexes retargeted to the ER are functional in vivo and in vitro and have enhanced RNA synthesis activity compared to mitochondrially targeted replication complexes.

MATERIALS AND METHODS

Yeast strain and plasmids. The haploid yeast strain BY4742 (*MATα his3Δ1 leu2Δ0 ura3Δ0*) was used for all experiments. Yeast cells were transformed, cultured, and induced with galactose as previously described (32) unless otherwise indicated. Standard molecular biology procedures were used for all cloning steps, and all products generated by PCR or with synthesized oligonucleotides were verified by automated sequencing. Plasmids pFA and $pF1_{fs}$ have been previously described (27, 32, 38). For the present experiments, we changed $pF1_{fs}$ from a *HIS3*-selectable yeast 2μm plasmid to a centromeric plasmid based on the pRS313 backbone (laboratory designation, $pFHV1_{fs}$) to provide better control of plasmid copy number and stability. Plasmid pFA-del was generated by PCR with oligonucleotides designed to delete protein A amino acids 2 to 35 and insert a unique *Bsp*EI site. We generated chimeric protein A expression plasmids from pFA-del using mutually primed extension of overlapping nucleotides with flanking *Bsp*EI sites. Inserted sequences and plasmid designations of chimeric protein A expression plasmids are shown in Fig. 1A and described in Results below.

Antibodies. Mouse monoclonal antibodies (MAbs) against cytochrome oxidase subunit III (CoxIII), mitochondrial porin, dolichyl-phosphate β-D-mannosyltransferase (DPM), 3-phosphoglycerate kinase (PGK), vacuolar ATPase, and Oregon Green 488-labeled concanavalin A were from Molecular Probes (Eugene, Oreg.). All secondary antibodies for immunofluorescence and immunoblotting were from Jackson Immunoresearch (West Grove, Pa.). Rabbit polyclonal antisera against FHV protein A has been described previously (33). Mouse MAbs against FHV protein A were generated from mice immunized with a protein A-enriched insoluble pellet fraction from lysates of *Escherichia coli* BL21-Codon Plus (RIL) cells transformed with the expression vector pET-FHVPA (33). Hybridoma supernatants were screened for protein A reactivity by enzyme-linked immunosorbent assay using lysates from mock- and FHV-infected *Drosophila* S2 cells, and MAb specificity was confirmed by immunoblot and immunofluorescence analyses. The protein A epitope specificities of three hybridomas were further characterized by immunoblotting with lysates from yeast cells expressing protein A deletion mutants (32). The epitope for clones 2-2.2.2.5.3 and 3-4.1.1.2 was located between protein A amino acids 99 and 230, whereas the epitope for clone 2-1.1.2.4.8 was located between amino acids 230 and 399. Pooled ascites fluid from all three clones was used for immunoblot analyses.

RNA and protein analyses. Total RNA isolation, Northern blot analyses and quantitation, protein isolation, and immunoblot analyses and quantitation were done as previously described (32). Cell lysates were fractionated by flotation in Nycodenz gradients as previously described (32) with several modifications. To avoid rapid FHV protein A and RNA degradation during spheroplast preparation, yeast cells were disrupted by mechanical shearing with glass beads for 1 min at 4°C in the presence of a yeast protease inhibitor cocktail (Sigma, St. Louis, Mo.) and the RNase inhibitor RNasin prior to equilibrium density gradient centrifugation. Two equal-volume fractions were taken—one from the visible membrane layer at the upper 5 to 35% Nycodenz interface and the other from the lower region where the cell lysate was loaded—and designated the low-

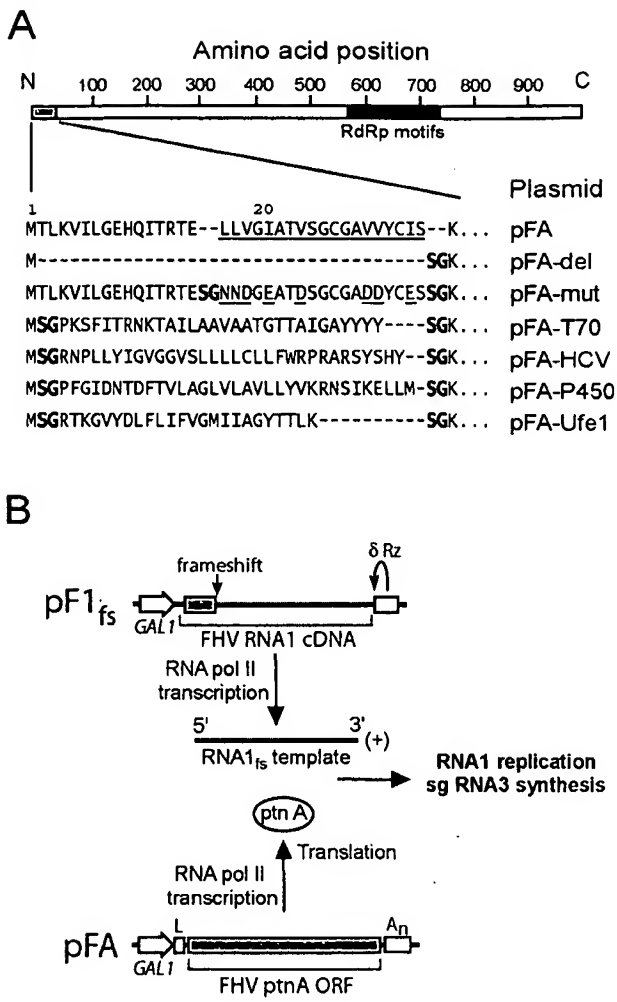

FIG. 1. (A) Chimeric FHV protein A sequences and plasmid designations. A schematic of protein A with the viral RdRp motif region represented by the solid bar is shown on top for reference. The core predicted protein A TMD from Leu 17 to Ser 35 is underlined (32). The hydrophobic-to-hydrophilic amino acid mutations in pFA-mut are also underlined. The unique *Bsp*EI site used to generate the chimeric protein A constructs introduced a Ser-Gly at the insertion sequence junctions (shown in boldface). The dashes indicate no amino acids and are included for alignment purposes. (B) Schematic of plasmid-directed FHV RNA replication in yeast. RNA1 templates with authentic viral 5′ and 3′ termini are generated from $pF1_{fs}$ through precise placement of the *GAL1* promoter start site and a hepatitis δ ribozyme (Rz), respectively, and the frameshift at the indicated location disrupts translation. The *GAL1* leader (L) and *CYC1* polyadenylation signal (A_n) flanking the protein A open reading frame (ORF) in pFA or derivatives thereof disrupt its activity as a viral RNA replication template but enhance its RNA polymerase II-directed transcription and translation. pFA-derived protein A (ptnA) subsequently directs RNA1 replication and subgenomic (sg) RNA3 synthesis from an RNA1 template transcribed from $pF1_{fs}$.

density (LD) and high-density (HD) fractions, respectively (32). The total protein concentration of each fraction was determined by Bradford assay using bovine serum albumin as the standard, and total protein was equalized for immunoblot and in vitro RdRp analyses. In vitro RdRp assays were done as previously described (58) with several modifications. Reaction mixtures containing LD or HD fractions plus 50 mM Tris (pH 8.0); 50 mM potassium acetate; 15 mM magnesium acetate; 5 μg of actinomycin D/ml; 40 U of RNasin/μl; 1 mM (each) ATP, GTP, and CTP; 50 μM UTP; and 10 μCi of [^{32}P]UTP in a 25-μl total volume were incubated for 3 h at 26°C, extracted once with phenol-chloroform, desalted with Sephadex G-50 columns, and analyzed in 1.2% nondenaturing agarose gels.

Immunofluorescence and EM. Confocal immunofluorescence and transmission electron microscopy (EM) analyses were done as previously described (32, 51).

RESULTS

Retargeting sequence selection and FHV RNA replication in yeast. We previously found that the N-terminal 46 amino acids of FHV protein A functioned as a mitochondrial outer membrane-targeting sequence (32). To investigate whether protein A and FHV RNA replication complexes could be retargeted to the ER, we constructed a series of chimeric protein A expression plasmids (Fig. 1A). Previous mapping studies showed that deletion of amino acids 9 to 45 disrupted protein A in vivo RdRp activity (32). Thus, we replaced the N-proximal region located between the initiator Met and Lys 36, the amino acid immediately downstream of the protein A TMD (32). For controls, we constructed pFA-del, in which amino acids 2 to 35 were deleted; pFA-mut, in which the protein A TMD hydrophobic amino acids Leu, Val, and Ile were mutated to the hydrophilic amino acids Asn, Asp, and Glu, respectively; and pFA-T70, in which wild-type (wt) protein A amino acids 2 to 35 were replaced with the outer mitochondrial membrane-targeting sequence from the yeast import receptor protein Tom70 (31). We initially searched for well-characterized ER-targeting sequences that contained an N-proximal TMD and were ~30 to 40 amino acids in length, similar in size to the deleted wt protein A region in pFA-del. Few sequences fulfilled these criteria, and thus, we expanded the search to include inverted C-proximal TMDs, based on the observation that membrane targeting of some yeast proteins depends on the TMD length and composition but not the precise sequence (40). We chose three ER-targeting sequences: (i) inverted amino acids 561 to 591 from the C terminus of the hepatitis C virus (HCV) NS5B protein (48), (ii) amino acids 1 to 34 from the N terminus of yeast NADP cytochrome P450 oxidoreductase (54), and (iii) inverted amino acids 326 to 346 from the C terminus of the yeast t-SNARE Ufe1p as modified by Rayner and Pelham (40). These sequences were inserted between wt protein A amino acids 1 and 36 to generate plasmids pFA-HCV, pFA-P450, and pFA-Ufe1, respectively (Fig. 1A).

For all experiments, unless otherwise indicated, yeast cells were cotransformed with pFA or derivatives thereof to provide protein A expression and with $pF1_{fs}$ to provide an RNA1 template for FHV RNA replication in *trans* (Fig. 1B) (27, 32, 38). All plasmids expressed protein A or RNA1 from the galactose-inducible, glucose-repressible *GAL1* promoter. The RNA1 transcribed from the plasmid $pF1_{fs}$ contains authentic FHV 5′ and 3′ termini and thus can serve as a template for viral RNA replication but cannot be translated due to a 4-nucleotide frameshifting insertion in the 5′ coding region (38). During RNA replication via a full-length genomic negative-sense (−)RNA1 intermediate, FHV produces a subgenomic, positive-sense (+)RNA3 that is colinear with the 3′ end of genomic (+)RNA1 (4). Thus, both genomic (−)RNA1 and subgenomic (+)RNA3 syntheses provide quantitative measurements of protein A-dependent FHV RNA replication.

Retargeted protein A chimeras localize to the ER. We used confocal immunofluorescence microscopy to examine the intracellular localization of protein A in yeast (Fig. 2). Consistent with previous observations (32), mitochondria from control yeast showed a peripheral distribution (Fig. 2A, top row), whereas mitochondria from yeast expressing pFA showed a clustered distribution that colocalized with protein A immunofluorescence (Fig. 2A, second row). Mitochondria from yeast expressing pFA-T70 also showed a clustered distribution that partially colocalized with protein A immunofluorescence, although the clustering was often not as prominent as that seen with wt protein A (data not shown). In contrast to pFA and pFA-T70, mitochondria from yeast expressing pFA-HCV showed a normal peripheral distribution that was distinct from the protein A immunofluorescence pattern (Fig. 2A, third row). The protein A distribution in yeast expressing pFA-HCV was predominantly centralized and perinuclear, similar to the distribution of the ER-targeted brome mosaic virus 1a and 2a replicase proteins in yeast (11, 41). A similar, largely perinuclear-type protein A distribution was seen in yeast expressing pFA-P450 (Fig. 2A, fourth row) or pFA-Ufe1 (Fig. 2A, bottom row). Immunofluorescence microscopy using a yeast ER marker confirmed that chimeric protein A localized to the ER in yeast expressing pFA-HCV (Fig. 2B, top row), pFA-P450 (Fig. 2B, second row), or pFA-Ufe1 (Fig. 2B, bottom row). As a control for other intracellular membrane compartments, immunofluorescence microscopy showed no significant localization of chimeric protein A to vacuoles in yeast expressing pFA-HCV (Fig. 2C, top row), pFA-P450 (Fig. 2C, bottom row), or pFA-Ufe-1 (data not shown). Thus, chimeric FHV protein A with specifically selected targeting sequences derived from the HCV NS5B polymerase, the yeast NADP cytochrome P450 oxidoreductase, or the yeast t-SNARE Ufe1p localized to the ER in yeast.

ER-targeted protein A chimeras increase FHV RNA synthesis in vivo. We analyzed FHV-specific RNA accumulation by Northern blot analyses to compare FHV RNA replication in yeast expressing wt protein A and in ER-targeted chimeras (Fig. 3). Both subgenomic (+)RNA3 (Fig. 3A, top blot) and (−)RNA1 template (Fig. 3A, bottom blot) accumulations were increased in yeast cells expressing pFA-T70, pFA-HCV, pFA-P450, and pFA-Ufe1. The increase in viral RNA accumulation was not due to increased FHV RNA polymerase expression, as protein A accumulations were similar in all constructs (Fig. 3B). Compared quantitatively to yeast expressing pFA, (+)RNA3 accumulation increased 5- to 11-fold and (−)RNA1 accumulation increased 2- to 12-fold in yeast cells expressing pFA-HCV, pFA-P450, and pFA-Ufe1 (Fig. 3C). The largest increases in FHV RNA accumulation were seen with pFA-T70, pFA-HCV, and pFA-P450, whereas pFA-Ufe1 showed a smaller, although still significant, increase. In contrast to subgenomic (+)RNA3 and genomic template (−)RNA1 accumulation, genomic (+)RNA1 accumulation was either unchanged or only slightly higher in yeast cells expressing pFA-T70, pFA-

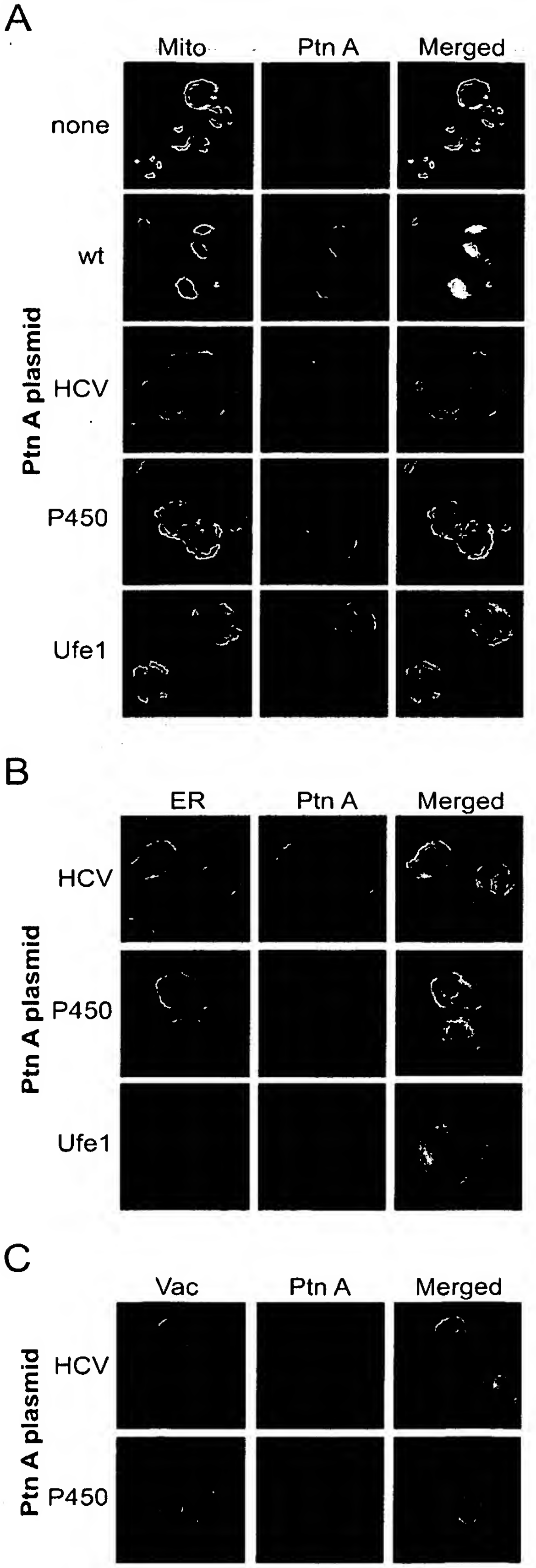

HCV, pFA-P450, and pFA-Ufel (Fig. 3C). Genomic (+)RNA1 accumulation reflects both FHV RNA replication and replication-independent yeast RNA polymerase II-directed transcription from plasmid DNA (Fig. 1B). We concluded from these data, in conjunction with the confocal-immunofluorescence results described above (Fig. 2), that FHV RNA replication complexes retargeted to the ER were active in vivo. Thus, FHV RNA replication complexes do not require a unique intracellular membrane for in vivo activity in yeast.

The increased RNA replication in yeast cells expressing pFA-T70, pFA-HCV, pFA-P450, and pFA-Ufe1 was not simply due to a change in the protein A TMD, as genomic (−)RNA1 and subgenomic (+)RNA3 accumulations in yeast expressing pFA-mut were negligible (Fig. 3). We changed the hydrophobic amino acids within the protein A TMD to hydrophilic amino acids in pFA-mut based on the hypothesis that a hydrophobic TMD was necessary for in vivo protein A RdRp activity. However, (+)RNA3 accumulation unexpectedly decreased only 40% in yeast expressing pFA-del compared to that in yeast expressing wt protein A, whereas (−)RNA1 accumulation increased almost twofold (Fig. 3). This suggests that the protein A N-terminal 35 amino acids are not essential for RdRp activity and that potential changes in secondary or tertiary structure may have been responsible for the absent in vivo RdRp activity with pFA-mut. Confocal immunofluorescence studies showed that protein A in yeast expressing pFA-del had a more diffuse distribution that did not colocalize with mitochondria (data not shown), similar to previously described

FIG. 2. Chimeric protein A is retargeted to the ER. (A) Yeasts expressing $pF1_{fs}$ plus a control plasmid lacking the protein A open reading frame (top row), pFA (second row), pFA-HCV (third row), pFA-P450 (fourth row), or pFA-Ufel (bottom row) were immunostained with rabbit anti-protein A (Ptn A) and mouse anti-CoxIII for mitochondria (mito), followed by Texas red-labeled goat anti-rabbit and fluorescein isothiocyanate-labeled goat anti-mouse secondary antibodies. Representative images for CoxIII (left; green), protein A (middle; red), and merged signals (right) are shown. The merged images represent a digital superimposition of red and green signals in which areas of fluorescence colocalization are yellow. The images for pFA-HCV (third row) are shown at approximately twice the magnification of the other immunofluorescence images. (B) Yeast cells expressing $pF1_{fs}$ plus pFA-HCV (top row), pFA-P450 (middle row), or pFA-Ufe1 (bottom row) were immunostained with rabbit anti-protein A and Oregon Green 488-labeled concanavalin A, followed by Texas red-labeled goat anti-rabbit secondary antibodies. Representative confocal images for conconavalin A (left; green), protein A (middle; red), and merged signals (right) are shown. The images for pFA-Ufe1 (bottom row) are shown at approximately twice the magnification of the other immunofluorescence images. Concanavalin A is a lectin that selectively binds α-mannopyranosyl and α-glucopyranosyl residues. Initial experiments demonstrated that the fluorescence pattern of concanavalin A reactivity in yeast colocalized with the immunofluorescence pattern of Kar2p, a yeast ER-resident protein (data not shown). (C) Yeast cells expressing $pF1_{fs}$ plus pFA-HCV (top row) or pFA-P450 (bottom row) were immunostained with rabbit anti-protein A and mouse anti-vacuolar ATPase for vacuoles (Vac), followed by Texas red-labeled goat anti-rabbit and fluorescein isothiocyanate-labeled goat anti-mouse secondary antibodies. Representative confocal images for vacuolar ATPase (left; green), protein A (middle; red), and merged signals (right) are shown. The images for pFA-P450 (bottom row) are shown at approximately twice the magnification of the other immunofluorescence images.

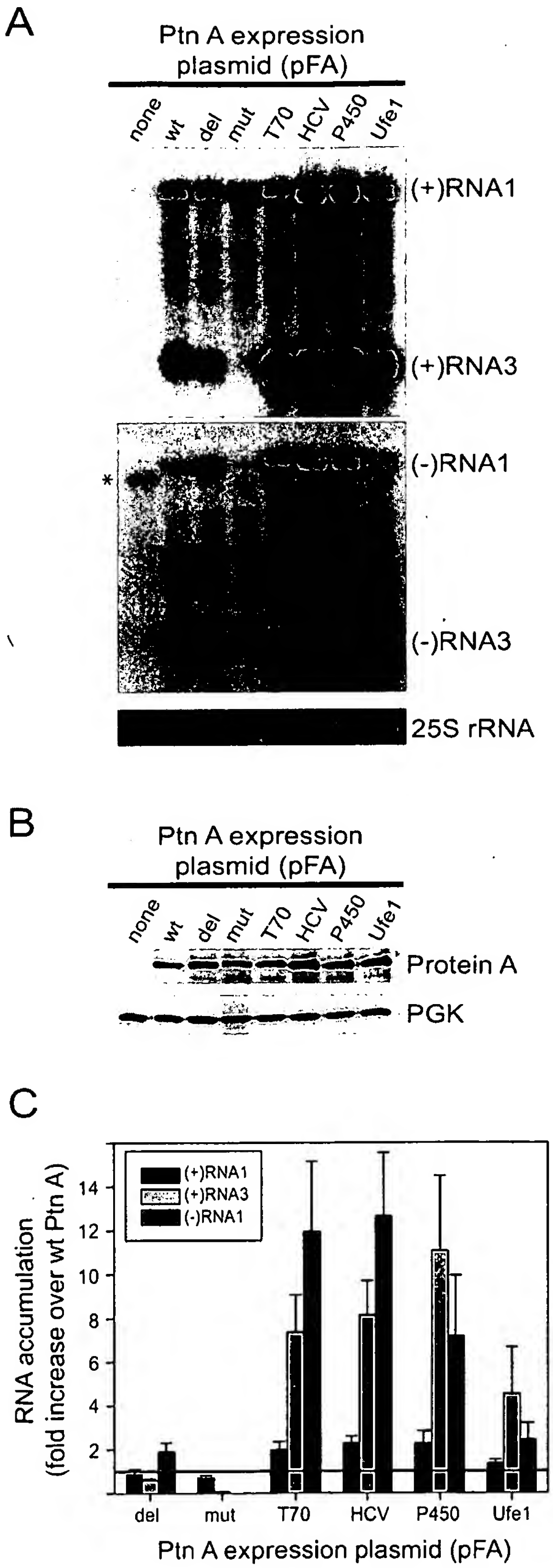

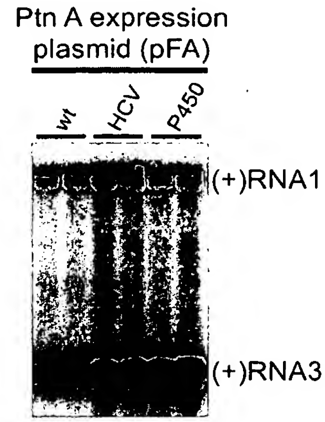

FIG. 4. ER-targeted protein A (Ptn A) chimeras maintain increased FHV RNA accumulation in vivo after 72 h of induction. Total RNA from equivalent numbers of cells was separated by electrophoresis and blotted with a ^{32}P-labeled complementary riboprobe that detected (+)RNA1 and (+)RNA3. Duplicate representative samples from yeast cells expressing pF1$_{fs}$ plus pFA, pFA-HCV, or pFA-P450 are shown.

protein A mutants with N-proximal deletions (32). Nevertheless, some protein A mutants with N-proximal deletions that include the TMD still maintain 40 to 60% membrane association (32). Thus, the retained in vivo RdRp activity of pFA-del

FIG. 3. ER-targeted protein A chimeras increase FHV RNA accumulation in vivo. (A) Viral RNA accumulation in yeasts expressing pF1$_{fs}$ plus the indicated protein A (Ptn A) expression plasmids. The lane labels correspond to the plasmid designations shown in Fig. 1A. Total RNAs from equivalent numbers of cells were separated by electrophoresis and blotted with ^{32}P-labeled complementary riboprobes that corresponded to nucleotides 2718 to 3064 from FHV RNA1 (38). Note that RNA3 is colinear with the 3′ end of RNA1 (13, 17) and that the probe sequence is present in both RNAs. Control Northern blots comparing known amounts of RNA1 and RNA3 in vitro transcripts showed that, with the probes and the transfer and hybridization conditions used, there was no significant difference between the detection efficiencies of RNA1 and RNA3. Thus, the band intensities reflect the molar ratios of RNA1 and RNA3. The riboprobes were either in the antisense or sense orientation and detected (+)RNA1 and (+)RNA3 (upper blot) or (−)RNA1 and (−)RNA3 (lower blot), respectively. The positions of RNA1 and RNA3 are shown on the right. The ethidium bromide-stained band of 25S rRNA is shown below the blots as a loading control. The asterisk indicates the position of a background band seen prominently in yeast expressing template only but also present to a lesser extent in all samples. This band was not present in total RNA preparations from FHV-infected *Drosophila* cells, whereas the (−)RNA1-labeled band was present (not shown). Subgenomic (−)RNA3 is produced in yeast replicating FHV RNA and in FHV-infected *Drosophila* cells and may function as a template for subgenomic (+)RNA3 synthesis (27, 38). (B) FHV protein A accumulation in yeast expressing pF1$_{fs}$ plus protein A expression plasmids. Total protein from equivalent numbers of cells was separated by electrophoresis and blotted with rabbit anti-protein A antiserum. The anti-PGK immunoblot is shown as a loading control. (C) Quantitative analysis of (+)RNA1, (+)RNA3, and (−)RNA1 accumulation. Northern blots were quantitated by phosphorimager analysis, and the results are expressed as the increase (n-fold) over yeast expressing pF1$_{fs}$ plus pFA. The horizontal line at 1 is placed for reference to the wt control. Averages and standard errors of the mean of at least three independent experiments are shown.

could be due to either residual membrane association or membrane-independent FHV RNA replication complex activity. The latter hypothesis is consistent with the observation that FHV negative-strand templates can be produced in vitro in the absence of membranes or phospholipids (57, 58). The observation that pFA-del retained some in vivo RdRp activity despite the lack of clear mitochondrial localization supports the conclusion that FHV RNA replication complexes do not require a unique intracellular membrane in yeast.

Effects of yeast growth and induction kinetics on viral RNA synthesis in yeast expressing chimeric protein A. To assess whether the increased FHV RNA synthesis in yeast expressing chimeric protein A might have been due to a slowing of yeast growth, thus allowing more time for viral RNA accumulation per cell before cell division, we measured doubling times over the entire 24-h induction period. When grown in selective medium with galactose, yeast expressing pFA plus $pF1_{fs}$ doubled every 9.7 ± 0.4 h (mean ± standard error of the mean), compared to 9.3 ± 1.2 h for control yeast. Doubling times were not significantly different in yeast cells expressing pFA-del (9.5 ± 0.7 h), pFA-mut (10.7 ± 0.8 h), pFA-HCV (8.5 ± 0.2 h), pFA-P450 (9.4 ± 0.2 h), or pFA-Ufe1 (9.3 ± 0.5 h) when compared to those of yeast cells expressing pFA. In contrast, the doubling time in yeast expressing pFA-T70 was increased almost twofold to 17.7 ± 1.6 h ($P < 0.0004$ compared to pFA), which may explain the increased (+)RNA3 and (−)RNA1 accumulation seen in these yeast cells (Fig. 3). However, differences in yeast growth kinetics did not explain the increased FHV RNA accumulation in yeast expressing ER-localized pFA-HCV, pFA-P450, or pFA-Ufe1.

We also explored the impact of the induction period on FHV RNA accumulation in yeast cells expressing $pF1_{fs}$ plus pFA, pFA-HCV, or pFA-P450. Expression of FHV protein A and RNA1 replication templates was induced in selective medium with galactose, and the yeast cells were passed every 24 h into new media to maintain exponential growth and analyzed 72 h after induction (Fig. 4). FHV RNA accumulation after a 72-h induction was still increased in yeast expressing pFA-HCV or pFA-P450 compared to that in yeast expressing pFA, but the increase was less than that seen after the shorter 24-h induction period. Subgenomic (+)RNA3 accumulation in yeast expressing pFA-HCV or pFA-P450 was increased 2.5- ± 0.2- or 3.0- ± 0.2-fold, respectively, over yeast expressing pFA. Thus, enhanced FHV RNA synthesis kinetics or RNA stability may explain part of the increased FHV RNA accumulation in yeast expressing retargeted protein A.

ER-targeted FHV protein A chimeras are membrane associated and have increased in vitro RdRp activities. FHV protein A is membrane associated in infected *Drosophila* cells (33) and in yeast transformed with protein A expression vectors (32). To determine whether the ER-targeted protein A chimeras were also membrane associated, we used equilibrium density gradient centrifugation to examine the flotation behavior of protein A from yeast expressing $pF1_{fs}$ plus pFA, pFA-HCV, or pFA-P450 (Fig. 5A). As an additional control for subsequent in vitro RdRp assays, we also examined yeast cells expressing pFA alone, which produce protein A but do not support FHV RNA replication (27, 32, 38). Protein A from yeast cells expressing pFA, pFA-HCV, and pFA-P450 fractionated almost exclusively into the membrane-enriched LD fraction

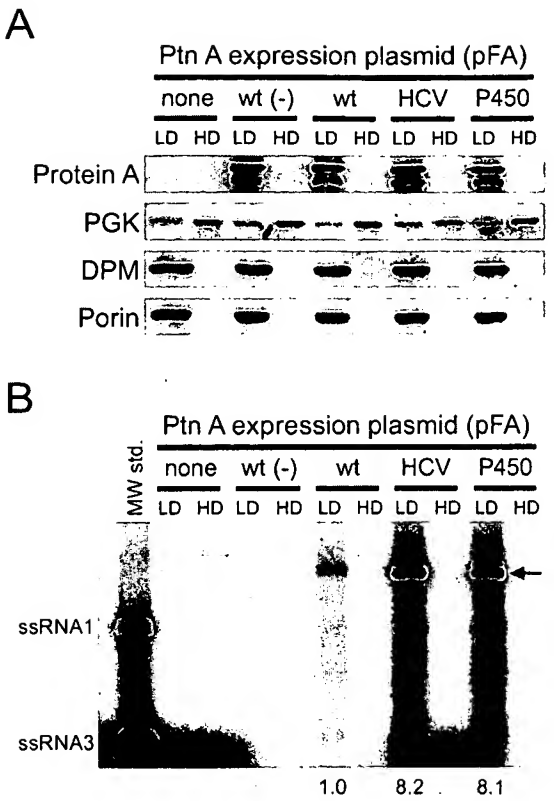

FIG. 5. ER-targeted protein A (Ptn A) chimeras are membrane-associated and have enhanced in vitro FHV RdRp activities. (A) Equilibrium density gradient fractionation of lysates from yeast cells expressing $pF1_{fs}$ alone (none), pFA alone [wt (−)], or $pF1_{fs}$ plus pFA (wt), pFA-HCV, or pFA-P450. Equal amounts of total protein from both LD and HD fractions were separated by sodium dodecyl sulfate-polyacrylamide gel electrophoresis and immunoblotted with mouse MAbs to protein A, PGK, DPM, or porin. Loading equal amounts of total protein resulted in an overrepresentation of individual proteins in the LD fraction relative to the HD fraction, thus exaggerating the residual PGK signal in the LD fraction. Protein A appears as a doublet in immunoblots of equilibrium gradient fractions, where the lower band represents a C-terminal degradation product (32). (B) In vitro RdRp assay of equilibrium density gradient fractions. Equal amounts of total proteins from both LD and HD fractions were incubated with [^{32}P]UTP and unlabeled ribonucleotides, and the reaction products were separated by nondenaturing agarose gel electrophoresis. The positions of in vitro-transcribed ssRNA1 and ssRNA3 are shown on the left. The major reaction products corresponding to ssRNA1, ssRNA3, and presumed replicative intermediate dsRNA1 (arrow) were quantitated by phosphorimager analysis in three independent experiments, and the numbers represent the increases (n-fold) in total radiolabeled products relative to the LD fraction of yeast expressing $pF1_{fs}$ plus pFA.

(Fig. 5A). The ER membrane protein DPM and the mitochondrial outer membrane porin protein were also present exclusively in the LD fraction, whereas the soluble cytosolic protein PGK partitioned predominantly into the membrane-depleted HD fraction. Thus, ER-targeted protein A chimeras were membrane-associated, consistent with the presence of TMDs in the sequences chosen to retarget protein A to the ER (Fig. 1A).

To assess the in vitro activities of ER-targeted protein A chimeras, LD and HD fractions from flotation gradients were

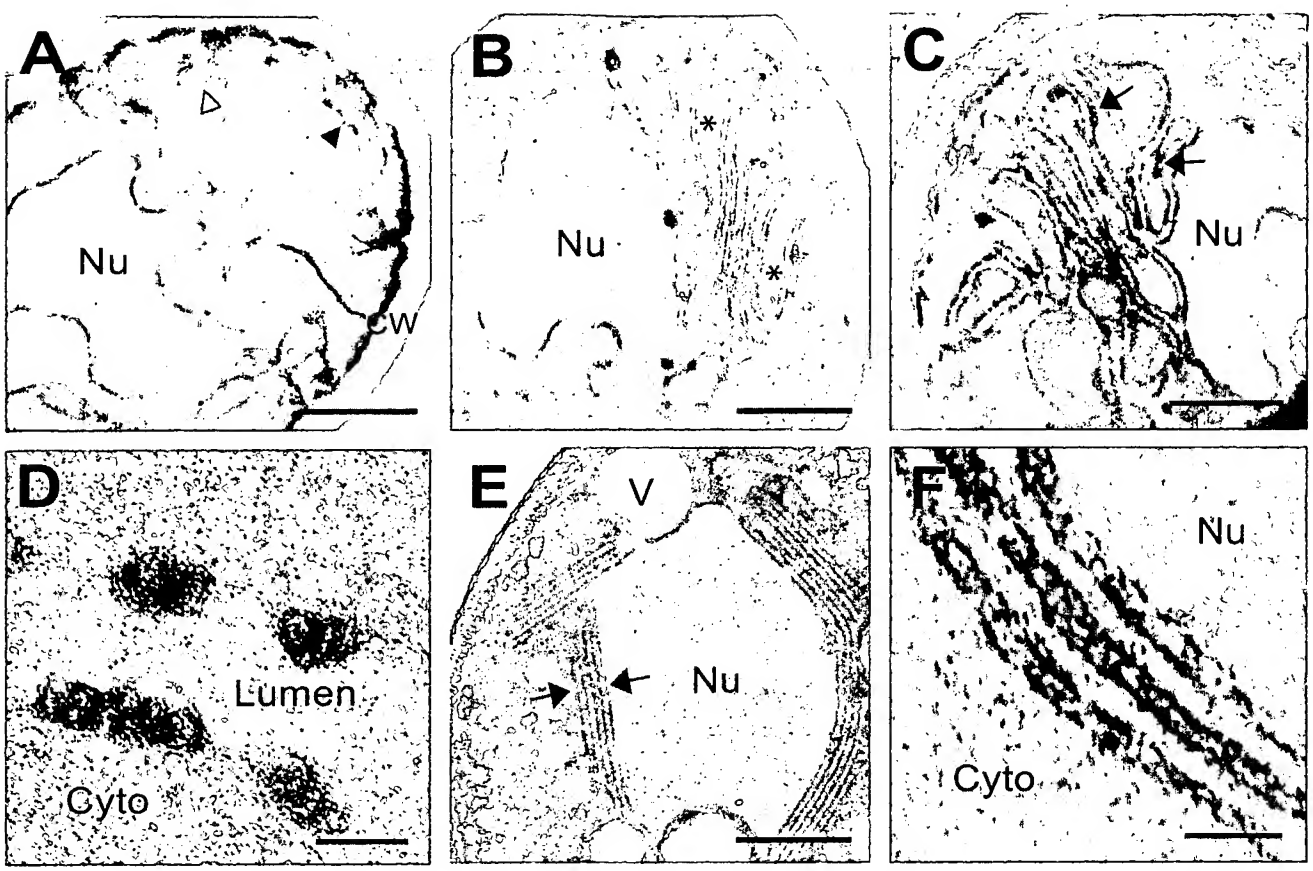

FIG. 6. FHV protein A expression and RNA replication induces distinct ultrastructural membrane alterations in yeast. (A) Electron micrograph of yeast expressing $pF1_{fs}$ only, showing normal nucleus (Nu), cell wall (CW), and mitochondria seen in longitudinal (black arrowhead) and transverse (white arrowhead) sections. (B) Electron micrograph of yeast expressing pFA only, showing clustering of membrane-bounded organelles (asterisks). (C) Electron micrograph of yeast expressing $pF1_{fs}$ plus pFA, showing clustered membrane-bounded organelles plus electron-dense structures (arrows). (D) Electron micrograph (higher magnification) of membrane-bounded structures projecting into the organelle lumen of yeast expressing $pF1_{fs}$ plus pFA. Cyto, cytoplasm. (E) Electron micrograph of yeast expressing $pF1_{fs}$ plus pFA-HCV, showing perinuclear membrane layers (arrows). V, vacuole. (F) Electron micrograph (higher magnification) of perinuclear membrane layers in yeast expressing $pF1_{fs}$ plus pFA-HCV, showing an irregular appearance. Bars = 500 (A, B, C, and E), 100 (D), and 150 (F) nm.

equalized for total protein content and used for in vitro RdRp assays (Fig. 5B). No exogenous FHV RNA template was added to the RdRp reactions, and thus, any in vitro activity in the gradient fractions represented functional replication complexes that contained protein A, template FHV RNA, and any accompanying host factors. Gradient fractions from yeast expressing either $pF1_{fs}$ or pFA alone showed only faint high-molecular-weight reaction products, predominantly in the HD fractions. In contrast, the LD fractions from yeast expressing $pF1_{fs}$ plus pFA, pFA-HCV, or pFA-P450 showed distinct reaction products that comigrated with in vitro-transcribed single-stranded (ss) FHV RNA1 and RNA3. The most prominent RdRp product migrated more slowly than ssRNA1 (Fig. 5B, arrow) and likely represented double-stranded (ds) RNA1, which is a replicative intermediate and the primary reaction product previously described in in vitro FHV RdRp assays (57, 58).

The in vitro RdRp activities of LD fractions from yeast cells expressing pFA-HCV and pFA-P450 were significantly greater than that of yeast cells expressing pFA. When expressed as an increase over pFA, the production levels of ssRNA1, ssRNA3, and the presumed replicative intermediate dsRNA1 in LD fractions from yeast cells expressing pFA-HCV were increased 6.4- ± 1.4-, 9.8- ± 1.9-, and 8.5- ± 1.1-fold, respectively. For yeast expressing pFA-P450, these increases were 5.7- ± 1.4-, 8.6- ± 1.8-, and 9.3- ± 1.3-fold. The increased in vitro RdRp activity was not due to increased protein A accumulation, as LD fractions from yeast cells expressing pFA, pFA-HCV, and pFA-P450 contained similar levels of protein A (Fig. 5A, upper blot). Thus, the in vitro RdRp activities of ER-targeted protein A chimeras mirrored their increased in vivo activities (Fig. 3).

FHV replication complexes targeted to mitochondria or the ER induce distinct ultrastructural membrane alterations in yeast. FHV infection of *Drosophila* cells induces distinct mitochondrial alterations, including mitochondrial clustering and the formation of 40- to 60-nm-diameter membrane-bounded spherical invaginations into the mitochondrial intermembrane space (33). Similar spherical membrane structures have been seen with a number of other positive-strand RNA viruses (7, 15, 18, 19, 24, 28, 51), and the localization of both viral replicase proteins and nascent viral RNA synthesis to these structures indicates that they are the intracellular sites of viral RNA

EXHIBIT A

replication complexes. To determine whether ultrastructural membrane changes similar to those in FHV-infected *Drosophila* cells (33) were also present in yeast cells replicating FHV RNA and to examine potential membrane changes induced by ER-targeted protein A chimeras, we used transmission EM to analyze yeast expressing pFA alone, $pF1_{fs}$ plus pFA, or pFA-HCV (Fig. 6). Compared to control yeast (Fig. 6A), yeast expressing pFA alone showed a proliferation of intracellular membranes and a marked clustering of membrane-bounded organelles (Fig. 6B). These structures were often located asymmetrically within cells and adjacent to nuclei, and normal-appearing mitochondria were not readily visible. A similar proliferation and ultrastructural appearance of intracellular membranes has been described in yeast expressing the mitochondrial-targeted Carnation Italian ringspot virus (CIRV) 36-kDa replicase protein (43). Yeast cells expressing $pF1_{fs}$ plus pFA had a similar appearance, with clustered membrane-bounded organelles (Fig. 6C). In addition, electron-dense structures were often visible along the clustered membranes (Fig. 6C), which at higher magnification appeared as tightly compressed membrane-bounded circular or ellipsoid structures (Fig. 6D). These structures protruded into the lumen of the organelle and had diameters of 30 to 50 nm, similar to the mitochondrial spherules located in the intermembrane spaces of FHV-infected *Drosophila* cells (33). However, the double external membrane and internal cristae that are characteristics of mitochondria were not readily apparent in the wt-protein A-induced clustered membrane structures in yeast. Nevertheless, the absence of normal mitochondria, the confocal immunofluorescence results demonstrating the localization of wt protein A to mitochondria in yeast (32) (Fig. 2A), and the similar ultrastructural appearances of FHV-infected *Drosophila* cells (33) and yeast expressing the CIRV 36-kDa replicase protein (43) suggest that the clustered membrane-bounded organelles in yeast expressing wt FHV protein A were mitochondria.

The ultrastructural appearance of the membrane alterations in yeast expressing $pF1_{fs}$ plus pFA-HCV were significantly different than that in yeast cells expressing wt protein A. Membrane proliferation was localized primarily to the perinuclear region (Fig. 6E), consistent with the confocal-immunofluorescence results that showed localization of chimeric protein A to the perinuclear ER (Fig. 2B). The number of membrane layers adjacent to the nucleus varied from three to more than six, and they often almost completely surrounded the nucleus. Although spherule-like structures were not readily evident, high magnification often demonstrated an irregular appearance of the perinuclear membrane layers (Fig. 6F), suggesting the presence of possible underlying structures not readily visible under the fixation conditions used. Similar perinuclear layers have been observed under some conditions for yeast replicating brome mosaic virus RNA (M. D. Schwartz, J. Chen, W. M. Lee, and P. Ahlquist, unpublished data). Thus, the EM ultrastructural studies were consistent with the confocal-immunofluorescence results (Fig. 2) and suggested that structural differences between mitochondrial- and ER-targeted FHV replication complexes, or their associated membranes, may have contributed to the functional differences observed both in vivo (Fig. 3) and in vitro (Fig. 5).

DISCUSSION

In this report, we investigated the roles of alternative intracellular membranes in the formation and function of viral RNA replication complexes by retargeting FHV protein A to the ER. We drew three main conclusions. First, the introduction of engineered sequences from the HCV NS5B polymerase, the yeast NADP cytochrome P450 oxidoreductase, or the yeast t-SNARE Ufe1p into the N terminus of protein A retargeted the FHV RNA polymerase from the mitochondria to the ER. Second, ER-targeted FHV RNA replication complexes were active in vivo and in vitro. Third, ER-targeted FHV RNA replication complexes had enhanced RNA synthesis activity compared to replication complexes targeted to mitochondria. These observations indicate that unique intracellular membranes are not required for FHV RNA replication complex formation and function and suggest that any membrane-associated host functions required for FHV RNA replication complexes are provided either by a factor or factors present on multiple membranes or by distinct, membrane-specific factors with similar functions. The ability of FHV to replicate its RNA on two different intracellular-membrane compartments in yeast makes it a potentially valuable tool to investigate the contributions of host membranes and other host factors to RNA replication complex assembly and function. The natures and functions of known host factors involved in positive-strand RNA virus genome replication have recently been reviewed (1).

The demonstration that FHV RNA replication complexes can be retargeted is consistent with the results of a previous study that suggested tombusvirus RNA replication complexes could be retargeted (10). Tombusviruses are positive-strand RNA viruses of plants whose infections are associated with the formation of membranous cytoplasmic inclusions called multivesicular bodies. These structures form on mitochondria or peroxisomes, respectively, in plants infected with the tombusviruses CIRV and cymbidium ringspot virus (45). Multivesicular bodies are surrounded by multiple 80- to 150-nm-diameter vesicles that contain RNA, as detected by RNase susceptibility (15), and viral replicase proteins (9), and thus they are thought to represent the sites of tombusvirus RNA replication. Multivesicular-body localization is dependent on determinants encoded by the 5′-terminal region of the tombusvirus genome. Replacement of 600 nucleotides from the 5′ region of the CIRV genome with a similar region from the cymbidium ringspot virus genome changes the localization of multivesicular bodies from mitochondria to peroxisomes (10). FHV and CIRV show several similarities, including the normal mitochondrial localization of viral RNA replication complexes and the formation of outer mitochondrial membrane spherules (15, 33) and the presence of TMDs within the mitochondrial localization sequence of the replicase protein responsible for intracellular targeting (32, 44, 55). In addition, both FHV and CIRV can replicate viral RNA in yeast and induce the formation of similar intracellular-membrane structures (34, 37–39, 43) (Fig. 6). Further retargeting studies with FHV, CIRV, and other positive-strand RNA viruses may identify broadly applicable principles that define the interactions between viral replicase proteins and host intracellular membranes that are nec-

essary for positive-strand RNA virus replication complex formation and function.

We retargeted FHV RNA replication complexes to the ER because that membrane compartment is used for viral RNA replication complex formation by a number of positive-strand RNA viruses (26, 29, 35, 42, 46–48, 51). The effectiveness of inverted C-terminal targeting sequences from the HCV NS5B polymerase and the yeast t-SNARE Ufe1p in retargeting FHV RNA replication complexes to the ER was consistent with the observation that the TMD amino acid composition and length, rather than the specific sequence, are important determinants for membrane localization (40). However, our results are not consistent with the results of the study by Kanaji et al. that showed a correlation between TMD hydrophobicity and intracellular-membrane localization, in which TMD hydrophobicities of <2.15 were associated with a mitochondrial localization while TMD hydrophobicities of >2.30 resulted in ER or Golgi localization (23). There was no correlation between TMD hydrophobicity and intracellular-membrane localization with the protein A chimeras used in this study. The wt protein A TMD has a hydrophobicity of 1.96, whereas the inverted HCV NS5B, P450 oxidoreductase, and inverted Ufe1p TMDs have average hydrophobicities of 2.27, 1.19, and 2.18, respectively. One potential explanation for this apparent discrepancy is that the Lys residue immediately downstream of the protein A TMD was present in all chimeric constructs (Fig. 1A), and the presence of charged residues surrounding TMDs can impact intracellular localization (23, 25). Alternatively, we cannot exclude the possibility that the ER was the default intracellular membrane target when protein A was no longer targeted specifically to the mitochondrial outer membrane, as we did not attempt to retarget FHV replication complexes to an alternative intracellular membrane other than the ER.

Previous studies that have examined FHV RNA replication in yeast (27, 38) have demonstrated significantly higher subgenomic RNA3/genomic RNA1 ratios in yeast expressing wt protein A than we found in this report (Fig. 3A and 4). Two differences in experimental design potentially contribute to this observation. We used the yeast strain BY4742, similar to the mapping study that identified the FHV protein A TMD as an important mitochondrial localization domain (32), whereas Price et al. (38) and Lindenbach et al. (27) used the yeast strain YPH500, which at 24 h after induction produces a higher subgenomic RNA3/genomic RNA1 ratio than BY4742 (P. McDowell and P. Ahlquist, unpublished data). Possibly due to the higher growth rate of BY4742, similar differences in subgenomic viral RNA accumulation between these yeast strains have been previously observed with brome mosaic virus (D. Kushner and P. Ahlquist, unpublished data). In addition, previous studies used a high-copy-number 2μm plasmid for FHV RNA1 template expression (27, 38), whereas we used a low-copy number centromeric plasmid to increase plasmid stability and reduce potential differences in DNA-dependent FHV RNA template expression levels between yeast cells expressing wt and ER-targeted protein A.

The observation that retargeting FHV protein A to ER membranes resulted in enhanced in vivo and in vitro RdRp activities compared to mitochondrial membrane-associated replication complexes was surprising, as nodavirus RNA replication is normally extremely robust. For example, in *Drosophila* cells infected with black beetle virus, an alphanodavirus whose RNA1 sequence shows 99% identity with FHV (4), viral RNA synthesis accounts for almost 50% of total RNA synthesis (17). Infectious-virion production in yeast spheroplasts transfected with FHV RNA is similar to that in FHV-infected *Drosophila* cells (39), and FHV RNA1 levels per microgram of total RNA are similar in infected *Drosophila* cells and yeast expressing pF1 (38). These observations suggest that FHV RNA replication efficiencies with wt protein A are similar in yeast and insect cells. The mechanisms responsible for the increased RNA accumulation observed in vivo (Fig. 3) and RNA synthesis observed in vitro (Fig. 5) with ER-targeted FHV replication complexes are unknown but could involve increased speed or efficiency of replication complex assembly, template RNA recruitment, or substrate utilization or increased stability of the template or product RNA. The reduced magnitude of the differences in (+)RNA3 accumulation between yeast cells expressing wt and ER-targeted protein A after prolonged induction (Fig. 4) implies that these differences reflect greater shifts in the early kinetics rather than in the final accumulation of RNA replication products. The observed differences in in vitro RdRp activities (Fig. 5B) and membrane ultrastructures (Fig. 6) also suggest the possibility that FHV RNA replication complexes targeted to mitochondrial or ER membranes may differ in accessibility to the cytoplasm for importing nucleotides or exporting product RNA, in host factor composition, or in other characteristics. Further experiments are being pursued to explore the underlying mechanisms responsible for the unexpected and interesting differences revealed by the retargeting of FHV RNA replication complexes.

ACKNOWLEDGMENTS

We thank Kathleen Wessels, Pricilla McDowell, and Aaron Eichhorn for assistance. We performed the confocal immunofluorescence microscopy and transmission EM at the Keck Neural Imaging Laboratory and the Medical School Electron Microscopy Facility at the University of Wisconsin—Madison, respectively.

This work was supported by National Institutes of Health grants K08 AI01770-1 and GM35072. P.A. is an investigator of the Howard Hughes Medical Institute.

REFERENCES

1. **Ahlquist, P., A. O. Noueiry, W. Lee, D. B. Kushner, and B. T. Dye.** 2003. Host factors in positive-strand RNA virus genome replication. J. Virol. 77:8181–8186.
2. **Ahola, T., A. Lampio, P. Auvinen, and L. Kaariainen.** 1999. Semliki Forest virus mRNA capping enzyme requires association with anionic membrane phospholipids for activity. EMBO J. 18:3164–3172.
3. **Ball, L. A.** 1995. Requirements for the self-directed replication of Flock House virus RNA 1. J. Virol. 69:720–727.
4. **Ball, L. A., and K. L. Johnson.** 1998. Nodaviruses of insects, p. 225–267. *In* L. K. Miller and L. A. Ball (ed.), The insect viruses. Plenum Publishing Corp., New York, N.Y.
5. **Ball, L. A., and Y. Li.** 1993. *cis*-acting requirements for the replication of Flock House virus RNA 2. J. Virol. 67:3544–3551.
6. **Barton, D. J., S. G. Sawicki, and D. L. Sawicki.** 1991. Solubilization and immunoprecipitation of alphavirus replication complexes. J. Virol. 65:1496–1506.
7. **Bashiruddin, J. B., and G. F. Cross.** 1987. Boolarra virus: ultrastructure of intracytoplasmic virus formation in cultured *Drosophila* cells. J. Invertebr. Pathol. 49:303–315.
8. **Bienz, K., D. Egger, T. Pfister, and M. Troxler.** 1992. Structural and functional characterization of the poliovirus replication complex. J. Virol. 66: 2740–2747.
9. **Bleve-Zacheo, T., L. Rubino, M. T. Melillo, and M. Russo.** 1997. The 33K protein encoded by cymbidium ringspot tombusvirus localizes to modified peroxisomes of infected cells and of uninfected transgenic plant. J. Plant Pathol. 79:179–202.

10. **Burgyan, J., L. Rubino, and M. Russo.** 1996. The 5'-terminal region of a tombusvirus genome determines the origin of multivesicular bodies. J. Gen. Virol. **77:**1967–1974.
11. **Chen, J., and P. Ahlquist.** 2000. Brome mosaic virus polymerase-like protein 2a is directed to the endoplasmic reticulum by helicase-like viral protein 1a. J. Virol. **74:**4310–4318.
12. **Chu, P. W. G., and E. G. Westaway.** 1992. Molecular and ultrastructural analysis of heavy membrane fractions associated with the replication of Kunjin virus RNA. Arch. Virol. **125:**177–191.
13. **Dasmahapatra, B., R. Dasgupta, A. Ghosh, and P. Kaesberg.** 1985. Structure of the black beetle virus genome and its functional implications. J. Mol. Biol. **182:**183–189.
14. **De Graaff, M., L. Coscoy, and E. M. Jaspars.** 1993. Localization and biochemical characterization of alfalfa mosaic virus replication complexes. Virology **194:**878–881.
15. **Di Franco, A., M. Russo, and G. P. Martelli.** 1984. Ultrastructure and origin of cytoplasmic multivesicular bodies induced by carnation Italian ringspot virus. J. Gen. Virol. **65:**1233–1237.
16. **Egger, D., B. Wolk, R. Gosert, L. Bianchi, H. E. Blum, D. Moradpour, and K. Bienz.** 2002. Expression of hepatitis C virus proteins induces distinct membrane alterations including a candidate viral replication complex. J. Virol. **76:**5974–5984.
17. **Friesen, P. D., and R. R. Rueckert.** 1982. Black beetle virus: messenger for protein B is a subgenomic viral RNA. J. Virol. **42:**986–995.
18. **Froshauer, S., J. Kartenbeck, and A. Helenius.** 1988. Alphavirus RNA replicase is located on the cytoplasmic surface of endosomes and lysosomes. J. Cell Biol. **107:**2075–2086.
19. **Grimley, P. M., I. K. Berezesky, and R. M. Friedman.** 1968. Cytoplasmic structures associated with an arbovirus infection: loci of viral ribonucleic acid synthesis. J. Virol. **2:**1326–1338.
20. **Guinea, R., and L. Carrasco.** 1990. Phospholipid biosynthesis and poliovirus genome replication, two coupled phenomena. EMBO J. **9:**2011–2016.
21. **Johnson, K. L., and L. A. Ball.** 1997. Replication of Flock House virus RNAs from primary transcripts made in cells by RNA polymerase II. J. Virol. **71:**3323–3327.
22. **Johnson, K. L., and L. A. Ball.** 1999. Induction and maintenance of autonomous Flock House virus RNA1 replication. J. Virol. **73:**7933–7942.
23. **Kanaji, S., J. Iwahashi, Y. Kida, M. Sakaguchi, and K. Mihara.** 2000. Characterization of the signal that directs Tom20 to the mitochondrial outer membrane. J. Cell Biol. **151:**277–288.
24. **Kujala, P., A. Ikaheimonen, N. Ehsani, H. Vihinen, P. Auvinen, and L. Kaariainen.** 2001. Biogenesis of the Semliki Forest virus RNA replication complex. J. Virol. **75:**3873–3884.
25. **Kuroda, R., T. Ikenoue, M. Honsho, S. Tsujimoto, J. Y. Mitoma, and A. Ito.** 1998. Charged amino acids at the carboxyl-terminal portions determine the intracellular locations of two isoforms of cytochrome b5. J. Biol. Chem. **273:**31097–31102.
26. **Lee, W. M., M. Ishikawa, and P. Ahlquist.** 2001. Mutation of host Δ9 fatty acid desaturase inhibits brome mosaic virus RNA replication between template recognition and RNA synthesis. J. Virol. **75:**2097–2106.
27. **Lindenbach, B. D., J. Y. Sgro, and P. Ahlquist.** 2002. Long-distance base pairing in Flock House virus RNA1 regulates subgenomic RNA3 synthesis and RNA2 replication. J. Virol. **76:**3905–3919.
28. **Magliano, D., J. A. Marshall, D. S. Bowden, N. Vardaxis, J. Meanger, and J. Y. Lee.** 1998. Rubella virus replication complexes are virus-modified lysosomes. Virology **240:**57–63.
29. **Mas, P., and R. N. Beachy.** 1999. Replication of tobacco mosaic virus on endoplasmic reticulum and role of the cytoskeleton and virus movement protein in intracellular distribution of viral RNA. J. Cell Biol. **147:**945–958.
30. **Maynell, L. A., K. Kirkegaard, and M. K. Klymkowsky.** 1992. Inhibition of poliovirus RNA synthesis by brefeldin A. J. Virol. **66:**1985–1994.
31. **McBride, H. M., D. G. Millar, J. M. Li, and G. C. Shore.** 1992. A signal-anchor sequence selective for the mitochondrial outer membrane. J. Cell Biol. **119:**1451–1457.
32. **Miller, D. J., and P. Ahlquist.** 2002. Flock House virus RNA polymerase is a transmembrane protein with amino-terminal sequences sufficient for mitochondrial localization and membrane insertion. J. Virol. **76:**9856–9867.
33. **Miller, D. J., M. D. Schwartz, and P. Ahlquist.** 2001. Flock House virus RNA replicates on outer mitochondrial membranes in *Drosophila* cells. J. Virol. **75:**11664–11676.
34. **Pantaleo, V., L. Rubin, and M. Russo.** 2003. Replication of carnation Italian ringspot virus defective interfering RNA in *Saccharomyces cerevisiae*. J. Virol. **77:**2116–2123.
35. **Pedersen, K. W., Y. van der Meer, N. Roos, and E. J. Snijder.** 1999. Open reading frame 1a-encoded subunits of the arterivirus replicase induce endoplasmic reticulum-derived double-membrane vesicles which carry the viral replication complex. J. Virol. **73:**2016–2026.
36. **Perez, L., R. Guinea, and L. Carrasco.** 1991. Synthesis of Semliki Forest virus RNA requires continuous lipid synthesis. Virology **183:**74–82.
37. **Price, B. D., P. Ahlquist, and L. A. Ball.** 2002. DNA-directed expression of an animal virus RNA for replication-dependent colony formation in *Saccharomyces cerevisiae*. J. Virol. **76:**1610–1616.
38. **Price, B. D., M. Roeder, and P. Ahlquist.** 2000. DNA-directed expression of functional Flock House virus RNA1 derivatives in *Saccharomyces cerevisiae*, heterologous gene expression, and selective effects on subgenomic mRNA synthesis. J. Virol. **74:**11724–11733.
39. **Price, B. D., R. R. Rueckert, and P. Ahlquist.** 1996. Complete replication of an animal virus and maintenance of expression vectors derived from it in *Saccharomyces cerevisiae*. Proc. Natl. Acad. Sci. USA **93:**9465–9470.
40. **Rayner, J. C., and H. R. Pelham.** 1997. Transmembrane domain-dependent sorting of proteins to the ER and plasma membrane in yeast. EMBO J. **16:**1832–1841.
41. **Restrepo-Hartwig, M., and P. Ahlquist.** 1999. Brome mosaic virus RNA replication proteins 1a and 2a colocalize and 1a independently localizes on the yeast endoplasmic reticulum. J. Virol. **73:**10303–10309.
42. **Restrepo-Hartwig, M. A., and P. Ahlquist.** 1996. Brome mosaic virus helicase- and polymerase-like proteins colocalize on the endoplasmic reticulum at sites of viral RNA synthesis. J. Virol. **70:**8908–8916.
43. **Rubino, L., A. Di Franco, and M. Russo.** 2000. Expression of a plant virus non-structural protein in *Saccharomyces cerevisiae* causes membrane proliferation and altered mitochondrial morphology. J. Gen. Virol. **81:**279–286.
44. **Rubino, L., and M. Russo.** 1998. Membrane targeting sequences in tombusvirus infections. Virology **252:**431–437.
45. **Russo, M., A. Di Franco, and G. P. Martelli.** 1987. Cytopathology in the identification and classification of tombusviruses. Intervirology **28:**134–143.
46. **Schaad, M. C., P. E. Jensen, and J. C. Carrington.** 1997. Formation of plant RNA virus replication complexes on membranes: role of an endoplasmic reticulum-targeted viral protein. EMBO J. **16:**4049–4059.
47. **Schlegel, A., T. H. Giddings, Jr., M. S. Ladinsky, and K. Kirkegaard.** 1996. Cellular origin and ultrastructure of membranes induced during poliovirus infection. J. Virol. **70:**6576–6588.
48. **Schmidt-Mende, J., E. Bieck, T. Hugle, F. Penin, C. M. Rice, H. E. Blum, and D. Moradpour.** 2001. Determinants for membrane association of the hepatitis C virus RNA-dependent RNA polymerase. J. Biol. Chem. **276:**44052–44063.
49. **Schneemann, A., and D. Marshall.** 1998. Specific encapsulation of nodavirus RNAs is mediated through the C terminus of capsid precursor protein alpha. J. Virol. **72:**8738–8746.
50. **Schneemann, A., W. Zhong, T. M. Gallagher, and R. R. Rueckert.** 1992. Maturation cleavage required for infectivity of a nodavirus. J. Virol. **66:**6728–6734.
51. **Schwartz, M., J. Chen, M. Janda, M. Sullivan, J. den Boon, and P. Ahlquist.** 2002. A positive-strand RNA virus replication complex parallels form and function of retrovirus capsids. Mol. Cell **9:**505–514.
52. **van der Heijden, M. W., J. E. Carette, P. J. Reinhoud, A. Haegi, and J. F. Bol.** 2001. Alfalfa mosaic virus replicase proteins P1 and P2 interact and colocalize at the vacuolar membrane. J. Virol. **75:**1879–1887.
53. **van der Meer, Y., E. J. Snijder, J. C. Dobbe, S. Schleich, M. R. Denison, W. J. Spaan, and J. K. Locker.** 1999. Localization of mouse hepatitis virus nonstructural proteins and RNA synthesis indicates a role for late endosomes in viral replication. J. Virol. **73:**7641–7657.
54. **Venkateswarlu, K., D. C. Lamb, D. E. Kelly, N. J. Manning, and S. L. Kelly.** 1998. The N-terminal membrane domain of yeast NADPH-cytochrome P450 (CYP) oxidoreductase is not required for catalytic activity in sterol biosynthesis or in reconstitution of CYP activity. J. Biol. Chem. **273:**4492–4496.
55. **Weber-Lotfi, F., A. Dietrich, M. Russo, and L. Rubino.** 2002. Mitochondrial targeting and membrane anchoring of a viral replicase in plant and yeast cells. J. Virol. **76:**10485–10496.
56. **Westaway, E. G., A. A. Khromykh, and J. M. Mackenzie.** 1999. Nascent flavivirus RNA colocalized in situ with double-stranded RNA in stable replication complexes. Virology **258:**108–117.
57. **Wu, S. X., P. Ahlquist, and P. Kaesberg.** 1992. Active complete in vitro replication of nodavirus RNA requires glycerophospholipid. Proc. Natl. Acad. Sci. USA **89:**11136–11140.
58. **Wu, S. X., and P. Kaesberg.** 1991. Synthesis of template-sense, single-strand Flockhouse virus RNA in a cell-free replication system. Virology **183:**392–396.
59. **Zhong, W., R. Dasgupta, and R. R. Rueckert.** 1992. Evidence that the packaging signal for nodaviral RNA2 is a bulged stem-loop. Proc. Natl. Acad. Sci. USA **89:**11146–11150.

THE JOURNAL OF BIOLOGICAL CHEMISTRY
Vol. 278, No. 50, Issue of December 12, pp. 50301–50308, 2003
Printed in U.S.A.

Hepatitis C Virus Non-structural Proteins in the Probable Membranous Compartment Function in Viral Genome Replication*

Received for publication, May 30, 2003, and in revised form, August 20, 2003
Published, JBC Papers in Press, September 8, 2003, DOI 10.1074/jbc.M305684200

Yusuke Miyanari, Makoto Hijikata‡, Masashi Yamaji, Masahiro Hosaka, Hitoshi Takahashi, and Kunitada Shimotohno

From the Department of Viral Oncology, Institute for Virus Research, Kyoto University, Kyoto 606-8507, Japan

The molecular mechanism of hepatitis C virus(HCV) RNA replication is still unknown. Recently, a cell culture system in which the HCV subgenomic replicon is efficiently replicated and maintained for a long period in Huh-7 cells has been established. Taking advantage of this replicon system, we detected the activity to synthesize the subgenomic RNA in the digitonin-permeabilized replicon cells. To elucidate how and where this viral RNA replicates in the cells, we monitored the activity for HCV RNA synthesis in the permeabilized replicon cells under several conditions. We obtained results suggesting that HCV replication complexes functioning to synthesize the replicon RNA are protected from access of nuclease and proteinase by possible cellular lipid membranes. We also found that a large part of the replicon RNA, including newly synthesized RNA, was present in such a membranous structure but a large part of each NS protein was not. A small part of each NS protein that was resistant to the proteinase action was shown to contribute sufficiently to the synthesis of HCV subgenomic RNA in the permeabilized replicon cells. These results suggested that a major subcellular site of HCV genome replication is probably compartmentalized by lipid membranes and that only a part of each NS protein forms the active replication complex in the replicon cells.

Infection of hepatitis C virus (HCV)[1] is estimated to occur in about 3% of the worlds population. HCV infection frequently causes chronic hepatitis, which often leads to the development of liver cirrhosis and hepatocellular carcinoma after a long period (1–3). Current combination therapy with interferon-α and ribavirin, a nucleotide analogue, is effective in many patients with chronic hepatitis C (4, 5). There still are, however, a lot of patients who do not respond to these treatments. Therefore, extensive studies have been performed to develop highly effective anti-HCV drugs. Such a drug, however, has not been produced yet, possibly because of the lack of detailed information about the life cycle of this virus.

HCV is a member of the *Flaviviridae* family and contains a single-strand RNA genome of positive polarity (6). The RNA genome is ~9.6 kb in length and consists of a 5′-untranslated region of 341 nucleotides, a large open reading frame encoding a single precursor polyprotein of ~3000 amino acids, and a 3′-untranslated region of variable length (6–8). The polyprotein is processed by the host and viral proteinases to generate at least 10 functional viral proteins: core (C), envelope (E) 1, E2, p7, non-structural protein (NS) 2, NS3, NS4A, NS4B, NS5A, and NS5B (from the amino- to the carboxyl-terminal) (9–12). C, E1, and E2 are believed to form viral particles as structural proteins. p7 was recently reported to form an ion channel-like structure (13, 14). NS molecules have been considered to function in the replication of HCV subgenomic RNA (15). Using recombinant proteins produced in either bacterial or insect cells, the proteinase and helicase activities of NS3 and RNA-dependent RNA polymerase activity of NS5B have been biochemically characterized (16–20). However, it was not clear whether these recombinant proteins function in HCV genomic replication as it has been revealed that HCV genomic sequences are highly variable among all isolates and furthermore, it is unclear whether the genes for these viral enzymes were derived from infectious HCV genomes.

Recently, HCV subgenomic RNA that replicates efficiently and is maintained for a long period in the human hepatoma cell line Huh-7 was developed and called the HCV subgenomic replicon (15). Functional replicons originating from different HCV isolates have been reported (15, 21–23). The HCV subgenomic RNA was constructed by replacing the structural and part of the non-structural protein-encoding regions (C-NS2) of the HCV genome with the neomycin phosphotransferase gene (*neo*^{r}) and an internal ribosome entry site of *encephalomyocarditis* virus (21). This implies that HCV proteins encoded in this subgenomic RNA (NS3-NS5B) are functional and sufficient for this RNA replication. In this model system, it has been suggested that mutations of particular amino acids in the NS region enhanced the efficiency of the replication (24–27). It was also demonstrated that the existence of the cis-acting elements in either the 5′- or 3′-untranslated regions were required for efficient replication (27–29). Recent observations indicated that the replication of the replicon RNA could be reproduced *in vitro* using particular cellular fractions from replicon cells (30–32). It remains, however, to be elucidated how and where the HCV RNA is synthesized in the cells. So, we intended to clarify these points using digitonin-treated replicon cells of which plasma membranes were permeabilized. This permeabilized cell system is often used to monitor several cellular events,

* This work was supported by grants-in-aid for cancer research and for the second-term comprehensive 10-year strategy for cancer control from the Ministry of Health, Labor, and Welfare, through grants-in-aid for scientific research from the Ministry of Education, Culture, Sports, Science and Technology, grants-in-aid of research for the future from the Japanese Society for the Promotion of Science, and by the Program for Promotion of Fundamental Studies in Health Science of the Organization for Pharmaceutical Safety and Research (OPSR) of Japan. The costs of publication of this article were defrayed in part by the payment of page charges. This article must therefore be hereby marked "*advertisement*" in accordance with 18 U.S.C. Section 1734 solely to indicate this fact.

‡ To whom correspondence should be addressed: 53 Kawahara-cho Shogo-in, Sakyo-ku, Kyoto 606-8507, Japan. Tel.: 81-75-751-4046; Fax: 81-75-751-3998; E-mail: mhijikat@virus.kyoto-u.ac.jp.

[1] The abbreviations used are: HCV, hepatitis C virus; NS, non-structural; ER, endoplasmic reticulum; DHFR, dihydrofolate reductase.

such as a nuclear protein transport as well as replication of positive-strand RNA viruses.

Cell biological and biochemical analyses have demonstrated that all HCV NS proteins are directly or indirectly associated with inner cellular membranes and colocalize on the rough endoplasmic reticulum (ER) membranes (33–36). So, we expected the active HCV replication complexes to be retained on the inner cellular membranes in permeabilized replicon cells. In this paper, we report that the functional replication complexes are retained in permeabilized replicon cells and its activity is easily detected by using this system. We also obtained data suggesting that a part of each NS protein in the cells, which is probably located in a membranous compartment, forms the active replication complex and contributes to the synthesis of HCV subgenomic RNA.

EXPERIMENTAL PROCEDURES

Cell Cultures—The human hepatoma cell line Huh-7 was grown in Dulbecco's modified Eagle's medium (Invitrogen) supplemented with 10% fetal bovine serum, 100 units/ml nonessential amino acids (Invitrogen), and 100 μg/ml penicillin and streptomycin sulfate (Invitrogen). MH-14 cells were cultured in the same medium with 500 μg/ml G418 (GENETICIN, Invitrogen).

Sequencing Analysis—The nucleotide sequence of the HCV subgenomic replicon RNA in MH-14 cells was determined by reverse transcription-PCR-based DNA sequencing as described previously (21).

Plasmid Construction—The plasmid pGEM-NN was constructed by inserting the cDNA fragment of the subgenomic replicon from pNNRZ2 (21) into the TA site of pGEM-T-Easy vector (Promega, Madison, WI). The cDNA fragment was obtained by PCR using the oligonucleotides 5′-GCCAGCCCCCGATTGGGGGCGACAC-3′ and 5′-ACATGATCTGCAGAGAGGCCAG-3′ and the plasmid pNNRZ2 as primers and a template, respectively.

In Vitro Transcription—pGEM-NN was linearized with PvuI or SpeI for plus or minus strand subgenomic HCV RNA synthesis, respectively, and used as a template for *in vitro* RNA synthesis with MEGA script Sp6 or T7 kit (Ambion, Austin, TX), respectively.

Preparation of RNA and Northern Blot Analysis—RNA was extracted from cells and a reaction mixture with Sepasol RNA I and II super reagent (Nacalai Tesque, Kyoto, Japan), respectively, according to the manufacturer's protocol. Northern blot analysis was performed as described previously (37). For the preparation of the ^{32}P-labeled probe, the EcoRI fragment of pNNRZ2 was labeled with a Ready-to-Go DNA labeling beads (-dCTP) kit (Amersham Biosciences) in the presence of 50 μCi of [α-^{32}P]dCTP (Amersham Biosciences).

Western Blotting—The preparation of the cell lysate, SDS-PAGE, and immunoblotting were performed as previously described (10). The antibodies used in the immunoblotting were those against HCV NS3, NS4A (α-NS4A), NS4B (NS4B-52), NS5A (α-NS5A), NS5B (NS5B-14) (21), dihydrofolate reductase (DHFR) (34), BiP/Grp78 (StressGen, Victoria, BC, Canada), and Calnexin-NT (StressGen). Anti-NS3 antibody was a gift from Dr. M. Kohara (Tokyo Metropolitan Institute of Medical Science).

Indirect Immunofluorescence—Indirect immunofluorescence analysis was essentially performed as described previously (38), with minor modifications. 1.0 × 10^5 cells were seeded on poly-L-lysine (Sigma)-coated coverslips. Three days post-seeding, the cells were fixed with 4% paraformaldehyde in phosphate-buffered saline (137 mM NaCl, 2.7 mM KCl, 4.3 mM Na_2HPO_4, and 1.4 mM KH_2PO_4) for 30 min at room temperature. The cells were treated with pre-chilled 100% methanol for 10 min at −20 °C after the fixation. In the case of permeabilized cells, permeabilization with digitonin followed by washing with buffer B (see below) was performed before or after fixation with 4% paraformaldehyde and then the cells were permeabilized completely with chilled 100% methanol after fixation. The antibodies against NS5A (α-NS5A), NS5B (NS5B-12), and protein-disulfide isomerase (StressGen) were used as primary antibodies. NS5B-12 was a gift from Dr. M. Kohara (Tokyo Metropolitan Institute of Medical Science). The fluorescent secondary antibodies were Alexa 568 goat anti-mouse IgG (H+L) and Alexa 488 goat anti-rabbit IgG (H+L) conjugates (Molecular Probes, Eugene, OR). The nucleus was visualized by staining with 4′,6-diamidino-2-phenylindole. All imaging experiments were performed on a Leica SP2 confocal microscope (Leica Microsystems, Germany).

Cell Permeabilization and Synthesis of HCV Subgenomic RNA—Cells of about 80% confluency in 12- or 6-well plates were precultured in complete Dulbecco's modified Eagle's medium containing 5 μg/ml actinomycin D (Nacalai Tesque) for 2 h, then washed with cold buffer B: 20 mM HEPES-KOH (pH 7.7 at 27 °C), 110 mM potassium acetate, 2 mM magnesium acetate, 1 mM EGTA, and 2 mM dithiothreitol. The cells were permeabilized by incubation in buffer B containing 50 μg/ml digitonin for 5 min at 27 °C and the reaction was stopped by washing twice with cold buffer B. The permeabilized cells were, then, incubated for 4 h at 27 °C in the labeling reaction mixture: 2 mM manganese(II) chloride, 1 mg/ml acetylated bovine serum albumin (Nacalai Tesque), 5 mM phosphocreatine (Sigma), 20 units/ml creatine phosphokinase (Sigma), 50 μg/ml actinomycin D, 500 μM ATP, CTP, and GTP (Roche Diagnostics), and 10 μCi of [α-^{32}P]UTP (Amersham Biosciences) in buffer B (pH 7.7), for 4 h at 27 °C unless otherwise specified. The reaction was terminated by the addition of Sepasol RNA I or II super reagent.

For the treatments with micrococcal nuclease and/or Nonidet P-40, the permeabilized cells were pre-washed twice with buffer D: 20 mM HEPES-KOH (pH 7.7 at 27 °C), 110 mM potassium acetate, 2 mM magnesium acetate, 2 mM dithiothreitol, and 1 mM $CaCl_2$. Then the permeabilized cells were incubated in buffer D containing 0.1 unit/ml micrococcal nuclease (United States Biochemical Corp.), with or without 0.5% Nonidet P-40 for 15 min at 37 °C or 0.5% Nonidet P-40 for 15 min on ice.

Slot Blot Hybridization—RNA products synthesized in the permeabilized cells in the presence of 200 μCi of [α-^{32}P]UTP were fractionated by denaturing agarose gel. The 8-kb RNA bands were eluted from the gel using RNade (BioOne, Carlsbad, CA). To increase the hybridization signal, the ^{32}P-labeled 8-kb RNA eluted from the gel was subjected to alkaline hydrolysis to generate fragments of ~250 nucleotides in length and used in hybridization. Newly synthesized replicon RNA in intact replicon cells was metabolically labeled by adding 1200 μCi of [^{32}P]orthophosphate to the culture medium (see below) and handled in the same manner. For detection of plus and minus strand replicon RNA, minus and plus strand replicon RNA were prepared as riboprobes by *in vitro* transcription, respectively, as described above. Then 2 μg of each riboprobe was applied to a nylon membrane filter (Hybond-N, Ambion). Slot blot hybridization was performed as described previously (39), except that ULTRAhyb (Ambion) was used for hybridization buffer.

Metabolic Labeling—For metabolic labeling of the replicon RNA, after a preculture in phosphate-free Dulbecco's modified Eagle's medium (Invitrogen) containing 2% dialyzed fetal bovine serum, 200 μg/ml G418, and 5 μg/ml actinomycin D for 2 h, 4 × 10^5 cells were cultured for 12 h in the same medium with 100 μCi of [^{32}P]orthophosphate (Amersham Biosciences), as described previously (21).

Proteinase K Treatment—After permeabilization of the replicon cells, the cells were scraped into 400 μl of cold buffer B and transferred to a siliconized tube. The cells were treated with various concentrations of proteinase K at 37 °C for 5 min. The reaction was terminated by the addition of 1 mM phenylmethylsulfonyl fluoride, and followed by trichloroacetic acid precipitation. The trichloroacetic acid precipitates were solubilized in 1× sample buffer containing 1 mM phenylmethylsulfonyl fluoride and used in Western blotting analysis.

RESULTS

Selection of Replicon Cell Clones in Which Replicon RNA Efficiently Replicated—We reported the establishment of a cell clone, NN 50-1, in which HCV subgenomic replicon RNA originating from the HCV genome isolated from the cultured human T cell line MT-2C infected with HCV *in vitro* efficiently replicated (21). Furthermore, we obtained a cell clone, MH-14, in which the HCV subgenomic RNA level is nearly 5-fold higher than that in NN 50-1 (data not shown). Nucleotide sequence analysis revealed that the replicon RNA in MH-14 cells bore two point mutations in the NS4B and NS5A encoding regions. One was a thymine to cytosine transition at nucleotide position 5985 (the number corresponds to the nucleotide number of the HCV genotype 1b genome) in the NS4B-encoding region without an amino acid substitution. Another was a cytosine to adenine transition at nucleotide 6953 in the NS5A-encoding region, resulting in the substitution of arginine for serine at amino acid position 2204. The substitution at amino acid 2204 has already been reported as one of the adaptive mutations enhancing the efficiency of viral replication (25). Then we used MH-14 cells, refereed as the replicon cells, in the following

experiments to analyze the mechanism of HCV genomic replication.

Replicon RNA and NS Proteins Were Retained in Digitonin-permeabilized Replicon Cells—Previous papers suggested that all HCV NS proteins are directly or indirectly associated with the inner cellular membranes, especially rough ER membranes, and form replication complexes on the membranes (10, 40). This suggested to us that functional HCV replication complexes could be retained in the replicon cells whose plasma membranes had been permeabilized with digitonin. To test this possibility, first, the fate of NS proteins in the replicon cells was investigated after digitonin treatment by Western blotting. In this experiment, ectopically expressed mouse DHFR was used as a cytoplasmic protein marker. After digitonin treatment, DHFR was not detected in the permeabilized cells (Fig. 1*A*, *lanes 2* and *3*), indicating that cytoplasmic soluble proteins were washed efficiently out of the cells under these conditions. On the other hand, HCV NS proteins (NS3-NS5B) were detected just like BiP/Grp78, an ER marker, in the permeabilized replicon cells as in the intact cells that were not treated with digitonin, as expected (Fig. 1*A*, *lanes 2* and *3*). Moreover, when we analyzed the RNA by Northern blotting, the retention of replicon RNA in the permeabilized replicon cells was observed (Fig. 1*B*, *lanes 2* and *3*). Treatment of the permeabilized replicon cells with the high salt buffer containing 2 M KCl did not greatly influence the amount of replicon RNA and NS proteins retained in the cells (data not shown). To investigate whether newly synthesized replicon RNA in the intact replicon cells was retained after permeabilization with digitonin, we performed metabolic labeling of the cells with [^{32}P]orthophosphate. As shown in Fig. 1*C*, newly synthesized replicon RNA was detected after permeabilization (Fig. 1*C*, *lane 3*), although the amount was slightly decreased compared with that in the intact cells (Fig. 1*C*, *lane 2*). The localization of NS5A and NS5B in the permeabilized replicon cells was also analyzed by indirect immunofluorescence. These proteins were seen to accumulate around the perinuclear region and to be mostly colocalized with protein-disulfide isomerase, an ER marker, in the permeabilized replicon cells (Fig. 1*D*, *panels i–p*), just as in the intact replicon cells (Fig. 1*D*, *panels a–h*). This indicated that treatment with digitonin did not markedly affect subcellular localization of these proteins. From all of these results, it seemed likely that the replication complexes including replicon RNA were retained in the permeabilized replicon cells just like in the intact cells.

The Replication Complexes in the Permeabilized Replicon Cells Functioned to Synthesize the HCV Subgenomic RNA—To see whether the replication complexes in the permeabilized replicon cells were active in HCV RNA synthesis, permeabilized or intact cells were incubated in reaction mixtures including [α-^{32}P]UTP for 4 h. Actinomycin D, which showed no inhibitory effect on the RNA-dependent RNA polymerase activity of HCV NS5B (15), was also added to the reaction mixture to inhibit the cellular activities of DNA-dependent DNA and RNA synthesis. After the reaction, total RNA of the cells and the reaction supernatants were extracted and analyzed by denaturing agarose gel electrophoresis followed by autoradiography. A radiolabeled product ~8 kb in length, which was equivalent to the subgenomic replicon RNA in size, was found in RNA from the permeabilized replicon cells but not from Huh-7 cells (Fig. 2*A*, *lanes 1–4*). When overexposed, the 8-kb band became detectable in RNA sample from the intact replicon cells, although the signal was much lower than that from the permeabilized replicon cells (data not shown). This 8-kb product, however, was not detected in all the reaction supernatants (Fig. 2*A*, *lanes 5–8*). The radiolabeled 8-kb product was degra-

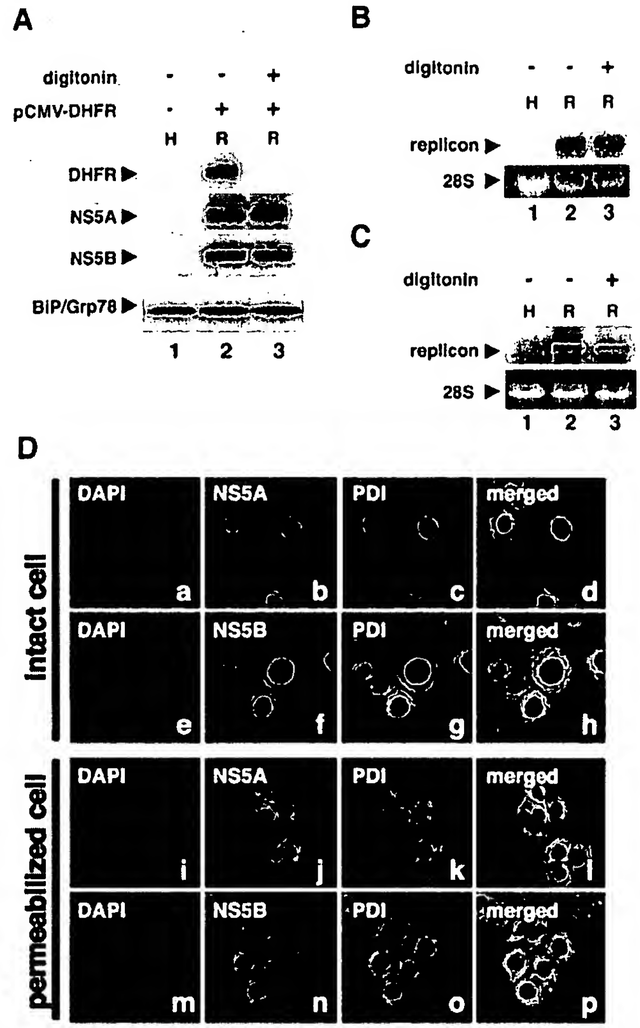

FIG. 1. **Detection of NS5A, NS5B, and subgenomic replicon RNA in permeabilized replicon cells.** *A*, total lysate from intact cells (*digitonin* −, *lanes 1* and *2*) or digitonin-treated permeabilized cells (*digitonin* +, *lane 3*) was analyzed by Western blotting with anti-DHFR, anti-NS5A, anti-NS5B, and anti-BiP/Grp78 antibodies. *H* and *R* indicate parental Huh-7 and replicon cells, respectively. DHFR produced ectopically by transient transfection of pCMV-DHFR and endogenous BiP/Grp78 were used as markers for cytoplasm and ER, respectively. *B*, total RNA extracted from the intact (*lanes 1* and *2*) or permeabilized cells (*lane 3*) was analyzed by Northern blotting using an HCV genome-specific probe (*upper panel*). The relative amount of total RNA in each lane is shown by 28 S rRNA (28S) stained with ethidium bromide (*lower panel*). *C*, the replicon RNA metabolically radiolabeled in the intact replicon cells was retained in cells after permeabilization with digitonin. After metabolic labeling of Huh-7 and replicon cells with [^{32}P]orthophosphate, radiolabeled RNA from the intact cells (*lanes 1* and *2*) or permeabilized cells (*lane 3*) was analyzed by denaturing agarose gel electrophoresis followed by autoradiography. Approximately 8-kb bands in length were indicated (replicon). *D*, the subcellular localization of NS5A (*red*), NS5B (*red*), and protein-disulfide isomerase (*PDI*) (ER marker, *green*) in the intact or permeabilized replicon cells was analyzed by indirect immunofluorescence using anti-NS5A (*panels b* and *j*), anti-NS5B (*panels f* and *n*), and anti-PDI antibodies (*panels c, g, k,* and *o*), respectively. Nucleus stained by 4′,6-diamidino-2-phenylindole (*DAPI*) is shown in *panels a, e, i,* and *m*. Merged panels are shown in *panels d, h, l,* and *p*.

dated by treatment with RNase A (data not shown), suggesting that it was HCV subgenomic RNA synthesized by the replication complexes in the permeabilized replicon cells. To examine whether the 8-kb RNA synthesized in the permeabilized cells was actually HCV subgenomic RNA, we performed slot blot hybridization analysis using each plus and minus strand HCV

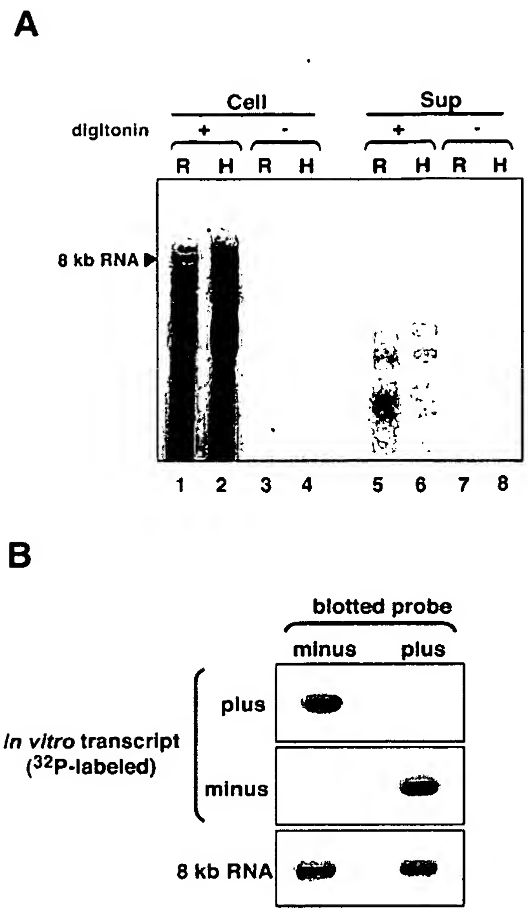

FIG. 2. **The activity for synthesis of the HCV subgenomic RNA was retained in the permeabilized replicon cells.** *A*, the replicon cells (*R*; *lanes 1, 3, 5,* and *7*) and the parental Huh-7 cells (*H*; *lanes 2, 4, 6,* and *8*) were used in this experiment after treatment with (*lanes 1, 2, 5,* and *6*) or without (*lanes 3, 4, 7,* and *8*) digitonin. Total RNA extracted from the cell fraction (*Cell*), as well as the reaction supernatant (*Sup*), of these cells after incubation in the reaction mixtures for 4 h was analyzed by denaturing agarose gel electrophoresis followed by autoradiography. The 8-kb RNA specifically found in the cell fraction of replicon cells is indicated by an *arrowhead*. *B*, characterization of the radiolabeled 8-kb RNA synthesized in the permeabilized replicon cells. Equal amounts of the unlabeled plus and minus strand replicon RNA synthesized *in vitro* were blotted on nylon membrane filter and used as specific probes for detection of the minus and plus strand replicon RNA synthesized and radiolabeled in the replicon cells, respectively, in the slot blot hybridization experiment (*8 kb RNA*). To show the strand specificity of this experiment, the results of the experiment performed by using the plus and minus HCV RNA ^{32}P radiolabeled *in vitro* instead of those in the replicon cells are presented (*in vitro* transcript, plus and minus).

RNA synthesized *in vitro* as probes on the nylon membrane filter. After denaturing agarose gel electrophoresis, the radiolabeled 8-kb RNA derived from the permeabilized replicon cells was eluted from the gel and hybridized with the probes on the filter. Then the radioactivity hybridized with either the plus or minus strand-specific probe on the filter was detected by autoradiography (Fig. 2*B*, *8 kb RNA*), whereas radiolabeled RNA prepared from permeabilized Huh-7 cells in the same way did not show any hybridization signals on the filter (data not shown). By the same procedure, we also confirmed that the metabolically radiolabeled 8-kb RNA in Fig. 1*C* was actually replicon RNA (data not shown). The ratio of plus to minus strand RNA synthesized in the permeabilized replicon cells was estimated to be 2.7 ± 0.4 (average ± S.D.) by three independent experiments. These results indicated that the radiolabeled 8-kb RNA was actually HCV subgenomic RNA synthesized in the permeabilized replicon cells and contained both plus and minus strands of the HCV RNA, implying that the functional HCV replication complexes were present in the permeabilized replicon cells.

Replicon RNA in the Permeabilized Replicon Cells Was Resistant to Nuclease—The production of radiolabeled HCV subgenomic RNA in the permeabilized cells seemed to continue until 4 h and reached a maximum until ~5 to 6 h (data not shown). Then the amount of radiolabeled HCV RNA was stably maintained even after 8 h. One possible explanation for this stability was the removal of RNase from the cell by permeabilization. Therefore, we examined the sensitivity of the newly synthesized HCV RNA in the permeabilized replicon cells to exogenously added nuclease. After the reaction for RNA synthesis, the permeabilized replicon cells were treated with micrococcal nuclease. As shown in Fig. 3*A*, the radiolabeled HCV RNA remained almost intact even after nuclease treatment (*lanes 1* and *2*), although 28 S rRNA was efficiently degradated under the same condition (*lanes 2* and *3*). This lower sensitivity of the replicon RNA to nuclease suggested that one of the reasons for the stability of the RNA in the permeabilized cells was its resistance to RNase activity. On the other hand, the radiolabeled HCV RNA was sensitive to nuclease in the presence of a nonionic detergent, Nonidet P-40 (Fig. 3*A*, *lane 3*), although a small portion of the HCV RNA was likely to remain resistant to nuclease. When the permeabilized replicon cells were treated with only Nonidet P-40, the radiolabeled HCV RNA in the cells was still detectable but apparently diminished. However, the radiolabeled molecules became detectable in the reaction supernatant, possibly because of leakage from the cells because of Nonidet P-40 (Fig. 3*A*, *lanes 4* and *8*). From these results, HCV subgenomic RNA newly synthesized in the permeabilized cells seemed resistant to nuclease in a cellular lipid membrane-dependent manner. Moreover, we also observed that the replicon RNA synthesis was equally carried out when the permeabilized cells were pretreated with nuclease before the reaction of the RNA synthesis (data not shown). This suggested that the HCV RNA used as a template in the viral RNA synthesis was also resistant to nuclease and present in the same environment as the newly synthesized RNA products mentioned above. Furthermore, we investigated the replicon RNA that was newly synthesized in the intact replicon cells. After metabolic labeling of the replicon cells with [^{32}P] orthophosphate, the cells were permeabilized with digitonin and treated with micrococcal nuclease as above. As shown in Fig. 3*B*, about 30% of radiolabeled replicon RNA in the intact replicon cells was found to be lost after permeabilization (*lanes 1* and *2*), probably implying that a part of the newly synthesized RNA flowed out with the cytoplasm from the permeabilized cells (see discussion). A large part of newly synthesized replicon RNA retained in the permeabilized cells showed resistance to the nuclease action in the absence of Nonidet P-40 (Fig. 3*B*, *lane 3*) but was tuned to be sensitive to nuclease in the presence of Nonidet P-40 (Fig. 3*B*, *lane 4*). This suggested that the fate of the newly synthesized replicon RNA in the permeabilized cells was similar to that retained in intact cells after permeabilization. Then we analyzed the nuclease sensitivity of total replicon RNA in replicon cells by Northern blotting. After permeabilization, replicon cells were treated with nuclease in the presence or absence of Nonidet P-40 as described above. As shown in Fig. 3*C*, we found that most of the replicon RNA was intact even after treatment (Fig. 3*C*, *lanes 2* and *3*). As in the case of the newly synthesized replicon RNA, the replicon RNA pre-existing in the replicon cells was sensitive to nuclease in the presence of Nonidet P-40 (Fig. 3*C*, *lane 4*). From these

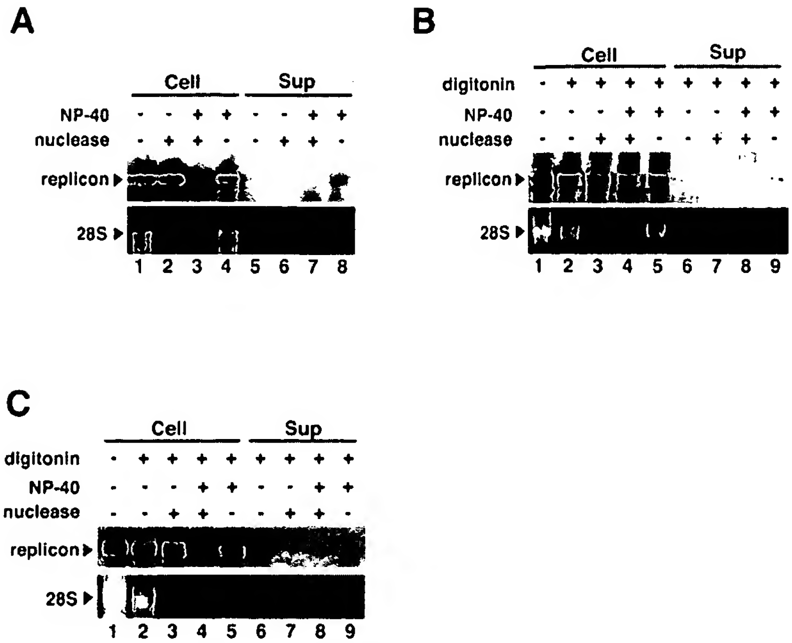

FIG. 3. **A large part of the replicon RNA was located in the nuclease-resistant environment in the replicon cells.** *A*, resistance of the newly synthesized HCV RNA in the permeabilized replicon cells to nuclease action. After the RNA synthesis reaction in the presence of [^{32}P]UTP, the permeabilized replicon cells were treated with (*nuclease +*, *lanes 2, 3, 6,* and *7*) or without microccocal nuclease (nuclease −, *lanes 1, 4, 5,* and *8*). The reactions were performed in the presence (*Nonidet P-40 +*, *lanes 3, 4, 7,* and *8*) or absence of 0.5% Nonidet P-40 (*Nonidet P-40 −*, *lanes 1, 2, 5,* and *6*). Total RNA extracted from the cells (Cell, *lanes 1–4*) and the reaction supernatant (Sup, *lanes 5–8*) was similarly analyzed as described in the legend to Fig. 2. *B*, resistance of the newly synthesized replicon RNA in the intact replicon cells to nuclease action. The intact replicon cells were metabolically labeled with [^{32}P]orthophosphate. After incubation, the cells were permeabilized and treated with (*lanes 3, 4, 7,* and *8*) or without micrococcal nuclease (*lanes 2, 5, 6,* and *9*), in the presence (*lanes 4, 5, 8,* and *9*) or absence of Nonidet P-40 (*lanes 2, 3, 6,* and *7*), as described above. *C*, resistance of the replicon RNA in replicon cells against nuclease action. After permeabilization of the replicon cells with digitonin, the cells were treated with (*lanes 3, 4, 7,* and *8*) or without micrococcal nuclease (*lanes 2, 5, 6,* and *9*), in the presence (*lanes 4, 5, 8,* and *9*) or absence of (*lanes 2, 3, 6,* and *7*) Nonidet P-40 as above. Total RNA from the cell fraction or the reaction supernatant after treatment was analyzed by Northern blotting using a HCV genome-specific probe to detect the replicon RNA (indicated by the *arrowhead* with replicon, *upper panel*). 28 S rRNA (*28S*) was detected by staining with ethidium bromide (*A–C*, *lower panels*). In *A*, the amount of 28 S rRNA seemed to be low probably because of degradation during incubation in the reaction mixture for 4 h.

results, it was suggested that replicon RNA existed in a subcellular compartment that was formed with cellular lipid membranes.

A Large Amount of Each NS Protein Was Not Required for Nuclease Resistance of Replicon RNA—To investigate the contribution of HCV NS proteins to the resistance of replicon RNA against nuclease, the sensitivity of the replicon RNA to nuclease was examined in permeabilized replicon cells after treatment with proteinase K at various concentrations. The condition of the replicon RNA and NS proteins in the cells after treatment was analyzed by Northern and Western blotting, respectively. An endogenous Calnexin, a type I transmembrane protein of ER, was detected by using an antibody specific to its NH_2-terminal region present in the ER lumen (Calnexin-NT) as a control for monitoring the efficiency of proteinase K digestion. At the dose of proteinase K that affected the amount of full-length Calnexin, a fragment, the size of which matched that of the NH_2-terminal region of Calnexin was detected (Fig. 4, *lanes 4–11*), indicating that proteins or segments on the cytoplasmic side of ER membranes were efficiently digested and those in the lumen were protected from the digestion by proteinase K as expected. Under these conditions, a large part of each NS protein was digested by proteinase K at higher concentrations, although the sensitivity of each NS protein to treatment varied (Fig. 4, *lanes 4–7* and *8–11*). On the other hand, we also observed that a small part of each NS protein remained resistant to even prolonged treatment of the permeabilized replicon cells with proteinase. Under these conditions, we observed that nuclease treatment did not affect replicon RNA despite efficient degradation of 28 S rRNA (Fig. 4, *lanes 8–11*), although amounts of 28 S rRNA and replicon RNA were not influenced by only the proteinase treatment (Fig. 4, *lanes 4–7*). These results indicated that the stability replicon RNA was not dependent on the large parts of the NS protein. This raised the possibility that the precise subcellular localization of replicon RNA was different from that of the majority of each NS protein.

The Active Replication Complex Was in a Similar Environment to the Replicon RNA—As shown above, the majority of each NS protein in digitonin-permeabilized replicon cells were sensitive to proteinase treatment. Furthermore, all NS proteins (NS3-NS5B) in replicon cells were detectable by indirect immunofluorescent analysis after permeabilization only with digitonin following fixation with 4% paraformaldehyde, although the proteins such as protein-disulfide isomerase and BiP/Grp78 that are present in the ER lumen were not detected under this condition (data not shown). These results indicated that a large part of each NS protein was exposed on the cytoplasmic side of the inner cellular membranes. To see whether these NS proteins function in the replication of HCV, the synthesis of the HCV subgenomic RNA was investigated in the permeabilized replicon cells pretreated with proteinase K. After treatment with proteinase at higher concentrations, each NS protein was almost degradated by the treatment as shown in Fig. 4 (Fig. 5*A*, *lanes 2–5*). Under these conditions, however, the HCV RNA was synthesized in a quite similar manner to that in the cells not treated with proteinase (Fig. 5*A*, *lanes 1–5*). These results suggested that the majority of active replication complex existed in the proteinase-resistant environment and a large part of each NS protein did not participate in the synthe-

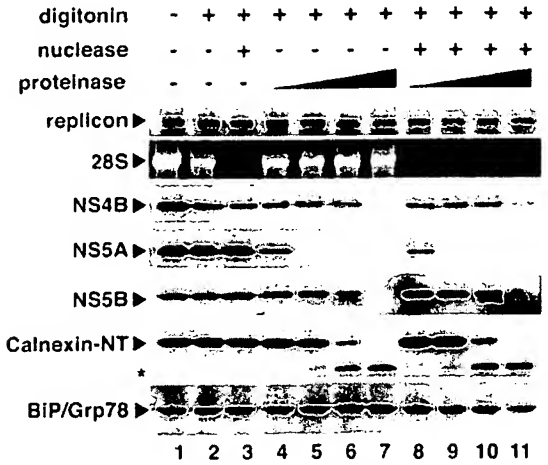

FIG. 4. **A large part of each NS protein was not required for the nuclease resistance of the replicon RNA.** The digitonin-permeabilized replicon cells were treated with proteinase K at various concentrations (0 μg/ml for *lanes 2* and *3*, 0.01 μg/ml for *lanes 4* and *8*, 0.1 μg/ml for *lanes 5* and *9*, 1 μg/ml for *lanes 6* and *10*, 10 μg/ml for *lanes 7* and *11*), followed by treatment with (*lanes 3* and *8–11*) or without (*lanes 2* and *4–7*) micrococcal nuclease. The samples from intact replicon cells without any treatments were similarly analyzed as shown in *lane 1*. After these treatments, total RNA and protein in the cells were analyzed by Northern and Western blotting, respectively. Antibodies used in the Western blotting were anti-NS4B (*NS4B*), anti-NS5A (*NS5A*), anti-NS5B (*NS5B*), anti-Calnexin (*Calnexin-NT*), and anti-KDEL (*BiP/Grp78*) antibodies. Each protein with original size is indicated by an *arrowhead*. An *asterisk* denotes the position of the Calnexin NH_2-terminal segment that is located in the lumen of the ER. BiP/Grp78, which located on the lumenal side of the ER membrane, was used as a negative control for proteinase digestion.

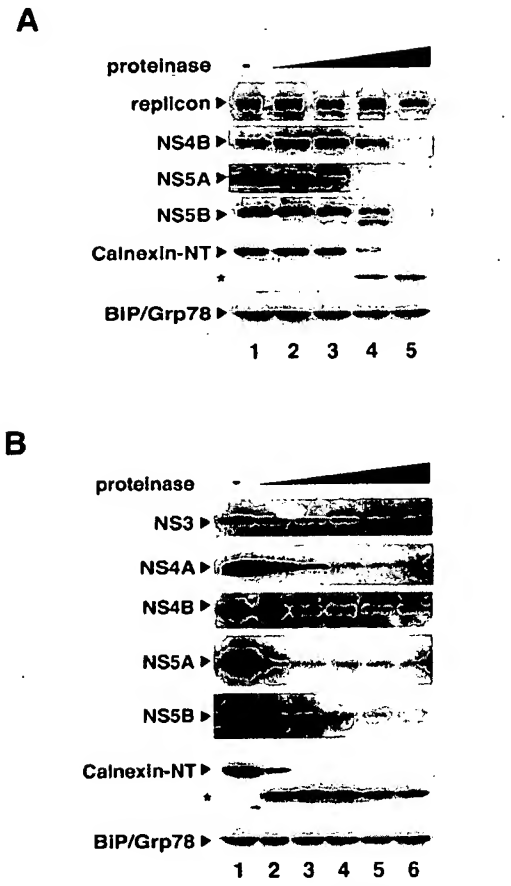

FIG. 5. *A*, the activity for the synthesis of HCV RNA in the permeabilized replicon cells was intact even after degradation of a large part of each NS protein by proteinase K treatment. After treatment of the permeabilized replicon cells with proteinase K as described in the legend to Fig. 4, the RNA synthesis reaction was performed. The concentrations of proteinase K used in this experiment were 0 (*lane 1*), 0.01 (*lane 2*), 0.1 (*lane 3*), 1 (*lane 4*), or 10 μg/ml (*lane 5*). Total protein of the cells prior to the RNA synthesis reaction was analyzed by Western blotting using anti-NS4B (*NS4B*), anti-NS5A (*NS5A*), anti-NS5B (*NS5B*), anti-Calnexin (*Calnexin-NT*), and anti-KDEL (*BiP/Grp78*) antibodies. Newly synthesized replicon RNA that was labeled with [^{32}P]UTP was indicated by the *arrowhead* with *replicon*, *upper panel*. *B*, a small part of each NS protein was located in the proteinase-resistant environment in the replicon cells. After permeabilization of the replicon cells with digitonin, fractions of the cells were treated with 0 (*lane 1*), 1 (*lane 2*), 5 (*lane 3*), 10 (*lane 4*), 50 (*lane 5*), and 100 μg/ml (*lane 6*) proteinase K. After the reaction, total protein was analyzed by Western blotting using anti-NS3 (*NS3*), anti-NS4A (*NS4A*), anti-NS4B (*NS4B*), anti-NS5A (*NS5A*), anti-NS5B (*NS5B*), anti-Calnexin (*Calenxin-NT*), and anti-KDEL (*BiP/Grp78*) antibodies.

sis of HCV RNA in the cells. This implied that a small part of each NS protein resistant to proteinase should be present in a similar situation to the active replication complexes in the cells. To clarify the existence of such proteins, we examined carefully the proteinase resistance of each NS protein in the permeabilized replicon cells. After treatment of the permeabilized replicon cells with proteinase K at various concentrations, total protein in the cells was analyzed by Western blotting. Under the conditions that the COOH terminus of Calnexin was efficiently digested by treatment as shown in Figs. 4 and 5*A*, we found that a small part of each NS protein was resistant to the treatment with proteinase K at even higher concentrations (Fig. 5*B*, *lanes 1–6*). These results strongly suggested that such proteinase-resistant NS proteins formed the functional replication complex in the cells. Furthermore, we did not detect any activity for the synthesis of the replicon RNA in the permeabilized replicon cells after treatment with nonionic detergents (data not shown). Summing up the above results, it was suggested that pre-existing replicon RNA and a small portion of each NS protein, which were resistant to nuclease and proteinase, respectively, form the replication complexes in lipid membrane structures to participate in the synthesis of replicon RNA in replicon cells.

DISCUSSION

By monitoring the synthesis of HCV RNA in permeabilized HCV replicon cells, we obtained results suggesting that the active HCV replication complexes function to synthesize the replicon RNA in subcellular compartments, which are probably formed by cellular lipid membranes. Recently, electron microscopic analysis showed that the expression of HCV proteins in Huh-7 cells induced the formation of a distinct membrane structure, designated a "membranous web," and all HCV proteins were found in the structure (40). Moreover, a similar web-like structure in livers of HCV-infected chimpanzees and HCV subgenomic replicon cells was reported (41, 42). Therefore, it seems likely that this membrane structure is a candidate for the site where the HCV RNA genome is mainly located and replicated. Until now the genomes of many positive-strand RNA viruses, such as brome mosaic virus, murine hepatitis virus, and Kunjin virus have been reported to replicate on inner cellular membranes in association with vesicles or other membrane structures (43–45). These membrane structures seemed to be constructed by viral proteins. For example, it was reported that brome mosaic virus 1a, the multifunctional RNA replication protein, selectively recruits brome mosaic virus 2a polymerase and viral RNA and forms membrane-bound spherules (43, 46). A subcellular site for the genome replication of these viruses including HCV has been suggested by the localization of brome uridine-incorporated genomic RNA, which is a

product of the replication reaction, in the cells (43, 47–49). It has not been biochemically analyzed, however, whether viral RNA is actually synthesized in or around such a membrane structure. In this paper, we showed that a quite similar activity for the synthesis of HCV subgenomic RNA was present in the permeabilized replicon cells even after proteinase treatment, which digested almost all the NS proteins including NS5B, to that in the cells not treated with proteinase. Furthermore, we found that a small part of each NS protein is actually present in the proteinase-resistant environment in the replicon cells. This suggested, therefore, that a small part of each NS protein forms the replication complex and functions in the membranous compartment.

A fairly large amount of each HCV protein accumulated in the perinuclear fraction in the replicon cells, which is exposed to the cytoplasmic environment. In this protein complex, no association of the HCV subgenomic RNA was observed and there was no activity to synthesize the viral RNA. Thus, the significance of the HCV protein complex regarding multiplication of the virus genome remains to be clarified. The replicon cells originating from Huh-7 may produce large numbers of HCV proteins in the perinuclear fraction as a consequence of overproduction and these proteins may play less important roles in the replication of the HCV genome than the active replication complex that we have noted in this paper. Conversely, the protein complex may play important roles in the regulation of not only the multiplication of the HCV genome but also further processes during the maturation of the virus. In this regard, it is important to analyze the presence as well as the function of the HCV protein complexes in cells where HCV proliferates with different degrees of multiplication. To date, several cellular proteins that interact with particular NS proteins have been reported. For example, double strand RNA-dependent protein kinase, soluble NSF attachment protein receptors-like protein, and karyopherin β3 are reported to interact with NS5A (50–52), although the physiological importance of these interactions has been obscure. This larger part of each NS protein might, therefore, participate in several cellular events and/or modulate the replication of the HCV genome through interactions with these cellular proteins.

The ratio of plus to minus strand RNA synthesized in the permeabilized replicon cells was estimated to be 2.7 ± 0.4 by slot blot hybridization analysis as shown in Fig. 2. On the other hand, that in the intact replicon cells was estimated to be 11.9 ± 2.0 as reported previously (data not shown and Ref. 15), when intact replicon cells were metabolically labeled with [^{32}P]orthophosphate and the newly synthesized and radiolabeled replicon RNA in the cells was analyzed by slot blot hybridization in a similar manner. The discrepancy in the ratio between the permeabilized and intact cells may be explained by the release of the replicon RNA synthesized in the permeabilized cells from the membranous compartment and degradated in the reaction mixture, although the possibility that the regulation of the plus to minus ratio of newly synthesized replicon RNA may be lost in the permeabilized replicon cannot be completely ruled out. Approximately 50% of the replicon RNA newly synthesized in the intact cells was actually lost by nuclease treatment following permeabilization (Fig. 3*B*, *lanes 1* and *3*), suggesting that some parts of replicon RNA newly synthesized in intact replicon cells is present in the cytoplasm. Slight degradation of the replicon RNA was also seen in permeabilized cells in the presence of Nonidet P-40 (Fig. 3). We also observed that *in vitro* synthesized replicon RNA added exogenously to the permeabilized cells was unstable in the reaction mixture (data not shown), as was observed in a recent report in which the replication activity of the HCV replicon was detected using the cell lysate fraction of replicon cells (30). These observations seem to support the former possibility indirectly. As the radiolabeled nucleotide substrate was incorporated in the newly synthesized replicon RNA in the permeabilized replicon cells, a channel-like structure should be present in the membranous compartment including the replication complex. In the case of spherules of brome mosaic virus, the channel-like structure connecting to the cytoplasm with the inside of the spherule was actually detected by the electron microscopic technique (43). This supported the idea that the replicon RNA that was present in the cytoplasm was probably exported from the membranous structure through the channel-like structure. A similar phenomenon was already reported for reovirus in that relatively large reoviral mRNA was exported from the viral core particles to the cytoplasm through the channel formed by a viral protein (53). The pore size of the putative channel of HCV, however, seemed to be limited, because nuclease and proteinase did not pass through the channel. The replicon RNA may be specifically recognized by some viral proteins and exported through the channel post- or co-replicationally. These mechanisms, however, have remained to be elucidated.

During the preparation of this article, Shi *et al.* (54) reported that almost all of the NS5A and part of the NS5B proteins were present in the membrane fraction that was resistant to treatment with 1% Nonidet P-40. Because the replicational activity in that fraction from the cell lysate was not demonstrated, we do not know whether that kind of membrane fraction from the cell lysate would include the replication activity observed here. Furthermore, a part of replicon RNA was reported to localize in the non-ionic detergent-insoluble membrane fractions (54), whereas we showed that the RNase resistance of both total and newly synthesized replicon RNA was reduced in the presence of Nonidet P-40. This discrepancy may be explained by the different methods used for the detection of the replicon RNA, reverse transcriptase-PCR and Northern blotting in that paper and ours, respectively. We also showed data indicating that a negligible amount of replicon RNA was released from the permeabilized cells into the reaction mixture by the detergent as shown in Fig. 3. It may also be relevant to this discrepancy that we and others have observed instability of the free replicon RNA in the reaction mixture (30). We also observed the existence of nuclease-resistant replicon RNA, even in the presence of nonionic detergent (Fig. 3). Such RNA may represent the replicon RNA in the non-ionic detergent-insoluble fractions.

Here we showed the stable nature of the active HCV RNA replication complex in the replicon cells by permeabilization of the cells. Our data suggests that only a small part of each NS protein contributes to RNA synthesis in the replicon cells. This implied that careful investigation would be required for identification of the precise subcellular sites of replication in the replicon cells. Further investigation to reveal how and where this complex is formed in the cells and what is essential for its activity is required for understanding the mechanism of viral replication and the life cycle of HCV.

REFERENCES

1. Liang, T. J., Jeffers, L. J., Reddy, K. R., De Medina, M., Parker, I. T., Cheinquer, H., Idrovo, V., Rabassa, A., and Schiff, E. R. (1993) *Hepatology* **18**, 1326–1333
2. Shimotohno, K. (1995) *Intervirology* **38**, 162–169
3. Tanaka, K., Hirohata, T., Koga, S., Sugimachi, K., Kanematsu, T., Ohryohji, F., Nawata, H., Ishibashi, H., Maeda, Y., and Kiyokawa, H. (1991) *Cancer Res.* **51**, 2842–2847
4. Fried, M. W., and Hoofnagle, J. H. (1995) *Semin. Liver Dis.* **15**, 82–91
5. McHutchison, J. G., Gordon, S. C., Schiff, E. R., Shiffman, M. L., Lee, W. M., Rustgi, V. K., Goodman, Z. D., Ling, M. H., Cort, S., and Albrecht, J. K. (1998) *N. Engl. J. Med.* **339**, 1485–1492
6. Kato, N., Hijikata, M., Ootsuyama, Y., Nakagawa, M., Ohkoshi, S., Sugimura, T., and Shimotohno, K. (1990) *Proc. Natl. Acad. Sci. U. S. A.* **87**, 9524–9528
7. Tanaka, T., Kato, N., Cho, M. J., Sugiyama, K., and Shimotohno, K. (1996)

J. Virol. **70**, 3307–3312
8. Bartenschlager, R., and Lohmann, V. (2000) *J. Gen. Virol.* **81**, 1631–1648
9. Hijikata, M., Kato, N., Ootsuyama, Y., Nakagawa, M., and Shimotohno, K. (1991) *Proc. Natl. Acad. Sci. U. S. A.* **88**, 5547–5551
10. Hijikata, M., Mizushima, H., Akagi, T., Mori, S., Kakiuchi, N., Kato, N., Tanaka, T., Kimura, K., and Shimotohno, K. (1993) *J. Virol.* **67**, 4665–4675
11. Mizushima, H., Hijikata, M., Tanji, Y., Kimura, K., and Shimotohno, K. (1994) *J. Virol.* **68**, 2731–2734
12. Grakoui, A., Wychowski, C., Lin, C., Feinstone, S. M., and Rice, C. M. (1993) *J. Virol.* **67**, 1385–1395
13. Griffin, S. D., Beales, L. P., Clarke, D. S., Worsfold, O., Evans, S. D., Jaeger, J., Harris, M. P., and Rowlands, D. J. (2003) *FEBS Lett.* **535**, 34–38
14. Pavlovic, D., Neville, D. C., Argaud, O., Blumberg, B., Dwek, R. A., Fischer, W. B., and Zitzmann, N. (2003) *Proc. Natl. Acad. Sci. U. S. A.* **100**, 6104–6108
15. Lohmann, V., Korner, F., Koch, J., Herian, U., Theilmann, L., and Bartenschlager, R. (1999) *Science* **285**, 110–113
16. Behrens, S. E., Tomei, L., and De Francesco, R. (1996) *EMBO J.* **15**, 12–22
17. Yuan, Z. H., Kumar, U., Thomas, H. C., Wen, Y. M., and Monjardino, J. (1997) *Biochem. Biophys. Res. Commun.* **232**, 231–235
18. Lohmann, V., Korner, F., Herian, U., and Bartenschlager, R. (1997) *J. Virol.* **71**, 8416–8428
19. Oh, J. W., Ito, T., and Lai, M. M. (1999) *J. Virol.* **73**, 7694–7702
20. Shirota, Y., Luo, H., Qin, W., Kaneko, S., Yamashita, T., Kobayashi, K., and Murakami, S. (2002) *J. Biol. Chem.* **277**, 11149–11155
21. Kishine, H., Sugiyama, K., Hijikata, M., Kato, N., Takahashi, H., Noshi, T., Nio, Y., Hosaka, M., Miyanari, Y., and Shimotohno, K. (2002) *Biochem. Biophys. Res. Commun.* **293**, 993–999
22. Ikeda, M., Yi, M., Li, K., and Lemon, S. M. (2002) *J. Virol.* **76**, 2997–3006
23. Blight, K. J., McKeating, J. A., Marcotrigiano, J., and Rice, C. M. (2003) *J. Virol.* **77**, 3181–3190
24. Lohmann, V., Korner, F., Dobierzewska, A., and Bartenschlager, R. (2001) *J. Virol.* **75**, 1437–1449
25. Blight, K. J., Kolykhalov, A. A., and Rice, C. M. (2000) *Science* **290**, 1972–1974
26. Krieger, N., Lohmann, V., and Bartenschlager, R. (2001) *J. Virol.* **75**, 4614–4624
27. Lohmann, V., Hoffmann, S., Herian, U., Penin, F., and Bartenschlager, R. (2003) *J. Virol.* **77**, 3007–3019
28. Friebe, P., Lohmann, V., Krieger, N., and Bartenschlager, R. (2001) *J. Virol.* **75**, 12047–12057
29. Yi, M., and Lemon, S. M. (2003) *J. Virol.* **77**, 3557–3568
30. Ali, N., Tardif, K. D., and Siddiqui, A. (2002) *J. Virol.* **76**, 12001–12007
31. Lai, V. C., Dempsey, S., Lau, J. Y., Hong, Z., and Zhong, W. (2003) *J. Virol.* **77**, 2295–2300
32. Hardy, R. W., Marcotrigiano, J., Blight, K. J., Majors, J. E., and Rice, C. M. (2003) *J. Virol.* **77**, 2029–2037
33. Tanji, Y., Hijikata, M., Satoh, S., Kaneko, T., and Shimotohno, K. (1995) *J. Virol.* **69**, 1575–1581
34. Hijikata, M., Mizushima, H., Tanji, Y., Komoda, Y., Hirowatari, Y., Akagi, T., Kato, N., Kimura, K., and Shimotohno, K. (1993) *Proc. Natl. Acad. Sci. U. S. A.* **90**, 10773–10777
35. Brass, V., Bieck, E., Montserret, R., Wolk, B., Hellings, J. A., Blum, H. E., Penin, F., and Moradpour, D. (2002) *J. Biol. Chem.* **277**, 8130–8139
36. Schmidt-Mende, J., Bieck, E., Hugle, T., Penin, F., Rice, C. M., Blum, H. E., and Moradpour, D. (2001) *J. Biol. Chem.* **276**, 44052–44063
37. Hijikata, M., Kato, N., Sato, T., Kagami, Y., and Shimotohno, K. (1990) *J. Virol.* **64**, 4632–4639
38. Marusawa, H., Hijikata, M., Chiba, T., and Shimotohno, K. (1999) *J. Virol.* **73**, 4713–4720
39. Sambrook, J., Fritsch, E. F., and Maniatis, T. (1989) *Molecular Cloning: A Laboratory Manual*, 2nd Ed., Cold Spring Harbor Laboratory, Cold Spring Harbor, NY
40. Egger, D., Wolk, B., Gosert, R., Bianchi, L., Blum, H. E., Moradpour, D., and Bienz, K. (2002) *J. Virol.* **76**, 5974–5984
41. Pfeifer, U., Thomssen, R., Legler, K., Bottcher, U., Gerlich, W., Weinmann, E., and Klinge, O. (1980) *Virchows Arch. B Cell Pathol. Incl. Mol. Pathol.* **33**, 233–243
42. Gosert, R., Egger, D., Lohmann, V., Bartenschlager, R., Blum, H. E., Bienz, K., and Moradpour, D. (2003) *J. Virol.* **77**, 5487–5492
43. Schwartz, M., Chen, J., Janda, M., Sullivan, M., den Boon, J., and Ahlquist, P. (2002) *Mol. Cell* **9**, 505–514
44. Gosert, R., Kanjanahaluethai, A., Egger, D., Bienz, K., and Baker, S. C. (2002) *J. Virol.* **76**, 3697–3708
45. Westaway, E. G., Mackenzie, J. M., Kenney, M. T., Jones, M. K., and Khromykh, A. A. (1997) *J. Virol.* **71**, 6650–6661
46. Chen, J., Noueiry, A., and Ahlquist, P. (2003) *J. Virol.* **77**, 2568–2577
47. Pedersen, K. W., van der Meer, Y., Roos, N., and Snijder, E. J. (1999) *J. Virol.* **73**, 2016–2026
48. Suhy, D. A., Giddings, T. H., Jr., and Kirkegaard, K. (2000) *J. Virol.* **74**, 8953–8965
49. Hagiwara, Y., Komoda, K., Yamanaka, T., Tamai, A., Meshi, T., Funada, R., Tsuchiya, T., Naito, S., and Ishikawa, M. (2003) *EMBO J.* **22**, 344–353
50. Gale, M., Jr., Blakely, C. M., Kwieciszewski, B., Tan, S. L., Dossett, M., Tang, N. M., Korth, M. J., Polyak, S. J., Gretch, D. R., and Katze, M. G. (1998) *Mol. Cell. Biol.* **18**, 5208–5218
51. Tu, H., Gao, L., Shi, S. T., Taylor, D. R., Yang, T., Mircheff, A. K., Wen, Y., Gorbalenya, A. E., Hwang, S. B., and Lai, M. M. (1999) *Virology* **263**, 30–41
52. Chung, K. M., Lee, J., Kim, J. E., Song, O. K., Cho, S., Lim, J., Seedorf, M., Hahm, B., and Jang, S. K. (2000) *J. Virol.* **74**, 5233–5241
53. Reinisch, K. M., Nibert, M. L., and Harrison, S. C. (2000) *Nature* **404**, 960–967
54. Shi, S. T., Lee, K. J., Aizaki, H., Hwang, S. B., and Lai, M. M. (2003) *J. Virol.* **77**, 4160–4168

EXHIBIT A

JOURNAL OF VIROLOGY, Nov. 2005, p. 13594–13605 Vol. 79, No. 21
0022-538X/05/$08.00+0 doi:10.1128/JVI.79.21.13594–13605.2005

Quantitative Analysis of the Hepatitis C Virus Replication Complex

Doris Quinkert, Ralf Bartenschlager, and Volker Lohmann*

Department Molecular Virology, Im Neuenheimer Feld 345, 69120 Heidelberg, Germany

Received 29 April 2005/Accepted 6 August 2005

The hepatitis C virus (HCV) encodes a large polyprotein; therefore, all viral proteins are produced in equimolar amounts regardless of their function. The aim of our study was to determine the ratio of nonstructural proteins to RNA that is required for HCV RNA replication. We analyzed Huh-7 cells harboring full-length HCV genomes or subgenomic replicons and found in all cases a >1,000-fold excess of HCV proteins over positive- and negative-strand RNA. To examine whether all nonstructural protein copies are involved in RNA synthesis, we isolated active HCV replication complexes from replicon cells and examined them for their content of viral RNA and proteins before and after treatment with protease and/or nuclease. In vitro replicase activity, as well as almost the entire negative- and positive-strand RNA, was resistant to nuclease treatment, whereas <5% of the nonstructural proteins were protected from protease digest but accounted for the full in vitro replicase activity. In consequence, only a minor fraction of the HCV nonstructural proteins was actively involved in RNA synthesis at a given time point but, due to the high amounts present in replicon cells, still representing a huge excess compared to the viral RNA. Based on the comparison of nuclease-resistant viral RNA to protease-resistant viral proteins, we estimate that an active HCV replicase complex consists of one negative-strand RNA, two to ten positive-strand RNAs, and several hundred nonstructural protein copies, which might be required as structural components of the vesicular compartments that are the site of HCV replication.

Hepatitis C virus (HCV) is an enveloped positive-strand RNA virus belonging to the genus *Hepacivirus* in the family *Flaviviridae*. The genome of HCV encompasses a single ~9600-nucleotide (nt) RNA molecule carrying one large open reading frame (ORF) that is flanked by nontranslated regions (NTRs). In addition to the polyprotein, the expression of a novel HCV protein with a yet-unknown function has recently been described, the so-called F-protein, which is generated by ribosomal frameshifting (78, 79). The 5′ NTR contains an internal ribosome entry site (IRES) that directs translation of the ORF (74). In addition, the 5′ NTR is required for RNA replication, as is the case with the 3′ NTR (25, 27, 42, 80). HCV proteins generated from the polyprotein precursor are cleaved by cellular and viral proteases into at least 10 different products (for reviews, see references 8 and 66). The structural proteins core, E1 and E2, are located in the amino terminus of the polyprotein (37), followed by p7, a hydrophobic peptide that is supposed to be a viroporin, forming an ion channel with a yet-unknown function (33, 63), and the nonstructural proteins (NS) NS2, NS3, NS4A, NS4B, NS5A, and NS5B. NS2 and the amino terminus of NS3 comprise the NS2-3 protease responsible for cleavage between NS2 and NS3 (31, 38). NS3 is a multifunctional protein, consisting of an amino-terminal protease domain required for processing of the NS3 to 5B region (6, 32) and a carboxy-terminal helicase/nucleoside triphosphatase domain (39, 71). NS4A is a cofactor that activates the NS3 protease function by forming a heterodimer (9, 21, 48, 72). The hydrophobic protein NS4B induces the formation of a cytoplasmic vesicular structure, designated the membranous web, that appears to contain the replication complex of HCV (18, 30). NS5A is a phosphoprotein that seems to play an important role in viral replication since most of the cell culture-adaptive mutations described thus far are located within the central region of NS5A (12, 34, 43, 50). NS5B is the RNA-dependent RNA polymerase of HCV (11, 52).

Since the establishment of HCV replicons (53), the understanding of the mechanisms underlying HCV RNA replication has increased tremendously (for a review, see reference 7). It is clear that nonstructural proteins NS3 to 5B are necessary and sufficient for HCV RNA replication. They build up a multiprotein complex that in analogy to other positive-strand RNA viruses is associated with intracellular membranes (reviewed in references 17 and 59). Biochemical analyses of crude replicase complexes (CRCs) prepared from lysates of replicon cells provided deeper insights into the organization and structure of the viral replication complex (2, 5, 19, 36, 45, 57, 70); however, a detailed stoichiometric analysis of the HCV replication complex has not yet been carried out. The aim of our study was to determine the ratio of viral positive- and negative-strand RNA to proteins in replicon cells and CRCs and to analyze which portions are actively involved in viral RNA synthesis. We found that the nonstructural proteins are produced in large excess over viral RNA in replicon cells and that viral replication complexes contain a large number of nonstructural protein copies. These results suggest that the majority of HCV nonstructural proteins may serve some other function in the replication process apart from RNA synthesis such as formation or scaffolding of the viral replication complex.

* Corresponding author. Mailing address: Department Molecular Virology, Im Neuenheimer Feld 345, 69120 Heidelberg, Germany. Phone: 49-6221-566449. Fax: 49-6221-564570. E-mail: volker_lohmann@med.uni-heidelberg.de.

MATERIALS AND METHODS

Cell cultures. Cell monolayers of the human hepatoma cell line Huh-7 (60) were grown in Dulbecco modified Eagle medium (DMEM; Invitrogen, Karlsruhe, Germany) supplemented with 2 mM L-glutamine, nonessential amino

acids, 100 U of penicillin/ml, 100 μg of streptomycin/ml, and 10% fetal calf serum. G418 (Geneticin; Invitrogen) was added at a final concentration of 1 mg/ml in case of replicon cell clone 9-13 carrying a HCV replicon expressing neomycin phosphotransferase (53). In the case of cell clone 11-1 harboring a monocistronic replicon (24), the medium was supplemented with 25 μg of hygromycin (Invitrogen)/ml. Huh7-Lunet cells refer to a Huh-7 cell clone that was generated with a selectable replicon and cured from HCV by treatment with a specific inhibitor. Huh7-Lunet cells are more permissive for HCV replication than naive Huh-7 cells (26, 50).

In vitro transcription. In vitro transcripts of HCV positive and negative-strands were generated by using the protocol described recently (50). For transcription of positive-strand HCV RNAs, plasmid DNA was restricted with AseI and ScaI (New England Biolabs, Frankfurt/Main, Germany), in the case of negative-strand transcripts, DNA was restricted with PmeI (New England Biolabs). After restriction, DNA was extracted with phenol and chloroform, precipitated with ethanol, and dissolved in RNase-free water. In vitro transcription reactions contained 80 mM HEPES (pH 7.5), 12 mM $MgCl_2$, 2 mM spermidine, 40 mM dithiothreitol, a 3.125 mM concentration of each nucleoside triphosphate, 1 U of RNasin (Promega, Mannheim, Germany)/μl, 0.05 μg of restricted plasmid DNA/μl, and 0.6 U of T7 RNA polymerase (Promega)/μl for positive-strand synthesis or T3 RNA polymerase for transcription of negative strands, respectively. After 2 h at 37°C, an additional 0.3 U of T7 or T3 RNA polymerase/μl was added, and the reaction was incubated for another 2 h. Transcription was terminated by the addition of 1 U of RNase-free DNase (Promega) per μg of plasmid DNA, followed by incubation for 30 min at 37°C. After extraction with acidic phenol and chloroform, RNA was precipitated with isopropanol and dissolved in RNase-free water. The concentration was determined by measurement of the optical density at 260 nm (OD_{260}), and RNA integrity was checked by denaturing agarose gel electrophoresis.

Electroporation of HCV full-length genomes. For electroporation, single-cell suspensions of Huh7-Lunet cells were prepared by trypsinization of monolayers, detaching the cells from the culture dish by a rinse with complete DMEM, followed by one wash with phosphate-buffered saline (PBS), counting, and resuspension at 10^7 cells per ml in Cytomix (76) containing 2 mM ATP and 5 mM glutathione. Then, 10 μg of in vitro-transcribed RNA was mixed with 400 μl of the cell suspension by pipetting, electroporated, and immediately transferred to 8 ml of complete DMEM. Electroporation conditions were 975 μF and 270 V using a Gene Pulser system (Bio-Rad, Munich, Germany) and a cuvette with a gap width of 0.4 cm (Bio-Rad). Cells of several electroporations were combined and seeded in aliquots. At 24, 48, 72, and 96 h after seeding, cells were treated with trypsin and counted. Aliquots of the cells were either lysed in protein sample buffer and subjected to immunoblot analysis or used for preparation of total RNA and Northern hybridization.

Preparation of total RNA and quantification of HCV RNA by Northern hybridization. These methods have been described recently (50). In brief, total RNA from cells or CRCs was prepared by a single-step isolation method (15), denatured by treatment with 5.9% glyoxal in 50% dimethyl sulfoxide and 10 mM sodium phosphate buffer (pH 7.0), and analyzed after denaturing agarose gel electrophoresis by Northern hybridization. Prior to hybridization the membrane was stained with methylene blue and cut ~1 cm below the 28S rRNA band. The upper strip containing the HCV replicon RNA was hybridized with a ^{32}P-labeled negative-sense riboprobe complementary to NS4B-NS5A region (nt 5979 to 6699) to detect viral positive-strand RNA or a positive-sense riboprobe encompassing the same region for detection of HCV negative-strand RNA. The lower strip that was hybridized with a β-actin-specific antisense riboprobe was used to correct for total RNA amounts loaded in each lane of the gel. Specific bands were quantified by phosphorimaging with a Molecular Imager FX scanner (Bio-Rad), and the number of HCV molecules was determined by comparison with a serial dilution of in vitro transcripts corresponding to a known number of positive or negative strands of subgenomic replicons mixed with 2 μg of total RNA from naive Huh-7 cells loaded in parallel onto the gel. In vitro transcripts were checked by denaturing agarose gel electrophoresis to ensure that almost all RNAs are full length and quantified by measurement of the OD_{260}.

Preparation of CRCs and in vitro replicase assay. The protocol is adapted from a previously published procedure (73). In a standard CRC-preparation, 2×10^8 Huh-7 cells persistently harboring subgenomic replicons were washed with phosphate-buffered saline and then scraped in phosphate-buffered saline and pelleted by centrifugation at 800 × *g* for 10 min at 4°C. Cells were suspended to a density of 2.5×10^7 cells/ml in hypotonic buffer (10 mM Tris-HCl [pH 7.5], 10 mM KCl, 1.5 mM $MgCl_2$, 0.5 mM phenylmethylsulfonyl fluoride [PMSF], 2 μg of aprotinin/ml) and lysed by 75 strokes with a Dounce homogenizer. Nuclei and unbroken cells were removed by centrifugation at 1,000 × *g* for 10 min at 4°C. The intracellular membranes in the resulting supernatant (S1) were then sedimented on 300 μl of 60% (wt/wt) sucrose in 10 mM Tris-HCl (pH 7.5)–10 mM KCl–1.5 mM $MgCl_2$ in an ultracentrifuge at 68,500 × *g* for 1 h at 4°C. The resulting supernatant (S2) was carefully removed, and the membrane fraction containing the CRCs was resuspended in the sucrose cushion to obtain an ~500-μl CRC fraction from 2×10^8 cells and directly subjected to proteinase K, S7 nuclease, and/or Triton X-100 treatment. The total protein concentrations of standard CRC preparations were in the range of 5 mg/ml. Alternatively, S1 obtained from 2×10^8 cells was directly pelleted for 1 h at 68,500 × *g*, resuspended in 200 μl of 10 mM Tris-HCl (pH 8.0)–10 mM NaCl–15% glycerol to obtain the CRC fraction, and stored in aliquots at −70°C.

HCV in vitro replicase activity was determined in a reaction mixture containing 20 mM Tris-HCl (pH 7.5), 10 mM $MgCl_2$, 5 mM dithiothreitol, 5 mM KCl, 40 μg of actinomycin D/ml, 20 μCi of [α-^{32}P]CTP, 10 μM CTP, 1 mM concentrations each of ATP and UTP, 5 mM GTP, 2.5 mM phosphoenolpyruvate, 1 U of pyruvate kinase (Sigma, Taufkirchen, Germany), 1 U of RNasin, and a 4-μl sample fraction in a total volume of 10 μl at 35°C for 60 min. Reaction products were purified by phenol-chloroform extraction and isopropanol precipitation and then analyzed by denaturing glyoxal agarose gel electrophoresis, followed by autoradiography. A radioactively labeled in vitro transcript corresponding to the length of a replicon RNA was used to determine the size of the reaction products.

Proteinase K, S7 nuclease, and Triton X-100 treatment of CRCs. To test the protease and nuclease resistance of the CRCs, different amounts of proteinase K (0.8- or 8-mg/ml final concentrations), nuclease (0.2- or 2-U/μl final concentrations), and/or 1% (vol/vol) Triton X-100 were directly added to 50 μl of freshly prepared CRCs, followed by incubation for 60 min at 25°C. After the incubation, proteinase K and S7 nuclease were inactivated by the addition of 1 μl of 100 mM PMSF and 1 μl of 200 mM EGTA, respectively. Then, 4 μl of CRCs was directly analyzed by in vitro replicase assays, and 2 μl was mixed with Laemmli sample buffer and analyzed by sodium dodecyl sulfate-polyacrylamide gel electrophoresis (SDS-PAGE) and immunoblotting. A 10-μl portion of CRCs was used for total RNA preparation. Total RNA was dissolved in 10 μl of water, and half of it was subjected to Northern hybridization analysis.

Fivefold-concentrated fractions of proteinase K-treated CRCs were generated by trichloroacetic acid precipitation.

Immunoblot analysis and silver staining of proteins. For quantitative immunoblot analysis, cells or CRCs were directly lysed in Laemmli-sample buffer and proteins were separated by SDS–10% PAGE using standard techniques (68). After SDS-PAGE proteins were either stained with silver or transferred to a polyvinylidene difluoride membrane and detected with various primary antibodies and secondary antibodies conjugated with horseradish peroxidase (Sigma) and developed with an ECL plus Western blotting detection system according to the instructions of the manufacturer (Amersham Biosciences, Freiburg, Germany). Core protein was quantified by using a goat anti-rabbit secondary antibody conjugated with alkaline phosphatase (Dianova, Hamburg, Germany), an ECF substrate (Amersham Biosciences) and a FLA-3000 fluorescence scanner with a 570-nm filter (Fuji). For detection of Calnexin a rabbit polyclonal antibody (Stressgen) was used specific for the amino-terminal part, which is resident in the lumen of the endoplasmic reticulum (ER). Core-, NS3-, and NS4B-specific rabbit polyclonal antisera were raised against purified portions corresponding to a part of the core protein (amino acids [aa] 1 to 167 of the polyprotein), the helicase domain of NS3 (aa 1230 to 1526 of the polyprotein), or full-length NS4B of the HCV NC1 isolate (EMBL nucleotide sequence database accession no. AJ238800), respectively, differing only in a few residues to HCV Con1 (EMBL nucleotide sequence database accession no. AJ238799). Mouse monoclonal antibody 5B-3B1, specifically detecting a linear epitope encompassing aa 2791 to 2801 (58) was used to quantify NS5B.

For quantification of HCV proteins, bacterially expressed core protein and baculovirus-expressed full-length NS4B and NS5B proteins with C-terminal His_6 tags were purified by Ni-nitrilotriacetic acid affinity chromatography according to the instructions of the manufacturer (QIAGEN, Hilden, Germany) or as described recently (52). NS4B-C-His and core-C-His was further purified by preparative SDS-PAGE. The purity of both proteins was >90%, and the protein concentration was determined by Bradford assay and analytical SDS-PAGE using a serial dilution of bovine serum albumin as a reference. Core, NS4B, and NS5B sequences correspond to the NC1 isolate (see above and reference 41). Samples were quantified by comparison of band intensities to signals obtained from the serially diluted purified proteins.

EXHIBIT A

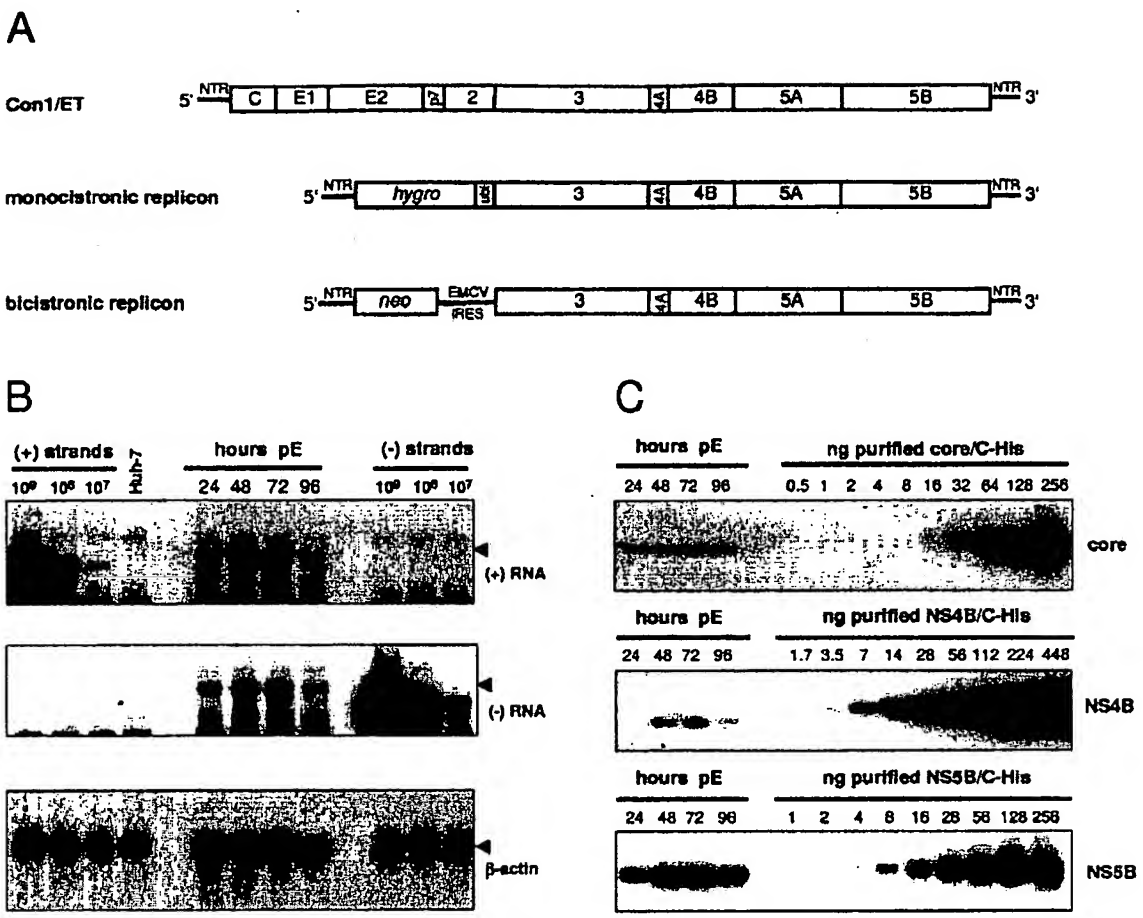

FIG. 1. Quantification of HCV RNA and nonstructural proteins in Huh-7 cells transfected with a full-length genome. (A) Structure of the HCV RNAs used in the present study. Con1/ET represents a full-length HCV genome harboring cell culture-adaptive mutations in NS3 and NS4B (64). The monocistronic replicon contains only a single ORF consisting of nt 342 to 389 of the core-coding region, the *hygro* gene (encoding the hygromycin phosphotransferase), the ubiquitin-encoding sequence (Ubi), and the HCV NS proteins NS3 to NS5B (24) and was used to select Huh-7 cell clone 11-1, which was analyzed in the present study (Table 1). The bicistronic replicon is composed of the first 377 nt of the HCV genome fused to the neo gene (encoding the neomycin phosphotransferase). Translation of the HCV NS proteins NS3-5B is initiated by the encephalomyocarditis virus-IRES. The bicistronic replicon was used to generate cell-clone 9-13 (53). (B) Time course of HCV positive- and negative-strand synthesis after transfection of Con1/ET RNA into Huh7-Lunet cells. Cells were harvested and counted at the time points indicated above the figure (pE, postelectroporation), and total RNA was prepared. A total of 5 μg of total RNA corresponding to 2.5×10^5, 2.1×10^5, 2.1×10^5, and 2.3×10^5 cells at 24, 48, 72, and 96 h, respectively, was subjected to Northern hybridization with radiolabeled riboprobes specific for the detection of HCV positive-strand (top panel), negative-strand (middle panel) or β-actin (lowest panel). Specific signals are indicated by arrowheads. Signals were quantified by phosphorimaging with known amounts of in vitro transcripts of positive or negative polarity corresponding to a subgenomic replicon and normalized for different loadings by the β-actin signal. Total RNA from naive Huh-7 cells was used as negative control (Huh-7). (C) Quantification of HCV core (upper panel), NS4B (middle panel), and NS5B (lowest panel) expression after transfection of Con1/ET RNA into Huh7-Lunet cells. An aliquot of the cells harvested for total RNA preparation at the time points given above each panel was lysed in Laemmli sample buffer and subjected to immunoblot analysis with monoclonal antibodies (NS5B) or polyclonal antisera (core, NS4B) with the specificities given on the right. Samples were quantified by comparison of signal intensities derived from known amounts of the respective antigens as indicated above each panel. The amount of loaded proteins correspond to 1.2×10^5, 1.8×10^5, 1.6×10^5, and 2.0×10^5 cells at 24, 48, 72, and 96 h, respectively.

RESULTS

Quantification of the HCV RNA to protein ratio in Huh-7 cells. The first question addressed in our study was how the number of HCV positive- and negative-strand RNA molecules correlates with the amount of different HCV proteins in cells with productive HCV RNA replication. Therefore, we chose a full-length HCV genome with cell culture-adaptive mutations (Con1/ET, Fig. 1A) (64), which was transfected into Huh7-Lunet cells, a cured replicon cell clone exhibiting high permissiveness for HCV replication. Cells were seeded in aliquots after electroporation, harvested at various time points, counted, and analyzed for the amount of HCV RNA and proteins. Figure 1B shows a typical Northern blot analysis of such a transient replication assay by using known numbers of in vitro transcripts to determine the quantity of positive and negative-strand RNA in cells transfected with Con1/ET. RNA

TABLE 1. Number of positive-strand RNA, negative-strand RNA, core, NS4B, and NS5B molecules per Huh-7 cell

HCV sequence	Mean no. of molecules/cell ± SD[a]				
	Negative-strand	Positive-strand	Core	NS4B	NS5B
Con1/ET (transient transfection)[b]	40 ± 4	(2.0 ± 0.3) × 10^2	(4.9 ± 1.4) × 10^6	(7.7 ± 1.8) × 10^5	(1.5 ± 0.4) × 10^6
Monocistronic replicon (cell clone 11-1)	81 ± 11	(4.4 ± 1.5) × 10^2	NA	(8.9 ± 3.2) × 10^5	(2.2 ± 0.8) × 10^6
Bicistronic replicon (cell clone 9-13)	94 ± 31	(7.6 ± 2.9) × 10^2	NA	(8.0 ± 0.4) × 10^5	(1.2 ± 0.5) × 10^6

[a] Data represent mean values and standard deviations of samples harvested at 48, 72, and 96 h after seeding. NA, not applicable.
[b] Per-cell data was not normalized for transfection efficiency, which was routinely 50 to 80%.

replication had already started 24 h after transfection (as judged by the clearly detectable negative-strand RNA signal), reached its maximum at 48 h and 72 h after transfection, and slightly decreased at 96 h, after the cells had reached confluence (Fig. 1B, top and middle panel). HCV core and nonstructural proteins 4B and 5B were quantified by Western blot analysis of cell lysates in comparison with defined amounts of purified proteins from the same HCV isolate (41, 52, 54) and by using antibodies raised against these particular antigens (Fig. 1C). The number of core, NS4B, and NS5B molecules in the transfected cells followed the same changes over time as the RNA, and the results obtained for the quantitative evaluation are summarized in Table 1. Previous analyses have shown that transfected RNA of replication-deficient genomes is degraded to trace amounts at 24 h after transfection and completely absent after 48 h (13, 64). To avoid any impact of transfected input RNA, the quantitative analysis was limited to the data obtained at 48 to 96 h. We found on average 40 copies of negative-strand RNA, a fivefold excess of positive-strand RNA and approximately one million copies of core, NS4B and NS5B per cell, indicating a vast excess of viral proteins to RNA molecules. Within the expected range of accuracy the ratio of the nonstructural proteins NS4B and NS5B was very similar. The three- to sixfold higher relative levels of core might be due to premature termination of translation leading to an overrepresentation of the amino-terminal portions of the HCV polyprotein. Nevertheless, the data were consistent in showing a tremendous excess of HCV proteins compared to RNA molecules.

Since we sought to determine the stoichiometry of RNA to protein in the HCV replication complex, we searched for the most appropriate biochemical equivalent. Every active replication complex must contain at least one negative-strand RNA molecule; therefore, the amount of negative-strand RNA gives the closest estimate of the maximal number of HCV replication complexes per cell. Based on this assumption, we found on average fewer than forty active replication complexes per cell, but each was accompanied by 20,000 to 40,000 copies of NS proteins.

Although the analysis of a HCV full-length genome should reflect the properties of viral translation and replication most closely, we wanted to confirm the data in a steady-state situation, which resembles a persistent infection. The most efficient and convenient systems to study persistent HCV RNA replication are Huh-7 cell clones with subgenomic replicons, keeping constant HCV RNA and protein levels over years, even in the absence of selective pressure (65). Therefore, we analyzed two different types of replicon cells to evaluate the data obtained with the full-length genome (Fig. 1A): (i) a Huh-7 cell clone designated 11-1, harboring a monocistronic replicon resembling closely the translational properties of a full-length genome (24) and (ii) a Huh-7 cell clone designated 9-13 (51, 53) with a bicistronic replicon representing the most efficient and most often used system to study persistent HCV replication. Cells harboring the respective replicons were seeded in aliquots and analyzed in the same way as the full-length genome at different time points after seeding. Despite the different architecture of the replicons and the assay format (transient replication versus stable replicon cell clones), we obtained very similar results (Table 1), with more than 10,000 NS4B or NS5B copies per negative-strand RNA molecule. This result indicated that the synthesis of a massive excess of NS-proteins over RNA seems to be an intrinsic property of HCV translation and replication in Huh-7 cells. Since the half-lives of the NS proteins (11 to 16 h) (65) were shown to be comparable to the half-life of RNA (about 11 h) (62) in replicon cells and HCV RNA and proteins are kept on similar steady-state levels over years of continuous passaging, HCV RNA and protein synthesis should also be quite constant. Therefore, based on the data shown in Table 1, each positive-strand RNA template is translated numerous times giving rise to 1,000 to 10,000 polyprotein copies. Another important conclusion was that the stoichiometry of HCV protein to RNA in replicon cell clones closely resembled the one found with full-length genomes. Therefore, replicon cell clones were an appropriate tool for further analyses.

Isolation of active replicase complexes from Huh-7 cell harboring subgenomic replicons. We wondered whether the massive surplus of nonstructural proteins really is directly involved in RNA synthesis or may serve some other function. To differentiate between these two possibilities, we isolated CRCs from replicon cells that could be further analyzed in vitro for their protein and RNA content. The method for the preparation of CRCs by pelleting heavy-membrane fractions from hypotonic cell lysates has been described for HCV and related viruses (5, 19, 36, 45, 73) and is shown schematically in Fig. 2A. To assay for in vitro replicase activity, cell lysates were incubated with radiolabeled nucleotides in the presence of actinomycin D and in the absence of exogenous template RNA. Reaction products were further analyzed by denaturing agarose gel electrophoresis (Fig. 2B). The dominant product of in vitro replication was a single band that corresponded in size to the full-length replicon RNA (arrowhead). HCV replicase activity was already detectable in the total hypotonic lysate of replicon cells but was enriched in CRCs that were obtained by pelleting the membranous material contained in supernatant 1. The resulting supernatant 2 did not contain detectable replicase activity. The distribution of the nonstructural proteins in

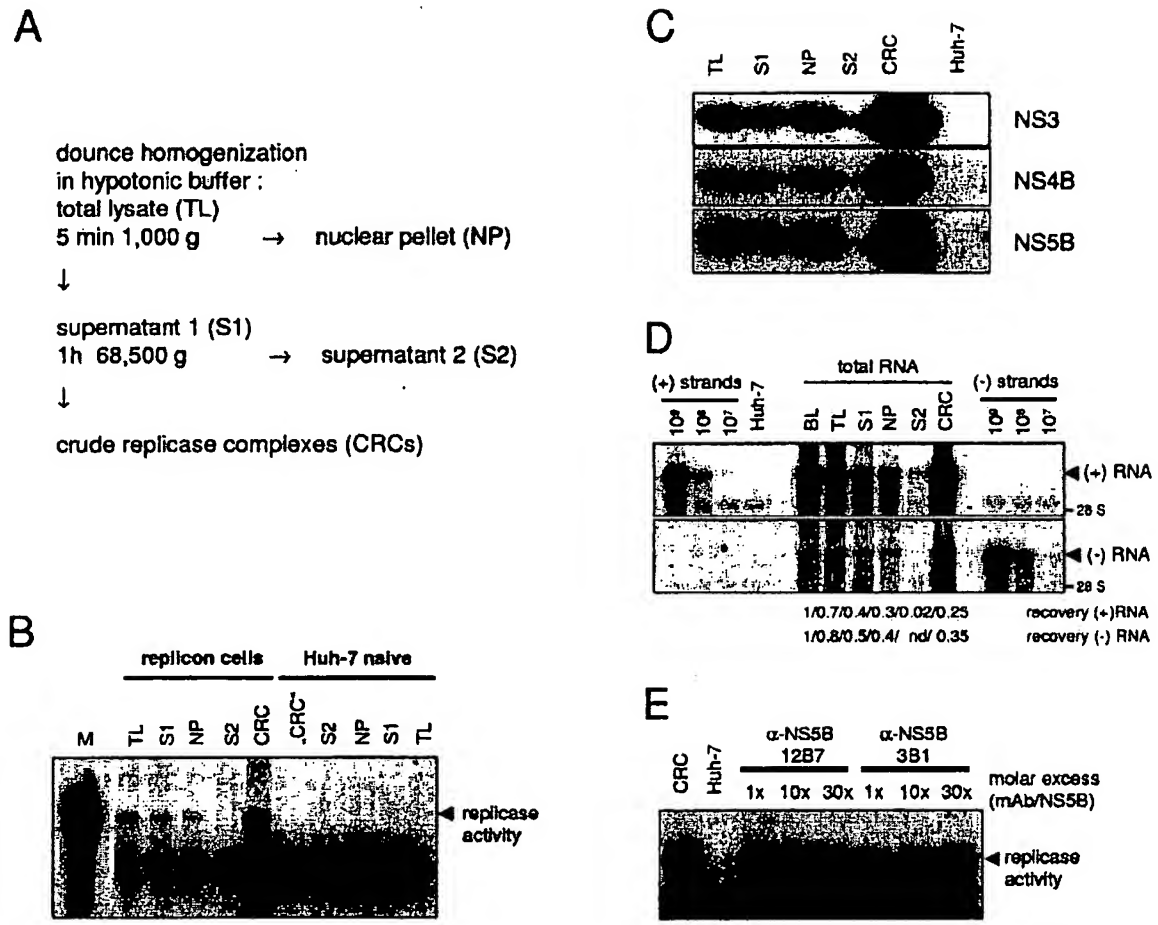

FIG. 2. Preparation and characterization of CRCs from HCV replicon cells. (A) Schematic diagram of the CRC preparation protocol. (B) Analysis of in vitro replicase activity in total lysates (TL) and different subcellular fractions of replicon cells (left half) and naive Huh-7 cells (right half). In vitro replicase activity was determined in 4 μl of each fraction, and reaction products were analyzed by denaturing glyoxal-gel electrophoresis, followed by autoradiography of the dried gel. A radioactively labeled in vitro transcript identical in size to the replicon was loaded as a marker (M). The major reaction product of the in vitro replicase assay is indicated by an arrowhead. (C) Detection of NS3, NS4B, and NS5B in different fractions of the CRC preparation. The volume of the NP fraction was adjusted to the volume of S1 and 10 μl of each fraction were analyzed by immunoblot with a polyclonal antiserum raised against HCV NS3 (upper panel) or NS4B (middle panel) or monoclonal antibodies specific for NS5B (lower panel) and compared to 10 μl of "CRC" fraction from naive Huh-7 cells (Huh-7). (D) Fate of viral positive and negative strands during hypotonic lysis and CRC preparation. Total RNA was prepared from 50 μl of a replicon cell suspension before lysis (BL) and from the same volumes of TL, S1, NP (adjusted to the volume of S1), S2, and CRC and subjected to Northern hybridization analysis with the same controls and probes to detect HCV positive- (upper panel) and negative-strand RNA (lower panel) as in Fig. 1B. To calculate the recovery rate samples were analyzed by phosphorimaging and correlated with the value obtained before cell lysis (BL). The data of the CRC fraction were corrected for the difference in total volume. (E) Effect of NS5B-specific monoclonal antibodies on in vitro replicase activity. Two μl of a standard CRC preparation containing 40 ng of NS5B were preincubated 5 min on ice with 0.1, 1, or 3 μg of purified monoclonal antibodies as indicated in the top, resulting in a 1×, 10×, or 30× molar excess or incubated in the absence of antibodies (CRC) and analyzed for in vitro replicase activity. The same amount of "CRC" fraction from naive Huh-7 cells was used as a negative control (Huh-7). For further details refer to the text.

different fractions of the CRC preparation is shown in Fig. 2C. Similar portions of NS3, NS4B, and NS5B were recovered in S1 and concentrated in parallel to the replicase activity in the CRC fraction, leaving only trace amounts in S2.

To exclude that the CRC fraction contains only a minor subpopulation of HCV replication complexes that might not be representative, we followed the fate of viral positive- and negative-strand RNA during CRC preparation (Fig. 2D). We found that 35% of the negative- and 25% of the positive-strand RNA present in the replicon cells before lysis were recovered in the CRC fraction. The remainder was either associated with the nuclear pellet (40% of negative-strand, 30% of positive-strand RNA) or was destroyed during cell lysis (20% of negative-strand, 30% of positive-strand RNA) or during centrifugation of CRCs (15% of negative-strand and positive-strand RNA, respectively); only traces of RNA were retained in S2. In consequence, about half of the positive-strand RNA and 25% of the negative-strand RNA were degraded, most likely by the action of cellular nucleases that were liberated during cell lysis. This fraction might include damaged replicase complexes and

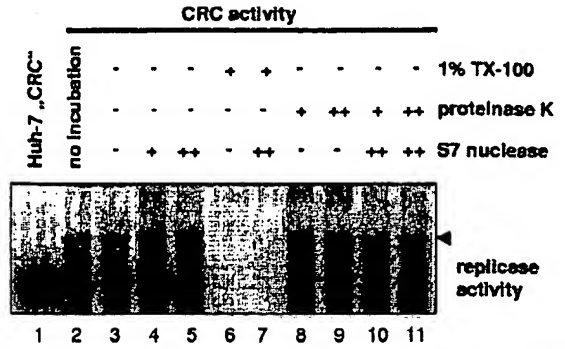

FIG. 3. HCV replicase activity is completely resistant to protease and nuclease treatment. A total of 50 μl of CRCs prepared from replicon cell clone 9-13 was incubated for 60 min at 25°C in the presence of 1% Triton X-100 and/or 0.8 (+) or 8 (++) mg of proteinase K/ml and/or 0.2 (+) or 2 (++) U of S7 nuclease/μl, respectively, as indicated above each lane. After termination of the proteinase K and S7 nuclease digest by the addition of 1.4 mM PMSF and/or 2.75 mM EGTA, respectively, equal amounts of each sample were analyzed for in vitro replicase activity. Reaction products were separated by denaturing glyoxal agarose gel electrophoresis and autoradiography. Lane 1 and 2 represent control reactions with CRCs from naive Huh-7 or replicon cells in the absence of any preincubation. CRCs in lane 3 were mock incubated for 60 min at 25°C prior to the in vitro replicase assay.

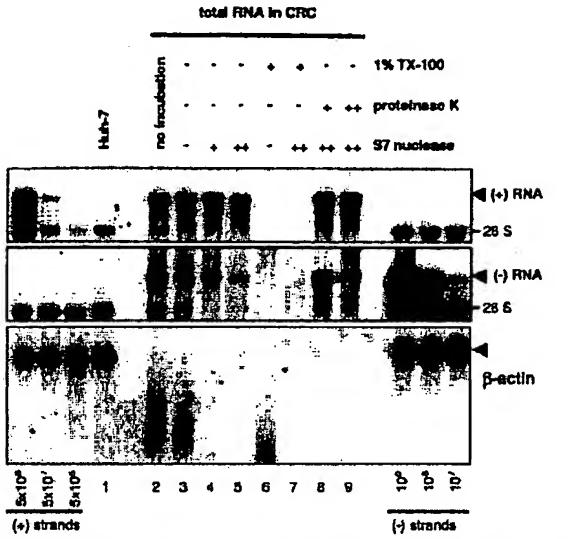

FIG. 4. Quantification of nuclease-resistant HCV positive- and negative-strand RNA and β-actin mRNA in CRCs. Total RNA equivalent to 5 μl of CRCs treated with 1% Triton X-100, 0.8 (+) or 8 (++) mg of proteinase K/ml and/or 0.2 (+) or 2 (++) U of S7 nuclease/μl for 60 min at 25°C or from mock-treated CRCs, as indicated on top, was subjected to Northern hybridization analysis with a negative-strand riboprobe to detect viral positive-strand RNA (top panel), a positive-strand riboprobe for HCV negative-strand detection (middle panel), and a riboprobe specific for the detection of cellular β-actin mRNA. The positions of viral positive- and negative-strand RNA and β-actin are indicated by arrowheads at the right. For quantification, in vitro transcribed replicons corresponding to known amounts of viral positive- and negative-strand RNA were mixed with 2 μg of total cellular RNA from naive Huh-7 cells and loaded as indicated at the bottom of the figure. We used 4 μg of total RNA from naive Huh-7 cells as a negative control (Huh-7, lane 1). We quantified the viral RNAs by phosphorimaging and found ca. 3×10^6 negative-strand and 3×10^7 positive-strand RNAs per μl of CRCs in this particular experiment.

positive-strand HCV RNAs that were not integrated into the replicase complex but engaged in some other processes such as RNA translation. A varying amount of NS proteins, HCV RNA, and replicase activity always stayed associated with the nuclear pellet and could not be recovered even by vigorous dounce homogenization, most likely due to the accumulation of replication complexes in the perinuclear region (30) and due to the mild extraction conditions omitting any detergents.

HCV replicase complexes act selectively on endogenous templates in vitro and are blocked by an inhibitor of NS3 helicase (36), indicating that replicase activity is distinct from RNA synthesis exerted by isolated NS5B polymerase. In addition, RNA synthesis activity of the native replicase complex was inhibited by 3′-deoxy-CTP, a chain-terminating nucleotide analog, but not inhibited by non-nucleoside NS5B polymerase inhibitors interfering with the activity of purified NS5B (56; data not shown). To gain further insights into the properties of the HCV replication complex, we analyzed the impact of monoclonal antibody NS5B 12B7 on replicase activity in CRCs. It has previously been shown that this antibody inhibits HCV polymerase activity by binding to a conformational epitope in NS5B (58), in contrast to antibody NS5B 3B1, that did not interfere with polymerase activity. We found that none of the antibodies affected replicase activity in CRCs in an up to 30-fold molar excess (Fig. 2E), further substantiating that in vitro replicase activity exhibits features distinct from isolated HCV polymerase.

Taken together, CRCs most likely contained a representative fraction of HCV replication complexes in replicon cell clones and were therefore appropriate to study the stoichiometry of RNA to NS proteins required for RNA replication. Since clone 9-13, which harbors a bicistronic replicon, was the most efficient source for the preparation of active replicase complexes, we chose this cell clone for further experiments.

In vitro replicase activity and viral RNA are fully resistant to nuclease and protease treatment. It has been shown previously that in vitro replicase activity is resistant to nuclease and protease treatment (2, 5, 19, 57). We exploited these results to evaluate which fraction of viral RNA and proteins is resistant to nuclease and protease, respectively, in order to determine the stoichiometry of the viral components of the HCV replication complex. Therefore, we treated CRCs with high concentrations of proteinase K (0.8 or 8 mg/ml) and/or S7 nuclease (200 or 2,000 U/ml), stopped the reaction by adding PMSF or EGTA, respectively, and analyzed an aliquot of the pretreated CRCs for in vitro replicase activity. As shown in Fig. 3, in vitro replicase activity was not affected by pretreatment with either S7 nuclease (lanes 4 and 5) or proteinase K (lanes 8 and 9) alone or in combination (lanes 10 and 11). Protease and nuclease resistance was not restricted to replicase activity contained in the CRC fraction but was also found for replicase activity in total cell lysate, the nuclear pellet, and supernatant 1 (data not shown), indicating that the replication complexes in the CRC fraction were not a selected subpopulation with dis-

EXHIBIT A

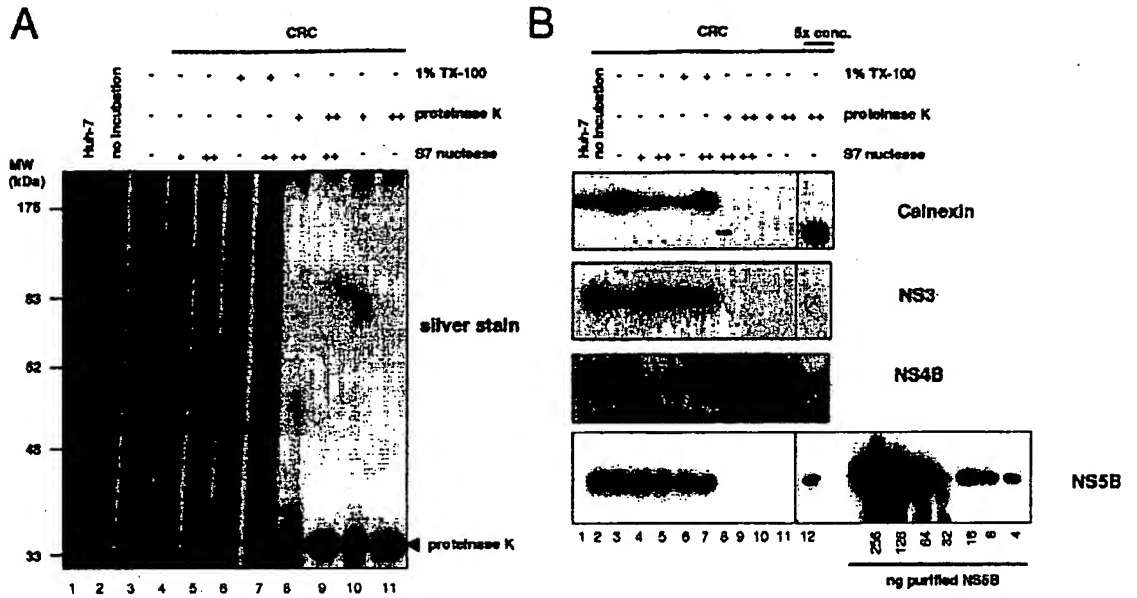

FIG. 5. Effect of proteinase K digest on cellular proteins and quantification of protease-resistant HCV nonstructural proteins in CRCs. Equal amounts of CRCs prepared from replicon cell clone 9-13 were incubated for 60 min at 25°C in the presence or absence of 1% Triton X-100 and/or 0.8 (+) or 8 (++) mg of proteinase K/ml and/or 0.2 (+) or 2 (++) U of S7 nuclease/μl, respectively, as indicated above each lane. The reaction was stopped by the addition of 1.4 mM PMSF and 2.75 mM EGTA and boiled in sample buffer, and total protein equivalent to 2 μl of the CRCs was subjected to SDS–10% PAGE. In the fivefold-concentrated samples, the proteins were trichloroacetic acid precipitated, and the equivalent of 10 μl of CRCs was loaded. Proteins were either visualized by silver staining (A) or subjected to immunoblot analysis (B) with monoclonal antibodies specific for the ER luminal part of calnexin (upper panel), a polyclonal antiserum raised against HCV NS3 or NS4B (middle two panels), and monoclonal antibodies specific for HCV NS5B (bottom panel), as indicated at the right. The concentrated fractions (lane 12) are shown from identical expositions of the same blot. A serial dilution of purified NS5B was loaded in parallel for quantification as depicted at the bottom of the figure.

tinct features. HCV replicase activity was only abolished by addition of 1% Triton X-100, in the absence (lane 6) or presence (lane 7) of additional nuclease, indicating that the resistance of HCV replicase to proteases and nucleases is mediated by detergent-sensitive structures. The full protease and nuclease resistance of in vitro replicase activity enabled us to analyze which portion of viral RNA and proteins were not affected by protease and nuclease and therefore were necessary and sufficient for RNA synthesis. To address this question, aliquots of the protease- and/or nuclease-treated CRCs were analyzed by Northern hybridization and immunoblotting to determine the ratio of HCV RNA and NS proteins involved in replication.

We first focused on the effect of S7 nuclease treatment on the fate of viral and cellular RNA (Fig. 4). Viral positive- and negative-strand RNAs were fully resistant to nuclease in CRCs, as shown by Northern blot analysis (Fig. 4, top and middle panels, compare lane 3 with lanes 4 and 5). The efficiency of the digest was indicated by the marked reduction of 28S rRNA in the S7 nuclease-treated samples (Fig. 4, top and middle panel, lanes 4, 5, 8, and 9). Protection from nucleases seemed not to be mediated by proteins, since further addition of proteinase K had no effect on RNA stability (lanes 8 and 9). In contrast, the addition of Triton X-100 resulted in complete degradation of both viral RNA species, even in the absence of exogenous nuclease (lanes 6 and 7), indicating that the RNA was protected by membranes rather than proteins and that the loss of replicase activity upon detergent treatment (Fig. 3) was primarily due to the destruction of template RNA by endogenous nucleases and S7 nuclease. In contrast to the viral RNAs, the cellular mRNA, exemplified by β-actin, was absent in CRCs because it was not attached to membranes or almost completely destroyed by the action of endogenous nucleases that were liberated during CRC-preparation (Fig. 4, lowest panel, lanes 2 and 3) and the remaining traces were fully accessible to S7 nuclease (lanes 4 and 5).

Taken together, our data indicate that the viral positive- and negative-strand RNA in the replication complex is completely protected from nucleases and that this protection is mediated by detergent sensitive membrane structures rather than by proteins.

Only a minor portion of the HCV NS proteins is resistant to protease treatment. Since in vitro replicase activity was completely resistant to protease and nuclease treatment, the ratio of HCV NS proteins to RNA actively involved in RNA synthesis was determined by the number of nuclease resistant RNA molecules compared to protease-resistant protein molecules. To measure the fraction of viral NS proteins resistant to protease, we analyzed aliquots of the differently treated CRC samples for the impact of proteinase K incubation by Western blotting (Fig. 5B). Even with the lower protease concentrations, we found a massive degradation of almost all cellular proteins to nearly undetectable amounts (Fig. 5A, lanes 8 to 11), whereas detergent and nuclease treatment had, as expected, no significant effect (lanes 4 to 7). As an example for a

cellular protein we chose calnexin for a closer analysis by Western blotting with an antiserum directed against its N-terminal part, which is located in the lumen of the endoplasmic reticulum and therefore should be protected from proteases in an intact ER structure, whereas the carboxy terminus was expected to be protease sensitive in a cell lysate (57). As shown in Fig. 5B (top panel), no full-length calnexin was detectable after protease treatment, and only traces of a C-terminally truncated fragment were visible with the lower amount of protease (lanes 8 to 11). Only after fivefold concentration of the sample were we able to obtain a clear signal (lane 12). The absence of full-length calnexin even in the concentrated samples indicated that the amount of proteinase K we used was sufficient for a complete digest. Since the majority of the ER-luminal N-terminal calnexin fragments were also accessible to protease (Fig. 5B, top panel, signal strength in lanes 1 to 7 compared to lanes 8 to 11), it seemed that most of the regular ER structures were not intact after CRC preparation and protease digest. The HCV replication complex therefore appears to represent a more rigid structure due to the complete protease and nuclease resistance of in vitro replicase activity. However, when we analyzed the viral nonstructural proteins 3, 4B, and 5B after protease digest (Fig. 5B, second, third, and lowest panels, respectively, lanes 8 to 12), we found detectable amounts again only after fivefold concentration of the samples (lane 12). The absence of lower-molecular-weight products indicated the completeness of digestion. Based on densitometric analysis and including the dilution factor, we calculated that roughly 2.5% of NS5B was resistant to proteinase K digest but accounted for the full replicase activity (Fig. 3), suggesting that the majority of viral nonstructural proteins was not directly involved in RNA synthesis at a given time point. The portions of protease-resistant NS3 and NS4B were similar, indicating a 1:1 stoichiometry of the NS proteins in the replication complex. A serial dilution of purified NS5B applied on the same Western blot allowed us to quantify the number of NS5B molecules resistant to protease digest (Fig. 5B, lowest panel), and we detected ca. 5×10^9 molecules NS5B per μl CRCs in this experiment. Compared to 3×10^6 negative strands and 3×10^7 positive strands (Fig. 4), the surprising result was that, although only 2.5% of the NS5B molecules were engaged in replicase activity at a given time, we still found a 1,600-fold excess of NS5B compared to negative-strand RNA and a >100-fold excess compared to positive-strand RNA in CRCs.

The HCV replication complex contains multiple copies of the NS proteins. The data obtained from the experiment shown in Fig. 3 to 5 (experiment 1) and from an additional, independent experiment are summarized in Table 2. Both sets of data revealed very similar results. Viral positive- and negative-strand RNA was entirely resistant to nucleases in preparations of replication complexes compared to <3% of NS5B being protease resistant. The ratio of positive to negative-strand RNA varied and might be dependent on the physiological state of the cells at the time of harvest. Negative-strand RNA is the most limited component in HCV RNA replication and therefore the best indicator for the total number of active replication complexes. Given the data presented in Table 1 and assuming that each active replicase complex contains per definition at least one copy of negative-strand RNA, there were on average fewer than a hundred active replication complexes per replicon cell but more than a million polymerase molecules. After biochemical preparation of replicase complexes and excessive protease digest we still found more than 1,000 NS5B molecules per negative-strand RNA (Table 2) and similar amounts of NS4B and NS3, indicating that a huge excess of NS proteins is required to build up the viral replication complex.

TABLE 2. Portions and ratios of nuclease-resistant positive-strand, negative-strand, and protease-resistant NS5B in CRCs

Parameter[a]	Expt 1	Expt 2
% Protease-resistant NS5B	2.5	2.2
% Nuclease-resistant positive-strand RNA	~100	~100
% Nuclease-resistant negative-strand RNA	~100	~100
Positive-strand/negative-strand RNA ratio	12 ± 3	6 ± 2
NS5B/negative-strand RNA ratio	1,200 ± 400	700 ± 400
NS5B/positive-strand RNA ratio	100 ± 20	110 ± 50

[a] Ratios are given as the mean and standard deviation of four nuclease-treated samples.

DISCUSSION

In the present study we analyzed the stoichiometry of HCV RNA and proteins in cells with ongoing HCV replication and found a massive excess of structural and nonstructural protein molecules over RNA, indicating that each positive-strand RNA molecule is excessively translated before a replication complex is formed and RNA synthesis is initiated. In agreement with the polyprotein nature of the major HCV ORF, we found all analyzed cleavage products in similar amounts. A ca. 1,000- to 10,000-fold excess of viral proteins to positive-strand RNA as observed in our study might fit well to the requirements for particle formation, since virions of other enveloped positive-strand RNA viruses such as alphaviruses, tick-borne encephalitis virus, or Dengue virus usually contain several hundred copies of structural proteins per particle (22, 28, 44, 61).

We wondered whether a similar excess of nonstructural proteins was required for RNA replication and addressed this question by studying crude replicase complexes isolated from cells harboring persistent HCV replicons. It has been shown previously that in vitro replicase activity is resistant to protease and nuclease treatment in CRCs (2, 5, 19) and that in digitonin-solubilized replicon cells only a minor portion of the HCV NS proteins is protease resistant and therefore seems to be involved in replication (57). Our data here are in good agreement with these earlier results; however, although we find as well that <5% of the NS proteins in CRCs are protease resistant and account for full replication activity in vitro, this still results in a ca. 1,000:1 stoichiometry of NS proteins to active replicase complexes, as estimated by the number of negative-strand RNA molecules.

Based on our data and on previously published electron microscopic studies (18, 30), we propose a tentative model of

EXHIBIT A

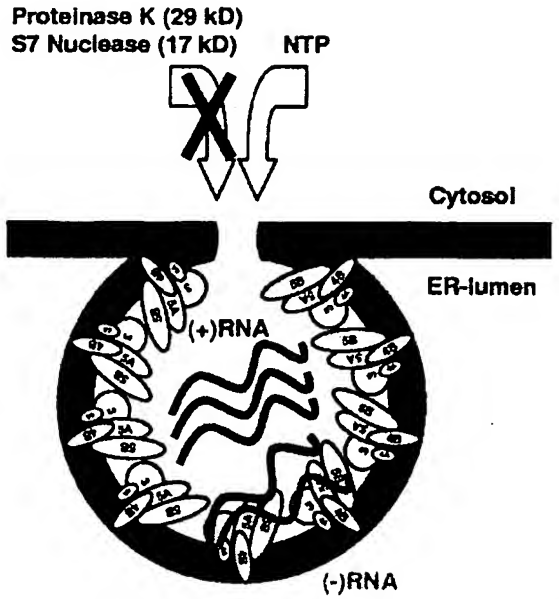

FIG. 6. Schematic model of the HCV replication complex. HCV NS proteins are indicated by ellipses; black and gray wavy lines represent viral positive- and negative-strand RNAs, respectively. Individual NS proteins and RNA are not drawn to scale. For closer explanations refer to the text.

the HCV replication complex (Fig. 6). This model is based on the well-supported assumption that polymerase activity as measured by CRC assays is a component of the replication complex and not of isolated enzyme. Multiple copies of HCV NS protein complexes encompassing NS3 to NS5B build up a vesicular membrane structure, which mediates the protection against nucleases and proteases and may hide double-strand RNA from detection by the host cells innate immune system. The existence of HCV NS protein complexes rather than individual proteins is indicated by similar fractions of NS3, NS4B, and NS5B being resistant to protease and seems plausible due to the numerous interactions within the NS proteins that have thus far been described (7, 16). Each vesicle should have a connection to the cytoplasm, allowing the constant supply with nucleotides for RNA synthesis, but preventing the access of molecules larger than 16 kDa, e.g., S7 nuclease and proteinase K. A number of these vesicles accumulate at distinct sites in the cytoplasm and form the membranous web, which was shown to be the site of RNA replication (30). Within every vesicle that contains an active replicase complex we find at least one negative-strand RNA, several positive-strand RNAs and up to 1,000 copies of each of the NS proteins. The precise stoichiometry of RNA to protein in the replicase complex is hard to tell, since a number of replication complexes might await initiation of negative-strand synthesis at a given time and therefore contain only NS proteins and positive-strand RNA. If this variant is frequent, ca. 100 to 200 copies of the nonstructural proteins per replicase complex would be a more realistic estimate. On the other hand, several replicase complexes might include more than one molecule of negative-strand RNA, and therefore the number of NS protein molecules per active replicase complex could even be higher. Finally, we cannot exclude the existence of vesicles without viral RNA, which still might render the included NS proteins protease resistant, because the induction of membrane alterations is an intrinsic property of NS4B (18), and we do not know whether the presence of RNA is necessary to induce protease resistance of the NS proteins.

Our picture of the HCV replication complex is very similar to a model suggested by Miyanari et al. (57); however, the data presented here provide the first experimental evidence that each HCV replication complex is composed of multiple copies of the viral nonstructural proteins. This resembles closely results obtained for brome mosaic virus (69). It has been shown that 400 copies of protein 1a form a spherular structure connected to the cytoplasm and containing viral RNA, together with a few copies of the viral polymerase 2a. In the case of HCV the majority of protease-resistant NS protein complexes might as well be required to build up the vesicular structure, whereas only a few complexes are required for polymerase activity. This calculation is based on the kinetics of RNA and protein synthesis in replicon cells: the intracellular levels of viral RNA and proteins remain relatively constant over years of continuous passaging (62), representing a steady-state situation at any given time point. Since the half-lives of viral NS proteins and viral positive-strand RNA in replicon cells have been shown to be 11 to 16 h (62, 65), the rate of newly synthesized RNA and protein per day should roughly be in the range we find in the steady-state situation (Table 1). Based on this knowledge and on our data, we estimate that only about 1,000 positive-strand RNA molecules are synthesized per day per cell by ca. 100 replicase complexes but more than 1,000,000 copies of NS proteins. In consequence, each newly synthesized positive strand has to be excessively translated to yield the ascertained surplus of proteins, whereas RNA synthesis is a rather rare event, which most likely is achieved only by a few NS protein complexes. Given our calculation, <0.1% of all NS5B molecules are required to be enzymatically active.

Many positive-strand RNA viruses have evolved strategies to regulate the amounts of active polymerase, either by expression from an independent cistron, like BMV (69); by the expression of a polyprotein containing rarely suppressed stop codons, like alphaviruses (47); or by producing stable precursor intermediates lacking polymerase activity, like poliovirus 3CD (10). In the case of HCV, polymerase activity could be regulated by different conformations of the NS protein complex, depending on its function. It has been shown that a carboxy-terminal region of NS5B, encompassing aa 545 to 562 inhibits polymerase activity (1) and that only a small fraction of purified NS5B containing this region is enzymatically active (14). Crystal structure analysis revealed that this carboxy-terminal domain protrudes into the RNA-binding cavity of NS5B and interferes with template binding (46). Deletion of this region increases polymerase activity, as well as RNA binding of NS5B (46); therefore, it is tempting to speculate that the majority of NS5B is inactive after translation by refolding of the carboxy terminus into the RNA binding cleft, whereas only those few molecules that stay bound to the viral RNA keep the template binding site in an open conformation and retain enzymatic activity. The ability to self-inactivate viral polymerase not required for RNA synthesis might represent an alternate

strategy to deal with the stoichiometric constraints of a polyprotein.

In contrast, the majority of NS protein complexes not directly involved in RNA synthesis may be required, e.g., as a structural component of the membrane vesicle. The viral NS protein primarily involved in this process is NS4B, since it is able to induce vesicular structures even in the absence of other HCV proteins (18). The different roles of nonstructural protein complexes might be regulated by the association with individual host cell factors, such as hVAP-A, a cellular protein that has been shown to interact with NS5A and NS5B (20, 75). Since this protein is involved in intracellular vesicle trafficking, it seems to be a good candidate for a cofactor of membrane structure rearrangements and has already been suggested to be involved in HCV replication complex formation (2, 29). In addition, other cellular factors might be required for RNA synthesis. A detailed biochemical analysis of the protease resistant NS protein fraction might reveal some of the cellular proteins that are directly involved in the formation of the replication complex and in RNA synthesis.

The functions of the protease sensitive portion of the NS proteins, encompassing >95%, remain obscure. Since our analysis presents a snapshot at a given time point and we have no precise data on the dynamics of replication complex formation and degeneration, parts of these proteins might be in the process of vesicle generation and disintegration. The remainder could simply be a by-product of structural protein synthesis, which might be required in excess amounts for virus production. Miyanari et al. (57) suggested potential roles of the NS proteins in virion formation or indirect modulation of viral replication by interaction with host cell proteins. Along the same line, the NS3/4A moiety might be required to block the IRF-3 induced pathway of the host cells' innate immune system, which has recently been shown to play a critical role in HCV replication (23).

In the present study we have shown that during the replication cycle of HCV a massive excess of nonstructural proteins is produced due to extensive translation. An interesting but yet unanswered question is how the transition of translation to replication is regulated. A number of proteins have been shown to bind to the HCV 5' NTR, which might be involved in this process (3, 4, 35, 40, 55); alternatively, the switch could rely on concentration-dependent inhibition of translation by an HCV protein. Interestingly, we found no significant differences in the ratio of HCV RNA and protein between an authentic HCV genome, a monocistronic replicon, and a bicistronic replicon (Table 1), indicating that the nature of the IRES-element directing translation of the NS proteins is not important for this stoichiometry. After translation, replication complex formation and RNA synthesis, the progeny RNA has to get back into the cytoplasm to enter a new round of translation/replication or packaging into particles. We currently do not know whether this process includes an active transport, as in the replication cycle of double-stranded RNA reoviruses (67), or if the progeny RNA accumulates in the replication complex and is released by disintegration of the vesicle.

An obvious limitation of our analysis is the fact that no viral particles are produced by the chosen replication systems (64). Since we do not know how many positive-strand RNA molecules would end up in virions and whether viral genomes undergo translation prior to packaging, it is very hard to predict the consequences of simultaneous RNA replication and particle morphogenesis on the ratio of RNA to proteins in infected cells. While the manuscript was in preparation, three independent studies demonstrated the production of infectious HCV particles in cell culture with the NS proteins of the JFH-1 HCV isolate (49, 77, 81). It will be interesting to evaluate our findings in this system covering the whole life cycle of HCV.

ACKNOWLEDGMENTS

We thank Darius Moradpour for the monoclonal NS5B antibodies, Joanne Tomassini for initial help with the establishment of CRC preparation and in vitro replicase assays, and Thomas Pietschmann for critically reading the manuscript.

This study was funded in part by the Deutsche Forschungsgemeinschaft (SFB 638 Teilprojekt A5) and within the National Genome Research Network by the German Ministry for Research and Education.

REFERENCES

1. Adachi, T., H. Ago, N. Habuka, K. Okuda, M. Komatsu, S. Ikeda, and K. Yatsunami. 2002. The essential role of C-terminal residues in regulating the activity of hepatitis C virus RNA-dependent RNA polymerase. Biochim. Biophys. Acta 1601:38–48.
2. Aizaki, H., K. J. Lee, V. M. Sung, H. Ishiko, and M. M. Lai. 2004. Characterization of the hepatitis C virus RNA replication complex associated with lipid rafts. Virology 324:450–461.
3. Ali, N., and A. Siddiqui. 1995. Interaction of polypyrimidine tract-binding protein with the 5' noncoding region of the hepatitis C virus RNA genome and its functional requirement in internal initiation of translation. J. Virol. 69:6367–6375.
4. Ali, N., and A. Siddiqui. 1997. The La antigen binds 5' noncoding region of the hepatitis C virus RNA in the context of the initiator AUG codon and stimulates internal ribosome entry site-mediated translation. Proc. Natl. Acad. Sci. USA 94:2249–2254.
5. Ali, N., K. D. Tardif, and A. Siddiqui. 2002. Cell-free replication of the hepatitis C virus subgenomic replicon. J. Virol. 76:12001–12007.
6. Bartenschlager, R., L. Ahlborn-Laake, J. Mous, and H. Jacobsen. 1993. Nonstructural protein 3 of the hepatitis C virus encodes a serine-type proteinase required for cleavage at the NS3/4 and NS4/5 junctions. J. Virol. 67: 3835–3844.
7. Bartenschlager, R., M. Frese, and T. Pietschmann. 2004. Novel insights into hepatitis C virus replication and persistence. Adv. Virus Res. 63:71–180.
8. Bartenschlager, R., and V. Lohmann. 2000. Replication of hepatitis C virus. J. Gen. Virol. 81:1631–1648.
9. Bartenschlager, R., V. Lohmann, T. Wilkinson, and J. O. Koch. 1995. Complex formation between the NS3 serine-type proteinase of the hepatitis C virus and NS4A and its importance for polyprotein maturation. J. Virol. 69:7519–7528.
10. Bedard, K. M., and B. L. Semler. 2004. Regulation of picornavirus gene expression. Microbes. Infect. 6:702–713.
11. Behrens, S. E., L. Tomei, and R. De Francesco. 1996. Identification and properties of the RNA-dependent RNA polymerase of hepatitis C virus. EMBO J. 15:12–22.
12. Blight, K. J., A. A. Kolykhalov, and C. M. Rice. 2000. Efficient initiation of HCV RNA replication in cell culture. Science 290:1972–1974.
13. Bukh, J., T. Pietschmann, V. Lohmann, N. Krieger, K. Faulk, R. E. Engle, S. Govindarajan, M. Shapiro, M. St Claire, and R. Bartenschlager. 2002. Mutations that permit efficient replication of hepatitis C virus RNA in Huh-7 cells prevent productive replication in chimpanzees. Proc. Natl. Acad. Sci. USA 99:14416–14421.
14. Carroll, S. S., V. Sardana, Z. Yang, A. R. Jacobs, C. Mizenko, D. Hall, L. Hill, J. Zugay-Murphy, and L. C. Kuo. 2000. Only a small fraction of purified hepatitis C RNA-dependent RNA polymerase is catalytically competent: implications for viral replication and in vitro assays. Biochemistry 39: 8243–8249.
15. Chomczynski, P., and N. Sacchi. 1987. Single-step method of RNA isolation by acid guanidinium thiocyanate-phenol-chloroform extraction. Anal. Biochem. 162:156–159.
16. Dimitrova, M., I. Imbert, M. P. Kieny, and C. Schuster. 2003. Protein-protein interactions between hepatitis C virus nonstructural proteins. J. Virol. 77:5401–5414.
17. Dubuisson, J., F. Penin, and D. Moradpour. 2002. Interaction of hepatitis C virus proteins with host cell membranes and lipids. Trends Cell Biol. 12: 517–523.
18. Egger, D., B. Wolk, R. Gosert, L. Bianchi, H. E. Blum, D. Moradpour, and K. Bienz. 2002. Expression of hepatitis C virus proteins induces distinct

EXHIBIT A

membrane alterations including a candidate viral replication complex. J. Virol. 76:5974–5984.
19. El Hage, N., and G. Luo. 2003. Replication of hepatitis C virus RNA occurs in a membrane-bound replication complex containing nonstructural viral proteins and RNA. J. Gen. Virol. 84:2761–2769.
20. Evans, M. J., C. M. Rice, and S. P. Goff. 2004. Phosphorylation of hepatitis C virus nonstructural protein 5A modulates its protein interactions and viral RNA replication. Proc. Natl. Acad. Sci. USA 101:13038–13043.
21. Failla, C., L. Tomei, and R. De Francesco. 1995. An amino-terminal domain of the hepatitis C virus NS3 protease is essential for interaction with NS4A. J. Virol. 69:1769–1777.
22. Ferlenghi, I., M. Clarke, T. Ruttan, S. L. Allison, J. Schalich, F. X. Heinz, S. C. Harrison, F. A. Rey, and S. D. Fuller. 2001. Molecular organization of a recombinant subviral particle from tick-borne encephalitis virus. Mol. Cell 7:593–602.
23. Foy, E., K. Li, C. Wang, R. Sumpter, Jr., M. Ikeda, S. M. Lemon, and M. Gale, Jr. 2003 Regulation of interferon regulatory factor-3 by the hepatitis C virus serine protease. Science 300:1145–1148.
24. Frese, M., V. Schwarzle, K. Barth, N. Krieger, V. Lohmann, S. Mihm, O. Haller, and R. Bartenschlager. 2002. Interferon-gamma inhibits replication of subgenomic and genomic hepatitis C virus RNAs. Hepatology 35: 694–703.
25. Friebe, P., and R. Bartenschlager. 2002. Genetic analysis of sequences in the 3′ nontranslated region of hepatitis C virus that are important for RNA replication. J. Virol. 76:5326–5338.
26. Friebe, P., J. Boudet, J. P. Simorre, and R. Bartenschlager. 2005. Kissing-loop interaction in the 3′ end of the hepatitis C virus genome essential for RNA replication. J. Virol. 79:380–392.
27. Friebe, P., V. Lohmann, N. Krieger, and R. Bartenschlager. 2001. Sequences in the 5′ nontranslated region of hepatitis C virus required for RNA replication. J. Virol. 75:12047–12057.
28. Fuller, S. D. 1987. The T = 4 envelope of Sindbis virus is organized by interactions with a complementary T = 3 capsid. Cell 48:923–934.
29. Gao, L., H. Aizaki, J. W. He, and M. M. Lai. 2004. Interactions between viral nonstructural proteins and host protein hVAP-33 mediate the formation of hepatitis C virus RNA replication complex on lipid raft. J. Virol. 78: 3480–3488.
30. Gosert, R., D. Egger, V. Lohmann, R. Bartenschlager, H. E. Blum, K. Bienz, and D. Moradpour. 2003. Identification of the hepatitis C virus RNA replication complex in huh-7 cells harboring subgenomic replicons. J. Virol. 77:5487–5492.
31. Grakoui, A., D. W. McCourt, C. Wychowski, S. M. Feinstone, and C. M. Rice. 1993. A second hepatitis C virus-encoded proteinase. Proc. Natl. Acad. Sci. USA 90:10583–10587.
32. Grakoui, A., D. W. McCourt, C. Wychowski, S. M. Feinstone, and C. M. Rice. 1993. Characterization of the hepatitis C virus-encoded serine proteinase: determination of proteinase-dependent polyprotein cleavage sites. J. Virol. 67:2832–2843.
33. Griffin, S. D., L. P. Beales, D. S. Clarke, O. Worsfold, S. D. Evans, J. Jaeger, M. P. Harris, and D. J. Rowlands. 2003. The p7 protein of hepatitis C virus forms an ion channel that is blocked by the antiviral drug, amantadine. FEBS Lett. 535:34–38.
34. Guo, J. T., V. V. Bichko, and C. Seeger. 2001. Effect of alpha interferon on the hepatitis C virus replicon. J. Virol. 75:8516–8523.
35. Hahm, B., Y. K. Kim, J. H. Kim, T. Y. Kim, and S. K. Jang. 1998. Heterogeneous nuclear ribonucleoprotein L interacts with the 3′ border of the internal ribosomal entry site of hepatitis C virus. J. Virol. 72:8782–8788.
36. Hardy, R. W., J. Marcotrigiano, K. J. Blight, J. E. Majors, and C. M. Rice. 2003. Hepatitis C virus RNA synthesis in a cell-free system isolated from replicon-containing hepatoma cells. J. Virol. 77:2029–2037.
37. Hijikata, M., N. Kato, Y. Ootsuyama, M. Nakagawa, and K. Shimotohno. 1991. Gene mapping of the putative structural region of the hepatitis C virus genome by in vitro processing analysis. Proc. Natl. Acad. Sci. USA 88: 5547–5551.
38. Hijikata, M., H. Mizushima, T. Akagi, S. Mori, N. Kakiuchi, N. Kato, T. Tanaka, K. Kimura, and K. Shimotohno. 1993. Two distinct proteinase activities required for the processing of a putative nonstructural precursor protein of hepatitis C virus. J. Virol. 67:4665–4675.
39. Kim, D. W., Y. Gwack, J. H. Han, and J. Choe. 1995. C-terminal domain of the hepatitis C virus NS3 protein contains an RNA helicase activity. Biochem. Biophys. Res. Commun. 215:160–166.
40. Kim, J. H., K. Y. Paek, S. H. Ha, S. Cho, K. Choi, C. S. Kim, S. H. Ryu, and S. K. Jang. 2004. A cellular RNA-binding protein enhances internal ribosomal entry site-dependent translation through an interaction downstream of the hepatitis C virus polyprotein initiation codon. Mol. Cell. Biol. 24: 7878–7890.
41. Koch, J. O., and R. Bartenschlager. 1999. Modulation of hepatitis C virus NS5A hyperphosphorylation by nonstructural proteins NS3, NS4A, and NS4B. J. Virol. 73:7138–7146.
42. Kolykhalov, A. A., K. Mihalik, S. M. Feinstone, and C. M. Rice. 2000. Hepatitis C virus-encoded enzymatic activities and conserved RNA elements in the 3′ nontranslated region are essential for virus replication in vivo. J. Virol. 74:2046–2051.
43. Krieger, N., V. Lohmann, and R. Bartenschlager. 2001. Enhancement of hepatitis C virus RNA replication by cell culture-adaptive mutations. J. Virol. 75:4614–4624.
44. Kuhn, R. J., W. Zhang, M. G. Rossmann, S. V. Pletnev, J. Corver, E. Lenches, C. T. Jones, S. Mukhopadhyay, P. R. Chipman, E. G. Strauss, T. S. Baker, and J. H. Strauss. 2002. Structure of dengue virus: implications for flavivirus organization, maturation, and fusion. Cell 108:717–725.
45. Lai, V. C., S. Dempsey, J. Y. Lau, Z. Hong, and W. Zhong. 2003. In vitro RNA replication directed by replicase complexes isolated from the subgenomic replicon cells of hepatitis C virus. J. Virol. 77:2295–2300.
46. Leveque, V. J., R. B. Johnson, S. Parsons, J. Ren, C. Xie, F. Zhang, and Q. M. Wang. 2003. Identification of a C-terminal regulatory motif in hepatitis C virus RNA-dependent RNA polymerase: structural and biochemical analysis. J. Virol. 77:9020–9028.
47. Li, G. P., and C. M. Rice. 1989. Mutagenesis of the in-frame opal termination codon preceding nsP4 of Sindbis virus: studies of translational readthrough and its effect on virus replication. J. Virol. 63:1326–1337.
48. Lin, C., J. A. Thomson, and C. M. Rice. 1995. A central region in the hepatitis C virus NS4A protein allows formation of an active NS3-NS4A serine proteinase complex in vivo and in vitro. J. Virol. 69:4373–4380.
49. Lindenbach, B. D., M. J. Evans, A. J. Syder, B. Wolk, T. L. Tellinghuisen, C. C. Liu, T. Maruyama, R. O. Hynes, D. R. Burton, J. A. McKeating, and C. M. Rice. 2005. Complete replication of hepatitis C virus in cell culture. Science 309:623–626.
50. Lohmann, V., S. Hoffmann, U. Herian, F. Penin, and R. Bartenschlager. 2003. Viral and cellular determinants of hepatitis C virus RNA replication in cell culture. J. Virol. 77:3007–3019.
51. Lohmann, V., F. Körner, A. Dobierzewska, and R. Bartenschlager. 2001. Mutations in hepatitis C virus RNAs conferring cell culture adaptation. J. Virol. 75:1437–1449.
52. Lohmann, V., F. Korner, U. Herian, and R. Bartenschlager. 1997. Biochemical properties of hepatitis C virus NS5B RNA-dependent RNA polymerase and identification of amino acid sequence motifs essential for enzymatic activity. J. Virol. 71:8416–8428.
53. Lohmann, V., F. Körner, J. O. Koch, U. Herian, L. Theilmann, and R. Bartenschlager. 1999. Replication of subgenomic hepatitis C virus RNAs in a hepatoma cell line. Science 285:110–113.
54. Lohmann, V., A. Roos, F. Korner, J. O. Koch, and R. Bartenschlager. 1998. Biochemical and kinetic analyses of NS5B RNA-dependent RNA polymerase of the hepatitis C virus. Virology 249:108–118.
55. Lu, H., W. Li, W. S. Noble, D. Payan, and D. C. Anderson. 2004. Riboproteomics of the hepatitis C virus internal ribosomal entry site. J. Proteome Res. 3:949–957.
56. Ma, H., V. Leveque, A. De Witte, W. Li, T. Hendricks, S. M. Clausen, N. Cammack, and K. Klumpp. 2005. Inhibition of native hepatitis C virus replicase by nucleotide and non-nucleoside inhibitors. Virology 332:8–15.
57. Miyanari, Y., M. Hijikata, M. Yamaji, M. Hosaka, H. Takahashi, and K. Shimotohno. 2003. Hepatitis C virus nonstructural proteins in the probable membranous compartment function in viral genome replication. J. Biol. Chem. 278:50301–50308.
58. Moradpour, D., E. Bieck, T. Hugle, W. Wels, J. Z. Wu, Z. Hong, H. E. Blum, and R. Bartenschlager. 2002. Functional properties of a monoclonal antibody inhibiting the hepatitis C virus RNA-dependent RNA polymerase. J. Biol. Chem. 277:593–601.
59. Moradpour, D., R. Gosert, D. Egger, F. Penin, H. E. Blum, and K. Bienz. 2003. Membrane association of hepatitis C virus nonstructural proteins and identification of the membrane alteration that harbors the viral replication complex. Antivir. Res. 60:103–109.
60. Nakabayashi, H., K. Taketa, K. Miyano, T. Yamane, and J. Sato. 1982. Growth of human hepatoma cells lines with differentiated functions in chemically defined medium. Cancer Res. 42:3858–3863.
61. Paredes, A. M., D. T. Brown, R. Rothnagel, W. Chiu, R. J. Schoepp, R. E. Johnston, and B. V. Prasad. 1993. Three-dimensional structure of a membrane-containing virus. Proc. Natl. Acad. Sci. USA 90:9095–9099.
62. Pause, A., G. Kukolj, M. Bailey, M. Brault, F. Do, T. Halmos, L. Lagace, R. Maurice, M. Marquis, G. McKercher, C. Pellerin, L. Pilote, D. Thibeault, and D. Lamarre. 2003. An NS3 serine protease inhibitor abrogates replication of subgenomic hepatitis C virus RNA. J. Biol. Chem.
63. Pavlovic, D., D. C. Neville, O. Argaud, B. Blumberg, R. A. Dwek, W. B. Fischer, and N. Zitzmann. 2003. The hepatitis C virus p7 protein forms an ion channel that is inhibited by long-alkyl-chain iminosugar derivatives. Proc. Natl. Acad. Sci. USA 100:6104–6108.
64. Pietschmann, T., V. Lohmann, A. Kaul, N. Krieger, G. Rinck, G. Rutter, D. Strand, and R. Bartenschlager. 2002. Persistent and transient replication of full-length hepatitis C virus genomes in cell culture. J. Virol. 76: 4008–4021.
65. Pietschmann, T., V. Lohmann, G. Rutter, K. Kurpanek, and R. Bartenschlager. 2001. Characterization of cell lines carrying self-replicating hepatitis C virus RNAs. J. Virol. 75:1252–1264.
66. Reed, K. E., and C. M. Rice. 2000. Overview of hepatitis C virus genome structure, polyprotein processing, and protein properties. Curr. Top. Microbiol. Immunol. 242:55–84.

EXHIBIT A

67. **Reinisch, K. M., M. L. Nibert, and S. C. Harrison.** 2000. Structure of the reovirus core at 3.6 Å resolution. Nature 404:960–967.
68. **Sambrook, J., Fritsch, E. F., and T. Maniatis.** 1989. Molecular cloning: a laboratory manual, 2nd ed. Cold Spring Harbor Laboratory Press, Cold Spring Harbor, N.Y.
69. **Schwartz, M., J. Chen, M. Janda, M. Sullivan, J. den Boon, and P. Ahlquist.** 2002. A positive-strand RNA virus replication complex parallels form and function of retrovirus capsids. Mol. Cell 9:505–514.
70. **Shi, S. T., K. J. Lee, H. Aizaki, S. B. Hwang, and M. M. Lai.** 2003. Hepatitis C virus RNA replication occurs on a detergent-resistant membrane that cofractionates with caveolin-2. J. Virol. 77:4160–4168.
71. **Suzich, J. A., J. K. Tamura, H. F. Palmer, P. Warrener, A. Grakoui, C. M. Rice, S. M. Feinstone, and M. S. Collett.** 1993. Hepatitis C virus NS3 protein polynucleotide-stimulated nucleoside triphosphatase and comparison with the related pestivirus and flavivirus enzymes. J. Virol. 67:6152–6158.
72. **Tanji, Y., M. Hijikata, S. Satoh, T. Kaneko, and K. Shimotohno.** 1995. Hepatitis C virus-encoded nonstructural protein NS4A has versatile functions in viral protein processing. J. Virol. 69:1575–1581.
73. **Tomassini, J. E., E. Boots, L. Gan, P. Graham, V. Munshi, B. Wolanski, J. F. Fay, K. Getty, and R. LaFemina.** 2003. An in vitro *Flaviviridae* replicase system capable of authentic RNA replication. Virology 313:274–285.
74. **Tsukiyama, K. K., N. Iizuka, M. Kohara, and A. Nomoto.** 1992. Internal ribosome entry site within hepatitis C virus RNA. J. Virol. 66:1476–1483.
75. **Tu, H., L. Gao, S. T. Shi, D. R. Taylor, T. Yang, A. K. Mircheff, Y. M. Wen, A. E. Gorbalenya, S. B. Hwang, and M. C. Lai.** 1999. Hepatitis C virus RNA polymerase and NS5A complex with a SNARE-like protein. Virology 263:30–41.
76. **van den Hoff, M. J., A. F. Moorman, and W. H. Lamers.** 1992. Electroporation in "intracellular" buffer increases cell survival. Nucleic Acids Res. 20:2902.
77. **Wakita, T., T. Pietschmann, T. Kato, T. Date, M. Miyamoto, Z. Zhao, K. Murthy, A. Habermann, H. G. Krausslich, M. Mizokami, R. Bartenschlager, and T. J. Liang.** 2005. Production of infectious hepatitis C virus in tissue culture from a cloned viral genome. Nat. Med. 11:791–796.
78. **Walewski, J. L., T. R. Keller, D. D. Stump, and A. D. Branch.** 2001. Evidence for a new hepatitis C virus antigen encoded in an overlapping reading frame. RNA. 7:710–721.
79. **Xu, Z., J. Choi, T. S. Yen, W. Lu, A. Strohecker, S. Govindarajan, D. Chien, M. J. Selby, and J. Ou.** 2001. Synthesis of a novel hepatitis C virus protein by ribosomal frameshift. EMBO J. 20:3840–3848.
80. **Yanagi, M., C. M. St, S. U. Emerson, R. H. Purcell, and J. Bukh.** 1999. In vivo analysis of the 3′ untranslated region of the hepatitis C virus after in vitro mutagenesis of an infectious cDNA clone. Proc. Natl. Acad. Sci. USA 96:2291–2295.
81. **Zhong, J., P. Gastaminza, G. Cheng, S. Kapadia, T. Kato, D. R. Burton, S. F. Wieland, S. L. Uprichard, T. Wakita, and F. V. Chisari.** 2005. Robust hepatitis C virus infection in vitro. Proc. Natl. Acad. Sci. USA 102: 9294–9299.

EXHIBIT A

CTMI (2004) 285:139–173

Viral RNA Replication in Association with Cellular Membranes

A. Salonen · T. Ahola · L. Kääriäinen (✉)

Program in Cellular Biotechnology, Institute of Biotechnology, Viikki Biocenter, University of Helsinki, P.O. Box 56, 00014 Helsinki, Finland
leevi.kaariainen@helsinki.fi

Abstract All plus-strand RNA viruses replicate in association with cytoplasmic membranes of infected cells. The RNA replication complex of many virus families is associated with the endoplasmic reticulum membranes, for example, picorna-, flavi-, arteri-, and bromoviruses. However, endosomes and lysosomes (togaviruses), peroxisomes and chloroplasts (tombusviruses), and mitochondria (nodaviruses) are also used as sites for RNA replication. Studies of individual nonstructural proteins, the virus-specific components of the RNA replicase, have revealed that the replication complexes are associated with the membranes and targeted to the respective organelle by the ns proteins rather than RNA. Many ns proteins have hydrophobic sequences and may transverse the membrane like polytopic integral membrane pro-

teins, whereas others interact with membranes monotopically. Hepatitis C virus ns proteins offer examples of polytopic transmembrane proteins (NS2, NS4B), a "tip-anchored" protein attached to the membrane by an amphipathic α-helix (NS5A) and a "tail-anchored" posttranslationally inserted protein (NS5B). Semliki Forest virus nsP1 is attached to the plasma membrane by a specific binding peptide in the middle of the protein, which forms an amphipathic α-helix. Interaction of nsP1 with membrane lipids is essential for its capping enzyme activities. The other soluble replicase proteins are directed to the endo-lysosomal membranes only as part of the initial polyprotein. Poliovirus ns proteins utilize endoplasmic reticulum membranes from which vesicles are released in COPII coats. However, these vesicles are not directed to the normal secretory pathway, but accumulate in the cytoplasm. In many cases the replicase proteins induce membrane invaginations or vesicles, which function as protective environments for RNA replication.

1 Introduction

The genome replication of all plus-strand RNA viruses infecting eukaryotic cells is associated with cellular membranes. The membranes can be derived from the endoplasmic reticulum (ER), or other organelles of the secretory pathway, mitochondria, chloroplasts, or from the endo-lysosomal compartment. The membrane association provides a structural framework for replication, it fixes the RNA replication process to a spatially confined place, increasing the local concentration of necessary components, and it offers protection for the alien RNA molecules against host defense mechanisms. The theme of immobilized polymerase and moving template may in fact be common also to most cellular DNA replication and transcription systems (Cook 1999) and might therefore reflect a primordial pathway in nucleic acid replication. The modes of membrane binding and targeting to specific intracellular organelles of the replication complexes of different viruses are so far poorly understood. However, this field at the interface of virology, cell biology, and biochemistry is attracting increased interest, as it represents an ancient feature shared by many virus groups. Some aspects have been nicely treated in earlier reviews (de Graaff and Jaspars 1994; Buck 1996). We will present in some detail relevant studies on alphaviruses, especially Semliki Forest virus (SFV), which has been the object of our own interest. We will then review recent work on other viruses based on their classification in three superfamilies (Koonin and Dolja 1993), except that we have treated nidoviruses as a separate group.

2 Alphaviruses as Models

2.1 RNA Replication in Cytoplasmic Vacuoles Derived from Endosomes

Association of SFV-specific RNA synthesis with membranes was demonstrated in several studies starting in the late 1960s (for reviews see Kääriäinen and Söderlund 1978; Kääriäinen and Ahola 2002). Simple fractionation of membranes derived from the postnuclear supernatant fraction of alphavirus-infected cells showed that essentially all RNA polymerase activity was associated with a "mitochondrial" pellet fraction sedimenting at 15,000 x *g*. On the other hand, early electron microscopic (EM) studies had revealed cytoplasmic structures typical for alphavirus-infected cells. These were designated as "cytopathic vacuoles type I" (CPV-I), hereafter referred as CPVs. Their size varied from 600 nm to 2,000 nm, and their surface consisted of small vesicular invaginations or spherules, of homogenous size, with a diameter of about 50 nm. EM autoradiography of SFV-infected cells pulse-labeled with tritiated uridine already suggested that CPVs, and possibly the spherules, were involved in virus-specific, actinomycin D-resistant RNA synthesis (Grimley et al. 1968).

However, the origin, nature, and function of CPVs remained unclear for about two decades until Froshauer et al. (1988) demonstrated that they were modified endosomes and lysosomes. Immunofluorescence and immuno-EM techniques showed that Sindbis virus-specific nonstructural proteins nsP3 and nsP4 were associated with CPVs. The authors proposed that CPVs were derived from endosomes, which were participating in the internalization of virus particles. This would have nicely explained the endosomal origin of CPVs as a direct consequence of fusion of the virus envelope with the endo/lysosomal membrane, which would bring the virus nucleocapsid and genome directly to the cytoplasmic surface of the organelle. Thus genome uncoating and subsequent synthesis of replicase components would result in the modification of endosomes to virus-specific CPVs. However, this hypothesis cannot explain why the amount of CPVs was not dependent on the amount of infecting virions. Moreover, typical CPVs were seen also in cells transfected with the genomic RNA of SFV, demonstrating that the endosomal targeting of the replication complexes must be a posttranslational event (Peränen and Kääriäinen 1991).

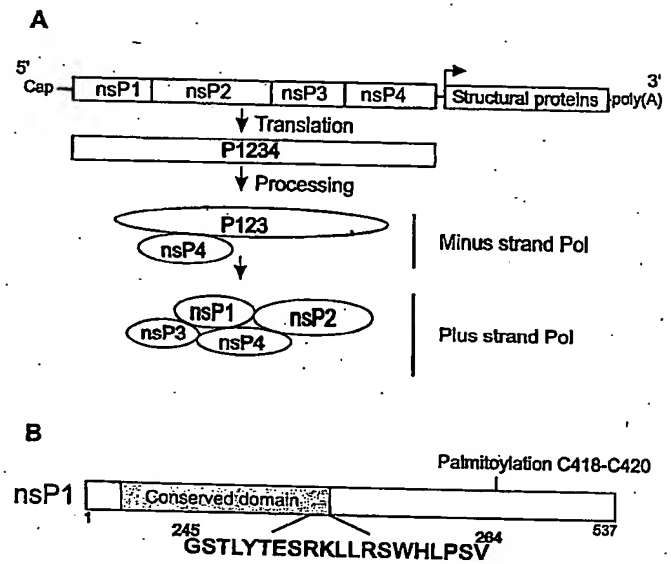

Fig. 1. A Genome organization of SFV. The translation and processing products relevant for SFV replication are shown. Physical interactions have been identified between nsP1 and nsP4, as well as nsP1 and nsP3 (Salonen et al. 2003). B Scheme of SFV nsP1 showing the two regions responsible for membrane binding. The amino acid sequence of the lipid binding peptide is given in *single-letter code*, and the position of palmitoylated cysteines is marked

Alphavirus nonstructural (=replicase) proteins are synthesized as a polyprotein precursor P1234, which is processed in a highly regulated manner into the individual components nsP1–nsP4 (Fig. 1A). Genetic and biochemical experiments have revealed many of the functions of the nsPs (reviewed in Strauss and Strauss 1994; Kääriäinen and Ahola 2002). Thus nsP4 is the catalytic RNA-dependent RNA polymerase subunit, nsP2 is involved in the regulation of the synthesis of the subgenomic 26S mRNA coding for structural proteins of the virion, whereas nsP1 is needed in the synthesis of the complementary (minus strand) RNA early in infection. nsP3 is essential for infection, but no specific function has been assigned for it as yet. Expression of the individual nsPs in *E. coli* and in insect cells revealed further functions of nsPs. nsP1 is an RNA capping enzyme with unique methyltransferase and guanylyltransferase activities (Mi and Stollar 1991; Ahola and Kääriäinen 1995), whereas nsP2 turned out to be a NTPase and RNA helicase (Gomez de Cedrón at

al. 1999), RNA triphosphatase (Vasiljeva et al. 2000), as well as the protease responsible for the processing of the nonstructural polyprotein precursor (Vasiljeva et al. 2001).

Creation of potent monospecific antibodies allowed the identification and localization of the ns proteins in SFV-infected cells (Peränen et al. 1988; 1995). After crude cell fractionation most of nsP1, nsP3, and nsP4 were associated with the P15 membrane fraction, whereas about 50% of nsP2 was found in the nucleus (Peränen et al. 1990). Pairwise double staining with different anti-nsP antibodies revealed costaining of CPV-like structures in immunofluorescence microscopy, suggesting that all four nsPs were associated with CPVs. This was confirmed by double-labeling in cryo-immuno EM (Kujala et al. 2001). Moreover, bromouridine given in short pulses also localized to CPVs and spherules together with the nsPs, indicating that these structures were the sites of RNA replication. The CPVs costained with late endosomal (lamp-1, lamp-2, and rab7) and lysosomal markers (LBPA and LysoTracker). Interestingly, all nsPs had localization sites also outside of the CPVs. nsP2 was found in the nucleus, nsP1 at the plasma membrane, nsP3 in cytoplasmic spotlike structures, and nsP4 diffusely in the cytoplasm (Kujala et al. 2001). Therefore, only a fraction of nsPs are present in the actual replication complexes.

2.2
nsP1 as the Membrane Anchor of the Replication Complex

As none of the alphavirus nsPs has sequences typical for transmembrane proteins, we have studied their membrane binding by expressing them individually in BHK, HeLa, and insect cells. These studies revealed that only nsP1 had a specific association with membranes (Peränen et al. 1995), whereas nsP2 on its own was transported almost quantitatively to the nucleus and nsP3 was in cytoplasmic aggregates (Salonen et al. 2003), which in light microscopy gives an impression of vesicles of variable size (Vihinen et al. 2001). Finally, nsP4 was distributed diffusely in the cytoplasm.

Thus nsP1 was a promising candidate as the membrane anchor of the SFV replication complex. nsP1 turned out to be very tightly membrane bound, as the association was not sensitive to high salt, EDTA, or alkaline sodium carbonate treatments, which release peripheral membrane proteins (Peränen et al. 1995). The tight binding was due to palmitoylation of cysteine residues 418–420 (Fig. 1B). When these residues were mutated to alanines, nsP1 was still membrane associated, but less tightly,

as it could now be released by high-salt treatment. Thus elimination of palmitoylation altered nsP1 from an "integral" to a "peripheral" membrane protein (Laakkonen et al. 1996).

To study the significance of the palmitoylation of nsP1, the C418–420A mutation was introduced to the infectious cDNA of SFV, followed by transcription of genomic RNA, which was used for transfection of BHK cells. Infectious virus was released to the medium, indicating that palmitoylation of nsP1 was not essential for virus replication. However, there was some retardation in the kinetics of virus growth. Analysis of the membrane association of wild-type and palmitoylation-negative mutant (1pa–) replicase proteins of SFV showed that 1pa– nsP1 was bound less tightly to the membranes than the wild-type protein. Typical CPVs with spherules, indistinguishable from those in wild-type SFV-infected cells, were seen in EM. The same results were obtained when the single palmitoylated cysteine residue (C420) of Sindbis virus nsP1 was mutated to alanine. However, the SFV 1pa– mutant was apathogenic for mouse. After intraperitoneal infection blood viremia was detected, but no infectious virus was found in the brain (Ahola et al. 2000).

2.3 Membrane Binding Mechanism of nsP1

Because palmitoylation was not the decisive mechanism for membrane binding of nsP1, we studied the peripheral binding by producing the wild-type protein in *E. coli*, which cannot palmitoylate proteins. Enzymatically active nsP1 was associated with bacterial membranes as judged by flotation in sucrose gradients. In vitro translated nsP1 also associated with liposomes containing 20%–50% phosphatidylserine (PS) or other anionic phospholipids, but not with liposomes containing only phosphatidylcholine (PC). Solubilization of membranes containing nsP1 by detergents, such as Triton X-100 or octylglucoside, resulted in loss of the protein's methyltransferase and guanylyltransferase activities, which could be reactivated by reconstitution of nsP1 into vesicle membranes or into mixed detergent-lipid micelles containing anionic phospholipids (Fig. 2A). Detergents also inhibited the binding of the methyl donor *S*-adenosylmethionine to nsP1, and the binding was resumed under the same conditions as enzymatic activity. Thus binding to anionic phospholipids causes a conformational change, which activates the protein (Ahola et al. 1999).

The membrane-binding site in nsP1 was identified by site-directed mutagenesis and deletion mapping in both bacterial and in vitro expres-

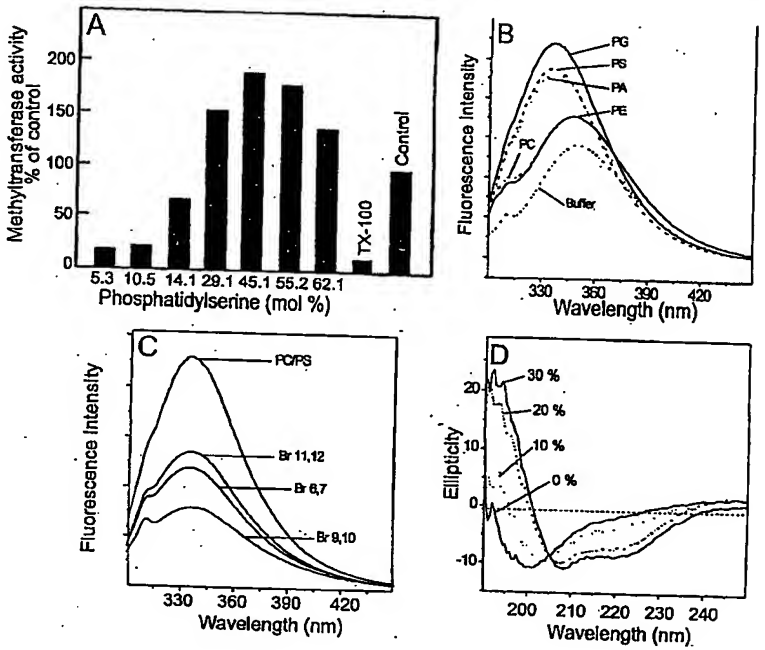

Fig. 2. Biochemical characterization of the lipid binding of SFV nsP1. A Inactivation and activation of nsP1 methyltransferase activity. Triton X-100 inactivates nsP1, compared with the control reaction in the absence of detergent (on the *right*). When TX-100 micelles containing increasing amounts of phosphatidylserine are added, nsP1 regains activity, even exceeding control levels at optimal concentration of the lipid. (Reproduced from Ahola et al. 1999, with permission). B Negatively charged phospholipids increase the intensity of tryptophan fluorescence of the lipid binding peptide. Tryptophan emission spectrum was recorded in the buffer or in the presence of small unilamellar vesicles consisting of phosphatidylcholine (*PC*) or PC with 30 mol % of phosphatidylglycerol (*PG*), phosphatidylserine (*PS*), phosphatidic acid (*PA*), or phosphatidylethanolamine (*PE*). C Depth of tryptophan W259 penetration to membrane measured by quenching of tryptophan fluorescence by brominated PCs. The position of bromine in the acyl chains is indicated. D The peptide adopts an α-helical conformation in the presence of PC-containing vesicles, as measured by circular dichroism spectroscopy. The numbers indicate the mol % of PS in the vesicles. (B–D reproduced from Lampio et al. 2000 with permission by the American Society of Biochemistry and Molecular Biology)

sion systems. Flotation of nsP1 with membranes or liposomes in discontinuous sucrose gradients was used as a criterion for membrane association. By this means a putative binding region of about 20 amino acid residues, starting from Gly245, was identified (Fig. 1B). The corresponding synthetic peptide consisting of Gly245–Val264 (GSTLYTESRKLLRSWHLPSV) was able to compete with the binding of in vitro synthesized nsP1 to liposomes containing PS, strongly suggesting that this region of nsP1 is responsible for its membrane association (Ahola et al. 1999).

The interaction of the synthetic membrane binding peptide with liposomes was assayed by utilizing the fluorescence of tryptophan residue W259 (Lampio et al. 2000). Tryptophan emission spectrum changes when it is embedded into an apolar environment. There was a marked increase in the fluorescence intensity and a blue shift of the emission in the presence of monolamellar liposomes, which consisted of PC and negatively charged phospholipids (PS, phosphatidylglycerol, or phosphatidic acid) (Fig. 2B). By using phospholipids with bromide substitution in different carbon atoms of the acyl chain, for quenching of the tryptophan fluorescence, it was possible to estimate that W259 penetrated to the level of carbon atoms 9 and 10 of the PC acyl chains in the outer leaflet of the liposomes (Figs. 2C and 3A). The circular dichroism spectrum of the binding peptide was dependent on the content of the apolar constituents (liposomes or trifluoroethanol). In a buffer solution the binding peptide was mostly in a random coil, whereas in the presence of liposomes with 20%–30% PS or in 30%–50% trifluoroethanol the peptide attained an α-helical conformation (Fig. 2D). The solution structure of the binding peptide, determined by NMR spectroscopy in 30% trifluoroethanol, revealed an amphipathic α-helix (Fig. 3A). One face consisted of hydrophobic residues, leucines 248, 255, 256, and 261, valine 264, and residues S252 and W259 interacting with the apolar fatty acid chains on the cytoplasmic leaflet of the membrane (Fig. 3). The other face contained positively charged residues R253, K254, and R257 lying parallel to the polar head groups of the bilayer surface. The hydrophobic surface of the peptide is rather stable, whereas the polar residues show considerable mobility in trifluoroethanol.

Point mutations R253E and W259A in the nsP1 protein, when expressed in *E. coli*, resulted in the loss of enzymatic activity and the lack of ability to float with membranes in sucrose gradients (Ahola et al. 1999). Thus these two residues were considered to be essential in the interaction of nsP1 with membranes. This view was supported by competition experiments done with synthetic mutant peptides. Both were unable to inhibit the binding of in vitro synthesized nsP1 to liposomes, in

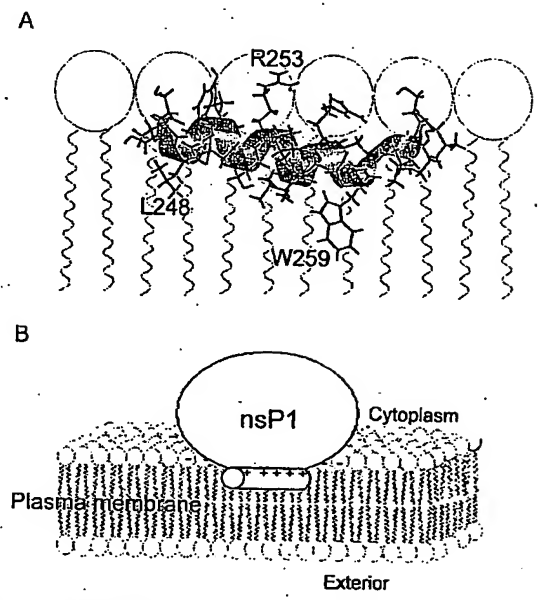

Fig. 3A, B. Monotopic binding of nsP1 to membrane via amphipathic α-helical peptide. A The NMR structure of the peptide is shown in interaction with the cytoplasmic leaflet of the lipid bilayer. B Highly schematic overview of interaction of nsP1 with a lipid bilayer

contrast to the synthetic wild-type binding peptide (Lampio et al. 2000). When the corresponding mutations were introduced to the SFV genome, neither W259A nor R253E was able to produce infectious virus after transfection (Salonen et al., unpublished data). Altogether, these results indicate that the interaction of nsP1 binding peptide with membranes is an essential and structurally finely tuned process, dependent on interaction with anionic phospholipids.

2.4 Polyprotein Conducts the Assembly and Targeting of the Replication Complex

The nsPs are derived from a common precursor P1234, the initial cleavage products of which (P123 plus nsP4) are necessary for the first step in the RNA replication, the synthesis of complementary RNA (Lemm et al. 1994, 1998) (Fig. 1A). To understand the role of this and other cleav-

age intermediates, we have produced them both in wild-type form and as noncleavable polyprotein variants, in which the autoprotease of nsP2 was inactivated by a mutation of the active site cysteine to alanine (superscript "CA"). The constructs were expressed in insect and mammalian cells, and the localization of individual proteins was followed by confocal microscopy and the complex formation by immunoprecipitation (Salonen et al. 2003).

The cleavable polyproteins (P12, P23, P123, P1234) containing an active nsP2 protease were processed to their constituents, most of which were distributed in the cell as though they were expressed alone. For instance, P12 yielded nsP1 and nsP2, which were targeted to the plasma membrane and nucleus, respectively. However, flotation analysis and immunoprecipitation recapture experiments showed that expression of P123 and P1234 resulted in membrane-bound complexes, containing all the individual proteins. This was different from the coexpression of all four nsPs individually, allowing us to conclude that the membrane association of the complex is guided by the polyprotein intermediate.

The uncleavable polyproteins were palmitoylated and had enzymatic activities typical for nsP1 and nsP2, and those containing nsP3 were phosphorylated, suggesting that the individual domains had folded properly in the context of the polyprotein. When $P12^{CA}$ was expressed in HeLa cells, it was localized exclusively at the cytoplasmic side of the plasma membrane and in long filopodia-like extensions (Fig. 4A), indistinguishable from those previously described for cells expressing nsP1 alone (Laakkonen et al. 1998). This indicated that the affinity to plasma membrane of nsP1 in the polyprotein overruled the attraction of nsP2 for nuclear transport. However, an interesting change in the localization was seen when $P12^{CA}3$ was expressed (Fig. 4B). No filopodia-like extensions were seen, and instead intracellular vesicular staining was observed, which in immuno-EM resembled CPVs (Fig. 4C and D). Double immunofluorescence with antisera against nsPs and lamp-2 suggested that at least a fraction of the vesicular structures were late endosomes or lysosomes (Salonen et al. 2003). Thus it seems that endosomal targeting is a joint action of nsP1 and nsP3 domains in the nonstructural polyprotein. The polyprotein is attached to the membrane first by the nsP1 binding peptide, which adopts α-helical structure. Concomitantly the nsP1 domain undergoes a conformational change, which activates the methyltransferase and guanylyltransferase. Palmitoylation of cysteine residues 418–420 thereafter anchors the protein irreversibly to the membrane. We propose that the targeting of nsP1 and polyproteins with this

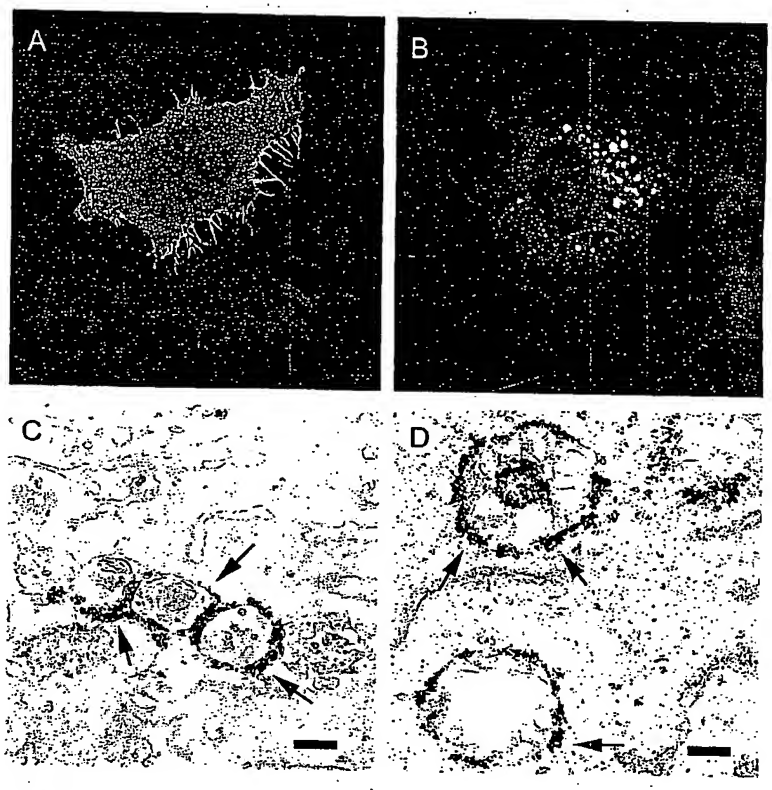

Fig. 4. Immunolocalization of SFV nonstructural polyproteins expressed by the aid of recombinant adenovirus vectors (A–C) and nsP3 during SFV infection (D) in HeLa cells. Cleavage-deficient $P12^{CA}$ (A) localizes to the plasma membrane and filopodia, whereas $P12^{CA}3$ (B) displays vesicular staining. At the ultrastructural level $P12^{CA}3$ (C) localizes to the outer membrane of cytoplasmic vesicles (*arrows*), which resemble the characteristic CPV structures carrying the viral replication complex in SFV-infected cells (D). *Bars* 200 nm

domain to the plasma membrane may simply be dictated by the optimal PS concentration in its cytoplasmic leaflet.

Early in alphavirus infection the minus-strand RNA synthesis is regulated by the processing of the nonstructural polyprotein. The first cleavage releases nsP4 from P1234 giving rise to the minus-strand polymerase (Fig. 1A). The further processing of P123 is regulated by the slow

in cis cleavage of the nsP1/2 site, which is essential for the next cleavage at the P2/3 site (Vasilieva et al. 2003). Thus the polyprotein has time to fold properly and bind to membranes by the aid of the nsP1 domain. The proper folding of the complex enables protein-protein interactions, which cannot be achieved when the components are expressed individually (Salonen et al. 2003). The polyprotein has a half-life of about 15 min before it is processed into the final components. During this time a replication complex synthesizes possibly only one minus-strand RNA before it is transformed into a stable plus-strand polymerase, which operates as the unit of replication within the spherule (Kujala et al. 2001).

3 Alphavirus-Like Superfamily

Rubella virus belongs to the *Togaviridae* family together with alphaviruses, and rubella virus replication complexes resemble in many ways those of SFV. Spherule-lined endo-lysosomal vacuoles are also found in rubella virus-infected cells (Magliano et al. 1998). Rubella virus replicase protein and newly synthesized RNA are located on the vacuoles, and specifically in spherule structures (Kujalā et al. 1999). The role of spherules as sites of RNA replication is supported by localization of double-stranded RNA to them by antibodies against dsRNA (Lee et al. 1994).

Plant viruses belonging to the alphavirus-like superfamily replicate on various intracellular membranes, for instance, brome mosaic virus (BMV) and tobacco mosaic virus (TMV) on the ER, alfalfa mosaic virus on the vacuolar (tonoplast) membrane, and turnip yellow mosaic virus on the chloroplast envelope (Restrepo-Hartwig and Ahlquist 1996; Más and Beachy 1999; Prod'homme et al. 2001; van der Heijden et al. 2001). For BMV (Fig. 5A; Table 1), the targeting determinant of the replication complex has been mapped to the 1a protein, and more precisely to its N-terminal domain, part of which is distantly related to alphavirus nsP1. 1a is peripherally but tightly bound to membranes and exposed to the cytoplasm. Relatively large regions of 1a are needed for membrane association and ER targeting, but the exact molecular basis for membrane binding is not yet known (den Boon et al. 2001). Further comparative studies are needed to determine whether replicase proteins in the alphavirus-like superfamily share similar mechanisms of membrane association and targeting, but in the case of several viruses the capping enzyme domain binds to membranes (Magden et al. 2001). Interestingly,

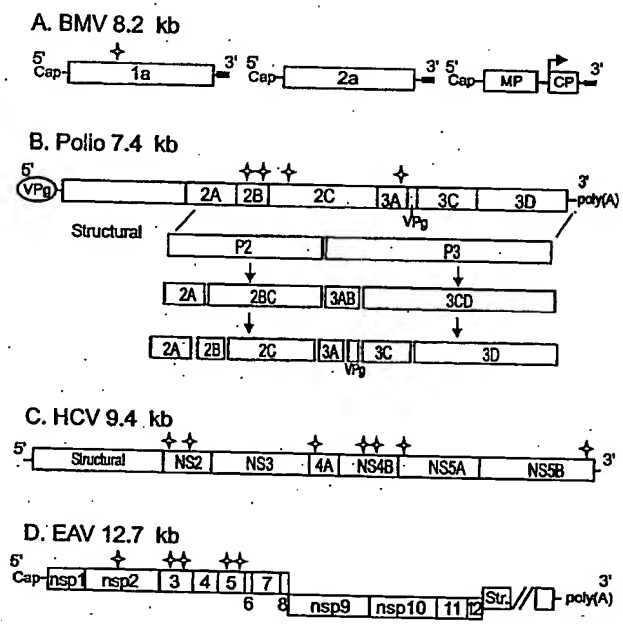

Fig. 5A–D. Genome organization of model viruses described in the text, representing the major groups of plus-strand RNA viruses. The different genomes are not in the same scale, and the structural region of the EAV genome is not represented. Regions attaching proteins to membranes are marked with *star symbols* (see also Table 1)

TMV replication in *A. thaliana* specifically and absolutely requires host genes TOM1 or TOM3. They encode related multipass transmembrane proteins, which seem to interact with the TMV replicase and are speculated to participate in its membrane anchoring (Yamanaka et al. 2002).

In cells infected with these plant viruses structures closely resembling the spherules, described above for alphaviruses, have been detected by EM-techniques (Prod'homme et al. 2001; Schwartz et al. 2002 and references therein). The spherules produced by BMV in yeast cells have recently been characterized in exquisite detail (Schwartz et al. 2002). BMV 1a protein alone, in the absence of other viral components, can induce spherule formation. When viral RNA is coexpressed with 1a, it is apparently protected inside the spherule in a membrane-associated, nuclease-resistant state. When the viral polymerase protein 2a is coexpressed, it associates with the spherules through interaction with 1a, and viral minus- and plus-sense RNA synthesis takes place in close association with

Table 1. Properties of replicase proteins

Virus	Replicase Proteins	Size aas	Function	Mode of membrane binding	Localization alone	Remarks	References
Togaviridae	nsP1	537	MT, GT	α-Helix; monotopic[1,2]	PM[3]	RC is in spherules	[1]Ahola et al. 1999
SFV	nsP2	799	NTPase, TP, Hel, Pro	–	Nucleus	In CPVs and at PM[5]	[2]Lampio et al. 2000
	nsP3	482	Unknown	–	CP; aggregates[4]		[3]Laakkonen et al. 1996
	nsP4	614	RdRp	–	CP	P123 is required for	[4]Salonen et al. 2003
	P123	1818	Early RC	Via nsP1	PM, endosomes[4]	targeting the RC[4]	[5]Kujala et al. 2001
Bromoviridae	1a	961	MT,GT,(Hel?)	Monotopic?[1]	ER	RC is in spherules,	[1]den Boon et al. 2001
BMV	2a	822	RdRp	–	CP	which can be induced by 1a alone[2]	[2]Schwartz et al. 2002
Picornaviridae	2A	149	Protease	–	CP	RC is in DMVs[4], which	[1]de Jong et al. 2003
Poliovirus	2B	97	Unknown	α-Helix[1] + TM[2]	ER, Golgi[1]	can be induced by the	[2]Agirre et al. 2002
	2C	329	NTPase	α-Helix; monotopic[3,4]	ER	coexpression of 2BC	[3]Paul et al. 1994
	3A	87	Unknown	HP C-term.[5]	ER	and 3A[5]	[4]Echeverri&Dasgupta 1995
	3B	22	VPg	–	CP		[5]Towner et al. 1996
	3C	182	Protease	–	CP		[6]Cho et al. 1996
	3D	461	RdRp	–	CP		[7]Lyle et al. 2002
	2BC	426	Unknown	Via 2B and 2C[6]	ER, Golgi, PM?		
	3AB	109	RNA priming	Via 3A[5,7]	ER, Golgi, PM?		
	3CD	643	Protease (main)	–	CP		
Flaviridae	NS2	149	Protease	TM; polytopic[1]	ER	Membranous web is the	[1]Yamaga et al. 2002
HCV	NS3	631	Pro, NTPase,Hel	–	CP, Nucleus	potential site of RC	[2]Wölk et al. 2000
	NS4A	54	Pro cofactor	HP N-term.[2]	ER	NS4B alone is able to	[3]Hügle et al 2001
	NS4B	261	Unknown	TM; polytopic[3]	ER	induce the web[6]	[4]Brass et al. 2002
	NS5A	447	Unknown	α-Helix; monotopic[4]	ER		[5]Ivashkina et al. 2002
	NS5B	591	RdRp	TM, tail-anchored[5]	ER		[6]Egger et al. 2002

Table 1. (continued)

Virus	Replicase Proteins	Size aas	Function	Mode of membrane binding	Localization alone	Remarks	References
Arteriviridae	nsp1	260	Protease	–	Nucleus, CP	RC is in perinuclear	[1]van der Meer et al. 1998
EAV	nsp2	570	Protease	HP[1]	ER	DMVs[2], which can	[2]Pedersen et al. 1999
	nsp3	232	Unknown	HP[1]	ER	also be formed by	[3]Snijder et al. 2001
	nsp4	204	Protease (main)	–	CP	expression of self-	
	nsp5	163	Unknown	HP[1]	ER?	cleaving nsp2-nsp3[3]	
	nsp6–8	302	Unknown	–	CP		
	nsp9	643	RdRp	–	CP		
	nsp10	467	Hel, NTPase	–	CP		
	nsp11–12	338	Endonuclease?	–	CP		

Abbreviations: MT, methyltransferase; GT, guanylyltransferase; TP, triphosphatase; Hel, helicase; Pro, protease; RdRp, RNA-dependent RNA polymerase; RC, replication complex; PM, plasma membrane; CP, cytoplasm; CPV, cytopathic vacuole; ER, endoplasmic reticulum; HP, hydrophobic; DMV, double membrane vesicle; TM, transmembrane.

the spherules, possibly in their interior, from where plus-sense RNA is released to the cytoplasm. Calculations based on immunolabeling suggest that many (maximally a few hundred) 1a proteins may be present in a spherule; leading to a hypothesis that 1a may form a shell-like structure coating the inside of the spherule (Schwartz et al. 2002). BMV replication in yeast requires a certain concentration of unsaturated fatty acids, as demonstrated through a mutation in the host fatty acid desaturase gene and its complementation by addition of unsaturated fatty acids. Under restrictive conditions, 1a can still normally recruit viral RNA and 2a to membranes, but minus-strand synthesis is strongly inhibited. Unsaturated fatty acids, present in membrane lipids, generally increase membrane fluidity and plasticity. Therefore, proper assembly or function of the BMV replication complex seems to require a relatively fluid membrane (Lee et al. 2001).

Uniquely among positive-sense RNA viruses, a highly purified detergent-solubilized replication complex of cucumber mosaic virus can catalyze a complete cycle of minus-strand and plus-strand synthesis on an exogenously provided specific template (Hayes and Buck 1990). However, this preparation seems to be relatively unstable and it has not been characterized further. In contrast, partially purified template-dependent preparations, such as that isolated from TMV-infected cells (Osman and Buck 1996), will be useful in further analyzing the role of membranes in RNA replication.

4
Picornavirus-Like Superfamily

4.1
Poliovirus as a Model

Poliovirus is one of the best-characterized viruses. Its structure and replication have been described in recent reviews (Pfister et al. 1999; Racaniello 2001; Semler and Wimmer 2002). Even though poliovirus does not have an envelope, the synthesis of the structural and nonstructural proteins takes place in association with cytoplasmic membranes in close vicinity to the RNA replication site (Caliguiri and Tamm 1970). The entire positive-strand RNA genome is translated to a single polyprotein, which is nascently cleaved into three polyproteins, P1, P2, and P3. P1 is the precursor of virion structural proteins, whereas P2 and P3 represent nonstructural proteins participating in the replication of viral

RNA (Fig. 5B; Table 1). Protease 2A cleaves P1 from the nascent polyprotein, while cleavages between nonstructural and structural proteins are carried out by protease $3C^{pro}$ (or rather $3CD^{pro}$). Nonstructural protein P2 yields protease $2A^{pro}$ and 2BC, which in turn is cleaved to 2B and the NTPase 2C. P3 yields 3AB and $3CD^{pro}$, which are processed to 3A and 3B (=VPg) and to 3C and $3D^{pol}$, respectively (Fig. 5B). VPg, a terminal protein of 22 aa, is linked to the 5′ end of the genome. The 5′ nontranslated region consists of a cloverleaf structure and an internal ribosome entry site.

The incoming poliovirus genomes seem to migrate to specific perinuclear sites, where replication starts. RNA recombination, which occurs during the synthesis of the complementary (minus-strand) RNA, takes place in these perinuclear sites (Egger and Bienz 2002). Throughout infection plus- and minus-strand RNAs are synthesized in the same replication complexes approximately in a ratio of 100 to 1 (Bolten et al. 1998). Poliovirus replication complexes consist of clusters of vesicles of 70–400 nm in diameter, which after isolation are associated as large "rosettelike structures" of numerous vesicles interconnected with tubular extensions. The rosettes can dissociate reversibly into tubular vesicles, which carry poliovirus nonstructural proteins on their surface and synthesize poliovirus RNA in vitro (Semler and Wimmer 2002). Immunoisolated poliovirus-specific vesicles contain cellular markers for the ER, lysosomes, and trans-Golgi network, suggesting complex biogenesis of the RNA replication complexes (Schlegel et al. 1996).

Involvement of the secretory route in the biogenesis of poliovirus replication complexes was suggested by the finding that brefeldin A, which inhibits the transport of secretory proteins from the ER to the Golgi complex, also inhibits poliovirus replication both in vivo and in vitro (Racaniello 2001). The importance of ER as the primary source for poliovirus replication complexes was confirmed recently by experiments in which COPII coat components were shown to colocalize with poliovirus nonstructural proteins on budding vesicles upon their exit from ER. Resident ER proteins were excluded from the released vesicles, which were not destined to the Golgi complex, but accumulated in the cytoplasm (Rust et al. 2001). These results are in conformity with previous findings, which showed that poliovirus infection inhibits the transport of secretory and plasma membrane proteins (Doedens and Kirkegaard 1995). Thus it seems that in poliovirus-infected cells a continuous proliferation and loss of ER membranes takes place. This process does not supply the Golgi complex with its normal lipids. The sensitivity of poliovirus replication to lipid synthesis inhibitors such as cerulenin could be

EXHIBIT A

explained by this scenario (Racaniello 2001; Pfister et al. 1999). Overexpression of viral or cellular ER-associated proteins also inhibits poliovirus replication, possibly by competing for the capacity of ER to generate new membrane material (Egger et al. 2000).

Expression of P2 and P3 without structural proteins results in membrane alterations similar to those seen in infected cells (Teterina et al. 2001). However, vesicles formed from nonreplicating poliovirus RNA could not be recruited to support the replication of superinfecting poliovirus RNA, suggesting that functional replication complexes are formed only *in cis* by the direction of the incoming RNA. This must be first translated to yield the replicase proteins for its own replication in situ (Egger et al. 2000). Assuming that the newly synthesized plus-strands create in turn new replication complexes by a similar *in cis* process, the "rosette structures" might well consist of closely packed assemblies of a parent replication complex and its numerous daughters, which are loosely bound to each other (Semler and Wimmer 2002).

Numerous studies, in which poliovirus nonstructural proteins were expressed individually or in combinations, in the absence of RNA synthesis, have helped to understand the biochemical functions of nonstructural proteins and their role in membrane association during the biogenesis of the replication complexes (Racaniello 2001; Semler and Wimmer 2002). The 2B protein is targeted to ER membranes and to the Golgi complex. It interferes with the secretory pathway in mammalian and yeast cells (Barco and Carrasco 1995; Doedens and Kirkegaard 1995; de Jong et al. 2003). It has been reported to disassemble the Golgi complex (Sandoval and Carrasco 1997). 2B has a predicted cationic amphipathic α-helix within the N-terminal 34–49 aa and a potential transmembrane domain (aa 61–81), which according to modeling form tetrameric aqueous pores, which could be responsible, for example, for the observed hygromycin sensitivity and increased permeability of poliovirus-infected cells. To cause these effects 2B has to be transported to the plasma membrane, evidently on the cytoplasmic surface of the transport elements (Agirre et al. 2002; de Jong et al. 2003).

When 2C is expressed alone in mammalian cells it is localized to the ER, causing its expansion into tubular structures. As opposed to 2B, it does not prevent the transport of VSV G-protein to the plasma membrane (Suhy et al. 2000). The fragment responsible for the membrane binding of 2C has been mapped to the N-terminal part of 2C within aa 18–54 (Pfister et al. 1999). It has been predicted that this region has an amphipathic α-helix, which starts either from residue 10 (Paul et al. 1994) or 21 (Echeverri and Dasgupta 1995). 2C has NTPase activity,

which can be inhibited by guanidine, the well-known specific inhibitor of poliovirus replication (Pfister and Wimmer 1999). The ATPase activity of 2C is needed specifically in the initiation of minus-strand RNA synthesis, the only step inhibited by guanidine (Barton and Flanegan 1997). Because 2C binds specifically to the 3′ end of the minus-strand RNA, it may also have a function in the synthesis of the plus-strand RNAs, which takes place even in the presence of guanidine, that is, without ATPase activity. Anyhow, the tight membrane association of 2C and its intimate participation in minus-strand RNA synthesis mean that this process must also take place in association with membranes, although it has been difficult to prove (Egger and Bienz 2002). 2BC, like 2B, is a membrane protein, which interferes with the vesicular transport in both animal and yeast cells. Thus the 2B moiety in 2BC is responsible for the transport inhibition (Doedens and Kirkegaard 1995). 2BC induces vesicles similar to those seen in poliovirus-infected cells and causes permeability increase of the plasma membrane, like 2B (Teterina et al. 1997).

3A expressed alone efficiently inhibits the vesicular transport of secretory proteins from the ER to the Golgi. It remains associated with ER membranes but can be mobilized into secretory vesicles, similar to those in poliovirus-infected cells, by coexpression with 2BC (Dodd et al. 2001). In poliovirus-infected cells 3AB delivers the 22-aa-long VPg peptide to the 5′ end of both minus- and plus-strand RNA molecules. Only membrane-associated 3AB can be cleaved by the viral proteases ($3C^{pro}$ and $3CD^{pro}$), and thus serve as the source of VPg (Pfister et al. 1999). 3AB associates tightly with cellular membranes, resembling the binding of integral membrane proteins. The binding region has been mapped to the C-terminal amino acids 59–80 of 3A, specifically to a hydrophobic region consisting of aa 73–80. However, the exact binding mechanism is not known (Towner et al. 1996). The 3B (=VPg) portion of 3AB has affinity to the catalytic subunit $3D^{pol}$, and its precursor 3CD, which in turn recruits the template RNA into the membrane-associated replication complex by interaction with 3C and 3D (Egger et al. 2000; Pfister et al. 1999).

In summary, the assembly of the poliovirus replication apparatus is a complex process of specific membrane recognition, followed by protein-protein and RNA-protein interactions. At the same time the vesicles develop by a poorly understood autophagocytosis-like process to double-membrane vesicles (DMVs) and large rosettes containing proteins from ER, Golgi, and lysosomes (Schlegel et al. 1996; Suhy et al. 2000). Because of the extreme proliferation of the ER, the secretory apparatus becomes exhausted. The Golgi complex disappears, probably through retrograde

transport that is not compensated by normal lipid flow from the ER. Development of poliovirus-induced vesicles must be associated with multiple fusion events directed either by viral or cellular proteins. Another possibility would be that the membrane proteins from the Golgi complex, and perhaps beyond it, would be enclosed to the poliovirus-specific vesicles through retrograde transport via ER. In any case, the result is that the membranes of the secretory and endocytotic apparatuses become mixed.

4.2 Other Members of the Picornavirus Superfamily

Many plant viruses in the picornavirus superfamily appear to replicate in association with membranes derived from the ER. In comovirus- and nepovirus-infected cells the ER is proliferated and vesiculized, but in contrast to poliovirus-infected cells, the Golgi complex remains normal. Replicase proteins and newly synthesized RNA are associated with the ER-derived structures. Sensitivity to cerulenin, as an inhibitor of RNA synthesis, seems to be a common property in the picornavirus superfamily (Carette et al. 2000; Ritzenthaler et al. 2002). Cowpea mosaic comovirus 32-kDa and 60-kDa replicase proteins are both targeted to subregions of the ER when individually expressed, and they also cause morphological alterations of the membrane system. The 32-kDa protein is a hydrophobic component specific for comoviruses, whereas the 60-kDa protein may contain membrane binding regions analogous to poliovirus 2C and 3A (Carette et al. 2002). For tobacco etch potyvirus, the 6-kDa protein (analogous to poliovirus 3A) appears to be decisive in directing the replicase to the ER. The 6-kDa protein associates tightly with ER membranes by a single central hydrophobic domain (Schaad et al. 1997). The protein may be inserted to the membrane posttranslationally, but its exact binding mechanism and topology are not known.

Although the polymerase of the insect nodaviruses appears to be distantly related to the picornavirus-like superfamily (Koonin and Dolja 1993), these viruses have capped mRNAs and the ultrastructure of the replication complex resembles that of the alphaviruses. The outer mitochondrial membranes of flock house virus (FHV)-infected *Drosophila* cells contain numerous spherulelike invaginations, connected to the cytoplasm by narrow necks. The number of spherules increases during infection, leading finally to disruption of mitochondrial structure. The single virus-encoded replicase component, 112-kDa protein A, localizes to the outer mitochondrial membrane, which is also the site of viral

RNA synthesis (Miller et al. 2001). The N-terminal 46 aa of protein A contain a mitochondrial targeting signal and a transmembrane helix, such that the N-terminus is embedded in the mitochondrial matrix while most of protein remains on the cytoplasmic side (Miller and Ahlquist 2002). This transmembrane topology distinguishes nodavirus replicase from the replicase proteins of alphaviruses.

An interesting result has been obtained with the crude membrane-bound replication complex isolated from FHV-infected cells. When treated with micrococcal nuclease and supplied with an exogenous template, the FHV replicase synthesizes a complementary minus-strand resulting in a dsRNA product. However, when glycerophospholipids are added to the mixture, relatively large quantities of plus-strand RNAs are also produced, that is, a complete RNA replication cycle takes place. Several phospholipid species can stimulate this reaction, for instance, phosphatidylcholine bearing acyl chains of 14–18 carbons. It has been speculated that glycerophospholipid might directly interact with a component of the crude membrane preparation, perhaps activating an enzymatic function, or alternatively, that the lipid might facilitate a membrane modification or assembly process required specifically for plus-strand synthesis (Wu et al. 1992). Because of these advances and the simplicity of the nodavirus replicase, this virus group is promising for further analysis of membrane-associated replication.

5 Flavivirus-Like Superfamily

Of the members of the *Flaviviridae*, hepatitis C virus (HCV) and Kunjin virus are the best studied in the context of membrane-associated replication. Here they will be discussed only briefly, because these aspects of HCV and Kunjin virus have been reviewed recently (Dubuisson et al. 2002; Westaway et al. 2002).

Analogous to picornaviruses, the whole positive-strand RNA genome of flaviviruses is translated to a large polyprotein. The structural proteins consist of a capsid protein and envelope glycoproteins followed by nonstructural proteins (Fig. 5C; Table 1). Because the envelope proteins are translocated to and glycosylated in the ER, it would be expected that the nonstructural proteins would associate directly to the ER membrane. Nevertheless, in heterologous expression systems HCV nonstructural proteins NS2, NS4A, NS4B, NS5A, and NS5B each alone bind to the ER, whereas the soluble protease/helicase (NS3) associates with the mem-

brane by interaction with NS4A, a cofactor for the protease domain of NS3 (Dubuisson et al. 2002; Wölk et al. 2000).

NS2 is a polytopic integral membrane protein introduced to the ER membrane by internal signal sequences. It is a protease responsible for the cleavage between NS2 and NS3, but it is not essential for RNA replication (Yamaga et al. 2002). NS4B is also a polytopic membrane protein cotranslationally inserted into the ER membrane with its own internal signal sequences (Hügle et al. 2001). Although the exact function of NS4B is not known, its interaction with NS3 and NS5B modulates the RNA polymerase activity (Piccininni et al. 2002). NS5A phosphoprotein is tightly associated with membranes through an N-terminal amphipathic helix of about 30 residues. When these residues are joined to GFP, the fusion protein is associated with ER membranes, suggesting that the N-terminus of NS5A has also an address for the ER, in addition to membrane binding (Brass et al. 2002; Dubuisson et al. 2002). The monotopic binding of NS5A to membranes resembles the situation in alphaviruses, except that the binding peptide of NS5A is "tip-anchored," rather than residing in the middle of the protein like in nsP1 (Ahola et al. 1999). NS5B, the catalytic subunit of the HCV RNA polymerase, has a C-terminal membrane insertion sequence of 21 aa, which is targeted to the ER membrane posttranslationally, like typical tail-anchored membrane proteins (Ivashkina et al. 2002).

Expression of the entire HCV polyprotein induced a special ER-derived membranous web, where a cluster of tiny vesicles was embedded in a membranous matrix, often accompanied by tightly associated vesicles surrounding the web. According to immuno-EM analysis, all HCV proteins were associated with the web, but not with the vesicles. When the ns proteins were expressed individually or in combinations, NS4B alone induced the web, whereas NS3-NS4A complex induced a multitude of single vesicles having no direct analog in polyprotein-expressing cells (Egger et al. 2002). NS5A and NS5B did not modify the ER. In cells expressing functional HCV subgenomic replicons all ns proteins associated with ER membranes according to light and electron microscopic analysis (Mottola et al. 2002).

Even though the genome organization of HCV and flaviviruses is similar, there are some differences as well. Flaviviruses have a nonstructural glycoprotein NS1 (46 kDa), which is translocated into the lumen of ER and transported through the secretory route to the exterior of the cell. NS1 also plays an essential role in RNA replication, evidently by recognizing portions of the other replicase proteins penetrating the ER membrane (Westaway et al. 2002). Another difference is that there are

two small membrane-associated proteins, NS2A (25 kDa) and NS2B (14 kDa), preceding the soluble NS3 protein (60 kDa), which has protease-helicase-RNA triphosphatase activities. NS2B acts as a cofactor for the NS3 protease. NS4A (16 kDa) and NS4B (27 kDa) are poorly conserved membrane proteins. Finally, NS5 (104 kDa) protein is the catalytic subunit of the RNA polymerase complex. It is a soluble protein, unlike its homologous counterpart NS5B of HCV.

Extensive immunofluorescence microscopy studies of Kunjin virus-infected cells have established that NS1, NS2A, NS3, NS4A, and NS5 are regularly associated with dsRNA, which has served as marker for genuine replication complexes. These markers also colocalize with cellular markers of trans-Golgi membranes (Mackenzie et al. 1999), even in cells that do not express the viral glycoproteins (Mackenzie et al. 2001).

Electron microscopy of Kunjin virus-infected cells has revealed dramatic changes in the organization of the ER membrane. Proliferation of the ER leads to convoluted membranes (CM) and paracrystalline structures (PC) and to vesicle packets of smooth membranes (VP) (Westaway et al. 1997, 2002). The majority of NS proteins, dsRNA, as well as nascent labeled viral RNA have been immunolocalized to VPs, which are derived from trans-Golgi membranes late in infection. VPs are "vesicle sacs" consisting of a cluster of individual vesicles (diameter about 50–100 nm) surrounded by a membrane. Interestingly, VPs were not detected on expression of Kunjin replicons, whereas CMs and PCs were formed. In these cells the dsRNA was scattered throughout the cytoplasm in small isolated foci, suggesting that all membrane structures induced by the replicase proteins are not necessarily sites of RNA replication (Mackenzie et al. 2001; Westaway et al. 1999). Comparison between replicon cell lines producing RNA and NS proteins with different efficiencies suggests that the induction of virus-specific membranes is dose dependent and requires a certain level or concentration of viral products to manifest (Mackenzie et al. 2001).

Tombusviruses, plant viruses classified in the same supergroup with flaviviruses, replicate on peroxisomal or chloroplast membranes, or on the mitochondrial outer membrane depending on the virus species. Tombusvirus infection induces multivesicular bodies, where the limiting membrane of the organelle is transformed into numerous spherules (Rochon 1999). A putative polymerase of carnation Italian ringspot virus is a 92-kDa protein translated by read-through of an amber termination codon at the end of a 36-kDa protein. Both the 36-kDa and 92-kDa proteins are targeted to the mitochondrial membranes and anchored there via two hydrophobic domains located close to the N-terminus

(Weber-Lotfi et al. 2002). However, the expression of the 36-kDa protein alone was not sufficient to induce the vesiculation of mitochondria and hence the formation of spherules (Rubino et al. 2000).

6 Nidoviruses

Coronaviruses and arteriviruses, which are grouped in the order *Nidovirales*, express their replicase genes from two large open reading frames through complex proteolytic processing, leading to 12 or more end products, depending on the virus (Snijder and Meulenberg 2001; Lai and Holmes 2001). The replicase proteins of equine arteritis virus (EAV) (Fig. 5D; Table 1), as well as newly synthesized RNA, accumulate in perinuclear granules and vesicles, which are of ER origin (van der Meer et al. 1998). An electron microscopic study of EAV-infected cells revealed DMVs of approximately 80-nm diameter, carrying the replication complex (Pedersen et al. 1999). Usually the inner and outer membranes of the DMVs were tightly apposed but clearly separate. The mechanism for DMV formation appears to be a protrusion of paired ER-membranes, because DMVs having the outer membrane continuous with ER could be seen. These profiles sometimes contained a neck between the paired ER-membrane and a forming DMV, which had not yet pinched off. The formation of DMVs is not dependent on RNA synthesis, because DMVs strikingly resembling those seen in EAV-infected cells can be induced by heterologous expression of the nsp2-nsp3 region of the polyprotein (Snijder et al. 2001). On individual expression of these proteins, DMVs were not observed. The large nsp2 has a long central hydrophobic sequence, which may represent its membrane anchor, whereas nsp3 and nsp5 have several hydrophobic sequences, suggesting that they are polytopic membrane proteins. They all, and their precursors, also behave biochemically as integral membrane proteins (van der Meer et al. 1998).

DMVs are also the sites of coronavirus RNA replication (Gosert et al. 2002). Coronavirus-induced DMVs are larger than those induced by EAV, over 200 nm in diameter, and they are surrounded by tightly apposed membranes that have fused into a lipid trilayer. Viral RNA and replicase proteins are found on the surface of DMVs, where RNA synthesis also takes place. The coronavirus replicase proteins are membrane associated and include the integrally bound components p210 and p44, the coronavirus counterparts of EAV nsp2 and nsp3 (Gosert et al. 2002). At the moment, the origin of the coronavirus replication complexes (DMVs) is not clear; involvement of membranes from secretory and endosomal compartments has been suggested. It should be noted that the majority of the viral replicase proteins may be located elsewhere than in the active replication complexes, as in SFV-infected cells (Kujala et al. 2001).

7 Concluding Remarks

7.1 Targeting of the Replicase Complex

Many viruses replicate on the cytoplasmic side of the ER membrane. For instance, picornavirus nonstructural proteins are targeted to the ER through 2B, 2C, 3A, and their precursors, bromovirus replication complex by the 1a protein, and arterivirus replicase by the nsp2-nsp3 complex (Table 1). However, the targeting mechanisms remain to be solved, as no specific receptors for viral components on the ER have been identified. Because all HCV and flavivirus proteins are translated from the same polyprotein as their envelope glycoproteins, it might be expected that their ns proteins also remain at the ER membrane. However, their location is guaranteed by their own independent affinity for ER membranes. In the case of Kunjin virus the NS1 glycoprotein, which is translocated to the cisternal side of the ER, may be responsible for the transport of the replication complex to the trans-Golgi region by transmembrane contact.

For some viral replicase proteins, classic targeting sequences directing them to a specific compartment have been identified. FHV virus protein A is directed to the mitochondrial outer membrane by a specific targeting sequence. A similar mechanism seems to operate in the targeting of the tombusvirus replication complex to either mitochondria or chloroplasts, depending on the virus species. The RNA replication of alphaviruses on the membranes of the endosomal apparatus (plasma membrane, endosomes, and lysosomes) might be explained by direct interaction of the amphipathic α-helix of nsP1 with these PS-rich membranes. It is an interesting question whether specific lipid components, or the lipid composition of the target membranes, might attract replicase components of other viruses as well.

The genomes of animal viruses discussed in this review are expressed as polyproteins. Picornaviruses and flaviviruses express both structural and nonstructural proteins in the same polyprotein, whereas togaviruses

and nidoviruses express their nonstructural proteins as a separate polyprotein. The polyprotein strategy evidently guarantees the proper targeting and assembly of the membrane-associated RNA replication complex. For instance, in SFV-infected cells the delayed proteolysis of the ns polyprotein enables the folding and assembly of "soluble" components (nsP2-nsP4) with the nsP1 membrane anchor. In the case of picornaviruses and flaviviruses several membrane anchors are present.

7.2 Mechanisms of Membrane Binding

The modes of membrane attachment are also variable. Monotopic binding by amphipathic α-helix has been suggested for several replicase proteins, which lack continuous hydrophobic anchor sequences (Table 1). Except for SFV nsP1 (Lampio et al. 2000) and HCV 5A (Brass et al. 2002), these conclusions have been based only on sequence-based predictions and mutagenesis studies. The amphipathic α-helix strategy has been proposed for components of picornavirus and for several plant virus replication complexes. Monotopic hydrophobic anchors have been proposed for poliovirus 3A and related plant virus proteins, and polytopic membrane anchors have been demonstrated for HCV proteins NS2 and NS4B. Recent results have shown that the catalytic subunit of HCV RNA polymerase is a typical tail-anchored ER protein, whereas the polymerases of other viruses are soluble proteins (Table 1).

7.3 Membrane Modification by Replicase Proteins

Alphaviruses and rubella virus give rise to specific cytoplasmic vesicles with regular membrane invaginations, spherules (Fig. 6A and B), that

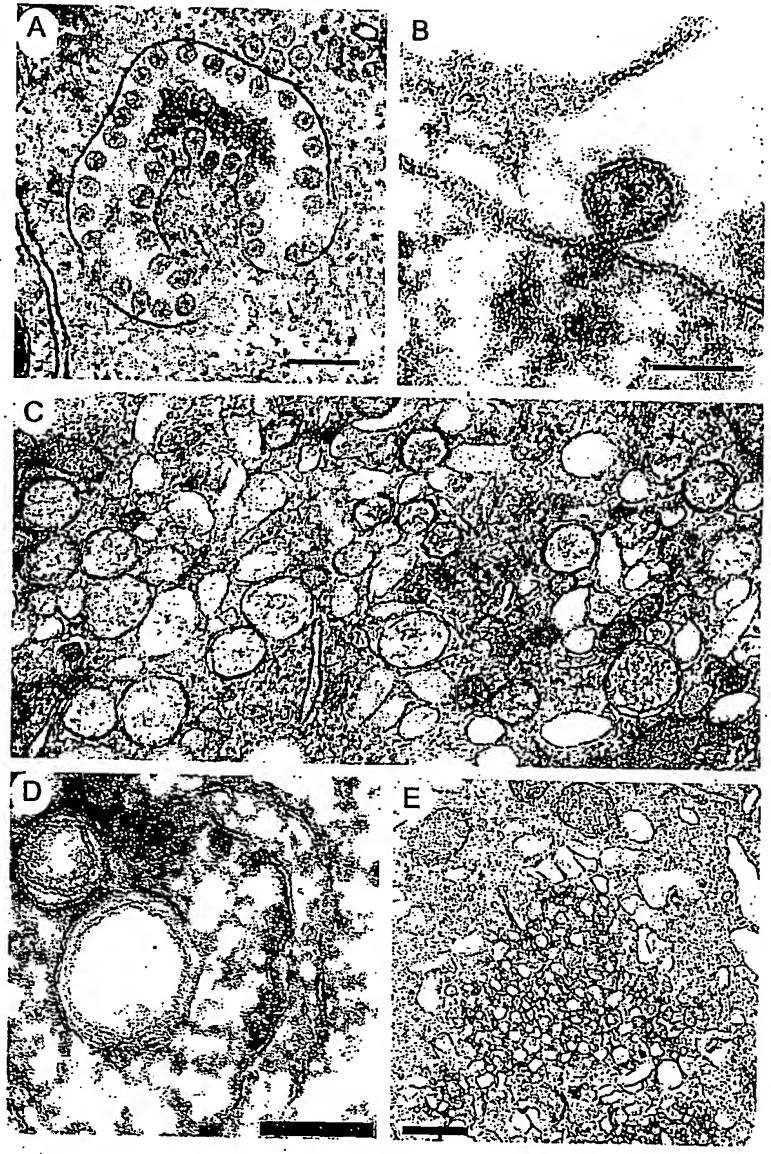

Fig. 6A–E. Ultrastructure of membranes involved in virus replication. A Typical cytopathic vesicles (CPVs) in SFV-infected BHK cell (4 h p.i.) with characteristic spherules inside. B A single spherule showing a neck opening to the cytoplasm with filled electron-dense material (courtesy of Dr. Ari Helenius and Dr. Jürgen Kartenbeck). C Poliovirus type 1-infected COS-1 cell (4 h p.i.) showing typical cytoplasmic vesicles ranging from 70 to 400 nm (courtesy of Dr. Karla Kirkegaard and Dr. Thomas Giddings). D EAV-infected BHK cell (4 h p.i) showing double membrane vesicles (DMVs) in close vicinity to RER (courtesy of Dr. Eric Snijder and Dr. Ketil Pedersen). E Membraneous web in UHCV-57.3 cell expressing the entire HCV open reading frame, 48 h after tetracycline removal (courtesy of Dr. Kurt Bienz). *Bars* 200 nm (A), 60 nm (B), 100 nm (D), 500 nm (E)

seem to be the actual units of RNA replication (Kujala et al. 2001). So far, it is not known how these structures arise. Similar spherules have been described in BMV-infected plant and in yeast cells expressing nonstructural proteins of the virus. It has been proposed that the internal surface of the spherules is covered by the replicase protein 1a of BMV (Schwartz et al. 2002). As the spherules seem to be a general feature for the members of the alphavirus superfamily, it will be interesting to see whether the suggested protein coating of the inner surface of spherules is a general mechanism within the whole superfamily. Involvement of host cell proteins cannot be excluded, as membrane bending and vesiculation in cells is a complex process requiring several factors (Hurley and Wendland 2002).

Membrane vesicles and multivesicular bodies induced by poliovirus (Fig. 6C) and other picornaviruses contain proteins from the Golgi complex, endosomes, and lysosomes, suggesting multiple fusion events during their development. Isolated membrane structures, "rosettes," consist of clusters of vesicles, which can be separated from each other at low ionic strength and low temperature. The individual vesicles represent units of replication (Egger et al. 1996). They have a tubular extension, which resembles the neck of a spherule through which the nascent RNA is proposed to be "secreted" from the site of synthesis (Froshauer et al. 1988). The DMVs (Fig. 6D) seem to the sites of arterivirus and coronavirus RNA synthesis as well. Evidently the vesicles wrap the template RNA, which in the case of poliovirus, alphaviruses, and flaviviruses is probably double-stranded, shielding it from host nucleases. During virus infection, translation and assembly of virus particles take place in close association with the replication complexes, utilizing nascent RNAs immediately after their synthesis.

A common feature for the viruses discussed in this review is that the nonstructural proteins, in the absence of RNA template, seem to be sufficient to induce the membrane modifications seen in the infected cells. Such is also the case for the membranous web seen during HCV polyprotein expression (Fig. 6E). Future studies at the molecular level should reveal how the different viruses and proteins can cause these fundamental structural changes in the membranes. A suitable lipid composition of the membrane may also be required for these dynamic membrane assembly and modification processes (Lee et al. 2001).

7.4 Functional Implications of Membrane Attachment

As the polymerase complex itself is firmly attached to the membrane, the template apparently has to move through the complex, which often also contains helicase, capping enzyme, and other subunits. In most instances, this would also mean that the same template would be repeatedly utilized by circling through the same replication complex. The dimensions of the membrane vesicles seen in EM images are such that the RNA would be relatively tightly packed within them, analogous to dsRNA virus cores. For picornavirus-like viruses there are special challenges, as for each round of RNA synthesis a protein component is consumed as a primer. It should also be emphasized that membrane lipids provide active components for the replication complex. They may directly bind to replicase proteins, thereby changing their conformation and activating them (Ahola et al. 1999).

Acknowledgements We thank Drs. Eija Jokitalo for the EM figures and Ilkka Kilpeläinen for help in presenting the peptide structure and Marja Makarow for critical reading of the manuscript. The work has been supported by the Academy of Finland (grants 8397 and 201687), Biocentrum Helsinki, and Helsinki University Research Funds. Drs. Kurt Bienz (University of Basel), Ari Helenius, (ETH, Zürich), Jürgen Kartenbeck (DKFZ, Heidelberg), Karla Kirkegaard (Stanford University), Thomas Giddings (University of Colorado), Eric Snijder (University of Leiden), and Ketil Pedersen (University of Oslo) are gratefully acknowledged for the electron micrographs.

References

Agirre A, Barco A, Carrasco L, Nieva JL (2002) Viroporin-mediated membrane permeabilization. Pore formation by nonstructural poliovirus 2B protein. J Biol Chem 277:40434–40441

Ahola T, Kääriäinen L (1995) Reaction in alphavirus mRNA capping: formation of a covalent complex of nonstructural protein nsP1 with 7-methyl-GMP. Proc Natl Acad Sci USA 92:507–511

Ahola T, Lampio A, Auvinen P, Kääriäinen L (1999) Semliki Forest virus mRNA capping enzyme requires association with anionic membrane phospholipids for activity. EMBO J 18:3164–3172

Ahola T, Kujala P, Tuittila M, Blom T, Laakkonen P, Hinkkanen A, Auvinen P (2000) Effects of palmitoylation of replicase protein nsP1 on alphavirus infection. J Virol 74:6725–6733

Barco A, Carrasco L (1995) A human virus protein, poliovirus protein 2BC, induces membrane proliferation and blocks the exocytic pathway in the yeast *Saccharomyces cerevisiae*. EMBO J 14:3349–3364

EXHIBIT A

Barton DJ, Flanegan JB (1997) Synchronous replication of poliovirus RNA: initiation of negative-strand RNA synthesis requires the guanidine-inhibited activity of protein 2C. J Virol 71:8482–8489

Bolten R, Egger D, Gosert R, Schaub G, Landmann L, Bienz K (1998) Intracellular localization of polio-virus plus- and minus-strand RNA visualized by strand-specific fluorescent in situ hybridization. J Virol 72:8578–8585

Brass V, Bieck E, Montserret R, Wolk B, Hellings JA, Blum HE, Penin F, Moradpour D (2002) An amino-terminal amphipathic alpha-helix mediates membrane association of the hepatitis C virus nonstructural protein 5A. J Biol Chem 277:8130–8139

Buck KW (1996) Comparison of the replication of positive-stranded RNA viruses of plants and animals. Adv Virus Res 47:159–251

Caliguiri LA, Tamm I (1970) The role of cytoplasmic membranes in poliovirus biosynthesis. Virology 42:100–111

Carette JE, Stuiver M, van Lent J, Wellink J, van Kammen A (2000) Cowpea mosaic virus infection induces a massive proliferation of endoplasmic reticulum but not Golgi membranes and is dependent on de novo membrane synthesis. J Virol 74:6556–6563

Carette JE, van Lent J, MacFarlane SA, Wellink J, van Kammen A (2002) Cowpea mosaic virus 32- and 60-kilodalton replication proteins target and change the morphology of endoplasmic reticulum membranes. J Virol 76:6293–6301

Cho MW, Teterina N, Egger D, Bienz K, Ehrenfeld E (1994) Membrane rearrangement and vesicle induction by recombinant poliovirus 2C and 2BC in human cells. Virology 202:129–145

Cook PR (1999) The organization of replication and transcription. Science 284:1790–1795

de Graaff M, Jaspars EMJ (1994) Plant viral RNA synthesis in cell-free systems. Annu Rev Phytopathol 32:311–335

de Jong AS, Wessels E, Dijkman HB, Galama JM, Melchers WJ, Willems PH, van Kuppeveld FJ (2003) Determinants for membrane association and permeabilization of the coxsackievirus 2B protein and the identification of the Golgi complex as the target organelle. J Biol Chem 278:1012–1021

den Boon JA, Chen J, Ahlquist P (2001) Identification of sequences in brome mosaic virus replicase protein 1a that mediate association with endoplasmic reticulum membranes. J Virol 75:12370–12381

Dodd DA, Giddings THJ, Kirkegaard K (2001) Poliovirus 3A protein limits interleukin-6 (IL-6), IL-8, and beta interferon secretion during viral infection. J Virol 75: 8158–8165

Doedens JR, Kirkegaard K (1995) Inhibition of cellular protein secretion by poliovirus proteins 2B and 3A. EMBO J 14:894–907

Dubuisson J, Penin F, Moradpour D (2002) Interaction of hepatitis C virus proteins with host cell membranes and lipids. Trends Cell Biol 12:517–523

Echeverri AC, Dasgupta A (1995) Amino terminal regions of poliovirus 2C protein mediate membrane binding. Virology 208:540–553

Egger D, Bienz K (2002) Recombination of poliovirus RNA proceeds in mixed replication complexes originating from distinct replication start sites. J Virol 76:10960–10971

Egger D, Teterina N, Ehrenfeld E, Bienz K (2000) Formation of the poliovirus replication complex requires coupled viral translation, vesicle production, and viral RNA synthesis. J Virol 74:6570–6580

Egger D, Wolk B, Gosert R, Bianchi L, Blum HE, Moradpour D, Bienz K (2002) Expression of hepatitis C virus proteins induces distinct membrane alterations including a candidate viral replication complex. J Virol 76:5974–5984

Froshauer S, Kartenbeck J, Helenius A (1988) Alphavirus RNA replicase is located on the cytoplasmic surface of endosomes and lysosomes. J Cell Biol 107:2075–2086

Gomez de Cedrón M, Ehsani N, Mikkola ML, García JA, Kääriäinen L (1999) RNA helicase activity of Semliki Forest virus replicase protein NSP2. FEBS Lett 448:19–22

Gosert R, Kanjanahaluethai A, Egger D, Bienz K, Baker SC (2002) RNA replication of mouse hepatitis virus takes place at double-membrane vesicles. J Virol 76:3697–3708

Grimley PM, Berezesky IK, Friedman RM (1968) Cytoplasmic structures associated with an arbovirus infection: loci of viral ribonucleic acid synthesis. J Virol 2:1326–1338

Hayes RJ, Buck KW (1990) Complete replication of a eukaryotic virus RNA in vitro by a purified RNA-dependent RNA polymerase. Cell 63:363–368

Hügle T, Fehrmann F, Bieck E, Kohara M, Krausslich HG, Rice CM, Blum HE, Moradpour D (2001) The hepatitis C virus nonstructural protein 4B is an integral endoplasmic reticulum membrane protein. Virology 284:70–81

Hurley JH, Wendland B (2002) Endocytosis: driving membranes around the bend. Cell 111:143–146

Ivashkina N, Wolk B, Lohmann V, Bartenschlager R, Blum HE, Penin F, Moradpour D (2002) The hepatitis C virus RNA-dependent RNA polymerase membrane insertion sequence is a transmembrane segment. J Virol 76:13088–13093

Kääriäinen L, Ahola T (2002) Functions of alphavirus nonstructural proteins in RNA replication. Prog Nucleic Acid Res Mol Biol 71:187–222

Kääriäinen L, Söderlund H (1978) Structure and replication of alphaviruses. Curr Top Microbiol Immunol 82:15–69

Koonin EV, Dolja VV (1993) Evolution and taxonomy of positive-strand RNA viruses: Implications of comparative analysis of amino acid sequences. Crit Rev Biochem Mol Biol 28:375–430

Kujala P, Ahola T, Ehsani N, Auvinen P, Vihinen H, Kääriäinen L (1999) Intracellular distribution of rubella virus nonstructural protein P150. J Virol 73:7805–7811

Kujala P, Ikäheimonen A, Ehsani N, Vihinen H, Auvinen P, Kääriäinen L (2001) Biogenesis of the Semliki Forest virus RNA replication complex. J Virol 75:3873–3884

Laakkonen P, Ahola T, Kääriäinen L (1996) The effects of palmitoylation on membrane association of Semliki Forest virus RNA capping enzyme. J Biol Chem 271:28567–28571

Laakkonen P, Auvinen P, Kujala P, Kääriäinen L (1998) Alphavirus replicase protein Nsp1 induces filopodia and rearrangement of actin filaments. J Virol 72:10265–10269

Lai MC, Holmes KV (2001) *Coronaviridae*: the viruses and their replication. In: Knipe DM, Howley PM (eds) Fields virology. Lippincott Williams & Wilkins, Philadelphia, pp 1163–1185

Lampio A, Kilpeläinen I, Pesonen S, Karhi K, Auvinen P, Somerharju P, Kääriäinen L (2000) Membrane binding mechanism of an RNA virus-capping enzyme. J Biol Chem 275:37853–37859

Lee J-Y, Marshall JA, Bowden DS (1994) Characterization of rubella virus replication complexes using antibodies to double-stranded RNA. Virology 200:307–312

Lee WM, Ishikawa M, Ahlquist P (2001) Mutation of host delta9 fatty acid desaturase inhibits brome mosaic virus RNA replication between template recognition and RNA synthesis. J Virol 75:2097–2106

Lemm JA, Rümenapf T, Strauss EG, Strauss JH, Rice CM (1994) Polypeptide requirements for assembly of functional Sindbis virus replication complexes: a model for the temporal regulation of minus- and plus-strand RNA synthesis. EMBO J 13:2925–2934

Lemm JA, Bergqvist A, Read CM, Rice CM (1998) Template-dependent initiation of Sindbis virus RNA replication in vitro. J Virol 72:6546–6553

Lyle JM, Clewell A, Richmond K, Richards OC, Hope DA, Schultz SC, Kirkegaard K (2002) Similar structural basis for membrane localization and protein priming by an RNA-dependent RNA polymerase. J Biol Chem 277:16324–16331

Mackenzie JM, Jones MK, Westaway EG (1999) Markers for trans-Golgi membranes and the intermediate compartment localize to induced membranes with distinct replication functions in flavivirus-infected cells. J Virol 73:9555–9567

Mackenzie JM, Khromykh AA, Westaway EG (2001) Stable expression of noncytopathic Kunjin replicons simulates both ultrastructural and biochemical characteristics observed during replication of Kunjin virus. Virology 279:161–172

Magden J, Takeda N, Li T, Auvinen P, Ahola T, Miyamura T, Merits A, Kääriäinen L (2001) Virus-specific mRNA capping enzyme encoded by hepatitis E virus. J Virol 75:6249–6255

Magliano D, Marshall JA, Bowden DS, Vardaxis N, Meanger J, Lee J-Y (1998) Rubella virus replication complexes are virus-modified lysosomes. Virology 240:57–63

Más P, Beachy RN (1999) Replication of tobacco mosaic virus on endoplasmic reticulum and role of the cytoskeleton and virus movement protein in intracellular distribution of viral RNA. J Cell Biol 147:945–958

Mi S, Stollar V (1991) Expression of Sindbis virus nsP1 and methyltransferase activity in *Escherichia coli*. Virology 184:423–427

Miller DJ, Ahlquist P (2002) Flock house virus RNA polymerase is a transmembrane protein with amino-terminal sequences sufficient for mitochondrial localization and membrane insertion. J Virol 76:9856–9867

Miller DJ, Schwartz MD, Ahlquist P (2001) Flock house virus RNA replicates on outer mitochondrial membranes in *Drosophila* cells. J Virol 75:11664–11676

Mottola G, Cardinali G, Ceccacci A, Trozzi C, Bartholomew L, Torrisi MR, Pedrazzini E, Bonatti S, Migliaccio G (2002) Hepatitis C virus nonstructural proteins are localized in a modified endoplasmic reticulum of cells expressing viral subgenomic replicons. Virology 293:31–43

Osman TAM, Buck KW (1996) Complete replication in vitro of tobacco mosaic virus RNA by a template-dependent, membrane-bound RNA polymerase. J Virol 70:6227–6234

Paul AV, Molla A, Wimmer E (1994) Studies of a putative amphipathic helix in the N-terminus of poliovirus protein 2C. Virology 199:188–199.

Pedersen KW, van der Meer Y, Roos N, Snijder EJ (1999) Open reading frame 1a-encoded subunits of the arterivirus replicase induce endoplasmic reticulum-derived double-membrane vesicles which carry the viral replication complex. J Virol 73:2016–2026

Peränen J, Kääriäinen L (1991) Biogenesis of type I cytopathic vacuoles in Semliki Forest virus-infected BHK cells. J Virol 65:1623–1627

Peränen J, Takkinen K, Kalkkinen N, Kääriäinen L (1988) Semliki Forest virus-specific non-structural protein nsP3 is a phosphoprotein. J Gen Virol 69:2165–2178

Peränen J, Rikkonen M, Liljeström P, Kääriäinen L (1990) Nuclear localization of Semliki Forest virus-specific nonstructural protein nsP2. J Virol 64:1888–1896

Peränen J, Laakkonen P, Hyvönen M, Kääriäinen L (1995) The alphavirus replicase protein nsP1 is membrane-associated and has affinity to endocytic organelles. Virology 208:610–620

Pfister T, Wimmer E (1999) Characterization of the nucleoside triphosphatase activity of poliovirus protein 2C reveals a mechanism by which guanidine inhibits poliovirus replication. J Biol Chem 274:6992–7001

Pfister T, Mirzayan C, Wimmer E (1999) Polioviruses (*Picornaviridae*): molecular biology. In: Granoff A, Webster RG (eds) Encyclopedia of virology, 2nd edition. Academic Press, San Diego, pp 1330–1348

Piccininni S, Varaklioti A, Nardelli M, Dave B, Raney KD, McCarthy JE (2002) Modulation of the hepatitis C virus RNA-dependent RNA polymerase activity by the non-structural (NS) 3 helicase and the NS4B membrane protein. J Biol Chem 277:45670–45679

Prod'homme D, Le Panse S, Drugeon G, Jupin I (2001) Detection and subcellular localization of the turnip yellow mosaic virus 66 K replication protein in infected cells. Virology 281:88–101

Racaniello VR (2001) *Picornaviridae*: the viruses and their replication. In: Knipe DM, Howley PM (eds) Fields virology, 4th edition. Lippincott Williams & Wilkins, Philadelphia, pp 685–722

Restrepo-Hartwig MA, Ahlquist P (1996) Brome mosaic virus helicase- and polymerase-like proteins colocalize on the endoplasmic reticulum at sites of viral RNA synthesis. J Virol 70:8908–8916

Ritzenthaler C, Laporte C, Gaire F, Dunoyer P, Schmitt C, Duval S, Piequet A, Loudes AM, Rohfritsch O, Stussi-Garaud C, Pfeiffer P (2002) Grapevine fanleaf virus replication occurs on endoplasmic reticulum-derived membranes. J Virol 76:8808–8819

Rochon DM (1999) Tombusviruses. In: Granoff A, Webster RG (eds) Encyclopedia of virology, 2nd edition. Academic Press, San Diego, pp 1789–1798

Rubino L, Di Franco A, Russo M (2000) Expression of a plant virus non-structural protein in *Saccharomyces cerevisiae* causes membrane proliferation and altered mitochondrial morphology. J Gen Virol 81:279–286

Rust RC, Landmann L, Gosert R, Tang BL, Hong W, Hauri HP, Egger D, Bienz K (2001) Cellular COPII proteins are involved in production of the vesicles that form the poliovirus replication complex. J Virol 75:9808–9818

Salonen A, Vasiljeva L, Merits A, Magden J, Jokitalo E, Kääriäinen L (2003) Properly folded nonstructural polyprotein directs the Semliki Forest virus replication complex to endosomal compartment. J Virol 77:1691–1702

Sandoval IV, Carrasco L (1997) Poliovirus infection and expression of the poliovirus protein 2B provoke the disassembly of the Golgi complex, the organelle target for the antipoliovirus drug Ro-090179. J Virol 71:4679–4693

Schaad MC, Jensen PE, Carrington JC (1997) Formation of plant RNA virus replication complexes on membranes: role of an endoplasmic reticulum-targeted viral protein. EMBO J 16:4049–4059

Schlegel A, Giddings JTH, Ladinsky MS, Kirkegaard K (1996) Cellular origin and ultrastructure of membranes induced during poliovirus infection. J Virol 70:6576–6588

Schwartz M, Chen J, Janda M, Sullivan M, den Boon J, Ahlquist P (2002) A positive-strand RNA virus replication complex parallels form and function of retrovirus capsids. Mol Cell 9:505–514

Semler BL, Wimmer E (eds) (2002) Molecular biology of picornaviruses. ASM Press, Washington, DC

Snijder EJ, Meulenberg JJM (2001) Arteriviruses. In: Knipe DM, Howley PM (eds) Fields virology. Lippincott Williams & Wilkins, Philadelphia, pp 1205–1220

Snijder EJ, van Tol H, Roos N, Pedersen KW (2001) Non-structural proteins 2 and 3 interact to modify host cell membranes during the formation of the arterivirus replication complex. J Gen Virol 82:985–994

Strauss JH, Strauss EG (1994) The alphaviruses: gene expression, replication, and evolution. Microbiol Rev 58:491–562

Suhy DA, Giddings THJ, Kirkegaard K (2000) Remodeling the endoplasmic reticulum by poliovirus infection and by individual viral proteins: an autophagy-like origin for virus-induced vesicles. J Virol 74:8953–8965

Teterina N, Gorbalenya AE, Egger D, Bienz K, Ehrenfeld E (1997) Poliovirus 2C protein determinants of membrane binding and rearrangements in mammalian cells. J Virol 71:8962–8972

Teterina NL, Egger D, Bienz K, Brown DM, Semler BL, Ehrenfeld E (2001) Requirements for assembly of poliovirus replication complexes and negative-strand RNA synthesis. J Virol 75:3841–3850

Towner JS, Ho TV, Semler BL (1996) Determinants of membrane association for poliovirus protein 3AB. J Biol Chem 271:26810–26818

van der Heijden MW, Carette JE, Reinhoud PJ, Haegi A, Bol JF (2001) Alfalfa mosaic virus replicase proteins P1 and P2 interact and colocalize at the vacuolar membrane. J Virol 75:1879–1887

van der Meer Y, van Tol H, Krijnse Locker J, Snijder EJ (1998) ORF1a-encoded replicase subunits are involved in the membrane association of the arterivirus replication complex. J Virol 72:6689–6698

Vasiljeva L, Merits A, Auvinen P, Kääriäinen L (2000) Identification of a novel function of the *Alphavirus* capping apparatus—RNA 5′ triphosphatase activity of Nsp2. J Biol Chem 275:17281–17287

Vasiljeva L, Valmu L, Kääriäinen L, Merits A (2001) Site-specific protease activity of the carboxyl-terminal domain of Semliki Forest virus replicase protein nsP2. J Biol Chem 276:30786–30793

Vasiljeva L, Merits A, Golubtsov A, Sizemskaja V, Kääriäinen L, Ahola T (2003) Regulation of the sequential processing of Semliki Forest virus replicase polyprotein. J Biol Chem 278:41636–41645

Vihinen H, Ahola T, Tuittila M, Merits A, Kääriäinen L (2001) Elimination of phosphorylation sites of Semliki Forest virus replicase protein nsP3. J Biol Chem 276:5745–5752

Weber-Lotfi F, Dietrich A, Russo M, Rubino L (2002) Mitochondrial targeting and membrane anchoring of a viral replicase in plant and yeast cells. J Virol 76: 10485–10496

Westaway EG, Mackenzie JM, Kenney MT, Jones MK, Khromykh AA (1997) Ultrastructure of Kunjin virus-infected cells: colocalization of NS1 and NS3 with double-stranded RNA, and NS2B with NS3, in virus-induced membrane structures. J Virol 71:6650–6661

Westaway EG, Khromykh AA, Mackenzie JM (1999) Nascent flavivirus RNA colocalized in situ with double-stranded RNA in stable replication complexes. Virology 258:108–117

Westaway EG, Mackenzie JM, Khromykh AA (2002) Replication and gene function in Kunjin virus. Curr Top Microbiol Immunol 267:323–351

Wölk B, Sansonno D, Krausslich HG, Dammacco F, Rice CM, Blum HE, Moradpour D (2000) Subcellular localization, stability, and trans-cleavage competence of the hepatitis C virus NS3-NS4A complex expressed in tetracycline-regulated cell lines. J Virol 74:2293–2304

Wu S-X, Ahlquist P, Kaesberg P (1992) Active complete in vitro replication of nodavirus RNA requires glycerophospholipid. Proc Natl Acad Sci USA 89:11136–11140

Yamaga AK, Ou J (2002) Membrane topology of the hepatitis C virus NS2 protein. J Biol Chem 277:33228–33234

Yamanaka T, Imai T, Satoh R, Kawashima A, Takahashi M, Tomita K, Kubota K, Meshi T, Naito S, Ishikawa M (2002) Complete inhibition of tobamovirus multiplication by simultaneous mutations in two homologous host genes. J Virol 76:2491–2497

EXHIBIT A

285
Current Topics in Microbiology and Immunology

EXHIBIT A

M. Marsh (Ed.)

Membrane Trafficking in Viral Replication

With 19 Figures

EXHIBIT A

Dr. Mark Marsh
Cell Biology Unit, MRC-LMCB
University College London
Gower Street
London, WC1E 6BT
United Kingdom

e-mail: m.marsh@ucl.ac.uk

Cover illustration: Lentivirus assembly. The principal image is an electron micrograph of simian immunodeficiency virus (SIV) budding from the surface of an infected T cell line. Budding figures, as well as immature and mature particles can be seen. The inset shows a fluorescence micrograph of a human immunodeficiency virus (HIV) infected macrophage stained to identify the viral gag protein. In these cells, virus assembly occurs intracellularly in late endosomes (see p 219). Micrographs were provided by Dr. Annegret Pelchen-Matthews, Cell Biology Unit, MRC-Laboratory for Molecular Cell Biology, University College London.

Library of Congress Catalog Card Number 72-152360

ISSN 0070-217X
ISBN 3-540-21430-5 Springer Berlin Heidelberg New York

Springer is a part of Springer Science+Business Media
springeronline.com

Printed in Germany

Editor: Dr. Rolf Lange, Heidelberg
Desk editor: Anne Clauss, Heidelberg
Production editor: Andreas Gösling, Heidelberg
Cover design: design & production GmbH, Heidelberg
Typesetting: Stürtz AG, Würzburg
Printed on acid-free paper 27/3150/ag – 5 4 3 2 1 0

Preface

Viruses are major pathogens in humans, and in the organisms with which we share this planet. The massive health and economic burden these agents impose has spurred a huge research effort to understand their most intimate details. One outcome of this effort has been the production, in many but certainly not all cases, of effective vaccines and therapies. Another consequence has been the realization that we can exploit viruses and put them to work on our behalf. Viruses are still seen to have the most potential as vehicles for gene delivery and other therapeutic applications. However, their ability to exploit cellular functions to their own ends makes viruses not only highly effective pathogens but also exquisite experimental tools. Work with viruses underpins much of our current understanding of molecular cell biology and related fields. For membrane traffic in particular, viruses have been crucial in providing insights into key cellular functions and the molecular mechanisms underlying these events.

Viruses can be regarded as enveloped or non-enveloped agents. In enveloped viruses, a membrane derived from a membrane-bound compartment of the host cell protects the genetic material. By contrast to enveloped viruses, non-enveloped viruses protect their nucleic acid with a protein shell assembled from polypeptides encoded in the viral genome. The fact that enveloped viruses contain a membrane has made these agents particularly useful for studies of membrane traffic. Some of the genetically less complex viruses encode just one or two membrane proteins and have the remarkable ability to take over a cell's protein synthetic capacity so that within a few hours of being infected, a cell is dedicated to making only one or two membrane proteins. These properties have made viruses such as the rhabdovirus vesicular stomatitis virus (VSV) and the alphaviruses Semliki Forest virus (SFV) and Sindbis virus extraordinarily useful in early studies of the exocytic pathway. Indeed, the VSV G protein has been used extensively in biochemical and morphological experiments, which have led to key insights into the molecular details of this pathway.

Similarly, analysis of the mechanisms through which these, and other viruses such as the orthomyxovirus influenza virus, generate new virions has led to insights into glycoprotein synthesis and glycosylation, protein folding, endoplasmic reticulum quality control, cell polarity, protein sorting, etc. But these agents have proved to be of use not only in biosynthetic events but in a variety of other processes involving cellular membrane sys-

EXHIBIT A

Molecular Cell, Vol. 9, 505–514, March, 2002, Copyright ©2002 by Cell Press

A Positive-Strand RNA Virus Replication Complex Parallels Form and Function of Retrovirus Capsids

Michael Schwartz,[1,2,4] Jianbo Chen,[1,4] Michael Janda,[1,2] Michael Sullivan,[1] Johan den Boon,[1] and Paul Ahlquist[1,2,3]
[1]Institute for Molecular Virology and
[2]Howard Hughes Medical Institute
University of Wisconsin, Madison
Madison, Wisconsin 53706

Summary

We show that brome mosaic virus (BMV) RNA replication protein 1a, 2a polymerase, and a *cis*-acting replication signal recapitulate the functions of Gag, Pol, and RNA packaging signals in conventional retrovirus and foamy virus cores. Prior to RNA replication, 1a forms spherules budding into the endoplasmic reticulum membrane, sequestering viral positive-strand RNA templates in a nuclease-resistant, detergent-susceptible state. When expressed, 2a polymerase colocalizes in these spherules, which become the sites of viral RNA synthesis and retain negative-strand templates for positive-strand RNA synthesis. These results explain many features of replication by numerous positive strand RNA viruses and reveal that these viruses, reverse transcribing viruses, and dsRNA viruses share fundamental similarities in replication and may have common evolutionary origins.

Introduction

Positive-strand RNA ([+]RNA) viruses, which contain messenger-sense, single-strand RNA in their virions, comprise over one-third of known virus genuses (van Regenmortel, 2000). One (+)RNA virus, hepatitis C virus, chronically infects nearly 3% of the world population, causing progressive liver damage and liver cancer. (+)RNA viruses also include West Nile virus, foot and mouth disease virus, and many other serious pathogens.

(+)RNA viruses replicate their genomes through negative-strand RNA ([−]RNA) intermediates. All known (+)RNA viruses replicate their RNA on intracellular membranes in association with vesicles or other membrane alterations (Froshauer et al., 1988; Westaway et al., 1997; Egger et al., 2000; Suhy et al., 2000). While membrane association is important for viral RNA synthesis (Wu et al., 1992; Molla et al., 1993; Lee et al., 2001), the nature and function of this membrane association and the organization of the replication complex are poorly understood.

One (+)RNA virus that has been studied as a model for RNA replication is brome mosaic virus (BMV), a member of the alphavirus-like superfamily of human, animal, and plant viruses. BMV has three genomic RNAs. RNA1 and RNA2 encode essential RNA synthesis proteins 1a and 2a. 1a (109 kDa) has a C-terminal helicase-like domain and an N-terminal domain with m^{7}G methyltransferase and covalent m^{7}GMP binding activities required for viral RNA capping in vivo (Kroner et al., 1990; Ahola et al., 2000). 2a (94 kDa) has a central polymerase-like domain and an N-terminal domain that interacts with the 1a helicase domain (Kao and Ahlquist, 1992). RNA3 encodes 3a, required for cell-to-cell spread in BMV's natural plant hosts, and coat protein (Figure 1A). Coat protein is translated from a subgenomic mRNA, RNA4.

1a and 2a direct BMV RNA replication in *Saccharomyces cerevisiae* (Janda and Ahlquist, 1993), duplicating all known features of BMV replication in plant cells. In plant cells and yeast, 1a targets itself and 2a to the endoplasmic reticulum (ER) for RNA synthesis (Restrepo-Hartwig and Ahlquist, 1996, 1999). In the absence of 2a, 1a dramatically stabilizes BMV genomic RNAs while blocking their translation (Janda and Ahlquist, 1998). This 1a-viral RNA interaction is required for (−)RNA synthesis and appears to reflect initial selection of viral RNA templates for replication. RNA2 and RNA3 sequences necessary and sufficient for 1a responsiveness are also required for RNA replication and contain a required, tRNA-like TΨC stemloop (Sullivan and Ahlquist, 1999; Chen et al., 2001). Separate, 3′-terminal tRNA-like sequences direct (−)RNA initiation (Sullivan and Ahlquist, 1997).

Another class of viruses encapsidating mRNA is the retroviruses, which replicate by tRNA-primed reverse transcription of a DNA intermediate (Coffin et al., 1997). All retroviruses encode Gag, a multidomain structural protein, and Pol, which has reverse transcriptase activity. Retroviruses express Gag and lesser amounts of a Gag-Pol fusion, which, for type C retroviruses and lentiviruses like HIV, accumulate at the plasma membrane. Acting through specific RNA signals, Gag encapsidates viral RNA and envelopes the capsid with plasma membrane. Gag-Pol is not required for encapsidation but, if present, is incorporated in the capsid. For most retroviruses, reverse transcription initially is blocked by a requirement for proteolysis of Gag and Gag-Pol, which occurs after virus budding. However, in the foamy retrovirus genus, substantial reverse transcription occurs before budding (Linial, 1999). Moreover, in hepadnaviruses, reverse transcription is completed in virion cores before budding (Seeger and Mason, 2000). tRNA-primed retroviral reverse transcription has been proposed to have evolved from initiation of RNA synthesis by an early RNA virus with a tRNA-like 3′ end similar to that of BMV and some other (+)RNA viruses (Weiner and Maizels, 1987; Wang and Lambowitz, 1993).

To better understand (+)RNA virus replication, we studied the nature of 1a-stabilized RNA3 and the BMV RNA replication complex. The results reveal strong parallels with conventional retrovirus and foamy virus cores, showing that 1a, 2a, and the 1a-responsive BMV RNA signals reprise the roles of Gag, Pol, and RNA encapsidation signals, respectively, to produce membrane-bound, partially budded spherules sequestering replication templates for synthesis. These results provide a mechanistic explanation for many features of (+)RNA

[3]Correspondence: ahlquist@facstaff.wisc.edu
[4]These authors contributed equally to this work.

EXHIBIT A

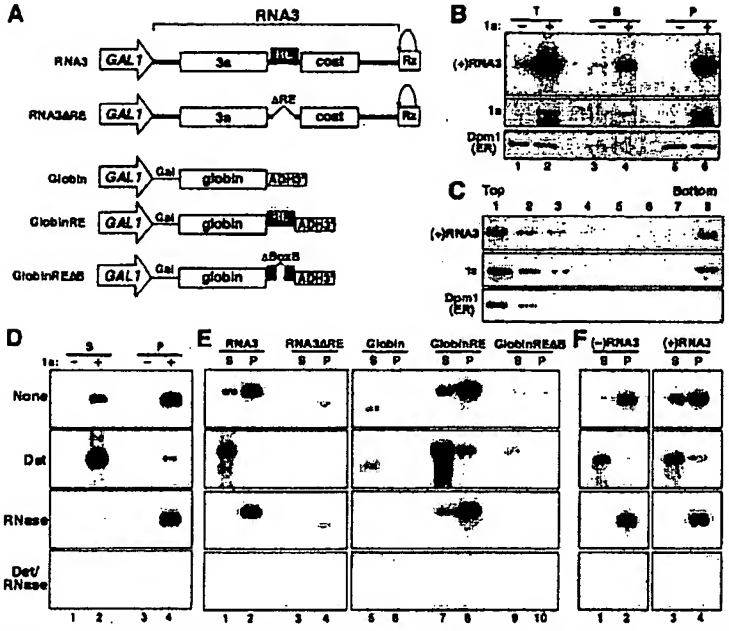

Figure 1. 1a Transfers RNA3 into a Membrane-Associated, RNase-Resistant State

(A) cDNA and flanking regions in RNA expression plasmids. The arrow depicts the yeast *GAL1* promoter and boxes denote open reading frames. A self-cleaving ribozyme (Rz) defined the RNA3 3′ end. RNA3ΔRE contains a deletion of the RE *cis* element. In globin mRNA, the human β-globin gene was flanked by the *GAL1* 5′ untranslated region and yeast *ADH1* poly(A) site. In globinRE, the BMV RE was inserted after the β-globin gene. GlobinREΔB contains the RE with a deletion of RNA3 nt 1100–1113, including box B.

(B) Northern and Western blot analysis of the distributions of RNA3, 1a, and integral ER membrane protein Dpm1 in total (T), 20,000 × g supernatant (S) and pellet (P) fractions from lysates of yeast expressing RNA3 with or without 1a.

(C) Distribution of RNA3, 1a, and Dpm1 after sucrose gradient flotation analysis of lysate from yeast expressing 1a+RNA3.

(D) Distribution of RNA3 in supernatant and pellet fractions as in (B) using lysates of yeast expressing RNA3 with or without 1a, fractionated after no additional treatment (None) or treatment with 0.5% NP-40 for 15 min at 0°C (Det), 0.01 U/μl micrococcal nuclease for 15 min at 30°C (RNase), or 0.5% NP-40 followed by micrococcal nuclease (Det/RNase).

(E) Analysis as in (D) of RNA3, RNA3ΔRE, and globin mRNA derivatives expressed with 1a.

(F) Analysis as in (D) of (−)RNA3 and (+)RNA in lysates of yeast expressing 1a+2a+RNA3 and replicating RNA3. To facilitate comparison, a light exposure of the (+)RNA3 blot is shown. See Figure 4A, lanes 1–4 to contrast amplified and unamplified (+)RNA3.

viruses in and beyond the alphavirus-like superfamily. They further imply that these (+)RNA viruses, reverse transcribing viruses, and dsRNA viruses, which all use mRNA replication intermediates, use related mechanisms for nucleic acid replication and may have evolved from common ancestors.

Results

1a Transfers RNA3 to a Membrane-Associated, Nuclease-Resistant State

ER membrane-associated BMV 1a protein increases the in vivo half-life of BMV genomic RNAs from 5 min to over 3 hr but renders these RNAs untranslatable (Janda and Ahlquist, 1998). Since these effects are closely linked to template selection for RNA replication (Sullivan and Ahlquist, 1999), we examined the state of 1a-stabilized BMV RNA3. Lysates of yeast expressing RNA3 alone or with 1a were centrifuged at 20,000 × g to yield a membrane-containing pellet and a supernatant fraction. Representative results are shown in Figure 1. When expressed alone, RNA3 was recovered exclusively in the supernatant (Figure 1B, lanes 1, 3, and 5). 1a increased the accumulation of RNA3 transcripts 20-fold (lane 2) and caused 85%–90% of this RNA3 to fractionate in the pellet, together with the majority of 1a and an integral ER membrane protein, Dpm1, followed as a control (lane 6). Retention of 10%–15% of RNA3 in the supernatant was paralleled by similar fractions of 1a and Dpm1 (lane 4). This suggests that the supernatant retained some membrane, perhaps as fragments or vesicles too small to pellet under these conditions. Thus, in addition to 1a-independent RNA3 pools, the supernatant may retain some 1a- and/or membrane-associated RNA3.

To confirm that 1a-induced RNA3 sedimentation reflected membrane association rather than aggregation, we used density gradient flotation (Figure 1C). Yeast lysate was loaded at the bottom of a sucrose gradient and centrifuged under conditions where membranes and membrane-associated factors float to the top fractions, while cytosolic proteins remain at the bottom. Without 1a, RNA3 remained at the bottom of such gradients (data not shown). In the presence of 1a, 75% of RNA3 floated to the top gradient fractions together with the majority of 1a and integral membrane protein Dpm1 (Figure 1C). Consistent with this, treating lysates of cells expressing 1a + RNA3 with nonionic detergent NP40 to disrupt membranes released 90% of RNA3 from the pellet into the supernatant (Figure 1D, top two panels).

1a also rendered RNA3 strikingly more nuclease resistant. In extracts from cells expressing RNA3 but not 1a, micrococcal nuclease degraded >95% of RNA3 (Figure 1D, third panel) and ribosomal RNA (data not shown) in the intact ribosomes of such lysates. After identical treatment of lysates from cells expressing 1a+RNA3, >95% of RNA3 fractionating to the pellet survived. Twenty percent of RNA3 in the supernatant also survived nuclease treatment, consistent with Figure 1B results, suggesting that the supernatant may contain some residual 1a- and/or membrane-associated RNA3 (see above). In both fractions, 1a-induced nuclease resistance was lost after treating with NP40 (Figure 1D, bottom panel).

1a-Induced RNA Protection Is Controlled by the RE *cis* Signal

Efficient 1a-mediated RNA3 stabilization and RNA3 replication require the 150 nt, *cis*-acting, intergenic replica-

tion enhancer (RE) element (Figure 1A) (Sullivan and Ahlquist, 1999). Deleting the RE suppressed 1a-induction of a rapidly sedimenting, nuclease-resistant, detergent-sensitive RNA3 fraction over 10-fold (Figure 1E, lanes 1–4). Conversely, adding the RE rendered β-globin mRNA highly 1a responsive, yielding a 1a-dependent, 10-fold stimulation of globin RNA accumulation and recovery of this RNA in a membrane-associated, nuclease-resistant form (Figure 1E, lanes 5–8). The RNA replication functions of the RNA3 RE and a related 1a-responsive signal in BMV RNA2 require a conserved sequence, box B, matching exactly the invariant nt and structure of tRNA TΨC stemloops (Sullivan and Ahlquist, 1999; Chen et al., 2001). Deleting box B from globinRE RNA suppressed 1a responsiveness (lanes 9–10).

Interestingly, even RE-defective RNAs RNA3ΔRE, globin, and globinREΔB showed weak, 1a-dependent accumulation of nuclease-resistant RNA in the pellet (Figure 1E, lanes 4, 6, and 10), although the level was only a few percent of that for RE-containing RNAs (lanes 2 and 8). This corresponds well with previously observed, low-efficiency interaction of 1a with nonviral RNAs (Sullivan and Ahlquist, 1999) and parallels nonspecific RNA interactions of Gag (see Discussion).

(−)RNA3 Is Retained in the Membrane-Associated, Protected State

Coexpressing 1a, 2a, and RNA3 leads to synthesis of (−)RNA3, which is copied to produce new (+)RNA3. Ninety percent of (−)RNA3 was recovered in the pellet in a highly nuclease-resistant state, similar to (+)RNA3 (Figure 1F). The residual (−)RNA3 in the supernatant was also almost completely nuclease resistant but detergent susceptible, suggesting that it was also 1a associated as discussed above.

1a Induces Perinuclear, ER Lumenal, Membrane-Bound Spherules

In plant cells and yeast, confocal microscopy shows that 1a directs itself, 2a, and viral RNA synthesis to ER membranes, predominantly in the perinuclear region (Restrepo-Hartwig and Ahlquist, 1996, 1999; Chen and Ahlquist, 2000). Since Figure 1 indicated that (+)RNA and (−)RNA replication templates are in a novel, 1a-induced, membrane-associated environment, we used thin section electron microscopy (EM) to examine wt yeast and yeast expressing 1a, 2a, and RNA3 individually, together, and in all pairwise combinations.

In cells expressing 1a, the lumen between inner and outer perinuclear ER membranes was expanded for much of the nuclear circumference and filled with numerous 50–70 nm vesicles or spherules (Figure 2B). Indistinguishable spherules were seen in cells expressing 1a, 1a+RNA3, 1a+2a, or 1a+2a+RNA3. Cells expressing 2a, RNA3, or both without 1a lacked spherules and were indistinguishable from wt yeast (Figure 2A). Thus, 1a was necessary and sufficient to induce spherules, and 2a, coat protein, or other BMV genes were not required. Results below show that these spherules were the major sites of 1a accumulation and, in cells expressing 1a+2a+RNA3, were the sites of BMV RNA synthesis. Moreover, these 1a-induced spherules and further details of their structure seen below correspond closely with spherules in bromovirus-infected plant cells and

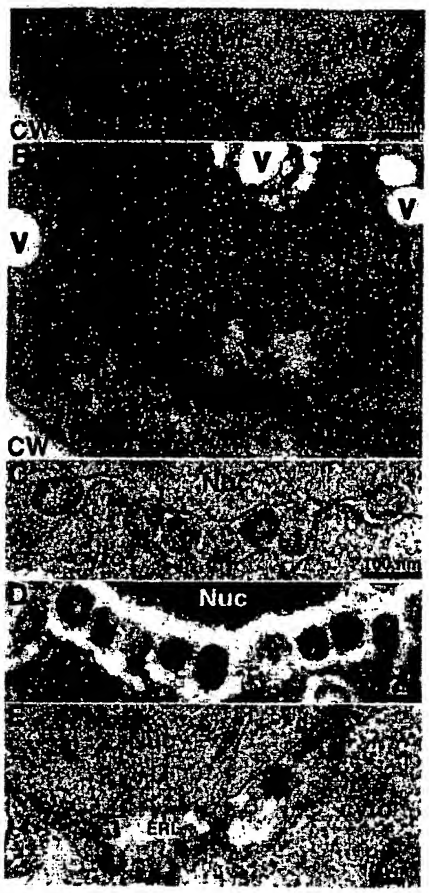

Figure 2. 1a Induces Perinuclear, ER Lumenal Spherules

Representative electron micrographs of yeast cells expressing (A) no BMV components, (B) 1a, or (C–E) 1a+2a+RNA3 are shown. Labels denote cell wall (CW), plasma membrane (PM), nucleoplasm (Nuc), cytoplasm (Cyto), vacuole (V), and ER lumen (ERL). Arrowheads indicate splitting/rejoining of the outer and inner nuclear envelope. Samples were postfixed with osmium except for (D) which was postfixed with tannic acid. For (E), yeast were spheroplasted prior to fixation.

plant and animal cells infected with diverse (+)RNA viruses (Hatta et al., 1973; Kim, 1977; Froshauer et al., 1988; Westaway et al., 1997; Kujala et al., 1999) (see also Discussion). Thus, such structures are a normal feature of replication by BMV and many other (+)RNA viruses in natural host cells. Cells expressing 1a also showed some fragmentation of the central vacuole (Figure 2B), which can be caused by general stress or modulation of vesicle traffic, possibly due to reduced availability of ER membrane (Payne et al., 1987).

In most sections, the ER lumenal spherules were crowded into overlapping masses. However, some sections showed discrete, membrane-bounded spherules surrounded by less electron dense lumen (Figure 2C). Similar rows of spherules were visible when cells were postfixed with tannic acid instead of osmium, allowing increased lipid extraction (Figure 2D). Since compression of spherules into overlapping masses obscured details, we spheroplasted cells to relieve osmotic pres-

EXHIBIT A

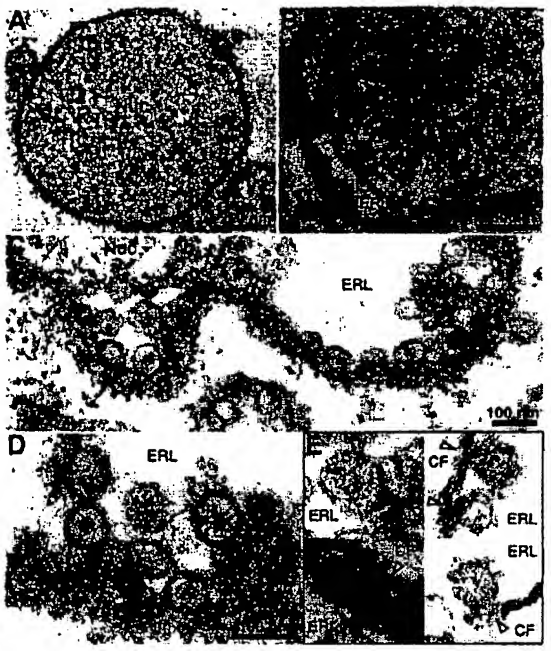

Figure 3. Details of Spherules Copurified with Nuclei

Representative electron micrographs of nuclei from yeast expressing (A) no BMV components or (B–E) 1a+2a+RNA3 are shown. Open arrowheads indicate potential connections between spherules and the outer nuclear envelope. ERL, ER lumen; CF, cytoplasmic face of outer ER membrane.

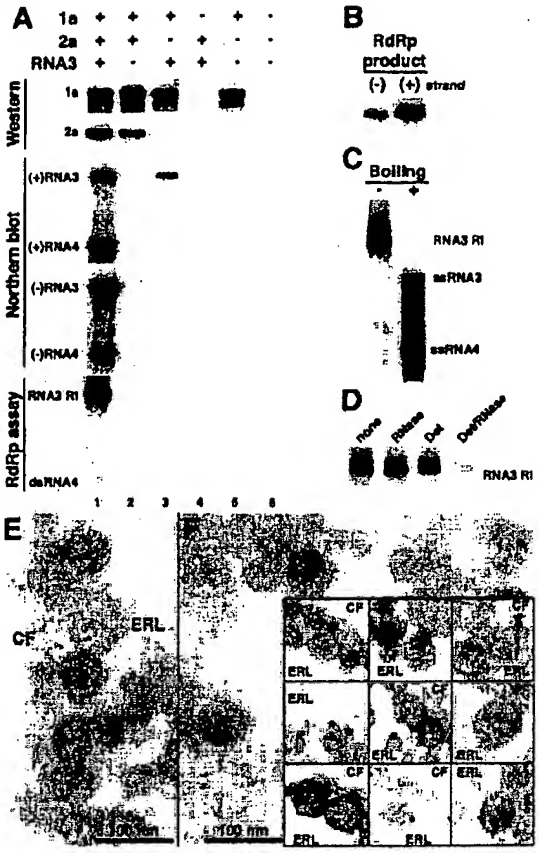

Figure 4. Association of BMV RNA Synthesis with Spherules

(A) Western, Northern, and RdRp analyses of nuclear preparations from yeast expressing the indicated BMV components.

(B) Excess of (+)RNA over (−)RNA in RdRp products synthesized by nuclear preparations from yeast expressing 1a+2a+RNA3. Equal amounts of unlabeled (+)RNA3 (left lane) and (−)RNA3 (right lane) in vitro transcripts were electrophoresed on an agarose gel, transferred to membrane, and hybridized to ^{32}P-labeled RdRp products. As a calibration standard, equal amounts of ^{32}P-labeled (+) and (−) in vitro transcript probes were hybridized to a parallel blot.

(C) Agarose gel electrophoresis of BMV RdRp products before and after denaturation by brief boiling.

(D) RNase and detergent susceptibility assays, as in Figure 1D, of membrane-associated RdRp products in nuclear preparations from yeast expressing 1a+2a+RNA3.

(E and F) Examples of incorporated BrUTP immunogold labeling of spherules from cells expressing 1a+2a+RNA3 and replicating RNA3 are shown.

sure. Under these conditions, the affected ER lumen dilated, and rows of adjacent, usually nonoverlapping spherules were seen (Figure 2E).

To further explore the nuclear association of these spherules, we isolated nuclei from yeast expressing 1a+2a+RNA3, 1a alone, or each paired combination. For each yeast type, hundreds of isolated nuclei were examined by thin section EM, and representative results are shown in Figure 3. Nuclei from wt yeast retained an intact double membrane with constant lumenal spacing and no lumenal spherules (Figure 3A). As in spheroplasted cells, nuclei from yeast expressing 1a+2a+RNA3, 1a+2a, 1a+RNA3, or 1a alone displayed extended regions of dilated perinuclear ER lumen-containing spherules (Figures 3B and 3C). Spherules had a single, bounding lipid bilayer and contained condensed or fibrillar material (Figures 3C and 3D). The diameter of spherule sections varied from 30 nm or less up to 70 nm, which must include variation due to different planes of sectioning as well as any variations in overall size. Spherules were primarily adjacent to the outer ER membrane (Figures 3B and 3C) and in many cases appeared connected to this membrane (Figures 3C–3E). In some sections, the spherule membrane appeared continuous with the outer ER membrane, forming an invagination connected by a neck (Figure 3E, top left panel; see also Figures 4F and 6C), as found for spherules in bromovirus-infected plant cells and alphavirus-infected animal cells (Kim, 1977; Froshauer et al., 1988).

BMV RNA Synthesis Is Associated with Spherules

Since BMV RNA synthesis occurs on perinuclear ER, and RNA-dependent RNA polymerase (RdRp) activity remains membrane-associated after lysis (Quadt et al., 1995), we tested nuclei from yeast expressing selected combinations of 1a, 2a, and RNA3 for RNA replication templates, products, and RdRp activity. All components and activities were distributed as expected for 1a-induced, nuclear-associated replication complexes. 1a was recovered with nuclei with or without 2a or RNA3 (Figure 4A, lanes 1–5). Without 1a, only trace amounts of 2a and RNA3 were present with nuclei (lane 4). With

1a, levels of 2a and RNA3 were greatly enhanced (lanes 2 and 3). Nuclei from yeast expressing 1a+2a+RNA3, but no lesser combination, carried amplified (+)RNA3 in addition to the other products and intermediates of RNA replication, i.e., (−)RNA3 and (+)RNA and (−)RNA4, the coat protein mRNA (lane 1).

Nuclear preparations from yeast expressing 1a+2a+RNA3 had the unique, actinomycin D-resistant ability to incorporate radiolabeled rNTPs into BMV replicative intermediate RNA that coelectrophoresed on agarose gels with dsRNA3 (Figure 4A, bottom panel). This BMV-specific, radiolabeled product contained a 6:1 excess of (+)RNA3 over (−)RNA3 sequences (Figure 4B), consistent with the excess of (+)RNA over (−)RNA produced by BMV replication in yeast or plant cells (Ishikawa et al., 1997b). After denaturing by brief boiling, the major products migrated with single-strand RNA3 and RNA4, together with smaller products consistent with partially completed RNA3 and RNA4 (Figure 4C). In undisrupted nuclear preparations, these RNA products sedimented with membranes and were highly nuclease resistant until treated with nonionic detergent (Figure 4D). Thus, their behavior paralleled 1a- and membrane-associated BMV (+)RNA3 and (−)RNA3 in Figure 1.

In plant and yeast cells, confocal microscopy shows that BMV RdRp incorporates BrU into RNA on perinuclear ER membranes at higher levels than nuclear transcription and in an actinomycin D-resistant manner (Restrepo-Hartwig and Ahlquist, 1996, 1999). To more precisely localize newly synthesized BMV RNA, we incubated isolated nuclei with ATP, CTP, GTP, and BrUTP and performed immunogold EM with an antibody recognizing BrU incorporated into RNA, but not unincorporated BrUTP, followed by a secondary antibody conjugated to gold particles. For nuclear preparations from yeast expressing 1a+2a+RNA3, spherules were the major site for incorporated BrU (Figures 4E and 4F). When over 400 gold particles on such sections were analyzed, 28% were found on nucleoplasm as expected for nuclear transcription, 45% were on 1a-induced spherules, and an additional 9% were within 10 nm of spherules, a distance readily spanned by a primary-secondary antibody complex (Hayat, 1991). In some cases, anti-BrU gold localized to the necks connecting spherules to the cytoplasm (Figure 4F, top row of inset images). As a control, we examined nuclei from yeast expressing 1a+2a, but no RNA3 replication template. Only 4% of gold particles were on or near spherules, leaving the nucleoplasm as the dominant accumulation site (70%). Some gold particles (18% for 1a+2a+RNA3 and 26% for 1a+2a) were not associated with clearly identifiable nucleoplasm or spherules, due to some damaged structures in the preparations, to immunolabeling background, and possibly to release of RNA products.

Individual Spherules Contain Many 1a Proteins and 2a Polymerase

Immunogold EM with an anti-1a antibody revealed that most BMV spherules labeled with multiple gold particles, typically 5–8 but with examples of 12 or more per spherule (Figure 5A). Similar 1a labeling was seen for spherules from all yeast expressing 1a, with or without 2a or RNA3. Anti-1a gold was also found on some outer

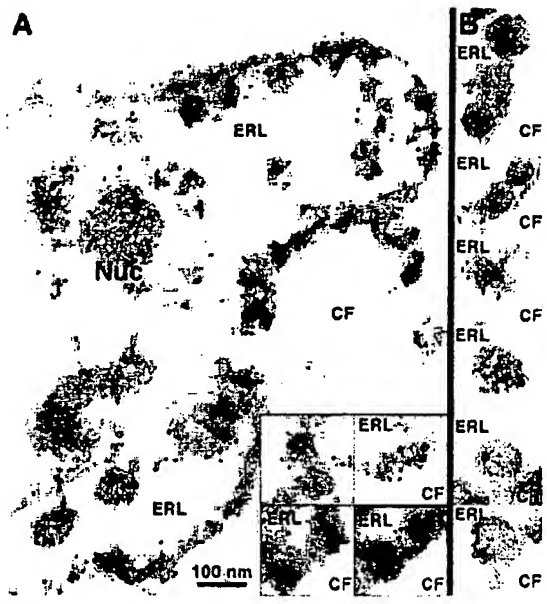

Figure 5. Multiple 1a Proteins and 2a Protein Are Localized in Spherules

Examples of (A) anti-1a and (B) anti-2a immunogold labeling of nuclear preparations from yeast expressing 1a+2a+RNA3 are shown. Cell components are labeled as in Figures 2 and 3. Reduced membrane definition was due to the need to (A) omit or (B) 10-fold reduce osmium fixation to preserve antigenicity.

nuclear membrane regions lacking obvious spherules (Figure 5A), although some spherules may have been obscured by sectioning near the spherule edge or by lower resolution due to the need to omit osmium fixation and staining to preserve 1a antigenicity. Nuclei from cells lacking 1a showed no labeling above background.

Since spherules were 50–70 nm in diameter and antibodies access at most 5 nm per section (Kellenberger et al., 1987), the multiplicity of 1a labeling per section implied that individual spherules contain at least 50–100 1a proteins. This is likely a significant underestimate due to immunogold labeling inefficiencies caused by difficulties in preserving antigenicity of samples fixed for EM (Figure 5, legend) and other factors.

To localize 2a, we constructed a 2a derivative with an N-terminal HA epitope tag, which gave wt levels of BMV RNA replication. For cells expressing 1a+HA-2a+RNA3 and replicating RNA3, immunogold EM with anti-HA antibody revealed labeling on spherules, with rarely more than one label per spherule section (Figure 5B). Much less frequently, gold particles were seen on the perinuclear membrane in regions lacking obvious spherules. ER membranes and spherules from cells expressing 1a, RNA3, and wt 2a lacking the HA epitope tag showed no labeling above background.

To further explore 1a and 2a levels in RdRp-active spherule preparations, we isolated nuclear membranes free of nucleoplasm (Kashnig and Kasper, 1969). Preparations from cells expressing no BMV components showed well-preserved nuclear membranes but no in-

EXHIBIT A

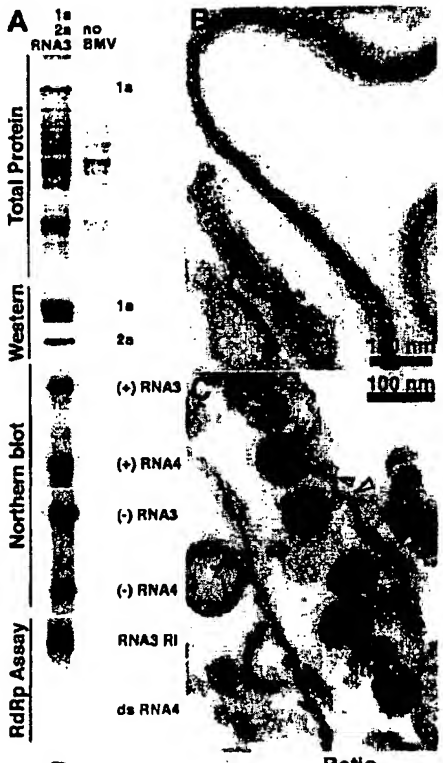

D

	Ratio
1a : (-)RNA3	402 ± 93
1a : (+) RNA3	252 ± 62
1a : 2a	26 ± 7
(+)RNA3 : (-)RNA3	1.6 ± 0.2
2a : (+)RNA3	10.1 ± 2.5
2a : (-)RNA3	15.6 ± 1.8

Figure 6. Levels of 1a, 2a, and RNA3 in RdRp-Competent Nuclear Membrane Preparations

(A) Total protein, Western, Northern, and RdRp analyses of nuclear membranes from yeast expressing the indicated BMV components.

(B and C) EM analysis of nuclear membrane preparations from cells expressing (B) no BMV components or (C) 1a+2a+RNA3 are shown. Open arrowheads indicate potential connections between spherules and the cytoplasm.

(D) Ratios between BMV components in nuclear membranes from cells expressing 1a+2a+RNA3 (see Results).

tact nuclei or nucleoplasm (Figure 6B). In contrast, nuclear membrane from cells expressing 1a+2a+RNA3 retained 1a, 2a, (+)RNA3 and (−)RNA3, RdRp activity whose product had identical characteristics to that from full nuclear preparations, and spherules (Figures 6A and 6C). In many cases, necks were visible connecting spherules to the membrane (Figure 6C).

Gel electrophoresis of total protein from these preparations revealed that 1a was one of the most abundant proteins in the spherule-bearing nuclear membranes (Figure 6A). 1a levels in these extracts were estimated by comparison with known amounts of coelectrophoresed, purified protein standards. 2a levels, which were not detectable by staining, were measured by quantitative Western blotting calibrated against known amounts of

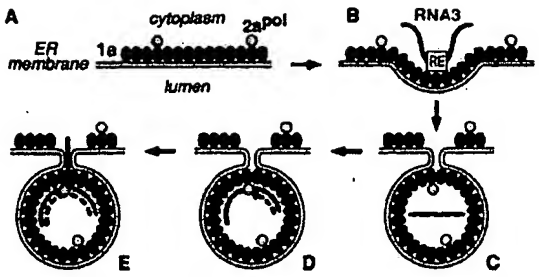

Figure 7. Model for BMV RNA Replication Complex Assembly and Function

Please see Discussion for details.

purified 2a. RNA3 levels were measured by quantitative Northern blotting calibrated with known amounts of (+)RNA3 and (−)RNA3 in vitro transcripts. Averaging the results over multiple preparations (Figure 6D) revealed that in these spherule-bearing nuclear membrane preparations with active RdRp, 1a was present in ~400-fold excess over (−)RNA3 templates, 250-fold excess over (+)RNA3, and 25-fold excess over 2a. The relation of these ratios to retroviruses is considered in the Discussion.

Discussion

The results presented here reveal close parallels between the functions of 1a, 2a polymerase, and the *cis*-acting RE signal in BMV RNA replication and Gag, Pol, and RNA packaging signals in retrovirus and foamy virus assembly and replication. Below we discuss similarities with other (+)RNA viruses, further parallels with reverse-transcribing and dsRNA viruses, and evolutionary implications. Figure 7 combines the results in a new model for BMV RNA replication complex assembly and function. In the presence or absence of 2a, 1a localizes to the cytoplasmic face of the ER membrane (Figure 7A) (Restrepo-Hartwig and Ahlquist, 1999). RNA3 templates initiate interaction with 1a via the RE signal (Figure 1E) and are sequestered by assembly of multiple 1a proteins into membrane-bound spherules (Figures 5A, 7B, and 7C), resulting in the 1a-induced, membrane-associated, RNase-resistant state. When 2a is present (Figures 7A–7C), it interacts with 1a and colocalizes to ER membranes (Chen and Ahlquist, 2000) at levels ~5% of those for 1a (Figure 6D) and is incorporated into spherules (Figure 5B). 2a, with 1a, then synthesizes a (−)RNA (dotted line) that is retained in the spherule (Figures 1F, 7D, and 7E) and used to synthesize progeny (+)RNA3 (Figures 4 and 7E) for export to the cytoplasm (see below). For simplicity, only one of several possible relationships between (+)RNA synthesis and export is shown in Figure 7E.

1a-Induced Spherules Parallel Gag-Induced Virion Budding

Like retrovirus Gag, 1a localizes by N-proximal sequences to the cytoplasmic face of its target membrane (den Boon et al., 2001), interacts with itself (O'Reilly et al., 1998), and is the sole protein required to induce

a membrane-invaginating spherule (Figures 2 and 3). Consistent with immunogold labeling (Figure 5A), there are hundreds of 1a's per spherule since (i) most 1a is in spherules with the remainder on flanking ER membrane (Figure 5A); (ii) there are similar numbers of spherules and (−)RNA3 per cell (Figures 1F, 2B, 6D, and similar results); and (iii) there are ~400 1a proteins per (−)RNA3 (Figure 6D). This appears sufficient for 1a to form an inner shell to induce and stabilize formation of the 50–70 nm spherules, since the ~60 nm shell of reovirus cores is formed by 120 copies of a slightly larger λ1 protein (Reinisch et al., 2000). In keeping with the high ratios of 1a per spherule and per viral RNA, 1a is one of the most abundant proteins in spherule-containing nuclear membranes (Figure 6A) and is the limiting factor for stabilizing RNA3 in vivo (Sullivan and Ahlquist, 1999) and wt BMV RNA replication (Dinant et al., 1993).

The necks connecting spherules to the outer nuclear membrane (e.g., Figures 3E, 4F, and 6C) were reminiscent of membrane stalks that connect budding retrovirions to the plasma membrane before separation, and thin stalks attached to newly budded retrovirions (Swanstrom and Wills, 1997). Moreover, mutations in Gag L domains block virion separation, producing large numbers of attached, budding virions similar to the ER fields of 1a-induced spherules (Swanstrom and Wills, 1997).

RE Parallels Retroviral Encapsidation Signals

Efficient 1a-induced sequestration of RNA3 derivatives in the membrane-associated, RNase-resistant state required the RE (Figure 1E), which is essential for efficient RNA3 replication and tightly linked to selection of RNA3 templates (Sullivan and Ahlquist, 1999). These RE functions parallel retroviral RNA encapsidation signals. Minimal retroviral packaging signals usually include structured regions, Ψ, between the LTR and Gag open reading frame. Other upstream or downstream sequences can contribute to packaging efficiency. Similarly, the extended stemloop of the RNA3 RE (Baumstark and Ahlquist, 2001) is necessary and sufficient for 1a-induced RNA capture (Figure 1E), but 5′ noncoding changes can modulate 1a interaction efficiency (Sullivan and Ahlquist, 1999). 1a-responsive signals in BMV genomic RNA2 are similar to packaging signals in murine leukemia retrovirus: for both, primary *cis* signals are structured elements in the 5′ untranslated region, and downstream coding sequences enhance efficiency (Berkowitz et al., 1996; Chen et al., 2001).

Retroviral Gags interact with Ψ^+ RNAs 20- to 200-fold more efficiently than Ψ^- RNAs (Swanstrom and Wills, 1997). 1a interacts with, stabilizes, and replicates RE^+ RNA3 derivatives 50- to 100-fold more efficiently than RE^- RNAs (Figure 1E) (Sullivan and Ahlquist, 1999). Thus, 1a and Gag both show high selectivity but not absolute specificity for their cognate RNA signals. As shown for Gag (Muriaux et al., 2001), such nonspecific RNA interaction may drive 1a-induced spherule formation in the absence of BMV RNAs (Figure 2B).

The 1a-2a Complex Parallels Gag-Pol

The 1a-2a complex parallels many aspects of retroviral Gag-Pol (Figure 7). Pol is fused to the Gag C terminus, and N-terminal 2a sequences interact with the C-terminal 1a helicase domain (Kao and Ahlquist, 1992; Chen and Ahlquist, 2000). Translational frameshift or readthrough yield a Gag to Gag-Pol ratio of ~10–20, and regulation of 2a translation and stability (Ishikawa et al., 1997a; Noueiry et al., 2000) yield a 1a:2a ratio of ~25 (Figure 6D). Pol and 2a are dispensable for selective capture of viral RNA by Gag and 1a but when present are incorporated into virions or replication complexes (Figure 5B) to allow viral RNA copying (Figures 1F, 4, and 7). Accordingly, nascent and newly synthesized BMV RNAs localized in spherules in a membrane-associated, RNase-resistant, detergent-susceptible state (Figures 4E and 4F) identical to that of (+)RNA3 templates and (−)RNA3 replication intermediates (Figure 1).

While (−)RNA3 templates were retained completely in the 1a-induced RNase-resistant state, amplified (+)RNA3 progeny were partly or temporarily retained but also released to a RNase-sensitive state (Figure 1F, lanes 1 and 3), consistent with their ability to translate reporter genes in vivo (Janda and Ahlquist, 1993; Ishikawa et al., 1997b). (+)RNA3 progeny release to the cytoplasm is underestimated in Figure 1F since cytoplasmic RNA3 has an in vivo half-life of ~5 min compared with >3 hr for membrane-associated, 1a-stabilized RNA3 (Janda and Ahlquist, 1998). As suggested by BrUTP labeling (Figure 4F, top row of inset images), the necks connecting spherules to the cytoplasm may serve as channels to export (+)RNA3 products and import rNTPs. Possible paradigms for RNA export are provided by dsRNA viruses (see below).

Similarities with Other (+)RNA Viruses

These findings likely have implications for many (+)RNA viruses. Spherules similar to those of BMV are associated with replication by many animal and plant (+)RNA viruses in the alphavirus superfamily and beyond (e.g., Chalcroft and Matthews, 1966; Grimley et al., 1968; Hatta et al., 1973; Kim, 1977). Potentially related multivesicle structures are produced by other (+)RNA viruses such as the HCV-related flaviviruses (Westaway et al., 1997). The retroviral parallels revealed here provide a mechanistic basis for understanding such spherules, including insights into their assembly, organization, function, and relation to other viruses.

While replication of many (+)RNA viruses involves BMV-like spherules, some induce alternate membrane structures, including other vesicle types or appressed membranes (Pedersen et al., 1999; Egger et al., 2000; Suhy et al., 2000). Further work is needed to resolve the relation of these structures to BMV RNA replication complexes. However, just as Gag assembles varied structures depending on conditions, distinct but topologically related membrane structures might be induced by modulating interactions among a set of RNA replication factors and might provide environments locally similar to those in spherules. Consistent with this, varied membrane structures can be induced by subsets of picornavirus replication factors (Teterina et al., 1997).

Similar to retroviral regulation of Gag-Pol, many (+)RNA viruses encode polymerase as a C-terminal fusion with other RNA replication proteins and downregulate its translation 10- to 20-fold by readthrough or frameshift (Ishikawa et al., 1986; Li and Rice, 1989). While

polymerase fusion and translational downregulation are common in reverse transcribing and (+)RNA viruses, other strategies exist. Like BMV 1a and 2a, foamy retrovirus Gag and Pol are expressed as separate proteins (Linial, 1999). Retrotransposon Tf1 (Levin et al., 1993) and some (+)RNA viruses such as picornaviruses express all replication factors at equal levels. Another common though not universal similarity of (+)RNA viruses to retroviruses is the use of proteolytic processing to release and activate replication proteins from a polyprotein precursor (e.g., Lemm et al., 1994).

Evolutionary Implications

An evolutionary link between retroviruses and (+)RNA viruses previously was proposed based on tRNA priming of reverse transcription and initiation of RNA replication by tRNA-like 3′ ends in BMV and some other viruses (Weiner and Maizels, 1987; Maizels and Weiner, 1999) and supported by the finding that initiation of reverse transcription by a *Neurospora* mitochondrial retroplasmid occurs without a primer at a tRNA-like CCA_{OH} 3′ RNA end and thus has characteristics intermediate between initiation of retroviral DNA synthesis and BMV RNA synthesis (Wang and Lambowitz, 1993; Weiner and Maizels, 1994). Acquisition of Gag functions was proposed to occur after reverse transcription diverged from RNA replication (Wang and Lambowitz, 1993). The results reported here show that similarities between retrovirus and (+)RNA virus replication extend beyond evolving roles of tRNA-like elements in initiation and include Gag-like functions and multiple parallels in replication complex assembly, form, and function. While no combination of characteristics can prove divergent over convergent evolution, these parallels strengthen the possibility that retroviruses and (+)RNA viruses may have arisen from a common ancestor. All major transitions for such evolution, including the transition between intracellular replication complex and extracellular virion, can be envisioned or have precedents. Reverse transcriptase uses RNA templates and can be mutated to use rNTPs (Gao et al., 1997), and BMV RdRp can use DNA templates (Siegel et al., 1999). As noted above, certain Gag mutations block separation of budding virions, yielding a spherule-like bud. Conversely, a fraction of alphavirus spherules occur on the plasma membrane and some may bud or break off from the cell (Kujala et al., 2001). This may be the source of novel infectious particles generated when vesicular stomatitis virus envelope protein G is expressed from an alphavirus replicon lacking all alphavirus virion proteins (Rolls et al., 1994). Finally, while most retroviruses bud from the plasma membrane, foamy viruses, hepadnaviruses, and intracisternal A-type particles of some endogenous retroviruses bud into the ER, like BMV spherules (Swanstrom and Wills, 1997; Linial, 1999; Seeger and Mason, 2000).

While initiation of BMV RNA synthesis is reminiscent of tRNA-primed retroviral DNA synthesis, most (+)RNA viruses lack detectable tRNA-like features. Membrane-associated RNA synthesis by picornaviruses initiates by protein priming with similarities to protein-primed DNA synthesis by the reverse-transcribing hepadnaviruses (Paul et al., 2000). Thus, different (+)RNA viruses may have evolutionary links with different groups of reverse transcribing agents.

In addition to retroviruses, Figure 7 bears striking similarities to RNA replication by dsRNA viruses, which also sequester RNA templates, RNA polymerase, and often RNA capping functions in a protein shell or core. Such packaging is perhaps best understood for dsRNA bacteriophage $\phi6$ (Poranen et al., 2001). Similar to retroviruses and BMV, packaging of $\phi6$ RNAs in the replicative core does not require the viral polymerase, although it does require three other core proteins and 5′-proximal packaging signals in each of the $\phi6$ RNAs. As with BMV, $\phi6$ cores containing polymerase synthesize and retain (−)RNAs and use them to produce progeny (+)RNA. Similarities with retroviruses have been noted in organization of the yeast L-A dsRNA virus core shell and polymerase genes, which are expressed analogously to Gag and Gag-Pol (Wickner, 1996). Structured RNA packaging signals are located internally in L-A mRNA, as in BMV RNA3. However, unlike retroviruses, BMV, or $\phi6$, selective packaging of L-A mRNA requires the viral polymerase. For the dsRNA reoviruses, the primary core shell protein contains a helicase-like domain, and (+)RNA products are released and capped through channels formed by a multifunctional RNA capping protein (Reinisch et al., 2000), in potential analogy to the helicase-like and capping domains of 1a. Rotavirus particles bud into the ER and are transiently membrane-enveloped like BMV spherules (Estes, 2001).

Thus, all classes of viruses replicating through mRNA intermediates, (+)RNA viruses, reverse transcribing viruses, and dsRNA viruses sequester mRNA templates in a multisubunit core that directs synthesis of the RNA or DNA intermediate from which more viral mRNA is made. Detailed similarities between members of each class suggest that all three classes may share evolutionary links. Understanding how the underlying common principles are applied in each class should provide synergistic insights into such evolution and the function of existing viruses, including important human pathogens in each class. This potentially ancient replicative strategy offers multiple advantages, including an additional level of template specificity and retention of negative-strand products for template use. For RNA viruses, an additional advantage may be reducing exposure to dsRNA-mediated host defenses such as PKR and RNase L (Biron and Sen, 2001) or RNA interference (RNAi) (Bass, 2000).

Experimental Procedures

Yeast, Plasmids, RNA, and Protein Analysis

Yeast strain YPH500, culture conditions, spheroplasting, RNA isolation, Northern and Western blots, and anti-1a and anti-Dpm1 antibodies were as described (Janda and Ahlquist, 1993; Chen and Ahlquist, 2000). BMV 1a, BMV 2a, and BMV RNA3 were expressed from pB1YT3H (Ahola et al., 2000), pB2CT15 (Janda and Ahlquist, 1993), and pB3MS82 (Ahola et al., 2000). RNA3ΔRE and globin mRNA derivatives were expressed as described (Sullivan and Ahlquist, 1999). To express HA-2a, the HA epitope tag was inserted by PCR between 2a codons 2 and 3 in pB2CT15. Antibodies against HA and incorporated BrU were from Santa Cruz Biotechnology (Santa Cruz, CA) and Roche (Indianapolis, IN), respectively.

Cell Fractionation

Spheroplasts were lysed in buffer YLB (50 mM Tris-Cl [pH 8.0], 2.5 mM EDTA, 1 mM PMSF, 5 ug/ml pepstatin, 10 ug/ml leupeptin, 10 ug/ml aprotinin, and 10 mM benzamidine) and centrifuged 5 min at

20,000 × g to yield pellet and supernatant fractions. For flotation analysis, 0.4 ml of lysate adjusted to 52% (w/w) sucrose in YLB was overlaid with 0.9 ml of 45% sucrose and 0.1 ml of 10% sucrose in YLB, and centrifuged to equilibrium at 100,000 × g. Nuclei (Dove et al., 1998) and nuclear membranes (Kashnig and Kasper, 1969) were isolated, and RdRp reactions (Quadt et al., 1995) were performed as described. BrUTP incorporation was performed at 30°C for 1 hr in 50 mM Tris-HCl (pH 8.0), 10 mM $MgCl_2$, 10 mM DTT, and 1 mM ATP, 1 mM CTP, 1 mM GTP, and 1 mM BrUTP.

Electron Microscopy

All steps were at room temperature unless noted. Yeast cells or nuclei were fixed for 1 hr in 2% glutaraldehyde, 4% paraformaldehyde, 50 mM KPO_4 (pH 6.8), 0.8 M sorbitol, 1 mM $MgCl_2$, and 1 mM EGTA. Cells were washed, incubated with 1% $NaIO_4$ for 15 min, and postfixed for 1 hr in 50mM KPO_4 (pH 7.2), 1% OsO_4, and 1% $K_3Fe(CN)_6$. For Figure 2D, 0.1% tannic acid was substituted for OsO_4 and $K_3Fe(CN)_6$. Cells then were incubated in 1% uranyl acetate overnight, dehydrated at 0°C in 50%, 70%, 90%, 95%, and 100% ethanol, and embedded in Spurrs resin.

For immunolabeling, nuclei were fixed with 0.5% glutaraldehyde and 4% paraformaldehyde in the above buffer, washed, and incubated 15 min in 50 mM NH_4Cl. For BrU or 2a immunolabeling, nuclei were postfixed for 15 min in 50 mM KPO_4 (pH 7.2), 0.1% OsO_4, and 0.1% $K_3Fe(CN)_6$, dehydrated, and embedded in LR White resin. For 1a, postfixation was omitted. 70 nm sections were incubated for 30 min in buffer AIB (PBS [pH 7.2], 0.1% BSA, 0.1% Tween-20, and 0.1% fish gelatin) and for 18 hr at 4°C in AIB containing rabbit antiserum against 1a, HA, or incorporated BrU. Sections were washed and incubated 2 hr in AIB containing goat anti-rabbit antibodies conjugated to 12 nm gold particles, washed, and incubated 15 min in 8% glutaraldehyde. All sections were poststained with 8% uranyl acetate and Reynold's lead citrate, and viewed with a Philips CM120 microscope.

Acknowledgments

We thank Randall Massey and Benjamin August of the University of Wisconsin Medical School Electron Microscope Facility for assistance with electron microscopy, members of our laboratory for helpful discussions, and Bill Sugden and John Young for comments on the manuscript. This research was supported by NIH grant GM35072. P.A. is an Investigator of the Howard Hughes Medical Institute.

Received September 17, 2001; revised January 3, 2002.

References

Ahola, T., den Boon, J., and Ahlquist, P. (2000). Helicase and capping enzyme active site mutations in brome mosaic virus protein 1a cause defects in template recruitment, negative-strand RNA synthesis and viral RNA capping. J. Virol. *74*, 8803–8811.

Bass, B.L. (2000). Double-stranded RNA as a template for gene silencing. Cell *101*, 235–238.

Baumstark, T., and Ahlquist, P. (2001). Brome mosaic virus RNA3 intergenic replication enhancer folds to mimic a tRNA TΨC stemloop and is modified in vivo. RNA *7*, 1652–1670.

Berkowitz, R., Fisher, J., and Goff, S.P. (1996). RNA packaging. Curr. Top. Microbiol. Immunol. *214*, 177–218.

Biron, C.A., and Sen, G.C. (2001). Interferons and other cytokines. In Fields Virology, D.M. Knipe, and P.M. Howley, eds. (Philadelphia, PA: Lippincott Williams & Wilkins), pp. 321–351.

Chalcroft, J., and Matthews, R.E. (1966). Cytological changes induced by turnip yellow mosaic virus in Chinese cabbage leaves. Virology *28*, 555–562.

Chen, J., and Ahlquist, P. (2000). Brome mosaic virus polymerase-like protein 2a is directed to the endoplasmic reticulum by helicase-like viral protein 1a. J. Virol. *74*, 4310–4318.

Chen, J., Noueiry, A., and Ahlquist, P. (2001). Brome mosaic virus protein 1a recruits viral RNA2 to RNA replication through a 5′ proximal RNA2 signal. J. Virol. *75*, 3207–3219.

Coffin, J.M., Hughes, S.H., and Varmus, H.E., eds. (1997). Retroviruses (Cold Spring Harbor, NY: Cold Spring Harbor Laboratory Press).

den Boon, J., Chen, J., and Ahlquist, P. (2001). Identification of sequences in brome mosaic virus replicase protein 1a that mediate association with endoplasmic reticulum membranes. J. Virol. *75*, 12370–12381.

Dinant, S., Janda, M., Kroner, P.A., and Ahlquist, P. (1993). Bromovirus RNA replication and transcription require compatibility between the polymerase- and helicase-like viral RNA synthesis proteins. J. Virol. *67*, 7181–7189.

Dove, J.E., Brockenbrough, J.S., and Aris, J.P. (1998). Isolation of nuclei and nucleoli from the yeast *Saccharomyces cerevisiae*. Methods Cell Biol. *53*, 33–46.

Egger, D., Teterina, N., Ehrenfeld, E., and Bienz, K. (2000). Formation of the poliovirus replication complex requires coupled viral translation, vesicle production, and viral RNA synthesis. J. Virol. *74*, 6570–6580.

Estes, M.K. (2001). Rotaviruses and their replication. In Fields Virology, D.M. Knipe, and P.M. Howley, eds. (Philadelphia: Lippincott Williams & Wilkins), pp. 1747–1785.

Froshauer, S., Kartenbeck, J., and Helenius, A. (1988). Alphavirus RNA replicase is located on the cytoplasmic surface of endosomes and lysosomes. J. Cell Biol. *107*, 2075–2086.

Gao, G., Orlova, M., Georgiadis, M.M., Hendrickson, W.A., and Goff, S.P. (1997). Conferring RNA polymerase activity to a DNA polymerase: a single residue in reverse transcriptase controls substrate selection. Proc. Natl. Acad. Sci. USA *94*, 407–411.

Grimley, P.M., Berezesky, I., and Friedman, R.M. (1968). Cytoplasmic structures associated with an arbovirus infection: loci of viral ribonucleic acid synthesis. J. Virol. *2*, 1326–1338.

Hatta, T., Bullivant, S., and Matthews, R.E. (1973). Fine structure of vesicles induced in chloroplasts of Chinese cabbage leaves by infection with turnip yellow mosaic virus. J. Gen. Virol. *20*, 37–50.

Hayat, M.A., ed. (1991). Colloidal Gold (San Diego, CA: Academic Press, Inc.).

Ishikawa, M., Meshi, T., Motoyoshi, F., Takamatsu, N., and Okada, Y. (1986). In vitro mutagenesis of the putative replicase genes of tobacco mosaic virus. Nucleic Acids Res. *14*, 8291–8305.

Ishikawa, M., Diez, J., Restrepo-Hartwig, M., and Ahlquist, P. (1997a). Yeast mutations in multiple complementation groups inhibit brome mosaic virus RNA replication and transcription and perturb regulated expression of the viral polymerase-like gene. Proc. Natl. Acad. Sci. USA *94*, 13810–13815.

Ishikawa, M., Janda, M., Krol, M.A., and Ahlquist, P. (1997b). In vivo DNA expression of functional brome mosaic virus RNA replicons in *Saccharomyces cerevisiae*. J. Virol. *71*, 7781–7790.

Janda, M., and Ahlquist, P. (1993). RNA-dependent replication, transcription, and persistence of brome mosaic virus RNA replicons in *S. cerevisiae*. Cell *72*, 961–970.

Janda, M., and Ahlquist, P. (1998). Brome mosaic virus RNA replication protein 1a dramatically increases in vivo stability but not translation of viral genomic RNA3. Proc. Natl. Acad. Sci. USA *95*, 2227–2232.

Kao, C.C., and Ahlquist, P. (1992). Identification of the domains required for direct interaction of the helicase-like and polymerase-like RNA replication proteins of brome mosaic virus. J. Virol. *66*, 7293–7302.

Kashnig, D.M., and Kasper, C.B. (1969). Isolation, morphology, and composition of the nuclear membrane from rat liver. J. Biol. Chem. *244*, 3786–3792.

Kellenberger, E., Durrenberger, M., Villiger, W., Carlemalm, E., and Wurtz, M. (1987). The efficiency of immunolabel on Lowicryl sections compared to theoretical predictions. J. Histochem. Cytochem. *35*, 959–969.

Kim, K.S. (1977). An ultrastructural study of inclusions and disease in plant cells infected by cowpea chlorotic mottle virus. J. Gen. Virol. *35*, 535–543.

Kroner, P.A., Young, B.M., and Ahlquist, P. (1990). Analysis of the

role of brome mosaic virus 1a protein domains in RNA replication, using linker insertion mutagenesis. J. Virol. *64*, 6110–6120.

Kujala, P., Ahola, T., Ehsani, N., Auvinen, P., Vihinen, H., and Kaariainen, L. (1999). Intracellular distribution of rubella virus nonstructural protein P150. J. Virol. *73*, 7805–7811.

Kujala, P., Ikaheimonen, A., Ehsani, N., Vihinen, H., Auvinen, P., and Kaariainen, L. (2001). Biogenesis of the Semliki Forest virus RNA replication complex. J. Virol. *75*, 3873–3884.

Lee, W.M., Ishikawa, M., and Ahlquist, P. (2001). Mutation of host Δ9 fatty acid desaturase inhibits brome mosaic virus RNA replication between template recognition and RNA synthesis. J. Virol. *75*, 2097–2106.

Lemm, J.A., Rümenapf, T., Strauss, E.G., Strauss, J.H., and Rice, C.M. (1994). Polypeptide requirements for assembly of functional Sindbis virus replication complexes: a model for the temporal regulation of minus- and plus-strand RNA synthesis. EMBO J. *13*, 2925–2934.

Levin, H.L., Weaver, D.C., and Boeke, J.D. (1993). Novel gene expression mechanism in a fission yeast retroelement: Tf1 proteins are derived from a single primary translation product. EMBO J. *12*, 4885–4895.

Li, G., and Rice, C.M. (1989). Mutagenesis of the in-frame opal termination codon preceding nsP4 of Sindbis virus: Studies of translational readthrough and its effect on virus replication. J. Virol. *63*, 1326–1337.

Linial, M.L. (1999). Foamy viruses are unconventional retroviruses. J. Virol. *73*, 1747–1755.

Maizels, N., and Weiner, A.M. (1999). The genomic tag hypothesis: what molecular fossils tell us about the evolution of tRNA. In The RNA World, R.F. Gesteland, T.R. Cech, and J.F. Atkins, eds. (Cold Spring Harbor, NY: Cold Spring Harbor Laboratory Press), pp. 79–111.

Molla, A., Paul, A.V., and Wimmer, E. (1993). Effects of temperature and lipophilic agents on poliovirus formation and RNA synthesis in a cell-free system. J. Virol. *67*, 5932–5938.

Muriaux, D., Mirro, J., Harvin, D., and Rein, A. (2001). RNA is a structural element in retrovirus particles. Proc. Natl. Acad. Sci. USA *98*, 5246–5251.

Noueiry, A.O., Chen, J., and Ahlquist, P. (2000). A mutant allele of essential, general translation initiation factor DED1 selectively inhibits translation of a viral mRNA. Proc. Natl. Acad. Sci. USA *97*, 12985–12990.

O'Reilly, E.K., Wang, Z., French, R., and Kao, C.C. (1998). Interactions between the structural domains of the RNA replication proteins of plant-infecting RNA viruses. J. Virol. *72*, 7160–7169.

Paul, A.V., Rieder, E., Kim, D.W., van Boom, J.H., and Wimmer, E. (2000). Identification of an RNA hairpin in poliovirus RNA that serves as the primary template in the in vitro uridylylation of VPg. J. Virol. *74*, 10359–10370.

Payne, G.S., Hasson, T.B., Hasson, M.S., and Schekman, R. (1987). Genetic and biochemical characterization of clathrin-deficient *Saccharomyces cerevisiae*. Mol. Cell. Biol. *7*, 3888–3898.

Pedersen, K.W., van der Meer, Y., Roos, N., and Snijder, E.J. (1999). Open reading frame 1-a-encoded subunits of the arterivirus replicase induce endoplasmic reticulum-derived double-membrane vesicles which carry the viral replication complex. J. Virol. *73*, 2016–2026.

Poranen, M., Paatero, A., Tuma, R., and Bamford, D.H. (2001). Self-assembly of a viral molecular machine from purified protein and RNA constituents. Mol. Cell *7*, 845–854.

Quadt, R., Ishikawa, M., Janda, M., and Ahlquist, P. (1995). Formation of brome mosaic virus RNA-dependent RNA polymerase in yeast requires coexpression of viral proteins and viral RNA. Proc. Natl. Acad. Sci. USA *92*, 4892–4896.

Reinisch, K.M., Nibert, M.L., and Harrison, S.C. (2000). Structure of the reovirus core at 3.6 A resolution. Nature *404*, 960–967.

Restrepo-Hartwig, M., and Ahlquist, P. (1996). Brome mosaic virus helicase- and polymerase-like proteins colocalize on the endoplasmic reticulum at sites of viral RNA synthesis. J. Virol. *70*, 8908–8916.

Restrepo-Hartwig, M., and Ahlquist, P. (1999). Brome mosaic virus RNA replication proteins 1a and 2a colocalize and 1a independently localizes on the yeast endoplasmic reticulum. J. Virol. *73*, 10303–10309.

Rolls, M.M., Webster, P., Balba, N.H., and Rose, J.K. (1994). Novel infectious particles generated by expression of the vesicular stomatitis virus glycoprotein from a self-replicating RNA. Cell *79*, 497–506.

Seeger, C., and Mason, W.S. (2000). Hepatitis B virus biology. Microbiol. Mol. Biol. Rev. *64*, 51–68.

Siegel, R.W., Bellon, L., Beigelman, L., and Kao, C.C. (1999). Use of DNA, RNA, and chimeric templates by a viral RNA-dependent RNA polymerase: evolutionary implications for the transition from the RNA to the DNA world. J. Virol. *73*, 6424–6429.

Suhy, D.A., Giddings, T.H., Jr., and Kirkegaard, K. (2000). Remodeling the endoplasmic reticulum by poliovirus infection and by individual viral proteins: an autophagy-like origin for virus-induced vesicles. J. Virol. *74*, 8953–8965.

Sullivan, M., and Ahlquist, P. (1997). *cis*-acting signals in bromovirus RNA replication and gene expression: networking with viral proteins and host factors. Semin. Virol. *8*, 221–230.

Sullivan, M., and Ahlquist, P. (1999). A brome mosaic virus intergenic RNA3 replication signal functions with viral replication protein 1a to dramatically stabilize RNA in vivo. J. Virol. *73*, 2622–2632.

Swanstrom, R., and Wills, J.W. (1997). Synthesis, assembly, and processing of viral proteins. In Retroviruses, J.M. Coffin, S.H. Hughes, and H.E. Varmus, eds. (Cold Spring Harbor, NY: Cold Spring Harbor Laboratory Press), pp. 263–334.

Teterina, N.L., Bienz, K., Egger, D., Gorbalenya, A.E., and Ehrenfeld, E. (1997). Induction of intracellular membrane rearrangements by HAV proteins 2C and 2BC. Virology *237*, 66–77.

van Regenmortel, M.H.V., ed. (2000). Virus Taxonomy (San Diego, CA: Academic Press).

Wang, H., and Lambowitz, A.M. (1993). The Mauriceville plasmid reverse transcriptase can initiate cDNA synthesis de novo and may be related to reverse transcriptase and DNA polymerase progenitor. Cell *75*, 1071–1081.

Weiner, A.M., and Maizels, N. (1987). tRNA-like structures tag the 3′ ends of genomic RNA molecules for replication: Implications for the origin of protein synthesis. Proc. Natl. Acad. Sci. USA *84*, 7383–7387.

Weiner, A.M., and Maizels, N. (1994). Unlocking the secrets of retroviral evolution. Curr. Biol. *4*, 560–563.

Westaway, E., Mackenzie, J., Kenney, M., Jones, M., and Khromykh, A. (1997). Ultrastructure of Kunjin virus-infected cells: colocalization of NS1 and NS3 with double-stranded RNA, and of NS2B with NS3, in virus-induced membrane structures. J. Virol. *71*, 6650–6661.

Wickner, R.B. (1996). Double-stranded RNA viruses of *Saccharomyces cerevisiae*. Microbiol. Rev. *60*, 250–265.

Wu, S.X., Ahlquist, P., and Kaesberg, P. (1992). Active complete in vitro replication of nodavirus RNA requires glycerophospholipid. Proc. Natl. Acad. Sci. USA *89*, 11136–11140.

EXHIBIT A

Alternate, virus-induced membrane rearrangements support positive-strand RNA virus genome replication

Michael Schwartz*, Jianbo Chen†, Wai-Ming Lee, Michael Janda, and Paul Ahlquist‡

Institute for Molecular Virology and Howard Hughes Medical Institute, University of Wisconsin, Madison, WI 53706

Contributed by Paul Ahlquist, June 11, 2004

All positive-strand RNA [(+)RNA] viruses replicate their RNA on intracellular membranes, often in association with spherular invaginations of the target membrane. For brome mosaic virus, we previously showed that such spherules serve as compartments or mini-organelles for RNA replication and that their assembly, structure, and function have similarities to the replicative cores of retrovirus and double-stranded RNA virus virions. Some other (+)RNA viruses conduct RNA replication in association with individual or clustered double-membrane vesicles, appressed double membranes, or other structures whose possible relationships to the spherular invaginations are unclear. Here we show that modulating the relative levels and interactions of brome mosaic virus replication factors 1a and 2a polymerase (2a^{pol}) shifted the membrane rearrangements associated with RNA replication from small invaginated spherules to large, karmellae-like, multilayer stacks of appressed double membranes that supported RNA replication as efficiently as spherules. Spherules were induced by expressing 1a, which has functional similarities to retrovirus virion protein Gag, or 1a plus low levels of 2a^{pol}. Double-membrane layers were induced by 1a plus higher levels of 2a^{pol} and were suppressed by deleting the major 1a-interacting domain from 2a^{pol}. The stacked, double-membrane layers alternated with spaces that, like spherule interiors, were 50–60 nm wide, connected to the cytoplasm, and contained 1a and 2a^{pol}. These and other results suggest that seemingly diverse membrane rearrangements associated with RNA replication by varied (+)RNA viruses may represent topologically and functionally related structures formed by similar protein–protein and protein–membrane interactions and interconverted by altering the balances among those interactions.

Positive-strand RNA [(+)RNA] viruses are the largest genetic class of viruses and include many pathogens, such as the severe acute respiratory syndrome (SARS) coronavirus, hepatitis C virus, and potential bioterrorism agents. Such (+)RNA viruses encapsidate messenger-sense genomic RNAs and replicate those genomes through negative-strand RNA intermediates. The RNA replication complexes of (+)RNA viruses invariably form on intracellular membranes, usually in association with vesiculation or other membrane rearrangements. Different (+)RNA viruses use distinct but usually specific membranes, ranging from the outer membranes of the endoplasmic reticulum (ER), later or mixed compartments of the secretory pathway, endosomes, mitochondria, and other organelles (1–7).

Many (+)RNA viruses, including alphaviruses, nodaviruses, bromoviruses, and many others form RNA replication complexes at virus-induced, vesicular invaginations of specific intracellular membranes (4–6, 8–11). One such virus is brome mosaic virus (BMV), a member of the alphavirus superfamily of human, animal, and plant viruses. BMV encodes two proteins that direct viral RNA replication in its natural plant hosts or yeast. Viral replication factor 1a contains a C-terminal helicase domain and a self-interacting N-terminal domain with m^{7}G methyltransferase and covalent m^{7}GMP-binding activities required for viral RNA capping (12–14). Viral replication factor 2a polymerase (2a^{pol}) contains a central polymerase domain and an N-terminal domain that interacts with the 1a helicase domain (15, 16). Replication factor 1a localizes to outer perinuclear ER membranes, where it induces membrane lipid synthesis and 50- to 60-nm vesicular invaginations or spherules, connected by means of necks to the cytoplasm, that serve as compartments or miniorganelles for RNA replication (6, 17–19). 1a also recruits viral RNA templates and 2a^{Pol} to these compartments, which concentrate replication factors, link successive replication steps, and protect double-stranded RNA intermediates from host RNA interference and IFN responses (6, 16, 20–22). The roles of 1a, 2a^{Pol}, and certain cis RNA signals in assembly and function of these intracellular spherular BMV RNA replication complexes parallel those of Gag-, Pol-, and RNA-packaging signals in the membrane-enveloped replicative cores of retrovirus virions (6). These roles also show similarities to double-stranded RNA virus virion cores, suggesting functional and possible evolutionary links among these three virus classes (6).

Although all (+)RNA viruses assemble their replication complexes on membranes, RNA replication by some (+)RNA viruses induce apparently distinct membrane rearrangements involving alternate vesicle types, appressed membranes, or both. Flavivirus replication factors and double-stranded RNA replication intermediates colocalize in packets of 50- to 100-nm vesicles enclosed in a second bounding membrane (1). Replication of the 12.5-kb arterivirus RNA localizes to 80-nm double-membrane vesicles (2), and the related coronaviruses replicate their >30-kb genomes in association with 200- to 350-nm double-membrane vesicles (23). Poliovirus RNA replication is associated with clusters of 150- to 300-nm, double-membrane-bounded vesicles (3, 24). RNA replication has been proposed to occur in the space between these clustered vesicles (25).

Here we show that modulating the relative levels of BMV replication factors 1a and 2a^{pol}, and, thus, the balance of their homotypic and heterotypic interactions, shifts the structure of membrane rearrangements associated with RNA replication from small spherular invaginations, as is found in natural infections by bromoviruses and many other (+)RNA viruses (4–6, 8–11), to large stacks of karmellae-like, appressed double-membrane layers that also support efficient viral RNA replication. We also show that 1a–2a^{pol} interaction motifs are critical for inducing this new membrane rearrangement. The results suggest that alternate membrane morphologies associated with RNA replication by various (+)RNA viruses may embody common, underlying principles of architecture and assembly. The results also have implications for other features of RNA replication, such as the frequent down-regulation of polymerase expression in (+)RNA and reverse-transcribing viruses.

Abbreviations: BMV, brome mosaic virus; (+)RNA, positive-strand RNA; (−)RNA, negative-strand RNA; ER, endoplasmic reticulum; EM, electron microscopy; 2a^{pol}, 2a polymerase.

*Present address: Department of Biological Sciences, Vanderbilt University, Nashville, TN 37235.

†Present address: HIV Drug Resistance Program, National Cancer Institute, Frederick, MD 21702.

‡To whom correspondence should be addressed at: Institute for Molecular Virology, University of Wisconsin, 1525 Linden Drive, Madison, WI 53706-1596. E-mail: ahlquist@wisc.edu.

EXHIBIT A

Materials and Methods

Yeast and Plasmids. Yeast strain YPH500 and culture conditions were as described in ref. 16. BMV 1a was expressed from the *GAL1* promoter by using pB1YT3H (26). BMV $2a^{pol}$ was expressed from pB2CT15 (*ADH1* promoter) (26), pB2YT5 (*GAL1* promoter) (14), or pAON55 (CUP1 promoter), a pB2YT5 derivative with the *GAL1* promoter replaced by that of *CUP1*. BMV RNA3 was expressed from pB3MS82, which encodes a full-length RNA3 derivative that does not express coat protein (14). Sec63-GFP was expressed from pJK59, kindly provided by J. Kahanab and P. Silver (Harvard Medical School, Cambridge, MA).

RNA and Protein Analysis. Cell fractionation, isolation of nuclei, RNA-dependent RNA polymerase reactions (6), and Northern (16) and Western blot analyses (17) were as described. RNA was purified from cell fractions by using Qiagen RNeasy columns.

Microscopy. Confocal and electron microscopy (EM) were performed as described in refs. 6 and 16. Under EM, not all cell sections in populations expressing 1a or 1a plus $2a^{pol}$ show nuclei or perinuclear membrane rearrangements because of the limited cell region revealed by the random plane of sectioning, incomplete plasmid segregation and consequent absence of plasmids from significant fractions of continuously selected yeast populations (27), and other effects. Thus, the relative frequencies of perinuclear membrane layers versus spherules were calculated as the percentage of cell sections with BMV-induced perinuclear membrane rearrangements that showed layers or spherules, respectively (see Figs. 4 and 5).

Results

Increased $2a^{pol}$ Levels Alter 1a-Induced Membrane Rearrangements. BMV 1a protein associates as a peripheral membrane protein with the cytoplasmic face of the outer ER membrane and induces invaginations of this membrane into the ER lumen to form vesicles or spherules whose interiors are connected through narrow necks with the cytoplasm (6). These spherules are induced either in yeast expressing 1a alone or in yeast expressing 1a and $2a^{pol}$ from plasmids by using the stronger *GAL1* and weaker *ADH1* promoters, respectively ($1a_G+2a_A$ yeast; Fig. 1C) (6). By contrast, in the great majority of yeast cells expressing both $2a^{pol}$ and 1a from plasmids by using the *GAL1* promoter ($1a_G+2a_G$ yeast), we discovered by EM that the perinuclear membrane did not form spherules but proliferated into a series of 2–7 appressed layers of double-membrane ER (Fig. 1 *D* and *E*). These karmellae-like, multilayer structures were formed by folding over continuous sheets of ramified, double-membrane ER with its enclosed lumen (Fig. 1*D*). The successive, double-membrane ER layers were separated by regular, 50- to 60-nm spaces (Fig. 1*E*), which at their ends were contiguous with the cytoplasm (Fig. 1*D*, top and bottom left). Yeast expressing $2a^{pol}$ from either the *GAL1* or *ADH1* promoters but lacking 1a lacked either layers or spherules and showed no detectable membrane changes from WT yeast (Fig. 1*B*). By contrast, yeast expressing 1a from either the *GAL1* or *ADH1* promoters but lacking $2a^{pol}$ contained perinuclear spherules but never layers (ref. 6 and results not shown).

Confocal imaging of live cells expressing a fusion of GFP to Sec63, an integral ER membrane protein, correlated well with the higher resolution ultrastructure obtained by EM. In cells not expressing BMV components, Sec63-GFP defined a perinuclear ER layer of relatively uniform thickness (Fig. 1*F*). Yeast expressing $1a_G + 2a_A$, which contained perinuclear spherules (Fig. 1*C*), showed modest thickening of some perinuclear sections (Fig. 1*G*). In $1a_G+2a_G$ yeast, which contained predominantly BMV-induced double-membrane layers, large sections of the GFP-fluorescent perinuclear layer showed a strikingly greater thickening (Fig. 1*H*). Thus, the Sec63-GFP results confirmed that, in the presence of 1a, $2a^{pol}$ expression from the stronger *GAL1* promoter induced alternate perinuclear membrane changes in live cells and not just in cells fixed for EM analysis.

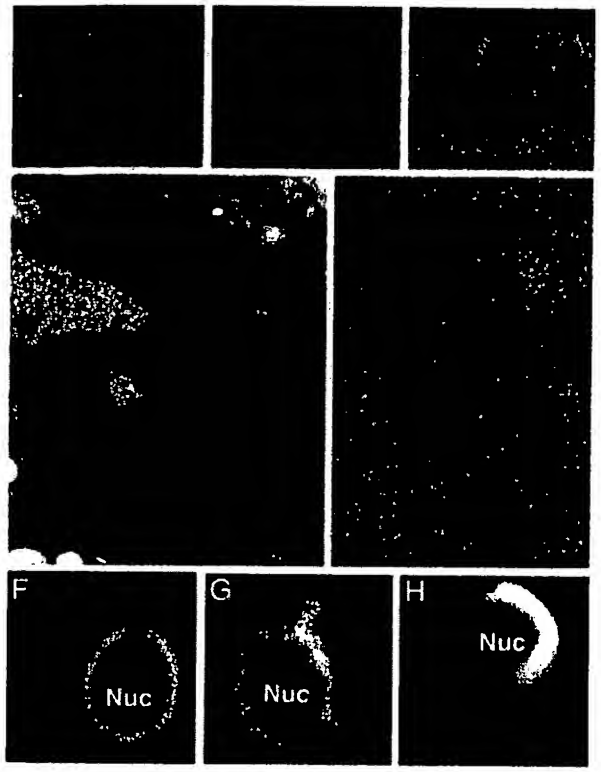

Fig. 1. Two alternate membrane rearrangements are induced by 1a and $2a^{pol}$. (*A–E*) Representative electron micrographs of yeast cells expressing no BMV components (*A*), *GAL1* promoter-driven $2a^{pol}$ (*B*), *GAL1* promoter-driven 1a and *ADH1* promoter-driven $2a^{pol}$ ($1a_G+2a_A$) (*C*), or *GAL1* promoter-driven 1a and $2a^{pol}$ ($1a_G+2a_G$) (*D* and *E*). (*F–H*) Representative confocal fluorescence images of live yeast cells expressing Sec63p-GFP and no BMV components (*F*), $1a_G+2a_A$ (*G*), or $1a_G+2a_G$ (*H*). Nuc, nucleus; Cyto, cytoplasm. (Scale bars, 100 nm.)

Double-Membrane Layers Contain 1a and $2a^{pol}$ and Support BMV RNA Replication. Yeast expressing BMV 1a, $2a^{pol}$, and BMV genomic RNA3 support RNA3 replication, including production of negative-strand (−)RNA3 that is copied to dramatically amplify (+)RNA3 and to produce the subgenomic mRNA RNA4 (26, 28). Northern blot analysis (Fig. 2*A*) showed that, when RNA3 was expressed from a third plasmid, similar levels of RNA3 replication and subgenomic RNA4 production occurred in $1a_G+2a_A$ and $1a_G+2a_G$ yeast, which contained membrane spherules or layers, respectively (Fig. 1). Thus, BMV RNA replication can occur in association with two distinct membrane architectures.

Yeast expressing $1a_G+2a_G$ accumulate 1a and $2a^{pol}$ in a $1a/2a^{pol}$ ratio of ≈25 (6). Western blot analysis confirmed that the levels of 1a accumulation were indistinguishable in $1a_G+2a_A$ and $1a_G+2a_G$ yeast (Fig. 2*A*). However, as expected, *GAL1*-promoted $2a^{pol}$ expression associated with membrane layers increased $2a^{pol}$ levels by >2-fold relative to the *ADH1*-promoted $2a^{pol}$ expression associated with spherules (Fig. 2*A*).

Confocal ImmunoGold EM and biochemical analyses showed previously that 1a localizes both itself and $2a^{pol}$ to the cytoplas-

EXHIBIT A

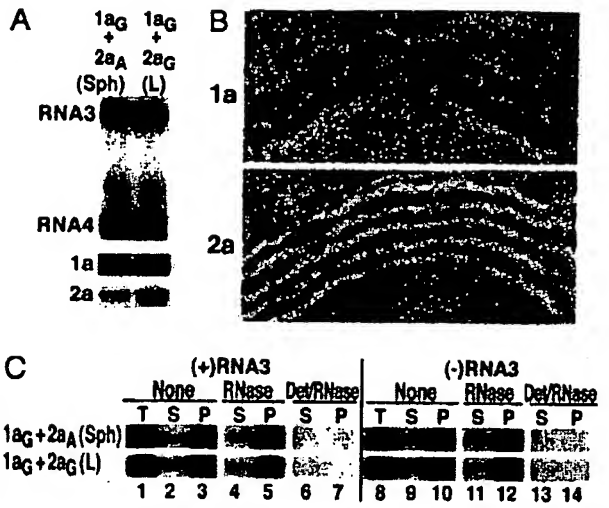

Fig. 2. Double-membrane layers induced by 1a/2a^{pol} contain 1a and 2a^{pol} and support BMV RNA replication and 1a-induced membrane association and nuclease resistance of viral RNAs. (*A*) Northern and Western blot analyses of RNA3, RNA4, 1a and 2a^{pol} accumulation in $1a_G+2a_A$ yeast that contain perinuclear spherules (Sph), or $1a_G+2a_G$ yeast that contain double-membrane layers (L). (*B*) ImmunoGold EM localization of 1a (*Upper*) and 2a^{pol} (*Lower*) in $1a_G+2a_G$ yeast containing double-membrane layers. Replication factor 1a was localized with polyclonal anti-1a antiserum (17). Because anti-2a antibodies gave weak ImmunoGold labeling, 2a^{pol} was localized by using an anti-GFP monoclonal antibody (JL-8, Clontech) to detect a 2a^{pol}-GFP fusion that supports BMV RNA replication (16) and induced ultrastructural changes indistinguishable from WT 2a^{pol} (compare with Fig. 1*D*). Nuc, nucleus; Cyto, cytoplasm. (Scale bars, 100 nm.) (*C*) Northern blot analysis of cell fractionation extracts from $1a_G+2a_A$ yeast that contain spherules (upper row) and $1a_G+2a_G$ yeast that contain double-membrane layers (lower row). The analysis shows the distribution of (+)RNA3 and (−)RNA3 in total lysate (T), 20,000 × *g* membrane-depleted supernatant (S), or membrane-enriched pellet (P) fractions after one of the following treatments: no additional treatment (none), addition of 0.01 units/ml micrococcal nuclease/1 mM $CaCl_2$ for 15 min at 30°C (RNase), or addition of 0.5% Nonidet P-40 for 15 min at 4°C followed by nuclease treatment (Det/RNase).

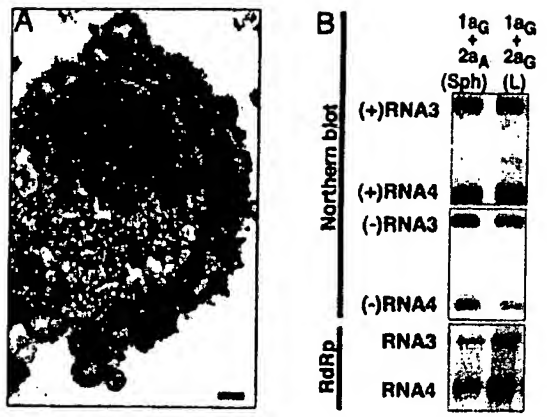

Fig. 3. Isolated nuclei retain perinuclear, double-membrane layers, BMV RNA templates, and BMV-specific RNA-dependent RNA polymerase (RdRp) activity. (*A*) Representative electron micrograph of a nucleus isolated from $1a_G+2a_G$ yeast and bearing 1a/2a^{pol}-induced, double-membrane layers. (Scale bar, 100 nm.) (*B*) Northern blot analysis of (+)- and (−)-strand RNA3 and RNA4 and BMV-specific RNA-dependent RNA polymerase activity found in preparations of nuclei isolated from $1a_G+2a_A$ yeast that contain perinuclear spherules (Sph) or $1a_G+2a_G$ yeast containing double-membrane layers (L).

mic face of the perinuclear ER membrane and that, in $1a_G+2a_A$ yeast, each BMV-induced spherule contains hundreds of 1a proteins and ≈10–15 2a^{pol} proteins (6, 17, 18, 29). ImmunoGold EM analysis showed that, in $1a_G+2a_G$ yeast, 1a and 2a^{pol} localized to the perinuclear membrane layers, with ≈80% of the ImmunoGold label in the cytoplasmic spaces between the double-membrane ER layers or on the cytoplasmic face of the outermost membrane layer (Fig. 2*B*). Some clustering of gold particles occurred, suggesting possible points of 1a and 2a^{pol} concentration within the layers (see also below).

Cells Containing Membrane Layers Sequester (+)RNA3 and (−)RNA3 Templates in a Membrane-Associated, Nuclease-Resistant State. In the absence of 2a^{pol}, 1a acts through a specific cis-acting RNA sequence to recruit RNA3 replication templates to a membrane-associated, nuclease-resistant state (6, 20, 21). This state appears to correspond to the interior of the 1a-induced spherules because, in $1a_G+2a_A$ yeast replicating RNA3, (+)RNA3 and (−)RNA3 templates and nascent RNA are retained in an indistinguishable, membrane-associated, nuclease-resistant state and ImmunoGold EM localizes BrUTP-labeled nascent RNA to spherules (6).

In $1a_G+2a_G$ yeast containing double-membrane layers, we found similar membrane association and protection of (+)RNA3 and (−)RNA3 (Fig. 2*C*). Samples of $1a_G+2a_A$ or $1a_G+2a_G$ yeast replicating RNA3 and containing spherules or layers, respectively, were treated with lyticase to remove cell walls and then lysed and centrifuged at 20,000 × *g* to yield a membrane-enriched pellet (P) and a cytosolic supernatant (S). In both cases, the majority of (+)RNA3 and (−)RNA3 was recovered in the membrane-containing pellet, with little RNA3 in the supernatant (Fig. 2*C*, lanes 1–3 and 8–10). This membrane-associated RNA3 was highly resistant to added nuclease (Fig. 2*C*, lanes 4–5 and 11–12) but became nuclease-susceptible after treatment with a membrane-disrupting, nonionic detergent (Fig. 2*C*, lanes 6–7 and 13–14). Thus, in association with both membrane architectures, (+)RNA3 and (−)RNA3 were found in a membrane-associated, nuclease-resistant, nonionic detergent-susceptible state.

Isolated Nuclei Retain Double-Membrane Layers, Viral (+)RNA and (−)RNA, and RNA-Dependent RNA Polymerase. To further characterize the perinuclear, double-membrane layers, nuclei were isolated from $1a_G+2a_G$ yeast. These nuclei retained double-membrane layers that were stable through nuclear isolation and EM analysis, suggesting relatively strong adhesion between the double-membrane layers (Fig. 3*A*). Similarly, nuclei isolated from $1a_G+2a_A$ yeast retain perinuclear spherules (6). Prior results show that 1a is required to direct RNA3 to nuclear membranes and that in the absence of 1a, RNA3 fractionates with the cytosol (6). Nuclei isolated from cells containing membrane layers or spherules contained similar levels of (+)RNA3, (−)RNA3, and RNA4 (Fig. 3*B*). Nuclei from both types of 1a- and 2a^{pol}-expressing yeast, but not from WT yeast, also incorporated radiolabeled ribonucleotides into BMV RNA replication intermediates (Fig. 3*B*) (6).

2a^{pol} Levels Modulate Layer Formation. To further explore the relationship between double-membrane layers and 2a^{pol} levels (Fig. 2*A*), the copper-responsive, linearly inducible *CUP1* promoter was used to regulate 2a^{pol} levels in cells coexpressing 1a from the standard *GAL1*-promoted 1a expression plasmid. As shown in Fig. 4, increasing $[Cu^{2+}]$ in the medium progressively increased 2a^{pol} accumulation, whereas 1a levels remained essentially constant. EM analysis showed that the percentage of cells with perinuclear membrane layers increased in parallel with 2a^{pol} (Fig. 4), whereas the percentage of cells with perinuclear spher-

EXHIBIT A

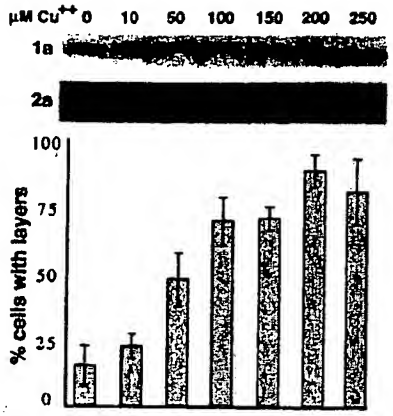

Fig. 4. Increasing $2a^{pol}$ levels promotes $1a/2a^{pol}$-mediated induction of double-membrane layers. Western analysis (*Top* and *Middle*) showing nearly constant 1a expression from the *GAL1* promoter and linearly increasing $2a^{pol}$ expression from the copper-inducible *CUP1* promoter in yeast grown in medium with the indicated levels of $CuSO_4$. For each $CuSO_4$ concentration, the histogram indicates the frequency of EM-visualized cell sections showing BMV-induced perinuclear double-membrane layers, relative to cells showing BMV-induced perinuclear spherules. The results show averages over two independent experiments, and in each experiment 150- to 200-cell sections with BMV-induced membrane rearrangements were scored for each indicated $CuSO_4$ concentration. Standard error bars are indicated.

ules declined correspondingly. In the absence of added Cu^{2+}, little $2a^{pol}$ was detected, but a low percentage of cells contained membrane layers. However, when the *CUP1*-$2a^{pol}$ plasmid was omitted, no membrane layers were seen at any $[Cu^{2+}]$ concentration tested, confirming that $2a^{pol}$ was required to induce layers and that Cu^{2+} alone did not promote layering.

Deleting a 1a-Interactive, N-Terminal $2a^{pol}$ Domain Inhibits Membrane Layer Formation. BMV 1a and $2a^{pol}$ interact *in vitro* and *in vivo* through the 1a C-terminal helicase domain and $2a^{pol}$ amino acids 50–113 (15, 16). To test the contribution of this $1a/2a^{pol}$ interaction to 1a- and $2a^{pol}$-dependent induction of perinuclear membrane layers, we constructed a series of $2a^{pol}$ deletions and assayed their ability to induce layers when expressed from the *GAL1* promoter in yeast coexpressing 1a (Fig. 5). Western blot analysis with multiple monoclonal antibodies against various regions of $2a^{pol}$ to visualize all deletion derivatives showed that

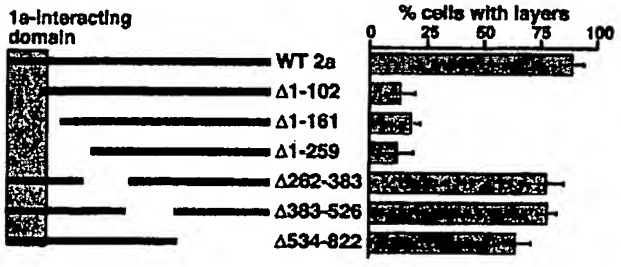

Fig. 5. Deleting the N-proximal 1a-interacting domain of $2a^{pol}$ inhibits induction of double-membrane layers. Diagram of $2a^{pol}$ deletion derivatives with the indicated amino acids deleted. The shaded box indicates the $2a^{pol}$ segment directing high-affinity interaction with the 1a helicase-like domain (15, 16). The histogram indicates the frequency of EM-visualized cell sections that show BMV-induced perinuclear double-membrane layers relative to cells showing BMV-induced perinuclear spherules. The results show averages over two independent experiments, and in each experiment 150- to 200-cell sections with BMV-induced membrane rearrangements were scored for each $2a^{pol}$ deletion derivative. Standard error bars are indicated.

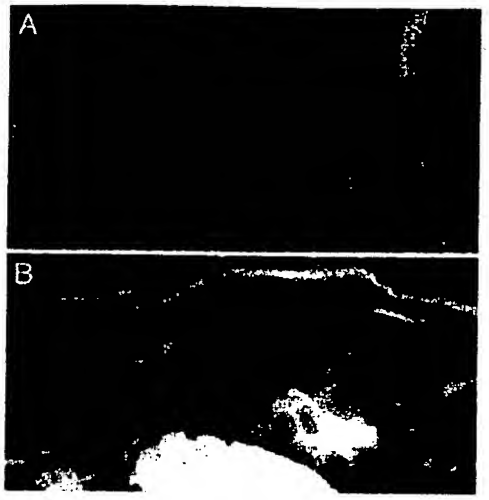

Fig. 6. Underlying structure in the cytoplasm-connected spaces between double-membrane layers in $1a_G+2a_G$ yeast. See *Results* for further comments. Nuc, nucleus; Cyto, cytoplasm. (Scale bar, 100 nm.)

each derivative accumulated to levels close to WT $2a^{pol}$ (results not shown). Deletions overlapping the polymerase domain but retaining the 1a-interactive domain (amino acids 262–383, 385–526, or 534–822) induced double-membrane layers at frequencies approaching those of WT (64–78%). By contrast, all deletions overlapping the N-proximal, 1a-interactive $2a^{pol}$ domain, including deleting the first 102, 161, or 259 amino acids, drastically reduced the frequency of perinuclear membrane layers (12–18%) relative to WT $2a^{pol}$ (92%). The low, residual frequency of membrane layering in the absence of the N-proximal $2a^{pol}$ domain may depend on lower affinity interaction between 1a and the central polymerase domain of $2a^{pol}$ (30).

Internal Structures Between Double-Membrane Layers. Although the BMV-induced double-membrane layers showed relatively smooth contours in most EM images of fixed cells (Fig. 1 *D* and *E*), most isolated nuclei (Fig. 3*A*) and a smaller percentage of fixed cells (Figs. 2*B* and 6*A*) showed perinuclear membrane layers with a distinctly ruffled or corrugated morphology. Thus, in at least some cases, the intermembrane space was not uniform but possessed some underlying variation or structure. Moreover, in rare instances, oblique sections of the membrane layers exposing significant areas of intermembrane space revealed the presence of spheres whose 50- to 60-nm diameters corresponded closely to those of spherules and to the average spacing of ER membrane layers (Fig. 6*B*). The possible relationship of membrane ruffling and these spherical structures to the underlying architecture of the intermembrane space is considered further in *Discussion*.

Discussion

As noted in the Introduction, the universal membrane association of (+)RNA virus RNA replication appears crucial to replication complex assembly and function, yet RNA replication by different (+)RNA viruses induces varied membrane rearrangements including invaginations, double-membrane vesicles, and layered membranes. The results presented here suggest that such apparently distinct morphologies may share underlying structural features. Specifically, modulating the relative expression or interactions of BMV RNA replication proteins 1a and $2a^{pol}$ switched the membrane rearrangements associated with RNA replication from the spherular invaginations (spherules)

EXHIBIT A

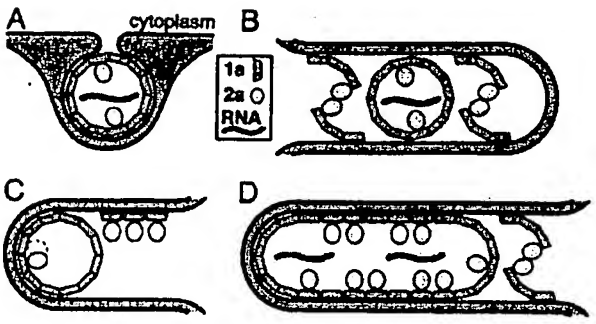

Fig. 7. Models for $2a^{pol}$ modulation of 1a-dependent membrane rearrangements. See *Discussion* for further comments. (*A*) Invagination of a spherule (~50 nm in diameter) into the outerperinuclear ER membrane by 1a formation of a membrane-enveloped, capsid-like shell with 1a recruitment of $2a^{pol}$ and viral RNA. Bold lines depict ER membranes and gray shading depicts the ER lumen. (*B*) High $2a^{pol}$ concentrations may promote zippering together of double-membrane layers by 1a–2a complexes. Replication factor 1a might participate as monomers or multimers (hexamers or pentamers). Self-interaction of $2a^{pol}$ might be direct or mediated by RNA or $2a^{pol}$-interacting host proteins (33). As suggested by Fig. 6, spherule cores may be trapped in such layers. (*C*) High $2a^{pol}$ concentrations may block 1a–1a curvature needed to form spherules by steric hindrance between $2a^{pol}$ factors bound to adjacent 1a factors (left side), tending to restrict 1a to planar lattices (right side). (*D*) Between the stacked double-membrane layers, extended planar lattices of 1a with bound $2a^{pol}$ might provide a local replication complex environment similar to spherule interiors and may be closed by occasional regions of 1a curvature.

found in natural infections by bromoviruses, the related alphaviruses, and many other (+)RNA viruses (4–6, 8–11) to stacked layers of double ER membranes (Fig. 1). Like spherules, these stacked, double-membrane layers were the sites of 1a and $2a^{pol}$ accumulation, protected viral RNA templates from nuclease, and supported RNA replication (Figs. 2 and 3). Below we discuss relevant interactions of 1a and $2a^{pol}$, the underlying structure of membrane spherules and layers, and possible relationships to other (+)RNA viruses.

Modulation of Replication-Associated Membrane Rearrangements by $2a^{pol}$. In the absence of other viral factors, 1a induces membrane spherules but never layers, whereas $2a^{pol}$ alone induces no membrane rearrangements (Fig. 1*B* and ref. 6). Formation of double-membrane layers required coexpressing 1a and $2a^{pol}$, was progressively favored by increasing $2a^{pol}$ levels (Fig. 4), and was inhibited by deleting the major 1a-interacting domain from $2a^{pol}$ (Fig. 5). Double-membrane layers also were promoted by reducing 1a expression relative to $2a^{pol}$. When 1a was expressed from the weaker *ADH1* promoter, cells formed layers when $2a^{pol}$ was expressed from either the *GAL1* or *ADH1* promoter (unpublished results).

Replication factor 1a interacts with ER membranes and itself (12, 29) and is present at hundreds of copies per spherule (6), suggesting that 1a may induce spherules by forming a virion-like shell (Fig. 7*A*) (6). At least two nonexclusive mechanisms could explain how increasing $2a^{pol}$ expression relative to 1a induces membrane layering rather than spherules. First, similar perinuclear layers of double ER membranes, termed karmellae, and other organized smooth ER double-membrane arrays, including whorls, sinusoidal arrays, and crystalloid ER, are formed when certain ER-associated proteins like 3-hydroxy-3-methylglutaryl CoA reductase are expressed above a threshold level (31). Such membrane stacking requires interaction between the cytoplasmic domains of the inducing membrane proteins but, when the responsible membrane protein is expressed at high levels, even low-affinity, dynamic interactions suffice (31).

At sufficient levels, $2a^{pol}$ may induce stable layer formation by mediating similar zippering interactions between opposing membranes. Clustering of $2a^{pol}$ *in vivo* (16) suggests that $2a^{pol}$ interacts with itself, and the related poliovirus 3D polymerase self-interacts to form planar or tubular lattices (32). In keeping with the dependence of membrane layering on $2a^{pol}$ interaction with 1a (Fig. 5), 1a–$2a^{pol}$ complexes might zipper together opposing membranes by means of $2a^{pol}$–$2a^{pol}$ interactions (Fig. 7*B*). Such $2a^{pol}$–$2a^{pol}$ interactions may be direct or mediated by RNA or $2a^{pol}$-interacting host proteins (33). Most proteins inducing organized ER membrane arrays induce a cytoplasmic space of 8–11 nm between the stacked layers of double-membrane ER (31). The ≈50-nm spacing between double-membrane layers induced by 1a and $2a^{pol}$ suggests bridging by larger complexes, such as whole-spherule cores (Fig. 6), 1a hexamers or pentamers (see below), $2a^{pol}$ dimers or multimers, or protein-RNA complexes. Spherule cores trapped in these layers (Figs. 6 and 7*B*) could support RNA replication.

Alternatively or in addition, $2a^{pol}$ overexpression might promote ER membrane layering by inhibiting 1a formation of spherules. Like the CA subunit of HIV Gag (34), 1a may assemble on membranes as a planar hexameric lattice, into which pentamer defects are introduced to generate curvature and invaginate the spherule replication compartments. The 1a–$2a^{pol}$ complex, which parallels many aspects of retroviral Gag-Pol fusion proteins, is incorporated into spherules at a 1a/$2a^{pol}$ ratio of ≈25, similar to the Gag/Gag-Pol virion ratio of ≈20 (6). Gag-Pol overexpression interferes with HIV virion assembly (35), possibly because the virion interior, to which Pol is localized, lacks room for Pol on more than a fraction of Gags (36). Similarly, $2a^{pol}$ association with adjacent 1a replication factors may sterically block the 1a–1a curvature needed to form spherules (Fig. 7*C*). Thus, above a threshold density, $2a^{pol}$ binding might tend to restrict 1a to planar lattices on ER membranes (Fig. 7 *C* and *D*). The resulting membranes may be linked by occasional 1a–$2a^{pol}$ bridges as noted above (Fig. 7*B*), and/or by occasional regions of curvature that allow the extended 1a lattice to close (Fig. 7*D*). The environment between such 1a and 1a–$2a^{pol}$ bearing lattices would be locally similar to spherule interiors and might support RNA replication.

Pol Down-Regulation in (+)RNA Viruses and Retroviruses. Because $2a^{pol}$ levels and interactions dramatically affect BMV replication complex ultrastructure, it is notable that bromoviruses and many other (+)RNA viruses have multiple mechanisms to reduce polymerase expression, accumulation, and interaction. Like retroviruses, many (+)RNA viruses, including alphaviruses, coronaviruses, tobamoviruses, and others, use translational frameshift or read-through to reduce polymerase expression 10- to 20-fold relative to upstream factors related to BMV 1a, and this regulation is linked to replicative fitness (37, 38). BMV, which encodes 1a and $2a^{pol}$ on separate genomic RNAs, inhibits $2a^{pol}$ translation at initiation (39). BMV and alphaviruses also regulate polymerase stability (40, 41). Bromovirus 1a–$2a^{pol}$ interaction is further down-regulated by competing intramolecular 1a–1a interaction and $2a^{pol}$ phosphorylation (12, 42). Picornaviruses and some other (+)RNA viruses express polymerase at levels equimolar with other replication factors. Some of these viruses, such as the picornavirus-like potyviruses, sequester large amounts of excess polymerase away from RNA replication in self-assembled nuclear inclusions (43).

Relation to Other (+)RNA Viruses. The ability to experimentally modulate 1a–$2a^{pol}$ interactions to switch the ultrastructure of functional BMV RNA replication complexes between small vesicular invaginations and extensive double-membrane layers suggests that seemingly diverse membrane rearrangements associated with RNA replication by varied (+)RNA viruses may

EXHIBIT A

represent related structures formed by similar protein–protein and protein–membrane interactions (Fig. 7). Similarly, retrovirus Gag proteins use a common set of underlying interactions to assemble sheets, tubes, cones, or isometric shells under various circumstances (34).

The varied membrane rearrangements associated with (+)RNA virus replication share some similarities. Flavivirus RNA replication localizes to packets of 50- to 100-nm vesicles surrounded by a second membrane (1). These vesicle packets appear similar to EM views of spherules invaginated into ER and mitochondrial lumens by BMV and nodaviruses, respectively, when sectioned perpendicular to the direction of invagination (refs. 6 and 9 and unpublished results). Picornavirus, coronavirus and arterivirus RNA synthesis occurs in or on double-membrane vesicles (2, 3, 23). Although BMV spherules typically are invaginated into a dilated perinuclear ER lumen and are tightly wrapped only by the outer ER membrane, the inner ER membrane constitutes a second bounding membrane surrounding the spherule, making them also double-membrane structures (Fig. 7*A*). Arterivirus double-membrane vesicles are thought to form similarly to spherules by invagination of appressed ER membranes (2). Poliovirus double-membrane-bounded vesicles appear to be formed by ER membranes wrapping around a portion of cytoplasm, which is topologically equivalent to invaginating a portion of ER membrane and its surrounding cytoplasm into the ER lumen (ref. 3; compare with Fig. 7*A*). Some EM sections of poliovirus double-membrane vesicles reveal a narrow neck at which, as for spherules, the inner and outer membranes are continuous and inner vesicle contents connect with the cytoplasm (44).

Like $1a/2a^{pol}$-induced double-membrane layers, picornavirus double-membrane vesicles cluster by interaction of surface membranes carrying viral RNA replication factors (24, 25, 32). Two of these factors, 2C and 2BC, induce ordered ER-membrane arrays, including stacked membrane layers, whorls, and crystalloid ER (45, 46). Similarly, nodavirus and tymovirus RNA replication occurs in association with BMV- and alphavirus-like spherules invaginated into the outer membranes of mitochondria and chloroplasts, respectively, and the replication factor-bearing surface membranes of these modified organelles cluster like poliovirus vesicle rosettes (9, 47). Retargeting nodavirus RNA replication protein A from mitochondria to ER also induces karmellae-like double-membrane layers that, just as for BMV, support RNA replication (48, 49).

We thank Natalie Pellechia for technical assistance, Randall Massey and Ben August (University of Wisconsin Medical School Electron Microscopy Facility) for assistance with EM, and Ann Palmenberg for comments on the manuscript. This work was supported by National Institutes of Health Grant GM35072. P.A. is an Investigator of the Howard Hughes Medical Institute.

1. Westaway, E., Mackenzie, J., Kenney, M., Jones, M. & Khromykh, A. (1997) *J. Virol.* **71**, 6650–6661.
2. Pedersen, K. W., van der Meer, Y., Roos, N. & Snijder, E. J. (1999) *J. Virol.* **73**, 2016–2026.
3. Suhy, D. A., Giddings, T. H., Jr., & Kirkegaard, K. (2000) *J. Virol.* **74**, 8953–8965.
4. Froshauer, S., Kartenbeck, J. & Helenius, A. (1988) *J. Cell Biol.* **107**, 2075–2086.
5. Hatta, T., Bullivant, S. & Matthews, R. E. (1973) *J. Gen. Virol.* **20**, 37–50.
6. Schwartz, M., Chen, J., Janda, M., Sullivan, M., den Boon, J. & Ahlquist, P. (2002) *Mol. Cell* **9**, 505–514.
7. Ahlquist, P., Noueiry, A. O., Lee, W. M., Kushner, D. B. & Dye, B. T. (2003) *J. Virol.* **77**, 8181–8186.
8. Kujala, P., Ahola, T., Ehsani, N., Auvinen, P., Vihinen, H. & Kaariainen, L. (1999) *J. Virol.* **73**, 7805–7811.
9. Miller, D. J., Schwartz, M. D. & Ahlquist, P. (2001) *J. Virol.* **75**, 11664–11676.
10. Kim, K. S. (1977) *J. Gen. Virol.* **35**, 535–543.
11. Hatta, T. & Francki, R. I. B. (1981) *J. Gen. Virol.* **53**, 343–346.
12. O'Reilly, E. K., Wang, Z., French, R. & Kao, C. C. (1998) *J. Virol.* **72**, 7160–7169.
13. Kong, F., Sivakumaran, K. & Kao, C. (1999) *Virology* **259**, 200–210.
14. Ahola, T., den Boon, J. A. & Ahlquist, P. (2000) *J. Virol.* **74**, 8803–8811.
15. Kao, C. C. & Ahlquist, P. (1992) *J. Virol.* **66**, 7293–7302.
16. Chen, J. & Ahlquist, P. (2000) *J. Virol.* **74**, 4310–4318.
17. Restrepo-Hartwig, M. & Ahlquist, P. (1996) *J. Virol.* **70**, 8908–8916.
18. Restrepo-Hartwig, M. & Ahlquist, P. (1999) *J. Virol.* **73**, 10303–10309.
19. Lee, W. M. & Ahlquist, P. (2003) *J. Virol.* **77**, 12819–12828.
20. Janda, M. & Ahlquist, P. (1998) *Proc. Natl. Acad. Sci. USA* **95**, 2227–2232.
21. Sullivan, M. & Ahlquist, P. (1999) *J. Virol.* **73**, 2622–2632.
22. Ahlquist, P. (2002) *Science* **296**, 1270–1273.
23. Gosert, R., Kanjanahaluethai, A., Egger, D., Bienz, K. & Baker, S. C. (2002) *J. Virol.* **76**, 3697–3708.
24. Egger, D., Pasamontes, L., Bolten, R., Boyko, V. & Bienz, K. (1996) *J. Virol.* **70**, 8675–8683.
25. Egger, D., Teterina, N., Ehrenfeld, E. & Bienz, K. (2000) *J. Virol.* **74**, 6570–6580.
26. Janda, M. & Ahlquist, P. (1993) *Cell* **72**, 961–970.
27. Christianson, T. W., Sikorski, R. S., Dante, M., Shero, J. H. & Hieter, P. (1992) *Genes* **110**, 119–122.
28. Ishikawa, M., Janda, M., Krol, M. A. & Ahlquist, P. (1997) *J. Virol.* **71**, 7781–7790.
29. den Boon, J., Chen, J. & Ahlquist, P. (2001) *J. Virol.* **75**, 12370–12381.
30. Smirnyagina, E., Lin, N. S. & Ahlquist, P. (1996) *J. Virol.* **70**, 4729–4736.
31. Snapp, E. L., Hegde, R. S., Francolini, M., Lombardo, F., Colombo, S., Pedrazzini, E., Borgese, N. & Lippincott-Schwartz, J. (2003) *J. Cell Biol.* **163**, 257–269.
32. Lyle, J. M., Bullitt, E., Bienz, K. & Kirkegaard, K. (2002) *Science* **296**, 2218–2222.
33. Tomita, Y., Mizuno, T., Diez, J., Naito, S., Ahlquist, P. & Ishikawa, M. (2003) *J. Virol.* **77**, 2990–2997.
34. Ganser, B. K., Cheng, A., Sundquist, W. I. & Yeager, M. (2003) *EMBO J.* **22**, 2886–2892.
35. Shehu-Xhilaga, M., Crowe, S. M. & Mak, J. (2001) *J. Virol.* **75**, 1834–1841.
36. Coffin, J. M., Hughes, S. H. & Varmus, H. E. (1997) (Cold Spring Harbor Lab. Press, Plainview, NY).
37. Ishikawa, M., Meshi, T., Motoyoshi, F., Takamatsu, N. & Okada, Y. (1986) *Nucleic Acids Res.* **14**, 8291–8305.
38. Li, G. & Rice, C. M. (1989) *J. Virol.* **63**, 1326–1337.
39. Noueiry, A. O., Chen, J. & Ahlquist, P. (2000) *Proc. Natl. Acad. Sci. USA* **97**, 12985–12990.
40. Ishikawa, M., Diez, J., Restrepo-Hartwig, M. & Ahlquist, P. (1997) *Proc. Natl. Acad. Sci. USA* **94**, 13810–13815.
41. deGroot, R. J., Rümenapf, T., Kuhn, R. J., Strauss, E. G. & Strauss, J. H. (1991) *Biochemistry* **88**, 8967–8971.
42. Kim, S. H., Palukaitis, P. & Park, Y. I. (2002) *EMBO J.* **21**, 2292–2300.
43. Restrepo, M. A., Freed, D. D. & Carrington, J. C. (1990) *Plant Cell* **2**, 987–998.
44. Schlegel, A., Giddings, J. T., Ladinsky, M. & Kirkegaard, K. (1996) *J. Virol.* **70**, 6576–6588.
45. Cho, M. W., Teterina, N., Egger, D., Bienz, K. & Ehrenfeld, E. (1994) *Virology* **202**, 129–145.
46. Teterina, N. L., Bienz, K., Egger, D., Gorbalenya, A. E. & Ehrenfeld, E. (1997) *Virology* **237**, 66–77.
47. Prod'homme, D., Le Panse, S., Drugeon, G. & Jupin, I. (2001) *Virology* **281**, 88–101.
48. Miller, D. J., Schwartz, M. D., Dye, B. T. & Ahlquist, P. (2003) *J. Virol.* **77**, 12193–12202.
49. Rubino, L., Di Franco, A. & Russo, M. (2000) *J. Gen. Virol.* **81**, 279–286.